THE PREPARATION OF CARBON FIBRES

"A study of the physics and chemistry
of the preparation of carbon fibres
from acrylic precursors."

by

PHILIP GEORGE ROSE M.Inst.P., M.Sc.

A thesis submitted to the University of Aston
in Birmingham for the award of the degree of Ph.D.

Rolls-Royce (1971) Ltd,
D.E.D. Laboratories,
Derby.

October 1971

SYNOPSIS.

High strength, high modulus carbon fibres are becoming increasingly important as high performance engineering materials. This thesis describes how they may be prepared by heat treatment from filaments spun from polyacrylonitrile and its copolymers.

The chemistry of the first stages of heat treatment is very important in controlling the mechanical properties of the carbonised product. A cyclisation reaction has been found to be responsible for the relatively high thermal stability of pyrolysed polyacrylonitrile, but without oxidation the fibres degrade and fuse. An initial oxidation stage is, therefore, essential to the preparation of fibre of high orientation. The cyclised product of pyrolysis is probably a poly 1,4 dihydropiridine and oxidation converts this to aromatic structures, and cyclised structures containing carbonyl and other oxygenated groups. Oxidation is found to assist the carbon fibre preparation process, by producing a product which condenses at an earlier stage of heat treatment, before fusion can occur.

Carbon fibre strength and modulus are dependent upon producing a highly oriented crystal structure. While oxidation of the polymer stabilises the fibre so as to prevent disorientation, further large increases in orientation, with a commensurate improvement in strength and modulus, can be obtained by stretching at temperatures above 1,700^{o}C. This process is analogous to the way fibre orientation is increased by the stretching of the precursor.

A lamellar graphite structure can be created in high temperature fibre, by carefully controlling the degree of oxidation. This type of graphite can produce very high values of Young's modulus. More often, however, graphite fibre has a fibrillar fine structure, which is explicable in terms of continuous graphite ribbons.

A ribbon model is the most satisfactory representation of the structure of carbon fibre, as it explains the mechanism of the development of long range order and the variation of Young's modulus with crystalline preferred orientation.

LIST OF CONTENTS

CHAPTER 1.

CARBON FIBRES; AN INTRODUCTION.

1.1 THE ENGINEERING ADVANTAGES OF CARBON FIBRE.

In this last decade, carbon fibre has emerged as potentially a very important engineering material. This is because of the increasing value to be found in employing composite materials in engineering applications. Composite materials are devised to combine the advantages of two or more materials in one component. An example of this is glass reinforced plastic (GRP), which combines the high strength of glass fibre with the light weight of a plastic matrix. Carbon fibres are at present being produced with properties which are highly competitive with glass fibre and they have a development potential, which promises further advances in the future.[1]

1.11 Carbon fibre composite material.

Metals possess a range of properties which amply justify their use in a large proportion of engineering applications. They include materials which have high strength and modulus and which can be applied over a wide range of temperatures. Metals are ductile in most cases and are capable of absorbing energy by plastic deformation. Many non-metallic materials are stiff and strong, but do not have this valuable characteristic.

A disadvantage of metals is their high density. In advanced technology some engineering designs are limited solely by the weight of their components, when produced in metal. This is particularly the case with aero-space systems and with machinery in which high centripetal forces are applied to components. Composite materials present the possibility of reducing this weight penalty in engineering design.

A method of measuring the efficiency of a material for use in engineering applications is to take the ratio of its strength and modulus to the specific gravity. These are known as the specific

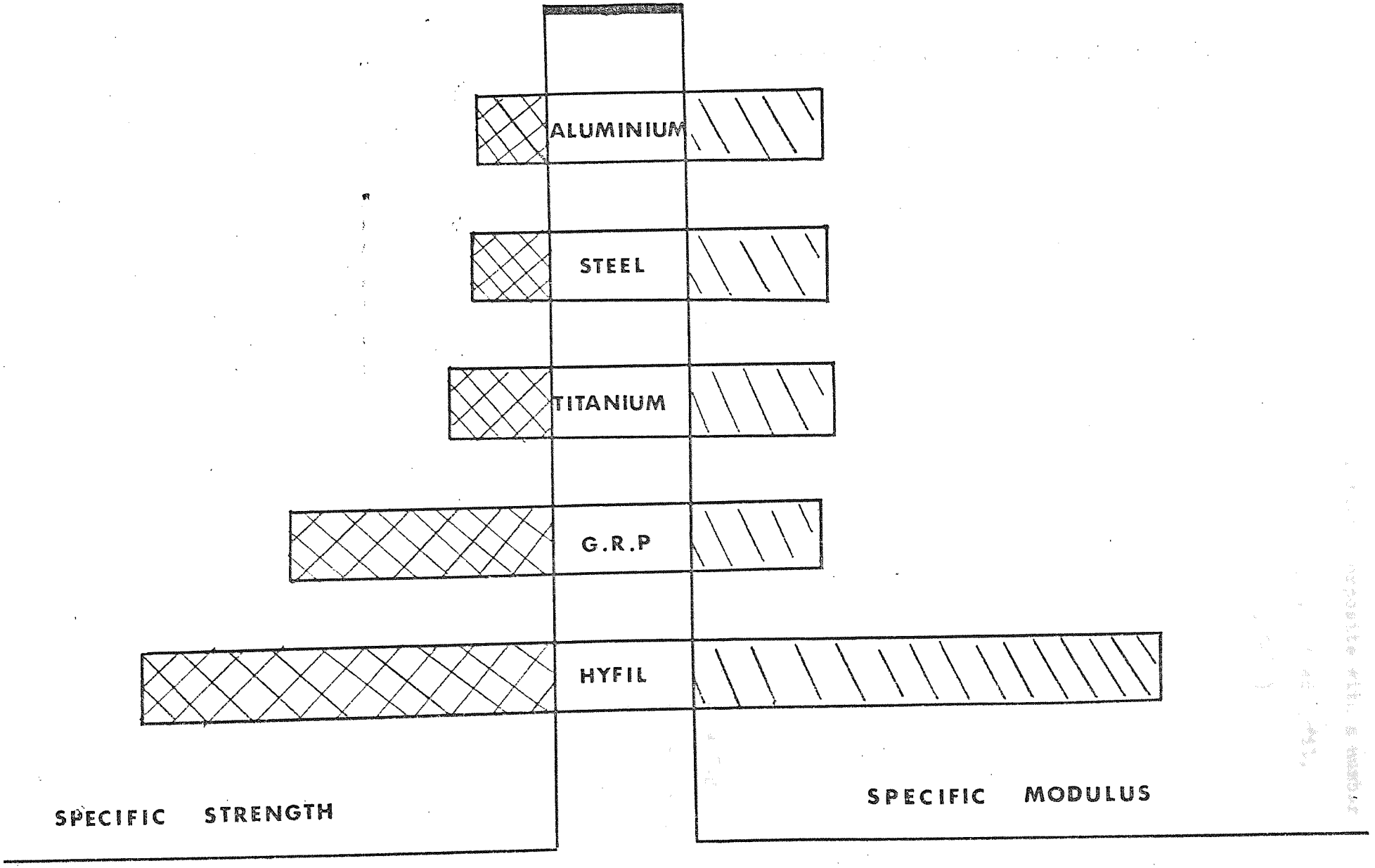

FIGURE 1·11 THE SPECIFIC PROPERTIES OF ENGINEERING MATERIALS

properties of the material. Figure 1.11 compares the specific properties of a Rolls-Royce Ltd carbon fibre composite with a number of typical engineering materials. This composite, called Hyfil, consists of a 70% volume fraction of carbonised (1,000°C) polyacrylonitrile fibres in a matrix of epoxy resin. The specific modulus of Hyfil is about three times as great as for the metals or G.R.P.. The specific modulus of metals is approximately constant, so there is little to be gained by changing the metal one is to use in this respect. The specific strength of both the composite materials in figure 1.11 is high compared to the metals and especially so for Hyfil. The properties of Hyfil are, therefore, quite exceptional.

It is not enough simply to have good specific properties; the absolute strength and modulus have to be good also. Carbon fibre composites also have advantages in this respect. A 70% volume fraction carbon fibre composite made with graphitised cellulose or polyacrylonitrile can have a tensile modulus of 350 GN/M^2; a figure which is similar to drawn tungsten wire and much better than glass or asbestos. The strength of this material would be 1.4 GN/M^2, quite an adequate value. It is, however, a simple matter to prepare a composite with a strength of 2.4 GN/M^2 by choosing the right processing temperature with a polyacrylonitrile precursor.[2,3] This is quite competitive with the finest grade steels.

1.12 Carbon fibre compared to other reinforcing agents.

There are a number of high performance reinforcing materials which can be used with metals and plastics to make composite materials. Each has its own peculiar advantage. Sometimes it is one of cost or possibly chemical stability, in addition to good mechanical properties. Figure 1.12 is a plot of a selection of the more promising materials, compared for their specific properties. Several examples of carbon fibre are shown in the figure. The high strength carbon fibre is a polyacrylonitrile based material, which has been pre-oxidised and

FIGURE 1·12 THE SPECIFIC PROPERTIES OF HIGH PERFORMANCE REINFORCING MATERIALS

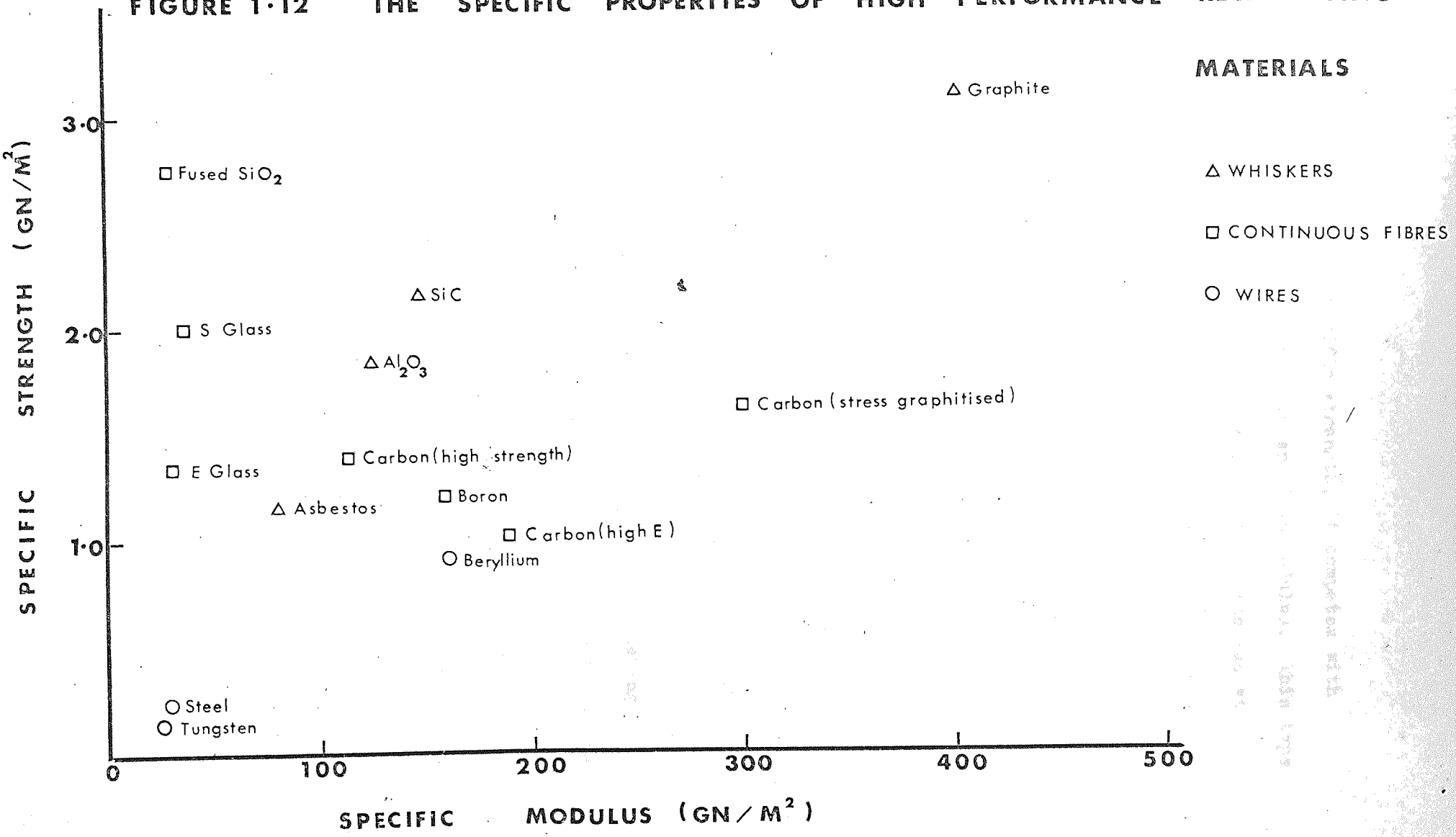

carbonised to 1,200°C. In specific strength, it competes with asbestos and E-glass and is superior in specific modulus. This type of carbon fibre is cheaper than any other, as it is prepared at comparatively low temperatures. When volume production becomes possible, it should compete with glass and asbestos in price. The high E (modulus) carbon fibre is prepared at very high temperatures; 2,500°C and above. For this reason it is more expensive than the high strength material. However, one gains by an improvement in specific modulus, although this is accompanied by a reduction in specific strength. Stress graphitised carbon fibre has a much higher specific modulus than most reinforcing materials. It can be prepared from cellulose or polyacrylonitrile to have the same properties. It is the most expensive continuous carbon fibre because it requires a very high temperature stretching process.

Carbon fibres have not so far been prepared with specific strengths as high as S-glass and silica. For most engineering applications, however, the glasses do not have a sufficiently large modulus. Whisker materials generally have high moduli and strengths, but because of their sophisticated methods of preparation they are extremely expensive. Another disadvantage of whiskers is that they are small and are hence not as efficient as continuous filaments in reinforcing a matrix. Also, there is greater difficulty in making fully aligned composites with them.

Carbon fibres are therefore highly competitive reinforcing materials, which can be obtained with a variety of properties. They are at an early stage of their existence and can be expected to improve with development. They have disadvantages, of course, such as their incompatibility with metals[4,5], and their susceptibility to oxidation. Otherwise they have a very great potential and should become an important engineering material.

1.13 The ultimate properties of carbon fibre: graphite whiskers.

Figure 1.12 includes values of specific strength and modulus for graphite whiskers. In both properties, these whiskers are far superior to any other currently available strong material. Bacon first described their preparation[6]. They require very exacting methods, being formed by a high pressure electrical arc, struck between carbon electrodes. The strengths and moduli quoted for the better examples approach 20 GN/M^2 and 1,000 GN/M^2 respectively. These values are remarkably close to the anticipated properties of perfect single crystal graphite, tested parallel to its basal planes. The reason for these high values is apparent from the structure of the whiskers. Each one consists of a scroll, formed by the apparent 'rolling up' of a single thin stack of graphite layer planes. The axis of the scroll becomes the axis of the whisker.

Graphite whiskers are often quoted as having the mechanical properties which should be ultimately realisable with carbon fibres. It is not theoretically necessary for carbon fibres to have the same scroll structure, but only that they should be very highly oriented, flaw free crystals. The author has achieved modulus values similar to graphite whiskers by producing graphite fibres having an oriented concentric lamellae structure (see chapter 8). The improvement of strength to the same degree remains for the future. Nevertheless, the prospects for very high performance carbon fibres are very exciting.

1.2 THE CRYSTAL STRUCTURE OF CARBON FIBRES.

1.21 The graphite single crystal.

There are two naturally occurring forms of crystalline carbon; diamond and graphite. Diamond is a very hard, transparent, electrical insulator, which has a characteristic cubic structure. Graphite is a very different material from diamond; in single crystal form it has a metallic appearance and can be easily cleaved. In

polycrystalline forms it is very soft to the touch and marks surfaces very easily. Graphite is an electrical conductor and is very much more anisotropic than diamond, a feature which is readily understood when their crystal structures are compared. The triple point for carbon, when both crystal types are in equilibrium with the liquid, occurs at 3,650°C and 100 atmospheres pressure. Of the two crystal forms, graphite is the more stable, as diamond graphitises in the region of 1,750°C.[7]

The unit cell of the graphite crystal is shown in figure 1.21. The structure of graphite was originally determined by Bernal,[8] to be a hexagonal layer structure, with the atoms in the layers closely packed, having a separation of 1.415 A°. The atoms in the layers are covalently bonded, but the layers themselves are bonded by the van der Waal's dispersion force. The interlayer spacing is therefore very great, having a minimum separation of 3.354 A°. The layers are stacked in an .ABABA ----- sequence. The hexagonal unit cell shown by hatched lines in figure 1.21 has a height of 6.708 A° and an edge dimension of 2.46 A°. The layer structure of graphite explains many of the peculiar features of the material, and in particular why orientation in polycrystalline graphite is so important. The crystal is extremely anisotropic: the modulus measured parallel to the layer planes is 1,020 GN/M^2, while measured perpendicularly it is 36.3 GN/M^2.[9] It is, therefore, necessary that an ideal carbon fibre should have the individual crystallites oriented with their layer planes parallel to the fibre axis.

Graphite materials only occasionally occur in an ideally crystalline form; examples are found in isolated geological formations, and some examples of highly crystalline material have been synthesised by precipitation from molten metals (e.g. kish graphite from iron) and by the high pressure graphitisation of pyrolytically deposited carbons. The degree to which a carbon is graphitic will depend upon the

FIGURE 1·21

THE GRAPHITE CRYSTAL UNIT CELL

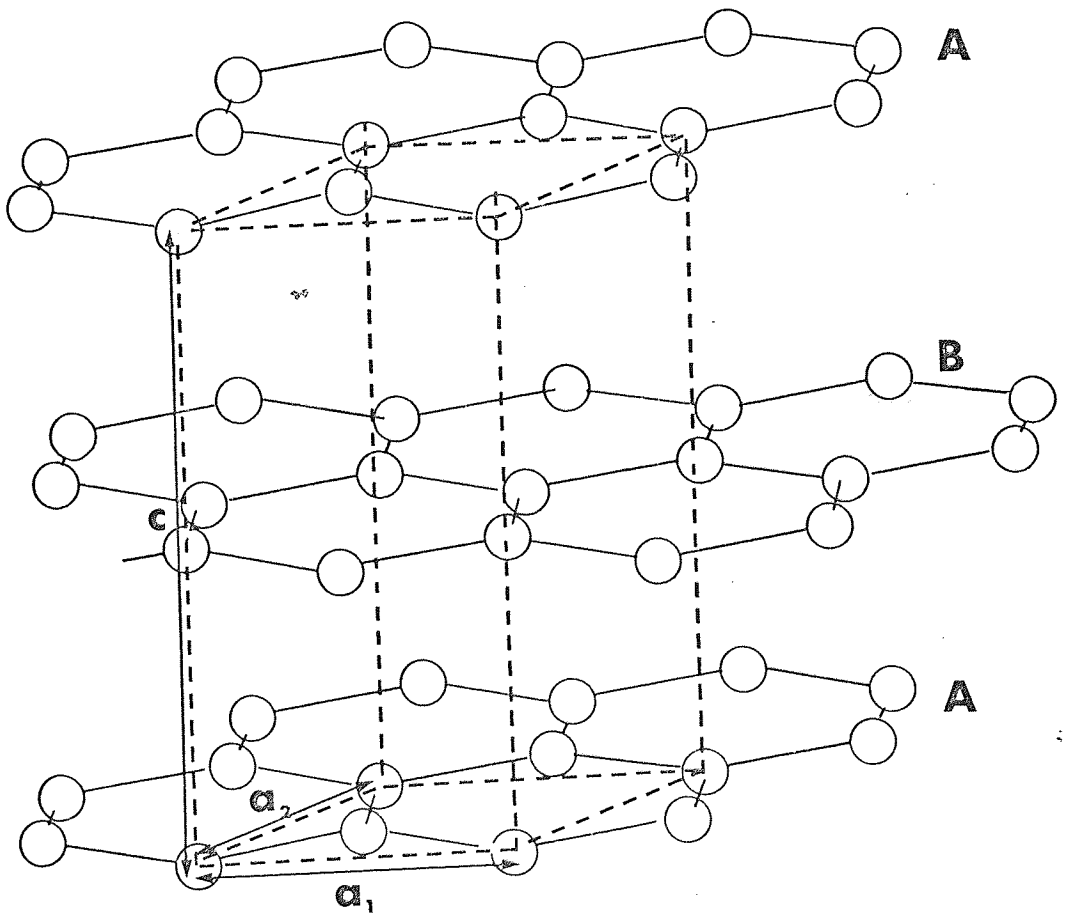

precursor material, the degree of heat treatment and the types of impurity element present.

Many carbons have an imperfect form of the graphite structure which is essentially two dimensional, lacking a regular stacking sequence of the layer planes. This type of graphite is called turbostratic graphite.[10] It has a fixed interlayer spacing and the atomic packing within the layers is identical to the single crystal. The lack of three dimensional order is due to the layers having a random stacking sequence, with neighbouring layers rotated out of register with each other about the crystal C-axis. This rotational disorder increases the spacing of the layers from 3.354 A^{o} (for a perfect crystal) to a minimum value of 3.44 A^{o}.

Turbostratic graphites produce X-ray diffraction patterns characteristic of a two dimensional diffracting system. Polycrystalline or powder specimens will only produce diffraction arcs of the type (o o ℓ) and (h k o) for which h and k cannot simultaneously be zero. This is assigning the arcs by conventional Miller indices.

The term lubricostratic [11] has been employed to describe an alternative imperfect form of graphite. In this case, the layers are in the right sequence, with no relative twist between them, but the interlayer lattice interval varies.

1.22 The graphitisability of carbons.

Carbons are generally classified according to their ability to form a three dimensional graphite lattice with a c-spacing of 3.354 A^{o}. If they do this, they are termed graphitising, or alternatively, soft carbons. Carbons which do not form three dimensional order for normal graphitising heat treatments are termed non-graphitising, or alternatively, hard carbons. A carbon which is turbostratic at 2,000^{o}C is not necessarily non-graphitising, because with heat treatment to 3,000^{o}C it may develop complete crystallinity. The

classification is really a measure of the ease with which complete crystallisation is achieved, because even a non-graphitising carbon should completely crystallise at 3,650°C, although it may not do this without sublimation, or the application of high pressure.

Carbons produced from organic polymers can be either graphitising or non-graphitising. An example of the former is polyvinylchloride and of the latter, polyvinylidine chloride.[12] The concept that all carbonised organic materials should belong to one of these two categories is now being questioned. A recent paper [13] describes how polymer carbons can have a range of crystal structures spanning the whole range of crystallinities between the non-graphitised and graphitised types. It will also be shown in this thesis that polyacrylonitrile carbon can be classed as either type depending upon the initial heat treatment, and often it has characteristics of both types simultaneously.

1.23 The structure of carbon fibres.

The chapter which considers the graphitisation of acrylic fibres (chapter 8) considers the subject of fibre structure in some detail. This section will be restricted to a brief review of the topic.

Shindo [14,15] made the first and most detailed study of the structure of acrylic based carbon fibre. For acrylic fibres which have been oxidised and carbonised to 1,000°C, he found that the structure was only poorly crystalline. Only the (002), (100) and (110) diffraction arcs could be identified. The crystal thickness L_c was 14 A° and the d-spacing 3.44 A°. This fibre, though very strong and stiff, is a turbostratic graphite. Other workers have confirmed this with alternative acrylic precursors. [16,17] Heat treatment of the fibre to higher temperatures is found to increase the size, perfection and preferred orientation of the crystals. This is accompanied by an increase in the density and Young's modulus of

the fibre.

Three dimensional graphite has been observed in a number of samples. Shindo observed it on the surface of his highest temperature material. [14] It has also been observed in ultrasonically disintegrated Rolls-Royce fibre.[17] Other authors have claimed that very large amounts of three dimensional crystal are possible,[18,19] and it will be shown later that it is a more important feature of fibre structure than previously believed.

Figure 1.23 is a reproduction of a model for the structure of Rolls-Royce, 2,800°C material [17] prepared from oxidised Courtelle acrylic fibre. This model has been to some extent superseded by the observation of continuous ribbon structures in graphitised fibre, using high resolution electron microscopy (chapter 8). However, it is a very good model for explaining the X-ray data produced by both high [17] and low angle [20] diffraction. The crystals are almost cubic in shape, having an edge dimension of about 60 A°. The crystals are turbostratic and oriented preferentially to the axis of the fibre; the high modulus is due to this arrangement. The crystals are organised in chains, which correspond to a fibrillar fine structure. This structure is believed to be the counterpart of the fibrous texture of the precursor fibre, retained in the graphite fibre as a crystal texture.[17,21,22]

Fibres prepared from other polymers are found to have a similar structure to polyacrylonitrile based material. The major difference appears to be that most alternative polymers do not produce such highly oriented graphite, unless a stretching process is applied at some stage of their preparation. Polyacrylonitrile fibres produce very highly oriented graphite, without stretching, although stretching can be used to improve its properties. It is the inherent ability of this polymer to conserve high preferred orientations during carbonisation that explains its attraction as a precursor.

FIGURE 1·23

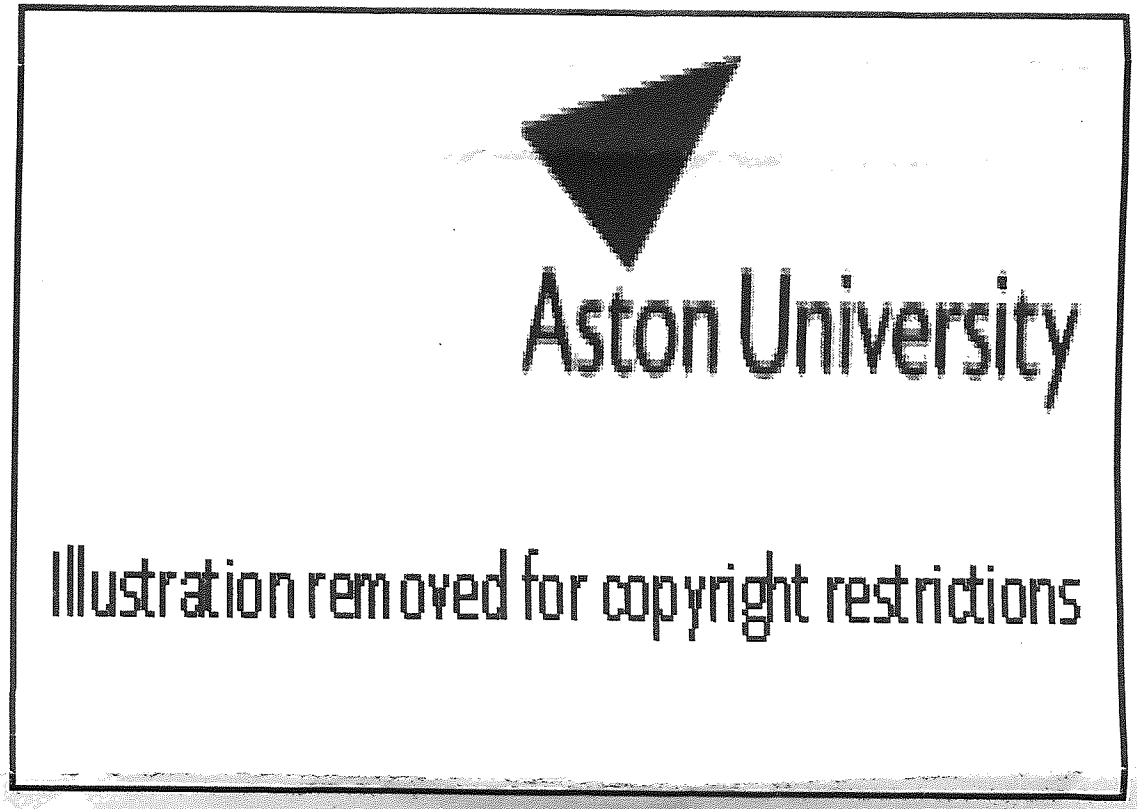

A MODEL OF CARBON FIBRE STRUCTURE
(Johnson & Tyson)

1.3 THE FORMATION OF CARBON FIBRE FROM TEXTILE PRECURSORS.

1.31 The early history of the preparation of carbon fibre.

The first patented carbon filament was produced from cellulose for use as an incandescent lamp filament.[22,23] We do not know the mechanical properties of this material, but they may well have been very good, as this use is quite an exacting application. Swann [24] was the first worker to spin synthetic, i.e. regenerated cellulose, fibres, for use as a carbon fibre precursor, as early as 1883. The use of very high temperatures had been developed by the turn of the century with the introduction of the Acheson method of producing graphite. Therefore, a large part of the technology for producing high performance carbon fibre was established at the beginning of this century. What has been lacking since then has been the stimulus of the demand for light and strong reinforcing materials, which is now making itself felt.

The carbon lamp filament was displaced in 1907 by the drawn tungsten wire and carbon fibres were for a long while neglected as a research topic.

1.32 The development of cellulose based carbon fibre as an engineering material.

Interest in using carbon fibres as an engineering material first arose in the early 1950's. It was found that by using very high tenacity rayons as precursors quite high mechanical properties were realised.[25,26] The method of heat treatment for cellulose can be very complex, with the periods spent at different temperatures having a great deal of significance. Chlorine is introduced into the furnace purge gas during heat treatment between 300 and 600^{o}C, as this is found to increase the yield and properties of the fibre. Since the use of pre-oxidation with polyacrylonitrile was publicised, it has been adopted for the early stages of the cellulose process. Ross [27] describes a typical continuous process with rayon as a precursor and

he also provides a very useful list of patent references, in which the details of the various carbon fibre processing methods can be found.

Cellulose fibres cannot be pyrolysed under restraint, otherwise they will break and shrivel. They must be allowed to relax to some extent. This appears to result in a reduction in the preferred orientation of the carbonised product and a low modulus. Typical properties for graphitised, unstretched cellulose based fibres are strengths of 0.9 GN/M^2 and moduli of 170 GN/M^2. Cellulose based material can be stretched at high temperatures, to produce properties equivalent to the high modulus polyacrylonitrile based material. It cannot, however, be used to produce the equivalent of the high strain material prepared by heating oxidised Courtelle acrylic fibre to 1,200°C. [3]

1.33 Carbon fibre prepared from polyacrylonitrile precursors.

The chemistry of the pyrolysis and oxidation of polyacrylonitrile is reviewed in chapter 3. This present section will be limited to a history of acrylic carbon fibre technology.

Shindo [14,15] was the first to publish details of a process which employed oxidised polyacrylonitrile as a method of preparing carbon fibre. His results are probably the basis of the original patent for the process.[28] The properties he quoted for his best material were very similar to those quoted in section 1.32, for cellulose based material. It is possible that he did not restrain his fibre during oxidation, and the resultant relaxation of the fibres could have reduced their ultimate mechanical properties.

Research workers at Rolls-Royce Ltd [29] and RAE (Farnborough) [30] originally developed distillation processes for preparing acrylic carbon fibre. (There is now some doubt, however, about them being thoroughly inert distillations.) The properties obtained with these processes were better than any obtained at that time by other methods. There appear to be two reasons for this. One is that restraint of

the acrylic fibre was used during the first stage of the process. The other was that an acrylic copolymer was used, Courtelle, which has an 8% weight content of methylacrylate.[31] This fibre is very much more easily processed than other acrylics, as it does not melt so easily and does not have such a violent exothermic reaction during initial pyrolysis. The properties obtained with distilled and graphitised Courtelle were strengths of 1.7 GN/M^2 and moduli of 410 GN/M^2. It was these properties that provided the initial stimulus for the use of carbon fibre composites in advanced technology in Britain.

The RAE workers discovered that the use of pre-oxidation with Courtelle, particularly 1.5 denier high tenacity fibre, produced improved properties. The strengths obtained were very high.[32,33] At the optimum heat treatment temperatures, strengths of 3.1 GN/M^2 and moduli of 450 GN/M^2 can be achieved. This process has now become an important commercial method for producing high strength carbon fibre.

Apart from the obvious advantages of good mechanical properties, polyacrylonitrile has other benefits as a precursor. It provides a high weight yield; 55% of the fibre is retained as carbon. Cellulose, at best, produces a 15% yield. Oxidised polyacrylonitrile is highly thermally stable. Pre-oxidised Courtelle fibres can be carbonised very rapidly, without excessive shrinkage. This allows the use of economic processing techniques. Cellulose has to be slowly programmed through carbonisation and this involves long expensive processing times.

1.34 Alternative precursors for carbon fibre.

There are a number of polymers which produce large carbon yields after distillation. Although at present cellulose and polyacrylonitrile are the favoured candidates, research with these alternative materials may very well lead to better properties and more

economic production.

Prominent amongst these materials is polyvinylidine chloride,[34,35] which can be used to form a carbon of high internal surface area. However, it is a non-graphitising carbon which has a structure similar to carbonised polyacrylonitrile. In fine filament form, it may well produce very good properties. High temperature polymers are also potential precursors that should produce high yields, and a number of patents have been taken out for processes which use them.[36,37]

The major precondition for a polymer fibre to be used for carbon fibre production is that it should not melt and disorient prematurely. The cross-linking and condensation of the chain molecules has to be accomplished without passing through a molten phase. This has been accomplished with polyolefines by the initial stabilisation of the polymer, either by filling with carbon black, or by cross-linking with ionising radiation.[38,39,40] Another method of dealing with polymers having low melting points is to pyrolyse them in the molten state and then spin them into fibres afterwards. The fibres can sometimes be stabilised by oxidation as they emerge from the spinnerette. This process works very successfully with polyvinylchloride.[41] Petroleum pitch [42] and bituminous tars (unpublished) can be spun and oxidised by similar methods.

The use of oxidation to stabilise unsaturated polymers, such as pitches and tars, is quite a standard practice and well known to the graphite technologist. It is quite possible that the oxidative stabilisation of polyacrylonitrile is related to the same basic mechanism.

The author has conducted several experiments with Nylon, polyamide filaments and has been able to obtain high carbon yields. However, the problem with most polyamides is that they tend to melt before achieving complete thermal stability. Nylon 6, which has a melting point of 200°C, could not be stabilised without fusing. Figure 1.34

FIGURE 1·34

OXIDISED NYLON 6 GRAPHITISED TO 3,000 °C .

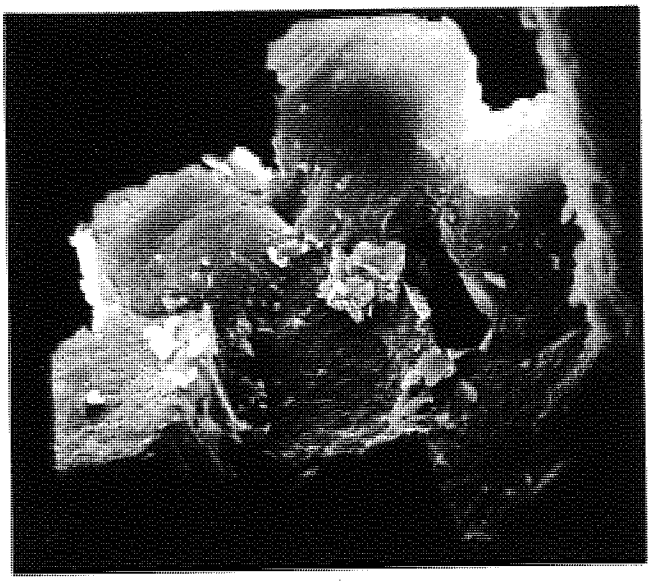

x 3,670

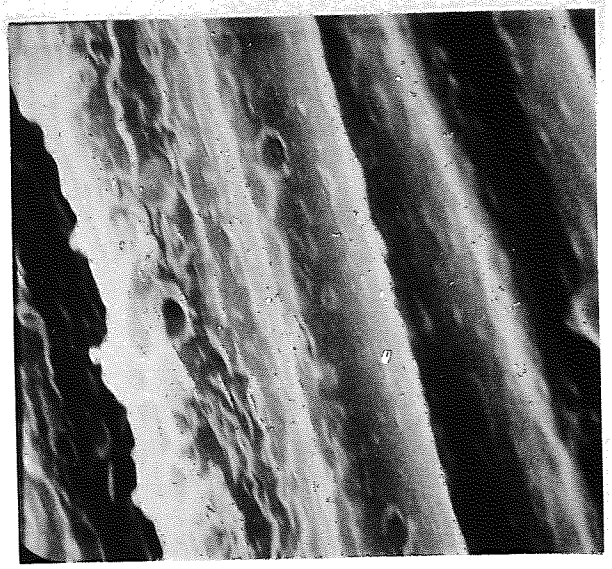

x 3,680

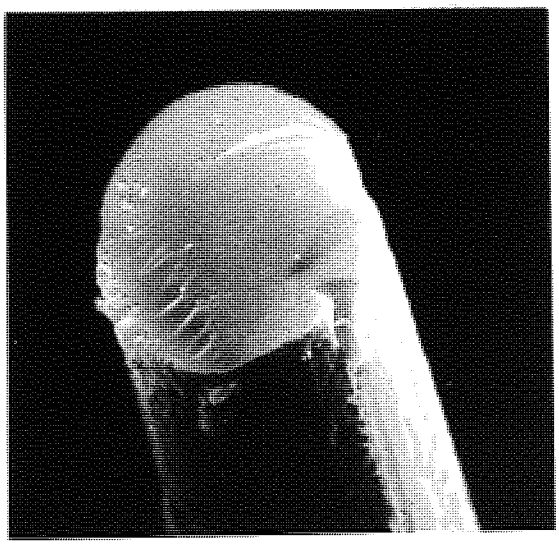

x 3,206

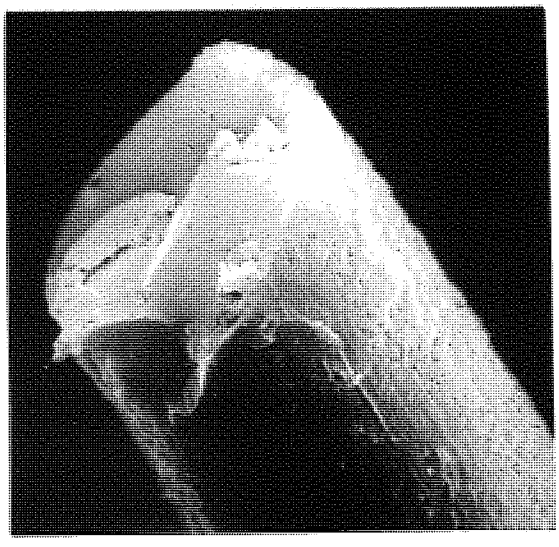

x 3,026

OXIDISED NYLON 6,6 GRAPHITISED TO 3,000 °C

shows scanning electron micrographs of a bundle of Nylon 6 fibre which has been oxidised and graphitised. The fibres have fused together, although their individual profiles are still apparent. Improved results were obtained with Nylon 6,6, which melts at 260°C and can hence be oxidised at higher temperatures. In spite of this, it was impossible to prevent shrinkage and some fibre adhesion. Although after carbonisation the fibres were separable, they had very poor properties. Micrographs of two of these fibres are shown in figure 1.34. They are glassy and the surfaces are very rough.

The best results were obtained with an aromatic polyamide fibre; Nomex Nylon. This has a melting point in excess of 400°C and can be satisfactorily oxidised at 300°C. Carbonisation produced fibres which were separable and which had moderately good mechanical properties. Ezekiel [43] has also found that aromatic polyamides can be used as precursors.

It is very important that the precursor is stabilised against melting during the early stages of heat treatment. This is a problem with polyvinylalcohol [44] as well as with the polyamides. It is also important with pure polyacrylonitrile fibres, as the rapid heating of these can easily result in fusion and excessive shrinkage.

CHAPTER 2.

APPARATUS AND EXPERIMENTAL TECHNIQUES.

The main purpose of this research was to relate the mechanical properties of carbon and graphite fibres to the method of preparation and to obtain an understanding of the behaviour of acrylic fibres under various processing conditions. It was, therefore, necessary to determine the fibre strength and tensile modulus following carbonisation and to monitor the physical and chemical changes accompanying heat treatment. For this purpose, quite a wide range of instruments and techniques have been employed and these will be described below.

2.1 X-RAY DIFFRACTION DETERMINATIONS.

The X-ray diffraction data reported in this thesis has been obtained by J. R. Marjoram of Rolls-Royce Ltd, who provided a routine service for the author. Two X-ray techniques were used for investigating fibre structure, the Debye-Scherrer powder diffraction method and the flat plate fibre diagram. The former method is very well known and can be studied in standard texts on crystallography.[45] The method of obtaining the fibre diagram is shown in figure 2.1. The fibre bundle to be investigated is mounted upon a frame, which in turn is mounted perpendicularly to the incident X-ray beam. A flat photographic plate is placed at an accurately determined distance from the fibre specimen, perpendicular to the incident beam and parallel to the axis of the bundle. The undeviated fraction of the incident beam is allowed to pass through a central aperture in the plate, so that only the diffracted X-rays are used in making the exposure. The precursor acrylic fibres and their carbonised products behave essentially as polycrystalline solids which have varying degrees of preferred orientation. The X-ray diffraction pattern, therefore, consists of numbers of concentric arcs about the axis formed by the incident X-ray beam. This is illustrated in figure 2.1. The number of arcs recorded is deliberately limited by the size of the

THE X ray Fibre Diagram

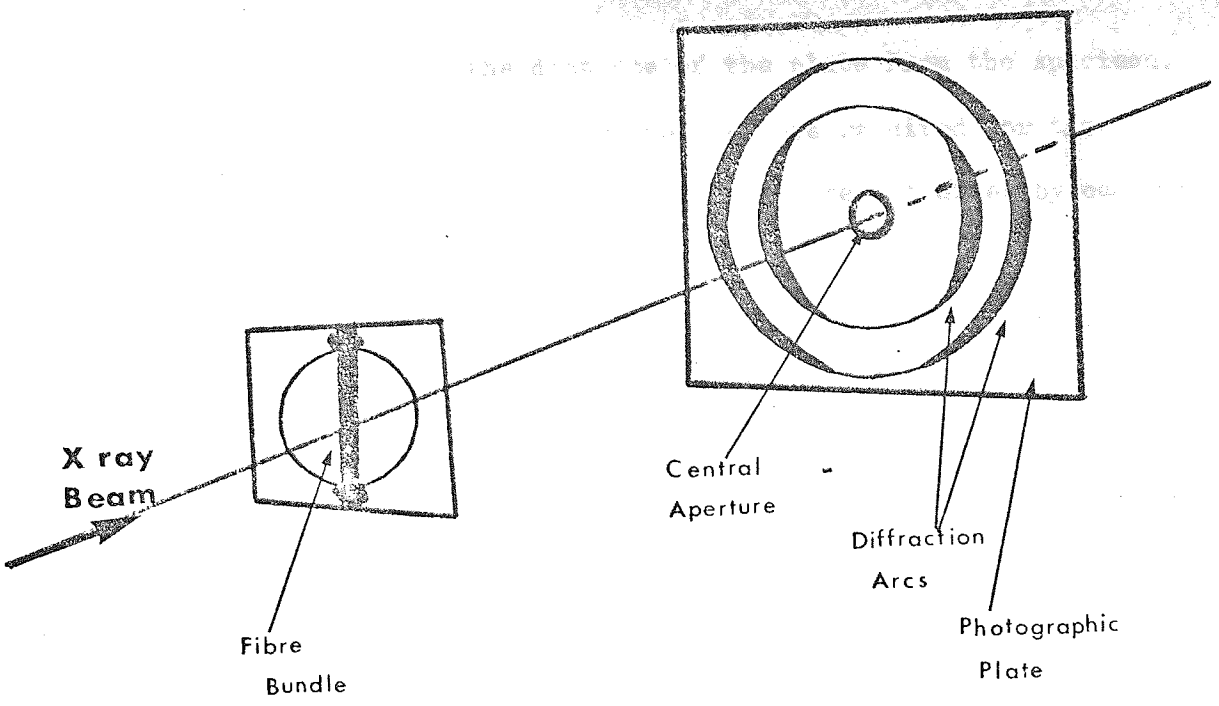

The Determination Of The Orientation Angle Z°

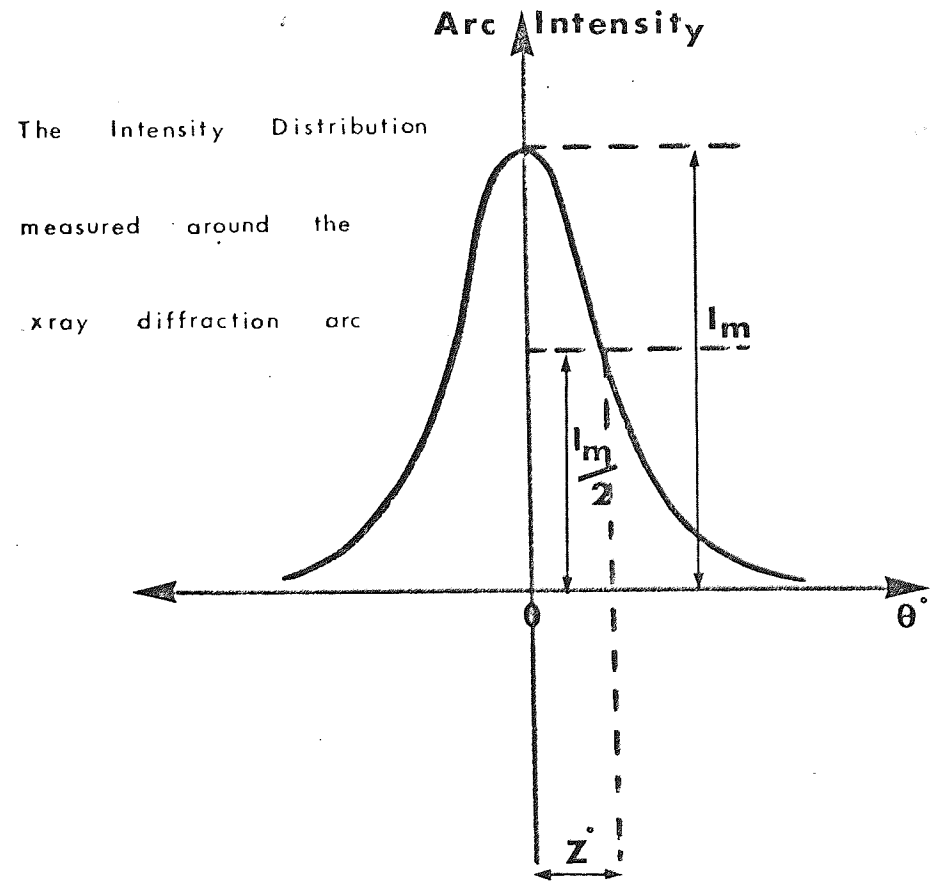

FIGURE 2·1

photographic plate and the distance of the plate from the specimen. This is done because only one or two arcs are required for the measurements to be made and the accuracy can be optimised by contriving to obtain as large an arc as possible.

The fibre diagram is used to determine accurate values of the Bragg angle for given crystal planes and the orientation angle for the fibre. The Debye-Scherrer powder diffraction method is used for the determination of the degree of crystallinity, as all the possible diffraction arcs can be obtained and indexed. It is also used for the determination of mean crystallite dimensions from the widths of some of the diffraction arcs. The acrylic precursor fibres only exhibit two diffraction arcs, which, using Miller indices, are the (100) and (200) arcs, and are both due to the lateral order of the molecular chain packing within the fibre. The preferred orientation of the precursor fibre is related to the orientation angle. The orientation angle is the half angular width of the intensity measured around the diffraction arc at half height. This is illustrated in figure 2.1. For the precursor fibre this measurement is made by taking a micro-densitometer plot around the (100) arc (the more intense of the two) and then by accurate measurement with the resultant intensity distribution. The smaller the orientation angle, the greater the degree of preferred orientation, i.e. the more perfectly aligned are the polymer molecules with the fibre axis.

With increasing heat treatment, the diffraction pattern changes. The (100) polymer arc disappears and new arcs develop. The strongest of these is the (002) arc, which is due to diffraction from planar structures, oriented approximately parallel to the fibre axis. These planar structures eventually become the layer planes of the graphite crystal structure. For oxidised fibres and their carbonised products, the orientation angle has been determined from this (002) arc intensity distribution.

The crystallite dimensions of the carbonised fibres have been determined from the width of the (002) and (100) diffraction arcs. The methods of calculating these dimensions can be found in the literature.[46,47,48]

2.2 THE DETERMINATION OF TEXTILE FIBRE MECHANICAL PROPERTIES.

The lack of three dimensional crystalline order in polyacrylonitrile precursor fibres, and their pyrolysed and oxidised products, renders the physical interpretation of the changes accompanying heat treatment rather difficult. Infra-red spectrophotometry and differential scanning calorimetry facilitate the chemical analyis of the changes that result from heat treatment. They do not, however, help a great deal in characterising changes in the physical structure of the fibre. For this reason, it was decided that it would be valuable to follow the changes in fibre mechanical properties with heat treatment. By this means it should be possible to judge if a loss of preferred orientation has taken place and whether polymer chain degradation has occurred. Another important possibility following from the oxidation of polyacrylonitrile is the cross-linking of the chains to produce a rigid intractable structure.[49,50] If this occurs it should have an appreciable effect on the mechanical properties.

The tensile properties and torsion modulus have been measured for 1.5 denier Courtelle fibres, heat treated in air and argon. The tensile properties, i.e. the Young's modulus, breaking strength and elongation at break,were measured using a specially designed textile extensometer.

2.21 Textile fibre extensometry.

The textile extensometer is shown in figure 2.21(a). This is a photograph taken from the front of the instrument. The instrument is driven by a 'Citenco' motor (A in the photograph) which is reversible and has a variable speed control. The motor drives a pair

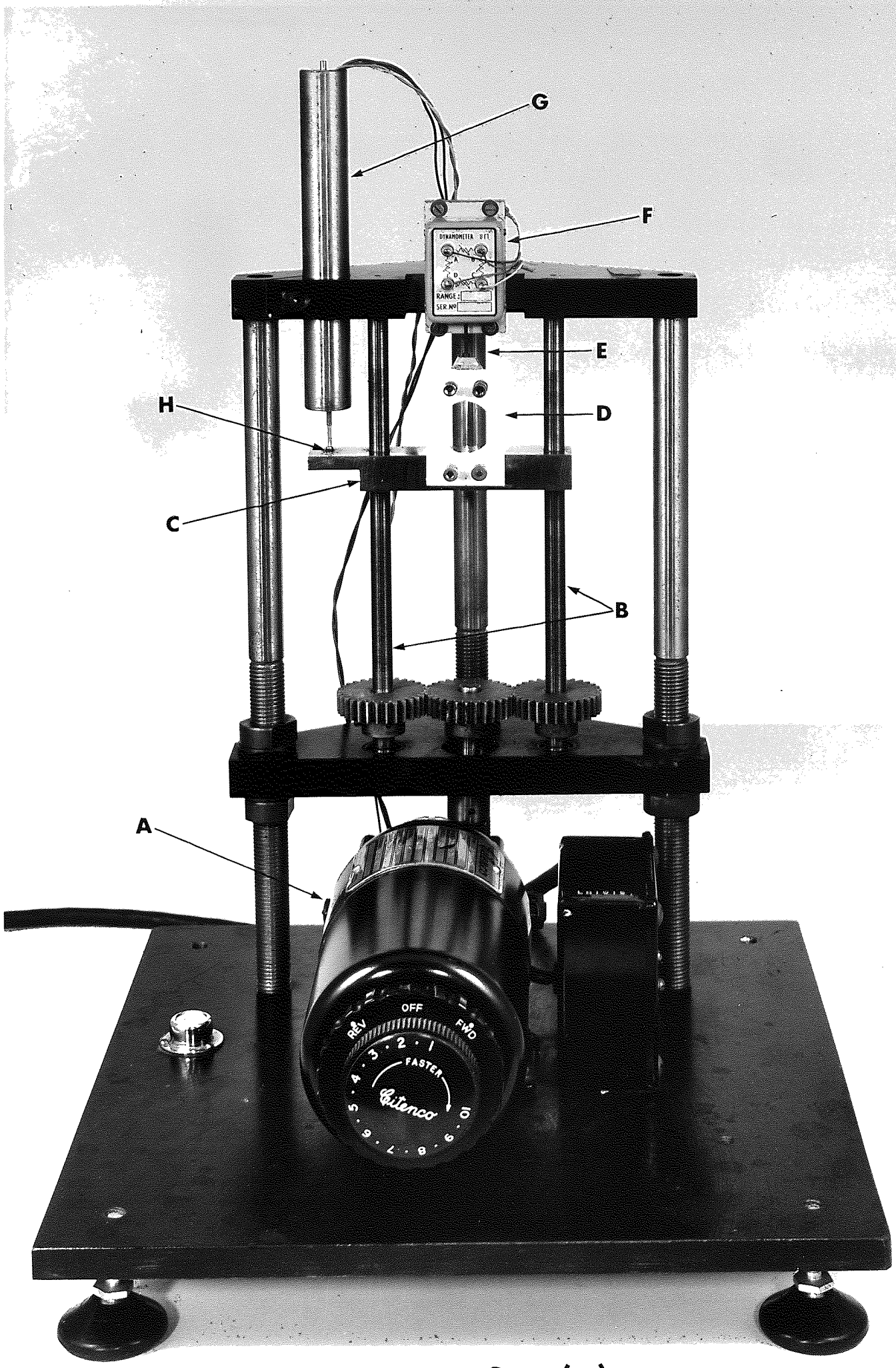

FIGURE 2·21(a)

TEXTILE EXTENSOMETER

of brass lead screws (B) which carry a brass cross-head (C). The fibre is mounted upon a card (D), which is of standard dimensions. An approximate gauge length was obtained for the fibre by mounting it across the central hole and securing it by spots of 'Durafix' glue at points 'a' and 'b' shown in the figure. The central line along which the fibre must lie was marked upon the card with a pencil, using a specially constructed jig. The card has a pair of small holes at the top and bottom, with which it is mounted upon pins on the top mounting block (E) and the cross-head, respectively. The card is fixed securely by brass caps, which are screwed down upon the pins.

The load upon the fibre is measured with an Ether Ltd U.F.1 Dynamometer, (F) measuring 2 ozs full scale. The full scale deflection of the Dynamometer is $\frac{1}{2}$ m.m., which will not introduce serious error into the measurement of modulus or extension at break, because the former is determined at small loads and the latter is normally in excess of 5% extension. The input voltage to the Dynamometer was supplied by a stabilised source and the output supplied to an amplifier and then to the y-terminals of an Advance Ltd x-y recorder. The extension of the fibre is measured with a linear voltage differential transformer (LVDT) (G), which was supplied by Scheavitz Ltd. The LVDT measures displacements of 0 to 1" with an accuracy of at least 10^{-3}". It was supplied by a stabilised 22 volt source and the output was applied directly to the x-terminals of the recorder. The transformer coil is contained in the barrel which is bolted into the top plate of the extensometer. The core of the transformer (H) is attached to the cross-head of the extensometer, and it is free to slide in the barrel with the movement of the cross-head. The position of the core within the barrel is linearly related to the out-put voltage.

The di meter of the fibre was measured with an optical microscope, in which the normal eye-piece was replaced by a Watson Ltd image shearing eyepiece. This instrument requires to be calibrated and this

FIGURE 2·21(b)

COURTELLE LOAD - EXTENSION CURVE

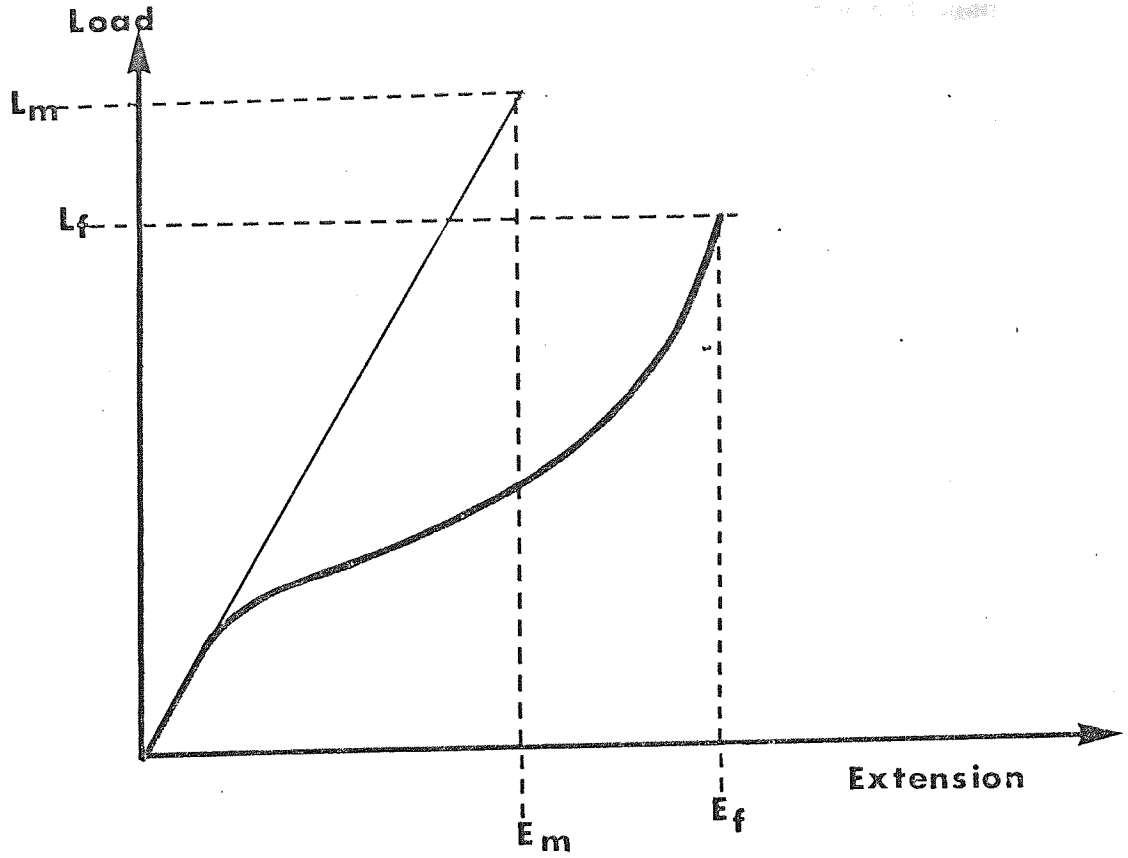

The calculation of fibre tensile properties

a = fibre cross-sectional area

l = fibre test gauge length

L_f = the breaking load

E_f = the breaking extension

L_m/E_m = the initial slope

$$\text{Strength} = L_f/a$$

$$\text{Elongation at Break} = E_f/l$$

$$\text{Young's Modulus} = (L_m/E_m) \times (l/a)$$

was done using wires of known diameter which covered the range of fibre diameters which were likely to be met. The wires had been accurately measured at high magnifications. A mean of three measurements along the gauge length were taken as the final diameter value. The microscope was calibrated prior to every set of fibre measurements. The usual test sample was of twelve fibres from each batch. These were selected randomly from the fibre bundle. Having determined the diameter, the fibre was mounted upon the extensometer and the card cut through to the left and right of the fibre. A vertical travelling telescope was then used to measure the gauge length of the fibre, after it had been pulled straight, so as to register a small load. The test speed was 75% extension/minute. This was quite an arbitrary choice that suited the response of the recorder. Before each test the load calibration was checked using accurately weighed metal rings and the strain measurement was checked with the travelling telescope, which was calibrated to 10^{-3}" with a vernier scale.

The load-extension curve obtained for a 1.5 denier Courtelle fibre is shown in figure 2.21(b), together with the formulae for obtaining the modulus, strength and elongation at break. The Young's modulus is for small strains and so it is determined from the initial straight line portion of the curve.

2.22 The determination of the torsion modulus of 1.5 denier Courtelle.

The torsion modulus of 1.5 denier Courtelle and its heat treated products has been determined by a modification of a method due to Meredith [51]. A torsion bar is suspended from the test fibre by means of a stirrup, which is glued to the end of the fibre. This was found to produce an unnecessary load upon the fibre, which is of low diameter and very weak after heat treatment. It was found to be more convenient and productive to attach the fibre directly to the torsion bar by means of 'Durafix' glue, hence eliminating the weight of the stirrup.

FIGURE 2·22

THE DETERMINATION OF FIBRE TORSION MODULUS

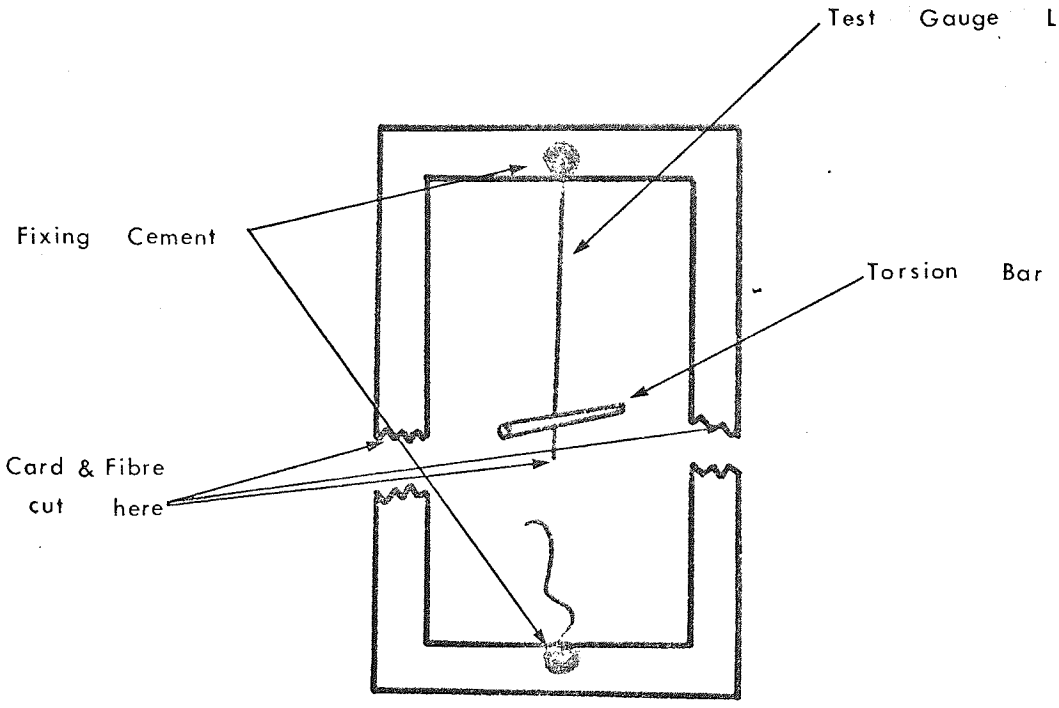

a = fibre cross-sectional area

L = fibre test gauge length

I = moment of inertia of the torsion bar

T = period of vibration of the pendulum

G = the torsion modulus

$$G = \frac{8\pi^3 I L}{T^2 a^2}$$

The fibre was first mounted upon a large frame card and the torsion bar attached with a spot of glue. When the glue had dried, the card could be clamped vertically and the card and fibre cut, so that it formed a torsion pendulum. This is shown in figure 2.22. The gauge length of the fibre was usually about $1\frac{3}{4}$", although weaker fibres were sometimes measured with shorter lengths. The period of the fibre was measured for five oscillations, with the fibre shielded from air disturbances. A mean of three measurements was taken for each determination. The torsion bar was 1 cm. long, 0.2 mm. in diameter and weighed 6.0×10^{-3} grams. Hence the tensile and torsional strains in the fibre were very small. The mean diameter of the fibre was measured after the completion of the test by remounting the fibre upon another card and using the microscope as with the extensometer samples. The formula for calculating the torsion modulus is shown in figure 2.22.

2.3 THE DETERMINATION OF CARBON FIBRE STRENGTH AND MODULUS.

The tensile testing of carbonised fibre has many features in common with the testing of the precursor. However, because carbon fibres are brittle, the accurate measurement of strain becomes an important consideration and the extensometer has to be designed accordingly. To differentiate it from the textile extensometer, the carbon fibre extensometer has been titled the carbon fibre modulus machine. A photograph taken from the front of the modulus machine is shown in figure 2.3. Many features of the machine will be recognised from the previous description of the textile extensometer. The same standard gauge length card as used for textile testing was used for mounting carbonised fibres. A card cut ready for testing is shown in position in the figure (F). Sealing wax was found by previous workers to give the best bond between the fibre and the card. Being a brittle material, it does not yield very much during the test.

FIGURE 2·3

THE SINGLE CARBON FIBRE MODULUS MACHINE

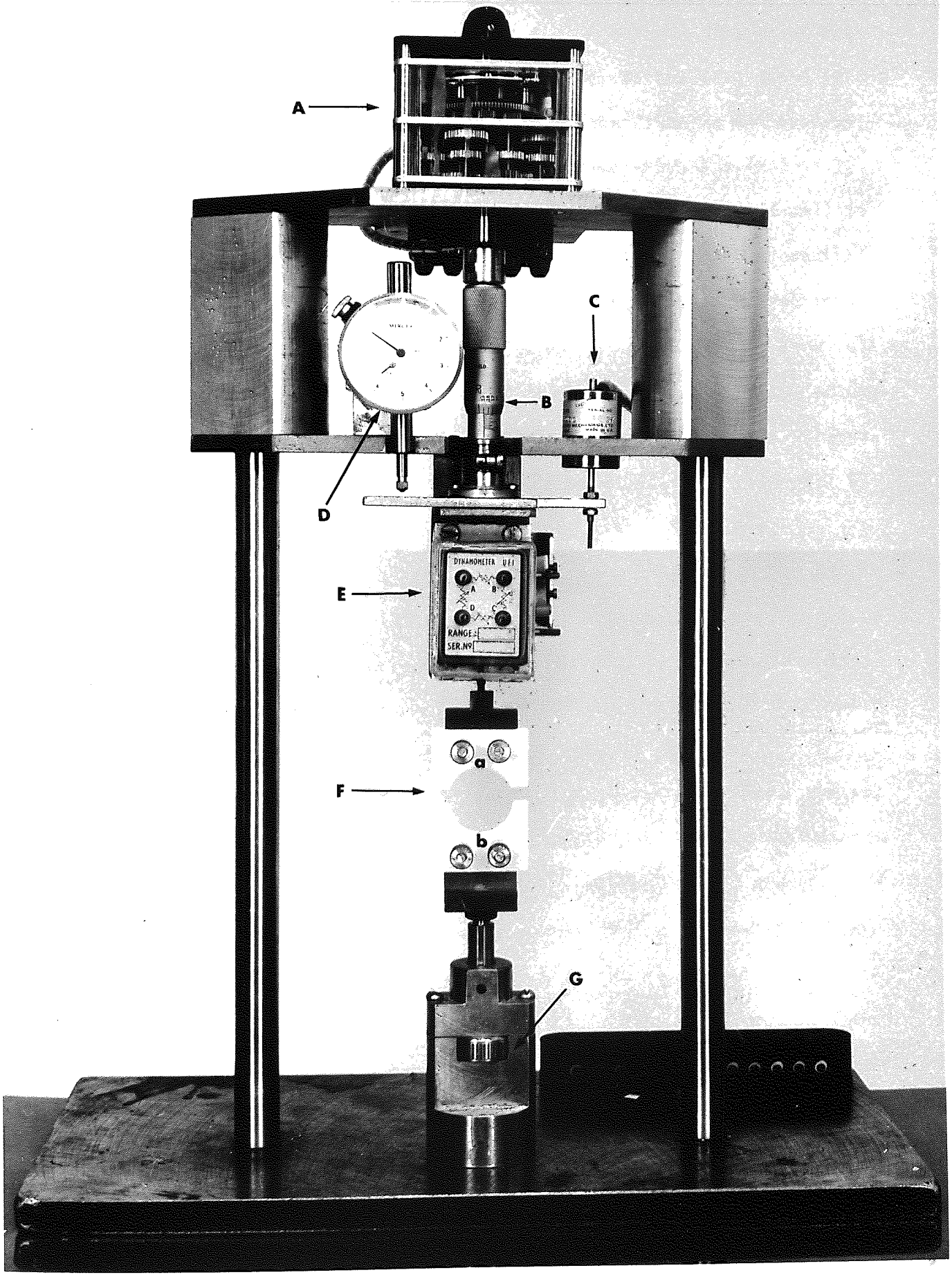

Durofix is too plastic and if this is used to secure the fibre the yielding of the glue causes an underestimation of the modulus.

The machine is driven by a synchronous motor and gear box (A) and is normally run at a strain rate of 0.1%/second. The properties are normally independent of the testing rate, so the test speed is not of any great importance. The extension of the fibre is achieved by the rotation of the micrometer screw, B, which draws the load cell, with the attached upper end of the fibre, upwards. The load cell is an Ether Ltd U.F.1. dynamometer which has a full scale load reading of 32 ozs. The maximum breaking load likely to be encountered with a carbon fibre is about $\frac{1}{2}$ oz. The reason for using a 32 oz load cell is that it minimises the deflection produced in the upper grip of the machine. On average carbon fibres reach a maximum extension of about 1%. This is very small, and a slight deflection of the load cell is likely to seriously reduce the measured modulus. The U.F.1. dynamometer has a maximum deflection of $\frac{1}{3}$ mm.; the use of the cell at very low loads, therefore, reduces the deflection to an acceptable error. The out-put voltage from the load cell is very low, however, and has to be amplified by a good quality d.c. amplifier. The load signal was applied to the y-terminals of an x-y recorder.

As with the textile extensometer, the extension of the fibre was measured with an LVDT, provided by Schaevitz Ltd (C). In this case a more sensitive model was used, having a range of 0 to 50 x 10^{-3}". This transducer is capable of measuring to 10^{-4}". The out-put from the LVDT was applied to the x-terminals of the x-y recorder. For accuracy it was necessary to calibrate the strain measurement before each test. This was done with the dial gauge (D), which can be seen in figure 2.3. The foot of the gauge was set to move with the transducer core and hence a simultaneous check could be made on the accuracy of the recorded displacement. The gauge records displacement to 10^{-4}". Coarse changes in the separation of the grips could be made

using the knurled screw (G) at the base of the machine. This was necessary when first straightening the fibre, after having cut the card. The gauge length of the fibre was measured using an accurately calibrated, vertical travelling telescope. The mean fibre diameters were measured by the same method as the precursor fibres.

2.4 THE HOT-STRETCHING EXTENSOMETER.

The problem of designing instruments for the hot stretching of carbon fibres is one of conveniently applying a relatively large load to the fibre without incurring a large frequency of breakages. If the stretch is obtained by suspending a weight from the fibre and allowing it to stretch with temperature, it is more difficult to obtain large extensions. With perseverance, however, fibres with high stretch ratios can be obtained, as reported by Johnson[52]. A better approach to the problem was found to be the use of a screw extensometer. This functions by using the fibre bundle in the form of a loop and applying the stretching load to it, through a push-rod driven by a lead screw. The advantage of using a screw to apply the load is that it does it smoothly and continuously. In order to control the load applied to the loop, the lead screw was driven through a torque controlled clutch, supplied by Kinetrol Ltd. A Citenco motor was used to turn the clutch and the torque applied to the lead screw was varied, either by a direct setting of the torque control, or by changing the speed of the motor. The advantage of this method is that a sensitive control of the stretching load can be achieved. The loop can be kept continuously stretching, with less risk of applying an excessive load.

Two extensometers were designed, each for a different graphite tube resistance furnace. The principle of both instruments was the same, but the dimensions differ because of the different sizes of the furnace tubes. A photograph of both extensometers can be seen in

FIGURE 2·4(a)

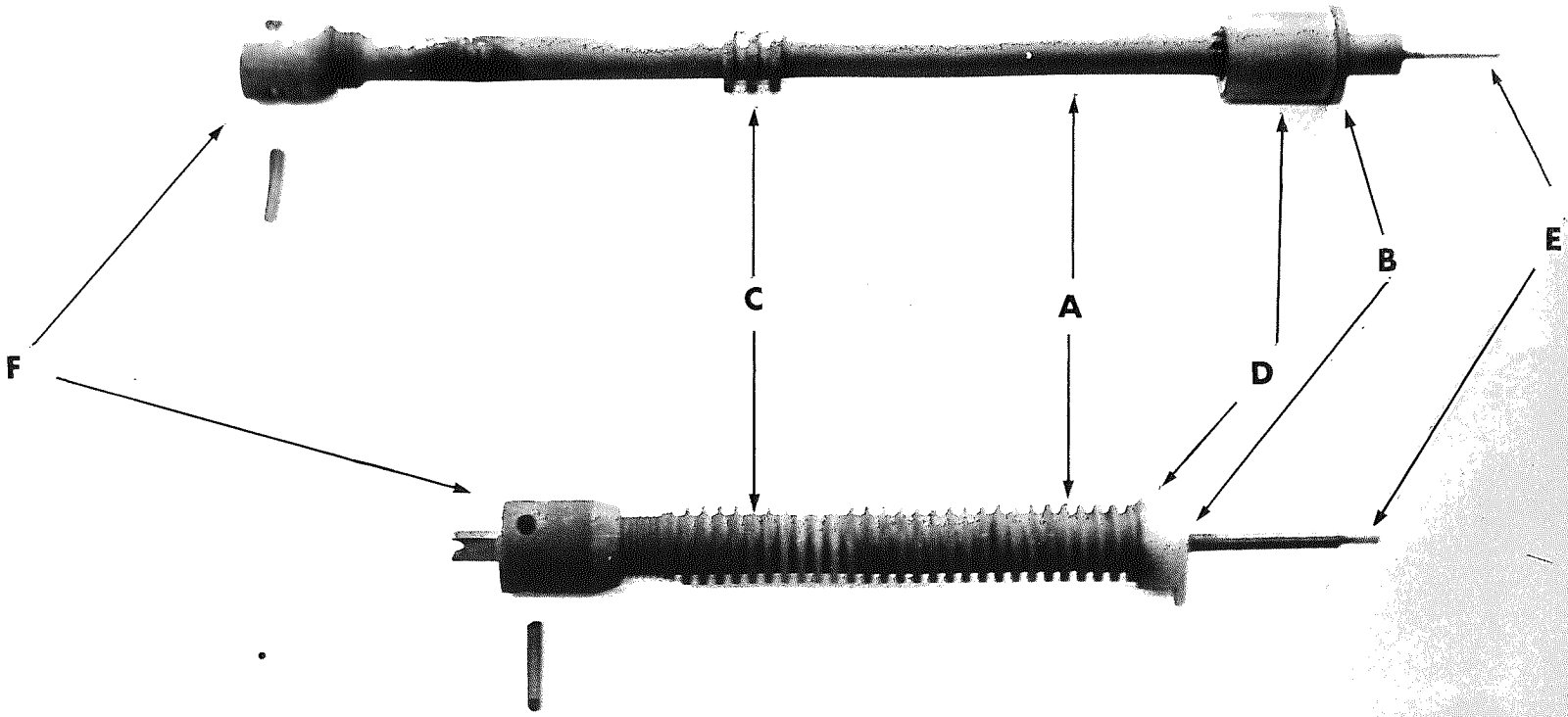

HOT-STRETCHING EXTENSOMETERS

figure 2.4(a). The main features of them have been lettered.

The main body of the extensometer, (A), is a graphite tube which contains the lead screw and push-rod. The lengths of the tubes have been calculated, so that the fibre loop will be in the middle of the furnace hot zone when the end flanges (B) are bolted into position. The flanges which are an integral part of the extensometer barrel (C) serve a dual purpose. A lot of the heat losses from the hot zone are by radiation, because of the very high temperatures, and the flanges help to reduce these losses simply by cutting off the radiation. The losses in the opposite direction of the furnace tube are cut-off by a set of heat shields, which are inserted ahead of the extensometer. The other advantage of the flanges is that they reduce the electrical contact between the extensometer and the inside of the furnace tube. The graphite resistance furnace functions by the application of low voltages (10 to 20 volts) from the secondary of a high power transformer, across a graphite tube which has a very low resistance (10^{-3} ohms). It is the very high currents that are drawn which provide the furnace power. If the extensometers were in greater contact with the furnace tube, they could act as shunt resistors which could create a short circuit. The presence of the flanges avoids this problem. The end bushes (D) were made from 'Tufnol' insulating composite, to provide thermal and electrical insulation to the external case of the furnace. The lead screw extension rods (E) pass through p.t.f.e. bushes to the outside of the furnace, where a drive sprocket is fitted. The extensometer is driven by a chain from the clutch and motor.

The holder in which the test loop is restrained is shown at (F) in figure 2.4(a). A drawing of the plan and elevation of this part of the extensometers (it is the same for both models) is shown in figure 2.4(b). Two rods are used to restrain the loop. These are

FIGURE 2·4(b)

THE HOT—STRETCHING OF CARBON FIBRE

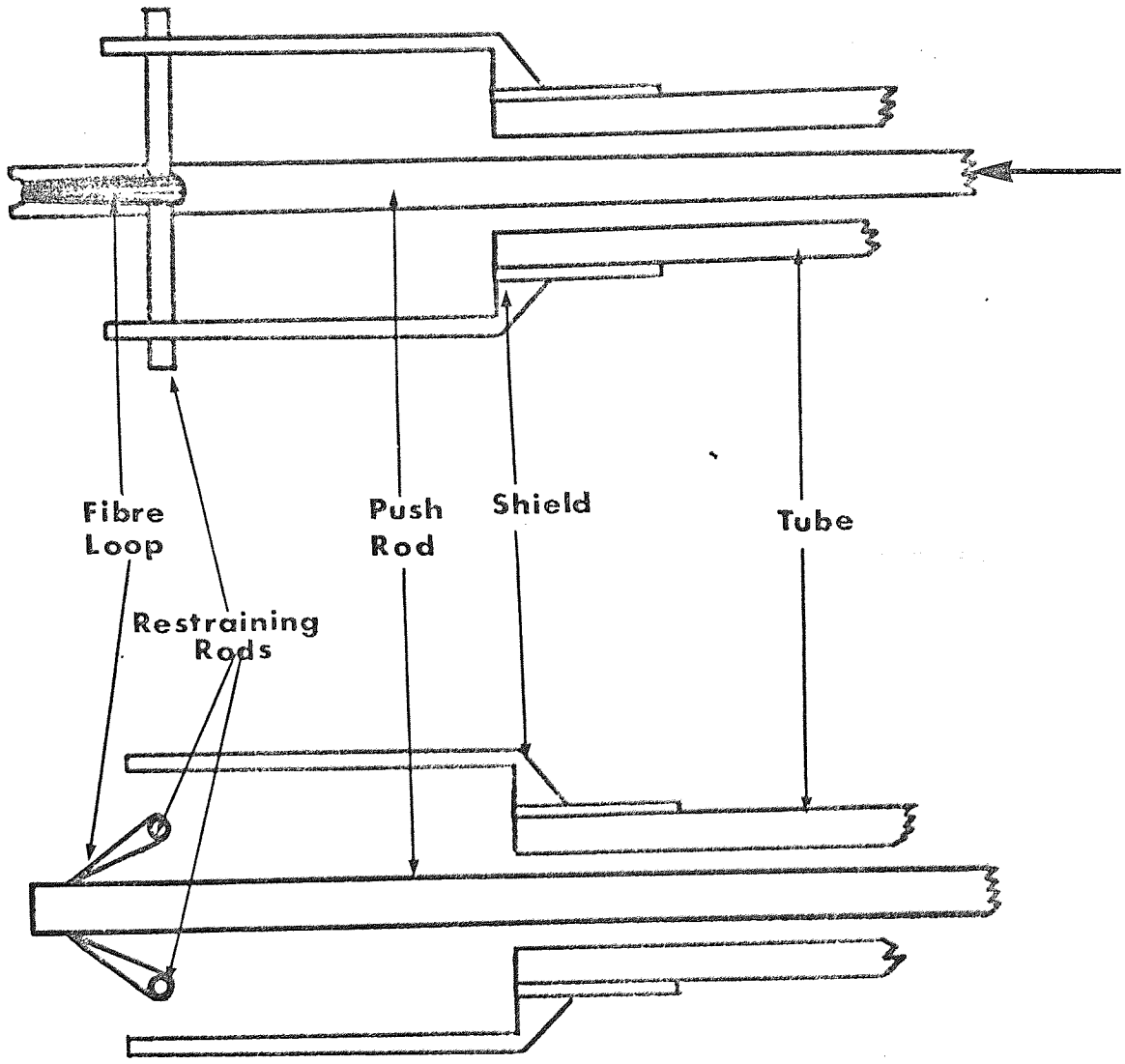

inserted through the shield after the loop has been formed and placed in position. The push-rod is pushed along by the rotation of the lead screw, to put the loop under load. It then forms a double loop in readiness for the hot stretching experiment. The loop was formed using a specially designed jig, which allowed a straight tow of fibres to be neatly clamped into a circle; 'Evostick' adhesive was then used to glue the ends together. At graphitising temperatures the 'Evostick' forms a very hard carbon, which does not itself stretch very much. It has proved a very useful substance for this purpose, as it withstood the stretching loads applied to the loop. To check for the accuracy of the stretch ratios, which were calculated from the number of turns made by the lead screw, the stretched fibre mean diameters were compared to their control values. This usually confirmed the results.

2.5 INFRA-RED SPECTROMETRY OF HEAT TREATED POLYACRYLONITRILE.

Most of the published work on the chemistry of the changes resulting from the heat treatment of polyacrylonitrile is concerned with the initial reactions responsible for colouration. Very few of the results are quantitative, and none of them extend so far as to describe the oxidised polymer at the stage where it would be considered satisfactory for carbonisation. In this work it was thought desirable to obtain quantitative measurements of the chemical changes following heat treatment, in order that the correlation between the physical and chemical changes might be investigated.

The KBr disc method was the best available, because it was necessary to keep the sample in a fibrous form during heat treatment. Thin films could not be prepared after heat treatment, as the sample was usually only partially soluble in any solvent. Spectroscopically pure KBr was used, which was kept completely free of moisture by storage in a dry vessel. The fibre samples were first thoroughly chopped with sharp scissors until they were very fine. They were then ground for long periods in a ball mill and subsequently dried

by being kept at 80°C for several hours in a vacuum oven. A concentration of 0.3% by weight of ground fibre sample to KBr was used for the preparation of each disc. The sample was carefully weighed each time using a Cahn microbalance, which weighed to 10^{-6} grams. The KBr mixture was then ground, sieved and dried. The KBr discs were prepared by pressing the sample mixture in a special die, which was evacuated during the application of pressure in a hydraulic press. Before recording the spectra, the disc was carefully checked to ensure that no moisture induced opacity of the surface had occurred and that it was otherwise unflawed.

The spectrophotometer used for the determinations was a Perkin Elmer Ltd 257 model. This is a double beam instrument. The slit width of the collimator was set at the normal value indicated by the instrument.

2.6 THERMAL ANALYSIS BY DIFFERENTIAL SCANNING CALORIMETRY

It has been shown that polyacrylonitrile exhibits a reaction exotherm during pyrolysis, which is probably attributable to the polymerisation of the nitrile groups[56]. The formation of a ladder polymer as a result could well be significant in the development of a thermally stable carbon fibre precursor. It is, therefore, valuable to quantify this exothermic reaction, in order that its importance to the formation of high strength carbon fibre might be assessed. Most of the published studies of the reaction have been made using differential thermal analysis (DTA). This method is not quantitative. Differential scanning calorimetry (DSC) is quantitative and for this reason it was adopted as the method of studying the effect of thermal pretreatment upon the reaction. Apart from the reaction exotherm, polyacrylonitrile undergoes thermo-physical changes which are of interest in understanding the behaviour of the fibre under different processing conditions.

Like DTA, DSC compares the sample with an inert reference. DTA measures the temperature difference between the sample and reference, as the average temperature of the calorimeter enclosure is raised. An endothermic change in the state of the sample results in the absorption of heat without a commensurate rise in temperature and so the sample temperature falls behind that of the reference. An exothermic change would have the opposite result. The DSC measures the amount of heat required to maintain the reference and sample at the same temperature. For an endothermic change, heat is supplied to the sample in order to keep it at the same temperature as the reference. For an exothermic change, the heat is supplied to the reference. Hence the magnitude of a thermodynamic transition can be determined with the DSC, while only the temperature effect of the change can be measured with DTA. The essential difference between the two methods is that the DSC is measuring the rate of change in specific heat with temperature. If the DTA was to be used quantitatively, then the change in specific heat of the sample with temperature would have to be determined separately.

The principles of the DSC method are illustrated in the block diagram shown in figure 2.6. The out-put of the instrument is a plot of the mean temperature of the calorimeter enclosure in ^{o}K, versus the rate of supply of heat to either the sample or reference pan, in calories/second. The latter reading remains constant until there is a transition in the state of the sample. The temperature of the calorimeter enclosure is measured independently of the sample and reference, by a resistance thermometer and the signal is amplified by the average temperature amplifier. The actual temperatures of the sample and reference are measured by resistance thermometers which are in extremely intimate contact with the cells. These cells are identical in every respect, so their specific heats will change in an identical manner. The differential temperature amplifier records

FIGURE 2·6

A.

Schematic circuit diagram for the DSC. 1B.

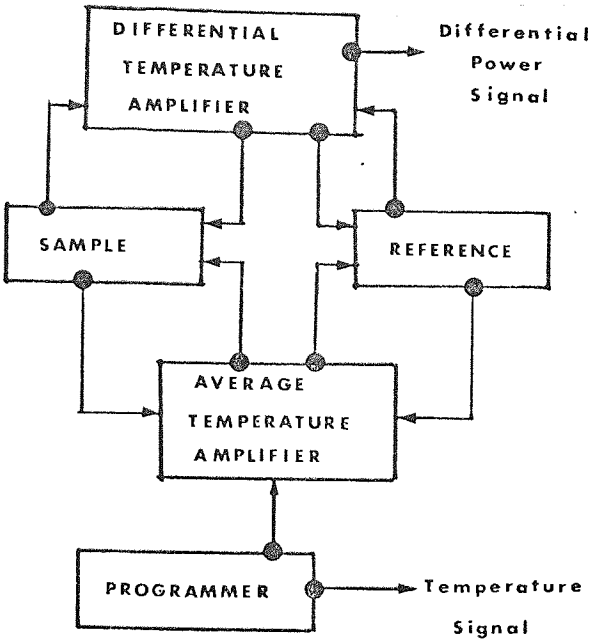

B.

Example of a DSC. scan

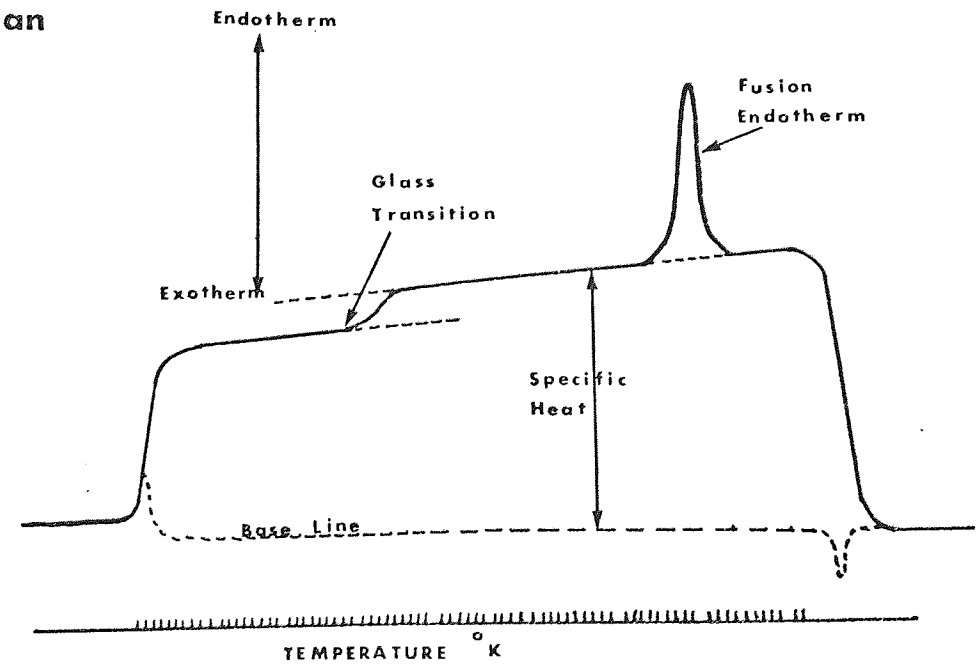

DIFFERENTIAL SCANNING CALORIMETRY

the difference in temperature between sample and reference, and the phase of the difference. It then supplies heat to the cooler cell until equilibrium is restored. The response of the amplifier and the size of the cells determines how rapidly this process is accomplished. The amount of power required to restore equilibrium is recorded with the average temperature.

The instrument used in these studies was a Perkin Elmer Ltd DSC 1B. At this time this was the most sensitive instrument available of the type. A detailed study of the DSC.1B [53] compares the performance of the instrument with the standard DTA method. The sample is encapsulated in thin walled aluminium pans which are supplied with the instrument. To ensure that the surface characteristics of the sample and reference are the same, an empty aluminium pan is used as the reference. To obtain as large a sample as possible, the fibres were chopped to a fine mat. Pans and lids were weighed using a microbalance and the samples were packed into the pans and the lids crimped onto them using a standard crimping press. The sample weight was determined by re-weighing. Before starting the experimental scan, the sample was kept in the instrument at 100°C for 30 minutes, to remove all moisture. The signal baseline settled at a fixed value once the sample had equilibriated. The scanning programme was started at 100°C, unless the glass transitions were to be studied, in which case it was first cooled to 30°C. Most of the measurements were carried out at a programme rate of 16°C/minute, unless the melting behaviour was being studied, in which case 64°C/minute was used. The out-put from the DSC was recorded on a specially modified strip chart potentiometer. The power signal was continuously recorded by the potentiometer pen, while the temperature was marked along the edge of the strip chart by a relay operated pen. This registered a mark upon the chart for every 1°C rise in temperature,

but left a gap every tenth degree for the convenience of recording the temperature.

A typical DSC scan is shown in figure 2.6. This is for a polymer which passes through a glass transition and eventually melts. The differential power signal changes as soon as the temperature programme is started. The resultant deflection is directly proportional to the specific heat of the sample. As the temperature is raised the deflection increases, as the specific heat of the sample increases. Other effects also influence the position of the signal base line with increasing temperature. The most important is due to the differences in emissivity between the sample and reference pans. A glass transition in the sample is seen as a discontinuity in the signal base line. The convention is to take the glass transition temperature as the temperature of the start of the discontinuity. This has been followed in this work. Thermal transitions which involve the absorption or evolution of heat produce a signal peak. In the case of the polymer studied in figure 2.6, the melting of the polymer has produced an endothermic peak. The determination of the area under this peak produces a value for the heat of fusion of the polymer. In the case of polyacrylonitrile, an exothermic peak is obtained which is similar in shape to a fusion peak, but as heat is supplied to the reference cell, it is formed by a contrary deflection in the power signal. The amount of exothermic heat evolved was determined by measuring the area under the peak with a rotating planimeter. Knowing the rate of feed of the strip chart, the full scale value of the power signal, the rate of heating and the mass of the sample; the amount of heat evolved per gram of sample was easily calculated.

To obtain accuracy with the DSC method, it is important to carefully calibrate the instrument. The calibration of the power

amplifier was checked regularly by the determination of the heat of fusion and crystallisation of a highly pure sample of indium. The result usually agreed very well to ± 1%. The temperature calibration had to be set regularly, though it did not depart from previous calibrations by more than ± 2°K. The temperature calibration was set by comparison with the melting points of pure indium, tin and lead. The average temperature amplifier was re-set until the temperatures recorded agreed exactly with all these melting points.

2.7 THE ELEMENTAL ANALYSIS OF PYROLYSED AND OXIDISED POLYACRYLONITRILE.

The analysis of the elemental composition of a large range of samples was carried out for the author by F. C. Johnson of Rolls-Royce Ltd as a routine service. The instrument used for this purpose was an F & M Automatic C, H & N Analyser, manufactured by the Hewlet Packard Company. This instrument is a gas chromatograph, which analyses the gaseous oxides produced by the total combustion of the specimen. The sample to be analysed was first accurately weighed and placed in a standard combustion cup. It was then covered with an excess quantity of manganese dioxide and catalysts (transition metal oxides). The instrument operated with a flow of helium gas at a pressure of four atmospheres. The sample cup was first placed in the cold zone of the instrument combustion tube, while sufficient time was allowed for the air to be purged from the system. The chromatograph was then allowed to come to equilibrium before combustion of the sample was commenced. Once the chromatograph had established a satisfactory base line, the sample was pushed into the hot zone, using a push rod which slides through a pressure seal. As soon as the sample reached the hot zone, the helium flow was diverted and the oxidation took place under static conditions; the evolved gases being retained in the combustion chamber. The hot zone was used at 1,100°C for all determinations.

The combustion process took about 70 seconds, after which the helium flow was resumed and the sample gases swept further into the system.

The carbon monoxide in the sample stream was completely converted to carbon dioxide by passing through copper oxide. The oxides of nitrogen were reduced to form pure nitrogen gas by passing over bright copper at 450 to 500°C. The sample entering the chromatograph column consisted of carbon dioxide, nitrogen, water and the helium carrier gas. The chromatograph column separated the gases and they were detected by a katherometer. The detector out-put signal was integrated electronically, to give the relative quantities of each gas. The instrument was calibrated prior to each determination, by a compound containing a similar carbon content to the experimental samples. Acetanilide was used in most cases, as this has the same approximate carbon content as the precursor polymer.

This method provided accurate values for the proportions of carbon, nitrogen, and hydrogen in the sample. The oxygen content was taken as the residual weight fraction; ignoring the trace quantities of other elements, which are possibly present in the precursor.

2.8 THE SCANNING ELECTRON MICROSCOPY OF HEAT TREATED FIBRES.

It is very useful to have a purely visual observation of fibres after heat treatment, in order to assess their condition. If melting has occurred, this is immediately apparent from direct observation in the microscope. The scanning electron microscope also reveals the fine structure of the fibre, if this is within its resolving power. The scanning electron microscope (SEM) used in these studies was a Stereoscan Mk 1. instrument, produced by Cambridge Instruments Ltd. It had an ultimate resolution of 150 A° and a maximum accelerating voltage of 20 kV.

Most of the studies made with the instrument were of fibre fracture surfaces. A specially designed tensile machine was used for

obtaining the fractured specimens. It was horizontal, which allowed the fibre, mounted on a card in the usual way, to be fractured while immersed in a liquid. A mixture of glycerol and water was found most suitable for this purpose. In this way the fractured ends were retained in the liquid and could be easily retrieved for mounting. After retrieval, the fractured pieces were washed in acetone and mounted on the ends of standard size steel pins, as parallel to the pin axis as possible, using Durafix cement. The normal type of SEM specimen stub was used for mounting the steel pins, which had holes drilled centrally for this purpose. After mounting, the fibre was given a thin coating of gold in a vacuum coating unit. This provided a conducting film, which prevented the charging of the fibre by the SEM primary beam, and also increased the yield of secondary electrons, necessary for a good specimen image.

The two major advantages of the scanning electron microscope, as compared to the optical microscope, are the higher magnifications possible and the very much greater depth of focus. These are major advantages with the study of carbon fibres, because they are usually very thin and have features which require a large depth of focus, such as the lamella structures considered later in the thesis. A detailed account of the operation of the scanning electron microscope and its application to physical investigations can be found in a book by Thornton [54].

CHAPTER 3.

THE PYROLYSIS AND OXIDATION OF POLYACRYLONITRILE; A REVIEW OF CURRENT KNOWLEDGE.

Polyacrylonitrile is a linear organic polymer which can be very simply represented by the following molecular formula.

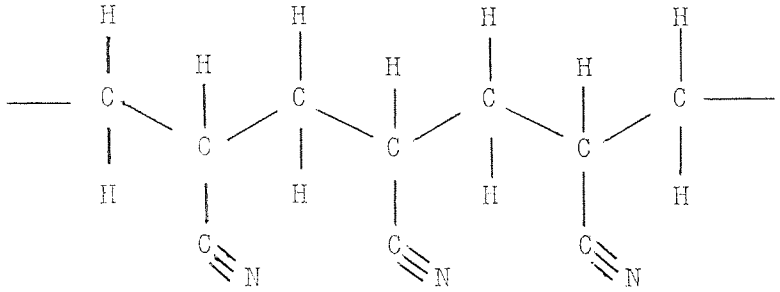

It does not necessarily have an isotactic conformation as represented by the formula and generally it is believed that it has a very irregular structure. The distorted configuration adopted by the polyacrylonitrile molecule in either the solid state or in solution makes a detailed structure analysis very difficult.

Compared to inorganic solids linear polymers are thermally unstable: if crystalline they have low melting points, - if not, they soften very considerably at relatively low temperatures. The reason for this behaviour is apparent from the long-chain structure of the molecule. Although within the molecule the atoms are covalently bonded as a rule, the molecules themselves are often only bound by van der Waal's forces, as in polyethylene for example. Polymer molecules are in some cases heterogeneously bonded, with additional attractive forces, such as hydrogen bonding found in the polyamides and polar bonding, found in polyvinylchloride, adding to the cohesive energy of the polymer. It is these relatively weak interchain forces which limit the physical stability at high temperatures, unless deliberate reinforcement or cross-linking of the polymer is used.

The low thermophysical stability of most linear polymers suggests

that they might be chemically unstable at high temperatures also. In fact, they are often found to be much more unstable than the simple chain model itself implies.[55] Degradation processes are observed before appreciable softening or melting of the polymer occurs, and early discolouration is often an indication of this. It is virtually impossible to synthesise polymers having the ideal chemical structure described by a simple linking together of the monomer or condensation product. A small probability of the building-in of chemical defects is always present. These defects are sometimes of a type which can initiate degradation processes, causing them to proceed more rapidly and at lower temperatures. The defects may take the form of the groups which terminate the chain molecule, or they may be branches in the chain. Sometimes degradation is initiated by copolymerised impurities, very small quantities often having a very considerable effect.

The presence of oxygen has an additionally deleterious effect on the stability of linear polymers (although it can have a favourable effect on the stability of any resultant char). Heat treatment in the presence of oxygen induces degradation at lower temperatures and accelerates the rate of chain scission.

3.1 THE FORMATION OF A CHROMOPHORE IN POLYACRYLONITRILE.

The pyrolysis of polyacrylonitrile is accompanied by a deterioration in mechanical properties, in common with the behaviour of other linear polymers.[56] This is probably due, in part, to the chain degradation of the polymer. Concurrently an increasing colouration of the polymer is observed. This is shown in figure 3.1(a) for a polyacrylonitrile copolymer fibre - Courtelle, which has a polyacrylonitrile content of 91%. The fibre has been heated at a rate of $\frac{15}{12}$ °C/minute, while under restraint in a dynamic atmosphere of pure argon. The maximum temperature achieved by each sample was as follows.

Figure 3.1

The development of colour in Courtelle fibre.

(a) Heated in Argon

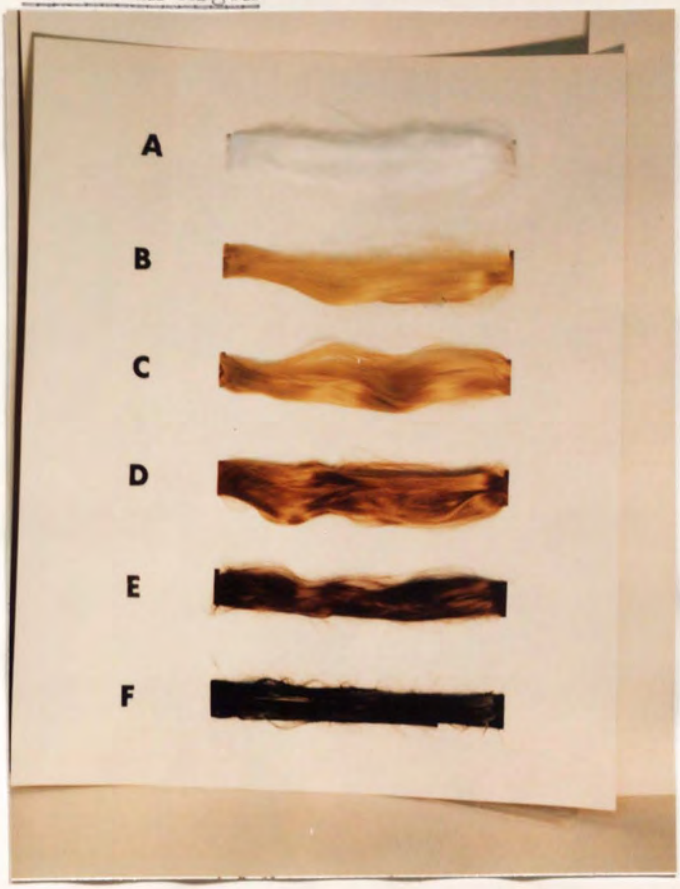

(b) Heated in Air

A = 20°C, B = 172°C, C = 200°C, D = 230°C, E = 262°C, F = 315°C.

With increasing degrees of heat treatment the fibre changes from white to bright yellow, to orange and finally to dark brown. For heat treatments above 400°C the fibre is completely black. Pure polyacrylonitriles undergo the same colour changes, except that the rate and temperature dependence is different.

The development of a chromophore is not unique to polyacrylonitrile. The thermal dehydrochlorination reaction in polyvinylchloride leads to the development of colour, which is due to the formation of sequences of unsaturation in the polymer chain.[57] An analogous process in polyacrylonitrile might be the dehydrocyanation reaction, but this does not occur until the major part of the colouration process is complete. Houtz [58] proposed that the chromophore was due to the formation of a cyclised structure. This, he suggests, is a consequence of the polymerisation of the nitrile groups and the partial dehydrogenation of the chain.

This structure is shown below:-

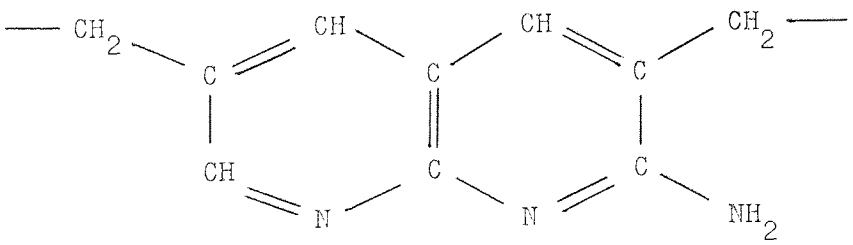

The degree of colouration with heat treatment is much greater under oxidising conditions, although the initial appearance of colour occurs at a higher temperature. This is shown by comparing figure 3.1(b) with 3.1(a). The samples in figure 3.1(b) have received similar heat treatments to their correspondingly lettered samples in 3.1(a), except that the treatment was carried out under a constant air flow. Sample B of the oxidised series is lighter than its pyrolysed comparitor. However, after further heat treatment, the oxidised

samples are darker than the equivalent pyrolysed fibres and remain so until complete blackening of the fibre occurs.

The chromophore following pyrolysis has been attributed by Grassie and co-workers [59], [60], [61] to the nitrile polymerisation reaction alone, which produces a hydrogenated naphthiridine structure:-

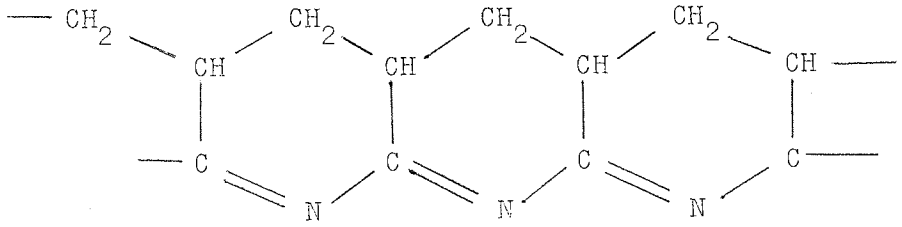

Other authors have attributed the chromophore to the formation of a polyene structure [62], [63], [64], [65] :-

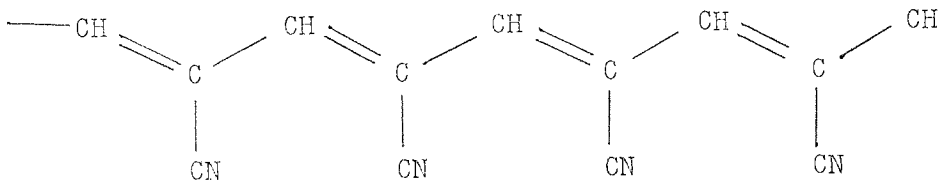

These latter workers conducted all their heat treatments in circulating air, though only one paper [62] attributes the structure to the effects of oxidation.

Schurz et al [66], [67] have suggested the formation of azomethine cross-links:-

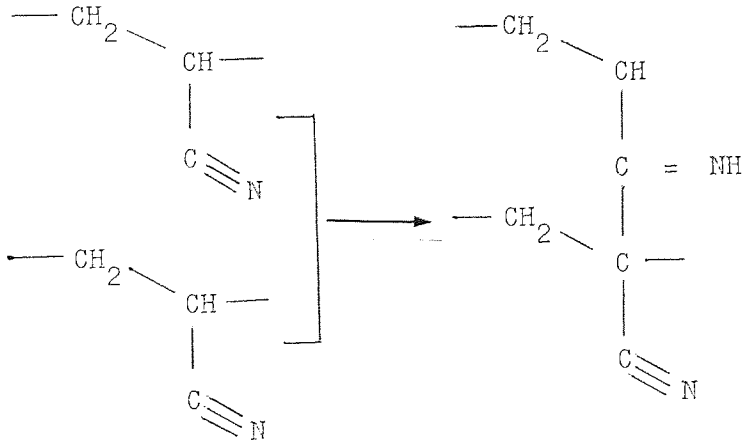

Various studies of model compounds have shown that this last reaction

is unlikely to be the origin of the chromophone.[68, 69]

Grassie proposes that the initiation of the nitrile polymerisation reaction might be either through copolymerised acid impurities (reaction A, below) or self initiation via the formation of an initiation ring (reaction B, below).

A - Acid Initiation

1. Initiation.

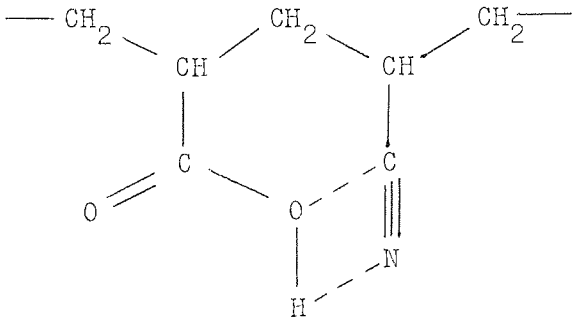

2. Propagation.

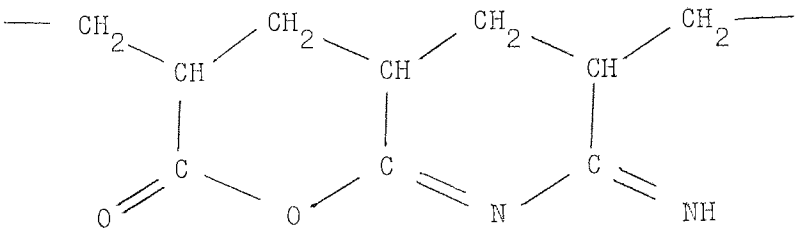

B - Self Initiation

1. Initiation.

(i)

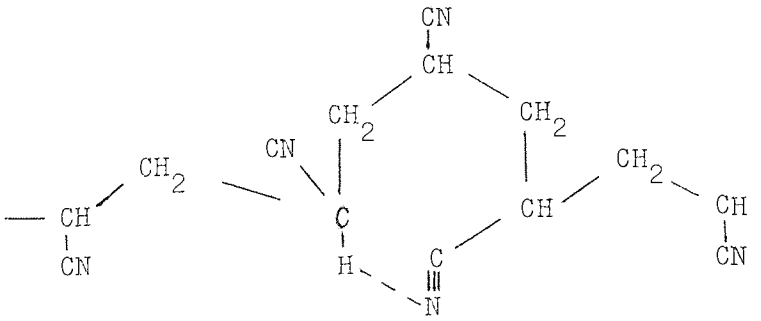

(ii)

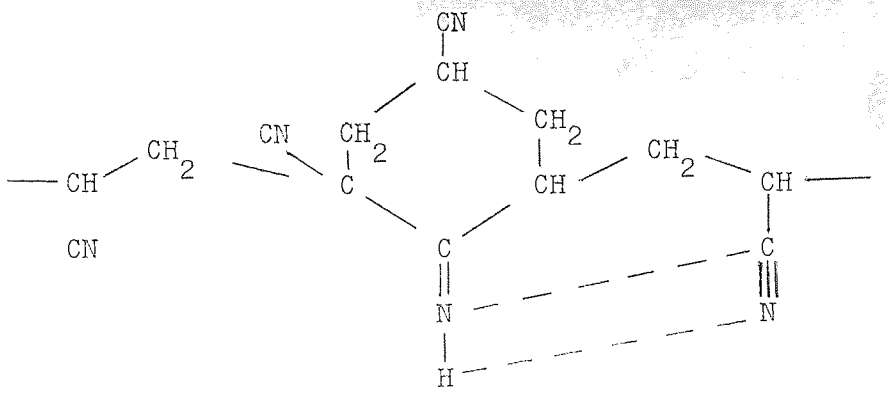

2. Propagation.

(i)

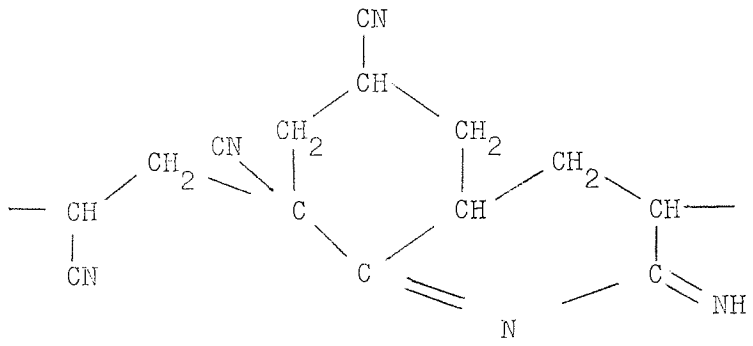

(ii)

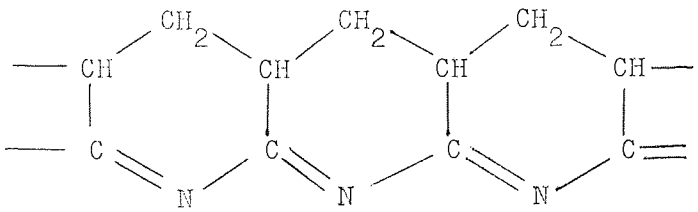

The self initiation reaction was proposed as an explanation of the ability of polyacrylonitrile to form a chromophore, even when it is completely pure. (Polymethacrylonitrile does not have this ability.) Peebles et al [70], [71] suggest that the pure polymer can contain a defect in addition to the acid impurity. This defect, the β-ketonitrile, has the ability to initiate the nitrile polymerisation reaction. These workers have shown that part of the free radical polymerisation of polyacrylonitrile can take place by addition to the nitrile group. This forms an enamine group which in slightly acidic aqueous conditions can hydrolise to form the β-ketonitrile group:-

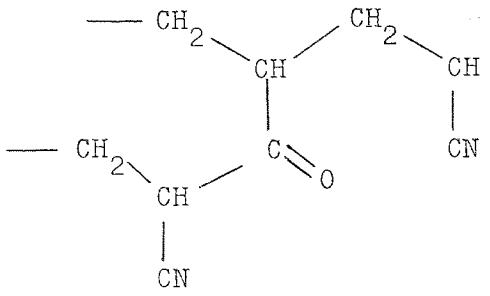

The initiation reaction is shown in section 3.5.

3.2 THE APPEARANCE OF INSOLUBILITY WITH HEAT TREATMENT.

The early appearance of insolubility with heat treatment in the normal solvents for polyacrylonitrile has led to the suggestion of cross-linking reactions, such as that of Schurz [66] mentioned above, and the propagation cross-link proposed by Grassie, [61] below:-

1.

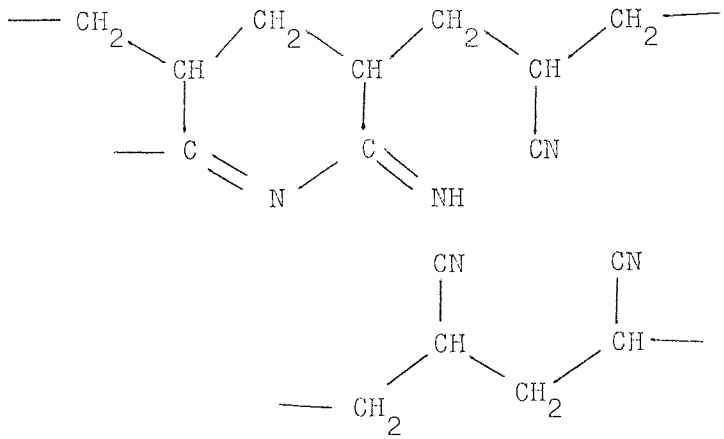

2.

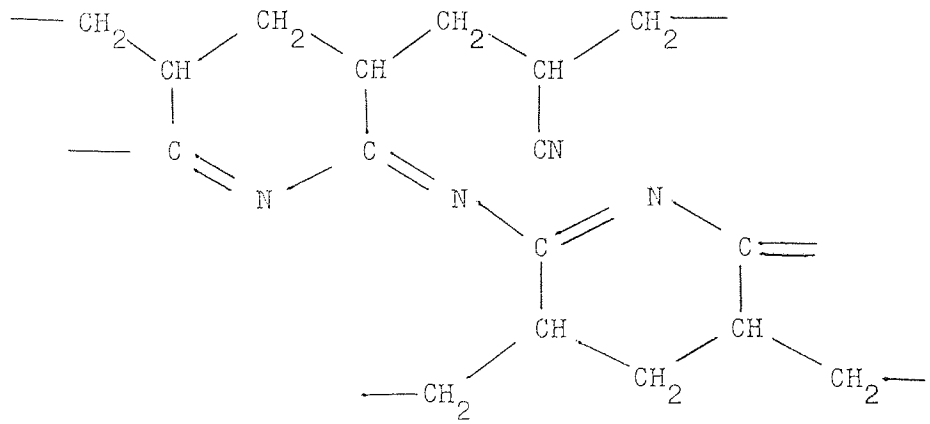

The propagation cross-link is formed when the nitrile polymerisation propagates between neighbouring chains.

If insolubilisation is due to a cross-linking reaction involving the nitrile group, then it will be the type of secondary bond which will determine whether the reaction proceeds according to the mechanism of Schurz, or that of Grassie. Some authors have suggested that polyacrylonitrile is hydrogen bonded,[72] with the α-hydrogens associated with neighbouring nitrile groups. As insolubilisation occurs below any observed melting temperature for the polymer,[61] the Schurz azomethine cross-link could form via such a hydrogen bond. Current evidence, however, favours the view that the secondary bonding in polyacrylonitrile is due to dipolar exchange forces, acting between neighbouring nitriles[73]. If this is the case, the propagation of the nitrile polymerisation reaction between chains is quite feasible and propagation cross-links would be formed.

It is quite possible, however, that insolubility at some stages of the heat treatment is due to the developing incompatibility of the molecule to the usual solvents. It has been reported that polyacrylonitrile exhibits increasing solubility in formic acid, as it develops insolubility in dimethylsulphoxide [74].

3.3 THE REACTION EXOTHERM UNDER INERT CONDITIONS.

The colouration reaction in polyacrylonitrile is accompanied by the evolution of heat, which has been described as an explosive reaction.[75] Thompson [76] has demonstrated that the temperature dependence and form of the exotherm, as measured by differential thermal analysis, can be strongly molecular weight dependent. He finds as a result that the exotherm peak temperature bears a constant relationship to the glass transition temperature.

Hay [77] has attributed the exotherm to the ammonia forming reaction which takes place within the same temperature interval and has the same

activation energy. The exotherm activation energy was calculated from the isothermal induction period. Hay postulated two reactions which could lead to the formation of ammonia; the aromatisation of the cyclised molecule (1. below) or the termination of two oppositely propagating imine sequences (2. below).

1.

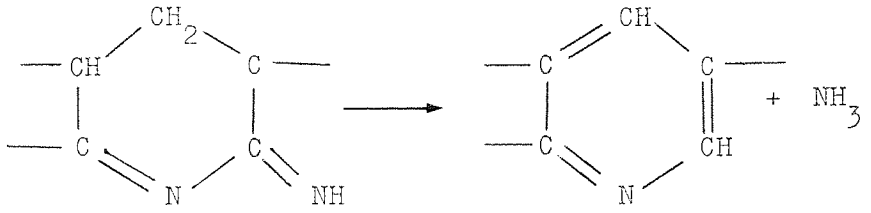

2.

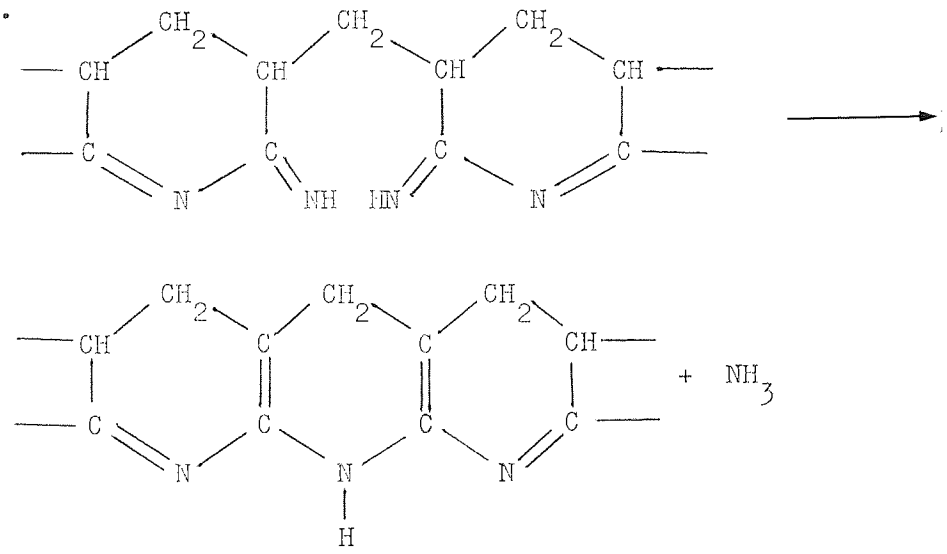

The sharp autocatalytic character of the exotherm is more characteristic of a chain reaction, such as the polymerisation of the nitriles, than of the random elimination of ammonia. Furthermore, Turner and Johnson [56] show that the evolution of ammonia in Courtelle fibre commences after the beginning of the reaction exotherm and the decay in the number of nitrile groups coincides exactly with the decay in the peak height of the exotherm.

3.4 THE THERMAL DEGRADATION OF POLYACRYLONITRILE.

In addition to the colouration and insolubilisation of the polymer with heat treatment, there exists the possibility that the polymer undergoes chain scission degradation reactions. The insolubility of the pyrolysed or oxidised material in suitable solvents makes the accurate determination of molecular weights impossible. There is, however, some published evidence for this opinion, though none of it is really conclusive.

The mechanical property changes accompanying pyrolysis indicate that chain scission occurs [56] (these are the author's own results). Kennedy and Fontana [75] found that following the exothermic reaction the polymer was soluble in formic acid and the intrinsic viscosity was very low for the solution. This suggested that the residue had a very low molecular weight. Beevers [81] has described how a crystalline solid can be produced by the extended heating of polyacrylonitrile at 540°C. The crystal structure was characteristic of the presence of several low molecular weight compounds. Chain scission is also supported by several observations of the evolution of low molecular weight tars during pyrolysis [78, 79, 80]. The proportion of tars can be very large if the heat treatment is in vacuo.

Chain scission reactions are likely to be in those parts of the chain where polymerisation of the nitriles hasn't occurred. It is well established that not all the nitrile groups participate in the formation of the chromophore. Some nitrogen is lost as ammonia and hydrogen cyanide. The fragmentation of the partial ladder molecule could take place when these gases are evolved and the tars might result from the volatilisation of the naphthiridine itself.

The high thermal stability of pyrolysed polyacrylonitrile is often attributed to the colouration reaction and its association with the formation of a ladder polymer.[82] A weight yield of 45% is quite

typical for polyacrylonitrile heated to 1,000°C in inert conditions, which compared to other vinyl polymers is very high indeed. The degraded products of pyrolysis must therefore undergo rearrangement and condensation sufficiently early in the carbonisation to avoid complete volatilisation. The author has observed, however, that the polymer undergoes some disorganisation before this occurs.

3.5 THE OXIDATION OF POLYACRYLONITRILE.

The oxidation of polymers is generally due to the formation and breakdown of hydroperoxides. The manner of the initiation and propagation of these reactions in different polymers will depend upon their molecular structure and for detailed accounts of this the reader should consult a book by Scott.[84] A generalised scheme for the oxidation of hydrocarbons is shown below:-

(1) Initiation:- Reaction to produce a radical R•

(2) Propagation:- $R\bullet + O_2 \rightarrow ROO\bullet$

$ROO\bullet + RH \rightarrow ROOH + R\bullet$

(3) Branching chain reactions:-

$ROOH \rightarrow RO\bullet + \bullet OH$

$2ROOH \rightarrow RO\bullet + H_2O + ROO\bullet$

$ROOH + RH \rightarrow RO\bullet + H_2O + R\bullet$

(4) Termination:-

$ROO\bullet + ROO\bullet \rightarrow$ Inactive products

where R is a hydrocarbon chain.

A great variety of oxygen containing groups can be detected in polymers following thermal oxidation. Groups such as carbonyl, hydroxyl, carboxylic acid and epoxides are quite common. In polyvinylchloride [57] polyvinyl alcohol [44] and polyacrylonitrile [65], olefin bonds are found, sometimes in long sequences. The rate of formation of these groups is dependent upon the rate of formation of the relevant hydroperoxide. In addition to the oxygenated products,

the decomposition of hydroperoxides usually produces a great deal of chain scission and there is a small probability of cross-linking through radical-radical interactions.

Vosborough [85] first described the oxidation of polyacrylonitrile fibre (Orlon) to produce a thermally stable, fireproof product. He attributed these properties to the formation of a ladder polymer having the structure originally proposed by Houtz [58]. He did not, however, provide an account of the chemistry of the process.

The nitrile group will have a very important influence on the mechanism of oxidative attack on polyacrylonitrile. Many authors propose that the initiation reaction is by attack at the α-position in the chain [62], [74], [86], [87], as follows.

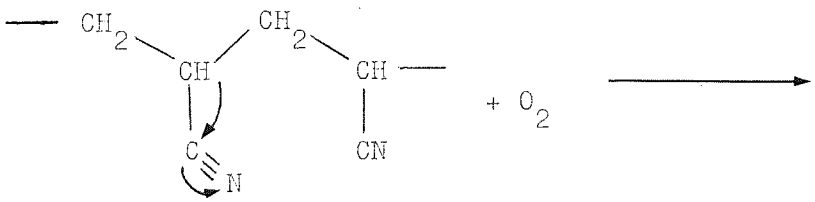

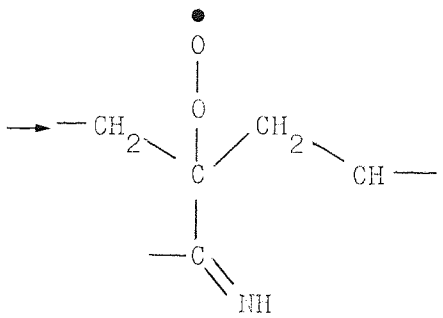

This scheme [87] also proposes that the α-hydrogen is responsible for forming an initiating imino group for the nitrile polymerisation reaction. The reason given for attack at the α-position is that the nitrile group is electron attracting which renders the α-carbon proton releasing. This argument is made by analogy with the behaviour of tertiary hydrogens in hydrocarbon polymers, but this cannot strictly apply in a nitrile polymer. As discussed by Scott [84] (pp.76) the

alkyl peroxy radical is electrophilic, which renders the β position i.e. the methylene hydrogens, most susceptible to attack in initiating and propagating reactions. Peebles et al [69] take this same viewpoint, and demonstrate quite convincingly that this is indeed the case. They found that three times the amount of oxidation takes place through attack on the methylene bridge than at the α-carbon. Other authors have since supported this interpretation [88], [92], [93].

The complete reaction scheme proposed by Peebles et al is shown below.

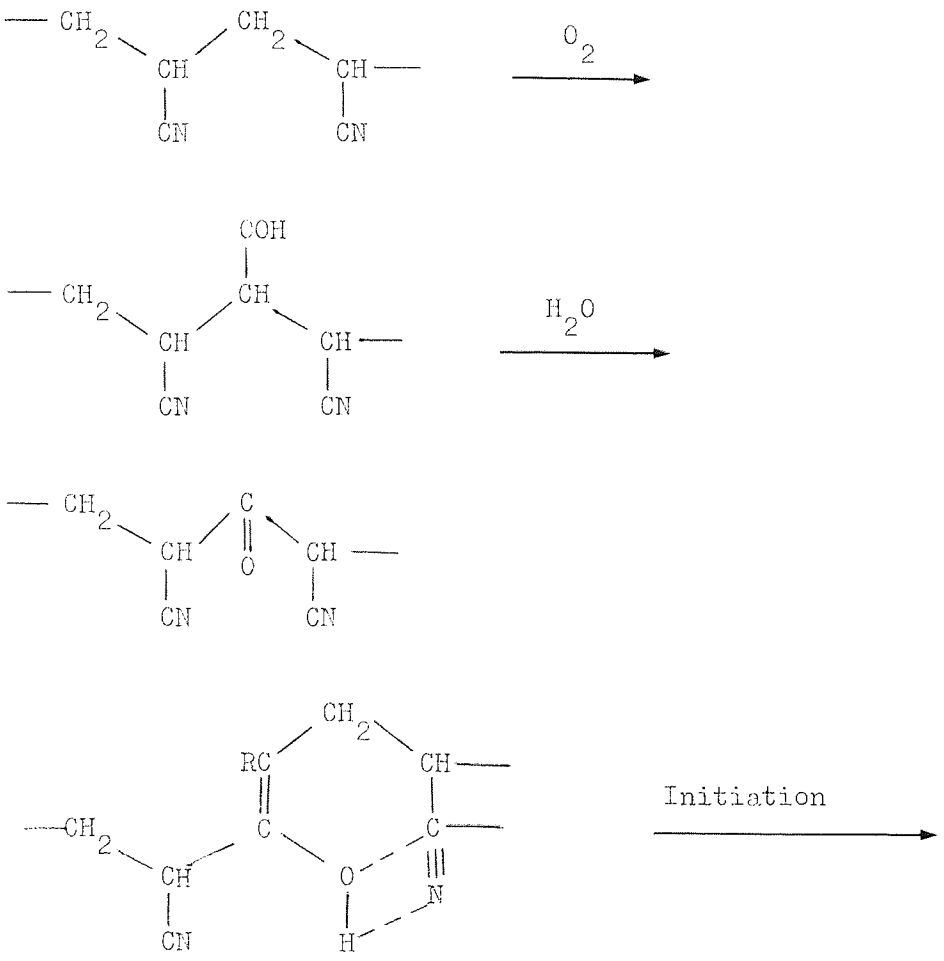

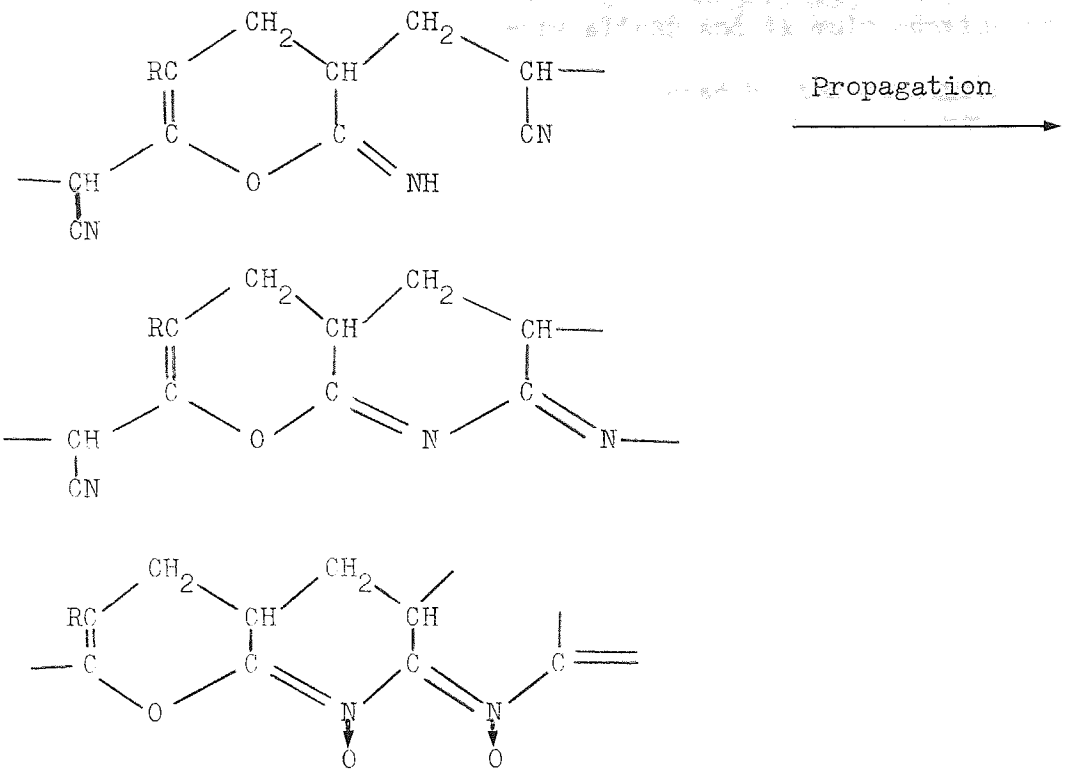

The oxygen attacks at the methylene bridge, to produce a hydroperoxide. This breaks down to yield water and a β-ketonitrile. These authors have demonstrated that β-ketonitriles can be formed during the free radical polymerisation of acrylonitrile also, and that they can initiate the polymerisation of the nitriles. The nitrile polymerisation scheme, above, can be due to initiation through either β-ketonitrile defect and the symbol R in the scheme represents polymer chain or a single nitrile group.

The formation of a polyimine, rather than a polyene had been demonstrated in a previous publication by Peebles [89], for similar heating conditions. Following this, nitrone formation is postulated by the addition of oxygen to the polyimine. This would increase the strength of the chromophore and is offered as the reason for the deeper colouration of oxidised material. It also explains the absorption of oxygen without any loss of hydrogen. However, the

evidence for nitrone formation is very slight and is only convincingly exhibited by one fraction of the products formed by the oxidation of isobutyronitrile. If present in polyacrylonitrile, it may represent only a small fraction of the oxidised product. As Brandup [91] himself points out, as little as 1% of the nitrone completely blackens the product.

The additional chromophore might be due to the formation of polyene in addition to the polyimine structure. The disagreement between Peebles [89] and Grassie [61] (the naphthiridine structure) and Fester [64, 65] and Berlin [63] (the polyene structure) over the source of the chromophore is probably mistaken. Both structures are quite possible and it will be demonstrated experimentally that heat treatment in oxygen can delay the polymerisation of the nitriles, while producing colouration through dehydrogenation of the chain. Both schools of thought can legitimately claim to have observed the structures they describe, due to their different methods of sample preparation. A further possible explanation of the increased colouration is simply that a greater degree of nitrile polymerisation takes place under oxidising conditions [92, 93], though this will be shown later to be rather doubtful.

An alternative structure for oxidised polyacrylonitrile, to that of Peebles et al, is that of Standage and Matkowsky [94]. They propose that polyacrylonitrile fibre oxidised to an arbitrary extent has a structure intermediate to (1) and (2) below.

(1)

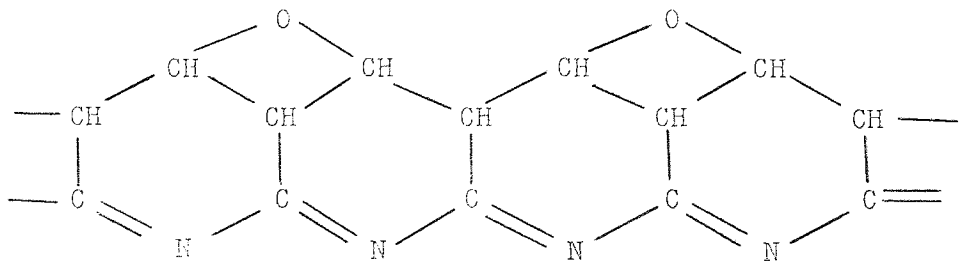

(2) 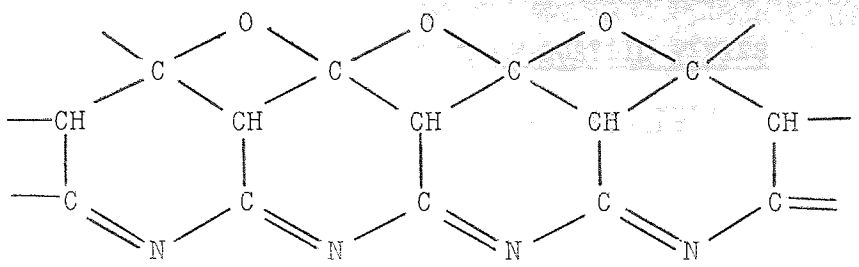

None of the studies reviewed above describes mechanisms which can fully explain all the phenomena associated with the carbonisation of polyacrylonitrile. The research to be described in following chapters is an attempt to isolate those mechanisms which are important. The work is basically physical in nature, so it will not be possible to offer a chemical phenomenology of the process of carbon fibre preparation from polyacrylonitrile. However, a description of the structural changes accompanying heat treatment has been attempted, and it is hoped that an increase in the understanding of the preparation of carbon fibre with good properties has been achieved.

CHAPTER 4.

THE PYROLYSIS AND OXIDATION OF ACRYLIC FIBRES STUDIED BY VISCOMETRY AND THERMAL ANALYSIS.

4.1 THE EXPERIMENTAL MATERIALS.

Most of the acrylic based carbon fibre available at present is prepared from Courtelle. This is because it is a good precursor for carbon fibre, as it is easy to process and produces excellent mechanical properties. Much of the research reported in this thesis is directed towards understanding why this particular acrylic is exceptional, in addition to understanding why polyacrylonitrile generally produces oriented carbon fibre of high strength and modulus.

Courtelle is produced by Courtaulds Ltd of Coventry, U.K.. It is a copolymer, consisting of approximately 91% polyacrylonitrile, 8% methylacrylate and a small fraction of itaconic acid.

Two pure polyacrylonitrile fibres have been studied; these are Dralon T, 2.2 denier fibre, produced by Farben Fabriken Bayer of Dusseldorf, West Germany, and Orlon 81 (approximately 2 denier) fibre, produced by the Dupont Company of Wilmington, U.S.A.. In addition to Courtelle, three other polyacrylonitrile copolymers have been studied: Dralon N (3 denier) fibre, which is produced by Bayer; Cashmilon, 60 denier mono-filament fibre, which is produced by the Asahi Company of Japan and Rhodiaceta acrylic fibre, produced by the Rhodiaceta Company of France. All these copolymers contain approximately 90% by weight of polyacrylonitrile, copolymerised with methylacrylate [95].

Of these acrylics, Courtelle and the Cashmilon mono-filament were wet spun and the remainder were dry spun. A polyacrylonitrile powder was also studied. This was a pure homopolymer prepared by a persulphate-bisulphite initiated polymerisation and was supplied by I.C.I. Limited.

4.2 THE MOLECULAR WEIGHTS OF COURTELLE AND THE DRALON ACRYLICS, BEFORE AND AFTER HEAT TREATMENT.

Solution viscometry was used to determine the intrinsic viscosities of these three acrylic precursors and a few examples of their heat treated products. The technique is well established in polymer science and the reader can obtain details of the methods used from standard texts on the subject [96]. These determinations were made using an Ubbelohde dilution viscometer. The measurements were made with the viscometer controlled at 25 ± 0.1°C, in a temperature controlled water bath. A 60% solution of nitric acid was used for the solvent. This was chosen because the fibres rapidly developed insolubility with colouration, in the usual organic solvents used for polyacrylonitrile. Although formic acid dissolves pyrolysed polyacrylonitrile [74], [75], it was found that the oxidised polymer was insoluble. Sulphuric and nitric acid were found to dissolve the largest proportion of the heat treated samples and as nitric acid fully dissolved the three precursors, it was considered the most suitable choice.

The molecular weight of a polymer is given by the formula

$$\eta_i = K M^n$$

where η_i is the intrinsic viscosity, M is the molecular weight and K and n are the Mark, Houwink, Sakurada constants.

The values for n and K were taken from the work of Fujisaki and Kobayashi [97] who also worked with a 60% nitric acid solution. These are

$$n = 0.75$$

$$K = 3.0 \times 10^{-4}$$

The plots of reduced viscosity versus concentration produced very good straight lines for the unheat-treated acrylics and accurate values of η_i were obtained by extrapolation to zero concentration. The

calculated molecular weights are recorded below,

Courtelle $7.4\ (3) \times 10^4$

Dralon T $7.2\ (0) \times 10^4$

Dralon N $3.0\ (8) \times 10^4$

The heat treated materials generally produced very poor reduced viscosity plots, whether the heat treatment was conducted under inert or oxidising conditions. The reduced viscosities were low in all cases, which indicated low molecular weights. In addition, a large number of the samples were only partially soluble, so the intrinsic viscosity was not completely characteristic of the material. (The variation of the degree of solubility with heat treatment has proved to be a useful parameter, however, and the results will be discussed again in chapter 5.) Accurate best fit straight lines were obtained for two heat treated Courtelle samples, by extrapolating from high values of solution concentration. Both samples were chosen because they were completely soluble and because they had been taken right through the colouration and exothermic reactions. The one sample had been pyrolysed at a rate of $\frac{15}{12}$ °C/minute to 260°C in pure argon and had an intrinsic viscosity of 0.09 dℓ/gram. The other had been oxidised to 290°C at 1°C/minute in circulating air and had an intrinsic viscosity of 0.10 dℓ/gram. Using the Mark, Houwink, Sakurada constants for polyacrylonitrile, the pyrolysed Courtelle molecular weight was 2,100 and the oxidised fibre's was 3,500. As the products of these treatments will have a completely altered molecular structure, the constants do not strictly apply. However, the evidence is quite conclusive that heat treatment reduces the molecular weight of polyacrylonitrile, whether conducted under inert conditions or in the presence of oxygen, because the decline in intrinsic viscosity is very great.

The similarity in molecular weight of Courtelle and Dralon T is

very useful, because the latter is a pure polyacrylonitrile fibre, which behaves quite differently from acrylic copolymer fibres. Molecular weight differences can now be ruled out as a major factor in the different behaviour of these two precursors.

4.3 THE GLASS TRANSITION TEMPERATURES IN ACRYLIC FIBRES.

Polyacrylonitrile exhibits two transition temperatures [72], [73], either of which could be described as a glass transition temperature. They are both very similar to second order thermodynamic phase changes and can be observed as a discontinuity in the rate of change of specific heat with temperature. These glass transitions have been measured for 1.5 denier Courtelle, the two Dralon acrylics, Orlon 81 and the pure polyacrylonitrile powder, with the differential scanning calorimeter. The results have been recorded in table 4.3, below.

Table 4.3

Polyacrylonitrile sample.	First glass transition temperature Tg 1.	Second glass transition temperature Tg 2.
1.5 denier Courtelle	94°C	154°C
3 denier Dralon N	99°C	162°C
Dralon T pure homopolymer	111°C	176°C
Orlon 81 pure homopolymer	110°C	178°C
Pure poly-acrylonitrile powder, I.C.I.	85°C	142°C

The determinations were carried out with the samples in a dynamic atmosphere of dry nitrogen, at a temperature scanning rate of

16°C/minute. The results are all higher than the published figures for relatively unoriented polyacrylonitrile powders and fibres, except for the I.C.I. powder. Andrews and Kimmel [73] quote values of 87°C and 140°C. The pure polyacrylonitrile fibres have very similar glass transition temperatures, which are significantly above the values for the two copolymers. This could be because of the diluent effect of th copolymerised methylacrylate, which has a relatively low glass transit temperature, at 9°C [98].

The transition temperatures for the fibres are probably higher th the unoriented polymer, because of their high preferred orientation. Experience with other fibre forming polymers has shown that the glass transition temperature can increase with increasing amounts of crystallinity and preferred orientation [99].

4.4 FIBRE RELAXATION WITH HEAT TREATMENT.

Bundles of 1.5 denier Courtelle and Dralon T fibre were laid flat and straight in a large diameter porcelain dish and their lengths measured very carefully with a travelling microscope. They were then heated slowly (1°C/minute) to a series of increasing temperatures and held at each temperature for 24 hours. The heat treatments were carried out in an air circulating oven with a constant supply of air provided by a pump. For this slow rate of heating the fibres remained straight and slight wrinkling only appeared at above 300°C. The degree of contraction was determined at each temperature stage, once the fibres had cooled. The results are plotted in figure 4.4(a) for both the acrylics, and straight lines have been drawn through the data points.

The two interesting observations made with this simple experiment are that the length and colour of the fibres change in step with each other and with the glass transition temperatures measured using the D.S.C. 1B. The colours developed during relaxation are indicated on

FIGURE 4·4(a)

THE FREE CONTRACTION OF ACRYLIC FIBRES IN AIR

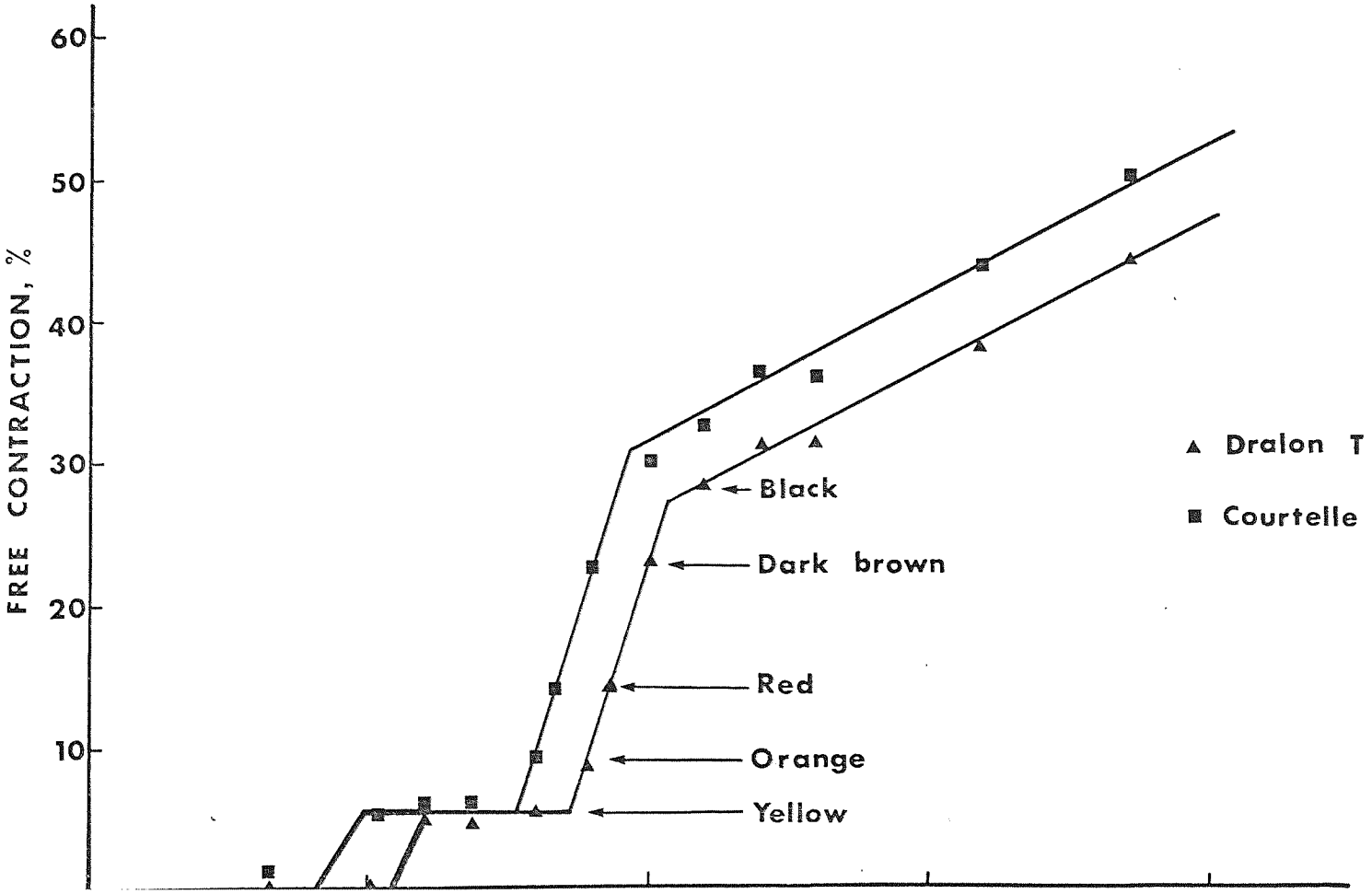

the figure. Dralon T developed the different colours at systematically higher temperatures than Courtelle, but each colour was achieved at approximately the same point of contraction. Contraction was first observed at the first glass transition temperature for each fibre i.e. 94°C for Courtelle and 110°C for Dralon T. No further contraction took place until the temperature reached the second of the glass transitions i.e. 154°C for Courtelle and 176°C for Dralon T. The fibre first coloured to a pale yellow with the first 5% contraction and remained at this colour until relaxation was resumed at the second of the transitions. The change in slope of the rate of contraction with temperature once the fibres have completely blackened corresponds to the completion of the exothermic reaction. Beyond this point, the fibres continue to contract to values of 50% and more, indicating that they still have the characteristic ability to relax which is typical of oriented polymers [100]. The rate of relaxation is now much slower than when the polymer was predominantly unmodified polyacrylonitrile, which indicates that the chain molecules are either more rigid or more firmly bound than previously.

The apparent correspondence between the physical changes in the polymer and the chemical reactions taking place with temperature is most interesting and suggests that the chain relaxation processes control the rates of the chemical reaction(s). A further interesting illustration of relaxation in Courtelle fibres is shown in figure 4.4(t The four curves in the figure have been obtained from four loops of Courtelle fibre, each consisting of 10,000 filaments which have been suspended in a glass fronted oven, with the indicated weights hung from them. The oven has been carefully controlled at each of the three temperatures shown in the figure and the length of each loop measured with a travelling telescope. For each increase in temperature there is a decrease in the length of the loop, if the weight does not

FIGURE 4·4(b)

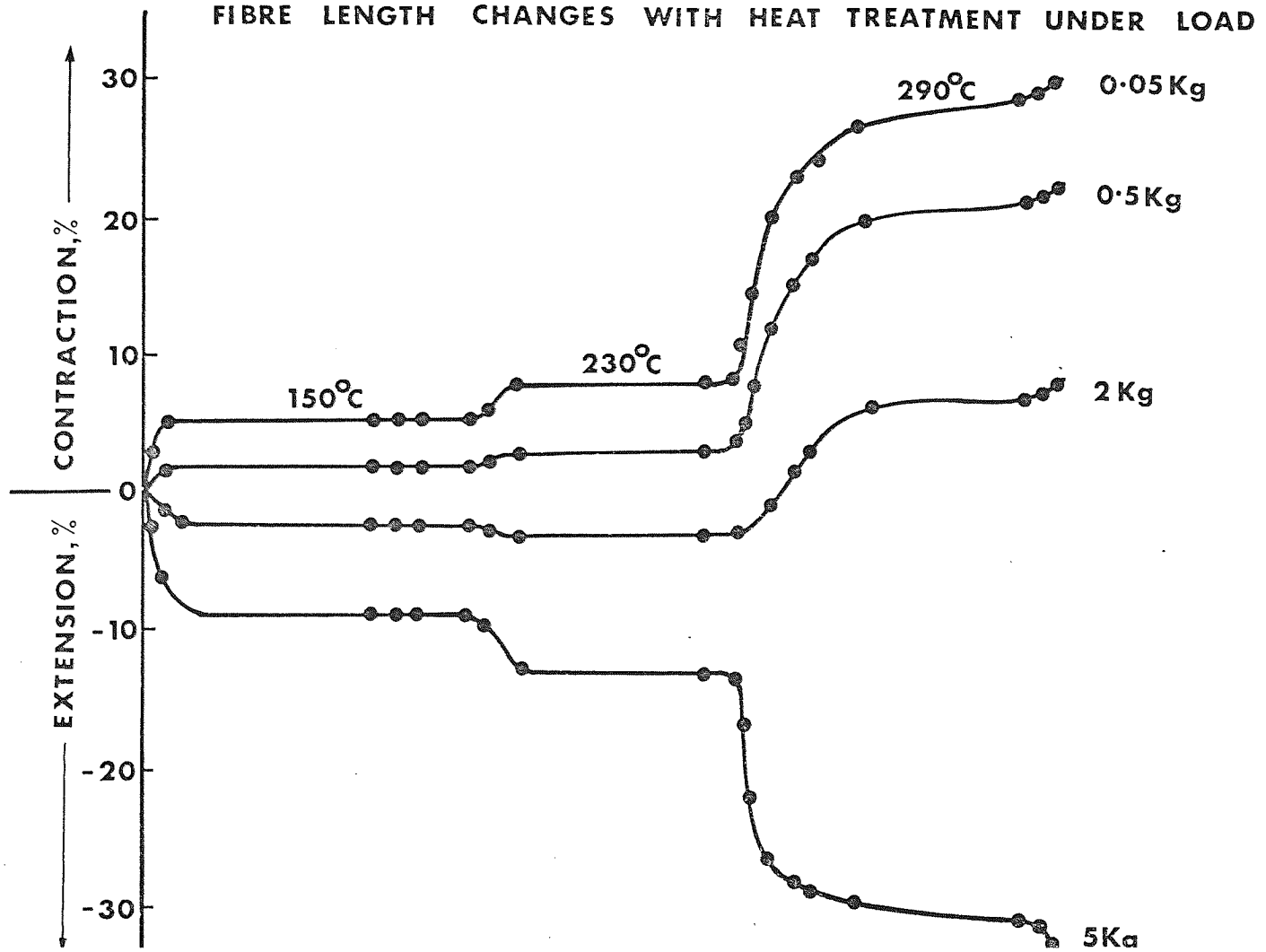
FIBRE LENGTH CHANGES WITH HEAT TREATMENT UNDER LOAD
CONTRACTION,%
EXTENSION,%
30
20
10
0
-10
-20
-30
150°C
230°C
290°C
0·05Kg
0·5Kg
2Kg
5Ka

exceed the plastic limit of the fibre. If it does, the fibre stretches but only to the extent that the retractive relaxation forces will allow. Any number of temperature steps could have been shown in the figure, as each increase in temperature produces a corresponding increase in the retractive force. The greater the load on the fibre the greater is the amount of work performed by the fibre in lifting the load. As the relaxation force is constant and dependent only on temperature, the loops with the heaviest weights contract the least (a plot of percentage contraction versus load is in fact a straight line).

The important observation here is that there is a relaxation time for each temperature, during which the retractive forces equilibriate and after which no reorganisation (i.e. disorientation) of the fibre occurs, unless the temperature is increased again. The usual pre-oxidation treatment for the fibre (e.g. 7 hrs at 220°C in air) does not remove this ability of the fibre to relax.

4.5 THE MELTING OF ACRYLIC FIBRES.

The melting of polyacrylonitrile is not usually observed, because the decomposition of the polymer to form a less tractable solid intervenes to prevent it. Melting has been observed for the polymer in dilute solution [101] and inflections in the reaction exotherm have been interpreted as being due to a melting endotherm [102]. The author has found that rapid scanning in the D.S.C.1.B resolves a melting endotherm immediately preceding the reaction exotherm. This is shown for Courtelle and the two Dralon acrylics in figure 4.5, and the effect has been observed for a very wide range of acrylics in addition to these.

The determinations were carried out at a scan rate of 64°C/minute, with the samples encapsulated in pressure sealed pans, in an external atmosphere of pure, dry nitrogen. The endotherm for the copolymers, Courtelle and Dralon N, are very small, and it is as if they have been

FIGURE 4·5

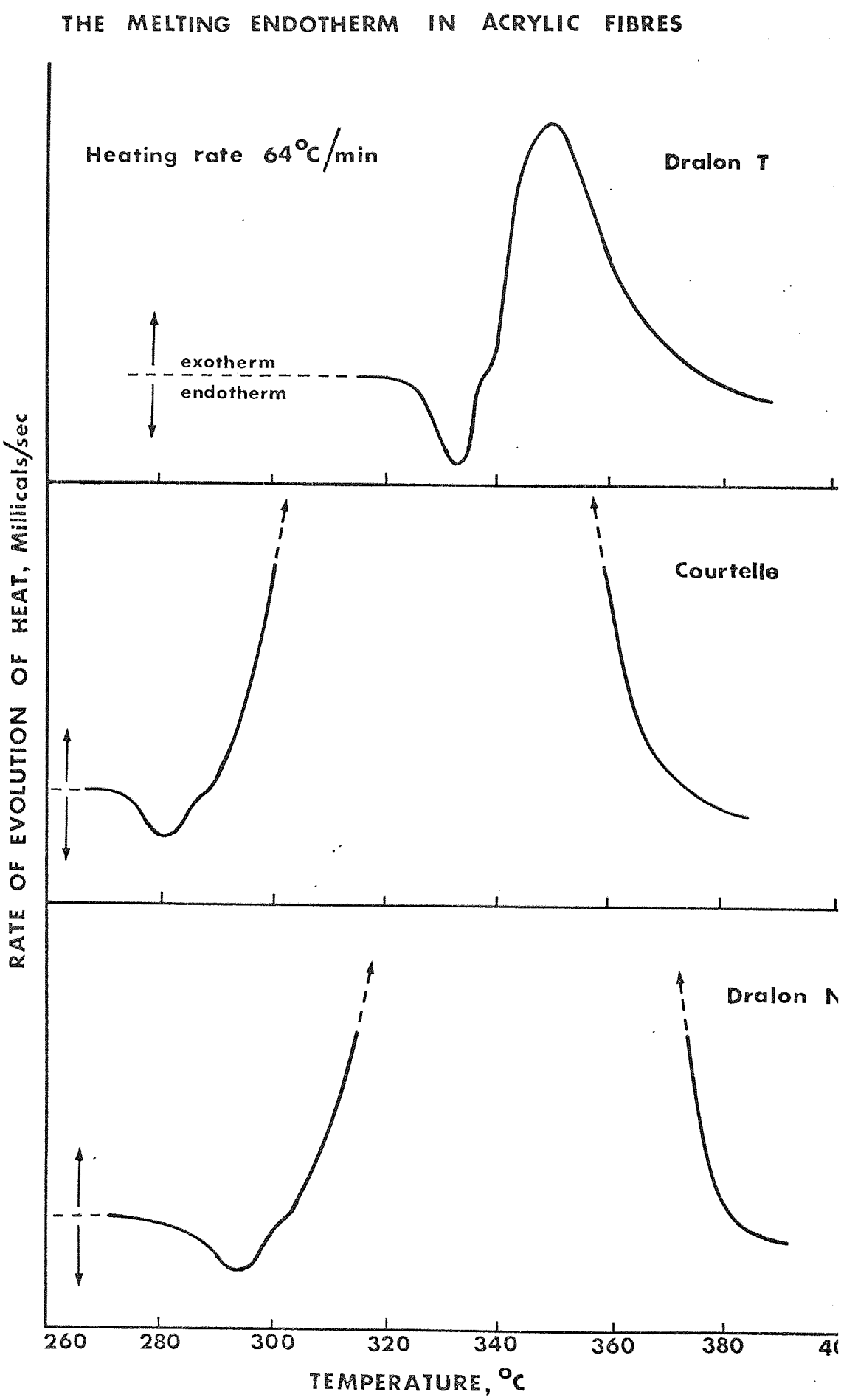
THE MELTING ENDOTHERM IN ACRYLIC FIBRES
Heating rate 64°C/min
Dralon T
exotherm
endotherm
Courtelle
Dralon N
RATE OF EVOLUTION OF HEAT, Millicals/sec
260
280
300
320
340
360
380
TEMPERATURE, °C

cut-off by the appearance of the very broad exotherms. For Dralon T, however, the endotherm and exotherm are very well resolved and there can be very little doubt that true melting is taking place. Layden [103] has shown similarly well resolved endotherms immediately prior to the exotherm, for copolymers of polyacrylonitrile with methylmethacrylate: these results have been reported since the author made his measurements

Table 4.5, below, lists the melting points for the endotherms in figure 4.5, and for Orlon 81 and the pure polyacrylonitrile powder. In addition, the glass transition temperatures from section 4.3 are repeated in the table for comparison.

Table 4.5

Acrylic Sample	Tg1 °C	Tg2 °C	Tm °C
Courtelle	94	154	281
Dralon N	99	162	294
Dralon T	111	176	333
Orlon 81	110	178	335
Pure PAN powder (I.C.I.)	85	142	340

The melting points for the pure polyacrylonitrile samples are very similar and in quite good agreement with the values quoted in the literature. The copolymer melting points are lower, which might be due to the diluent effect of the methylacrylate, reducing the cohesion of the fibres. Layden [103] has shown how increasing amounts of methylmethacrylate copolymer reduces the melting point of acrylic fibres. The melting points of the fibres are directly proportional to the glass transition temperatures, which is a general rule for semicrystalline polymers [104].

The thermodynamic changes in polyacrylonitrile appear to provide

boundary conditions to the occurrence of the colouration/exothermic reaction(s). (It will be assumed these are identical; evidence for this is provided in chapter 5.) Colouration does not take place until the temperatures of the glass transitions are exceeded. The glass transitions, therefore, provide a lower temperature limit to the reaction(s). For rapid heat treatment programmes the exotherm follows immediately upon the melting of the polymer, therefore melting represents the upper temperature limit to the appearance of the reaction(s). This suggests that the reaction(s) which produce the chromophore and exotherm are dependent upon the ability of the chain molecules to relax or rotate about their axes. Bond rotation in the chain does not appear until the first glass transition temperature and once the temperature is increased to the melting point all the molecule will be free to relax.

4.6 THE EFFECT OF PRE-OXIDATION UPON FIBRE MELTING.

The rapid heating of unpretreated acrylic fibres held under restraint results in their breakage and fusion, because of the appearance of the melting endotherm. If the fibres are first given a moderate inert heat treatment to produce the thermally stable coloured product and then given a further rapid heat treatment, the melting is less severe but the fibres nevertheless shrink and fuse at about 340°C. Oxidation of the fibres, however, renders them completely infusible. The standard pre-oxidation of Courtelle, for example, so stabilises the fibre that it can be carbonised almost instantaneously, without any fibre adhesion and with very little shrinkage.

The suppression of melting by pre-oxidation is illustrated with Dralon T in figure 4.6. Thermogram (a) is the 64°/minute D.S.C. scan of the fibre discussed above, which clearly exhibits the melting endotherm. Thermogram (b) shows that this endotherm has been almost completely suppressed by a relatively low degree of pre-oxidation. This second sample has initially received an oxidation treatment by

FIGURE 4·6

THE MELTING ENDOTHERM IN DRALON T

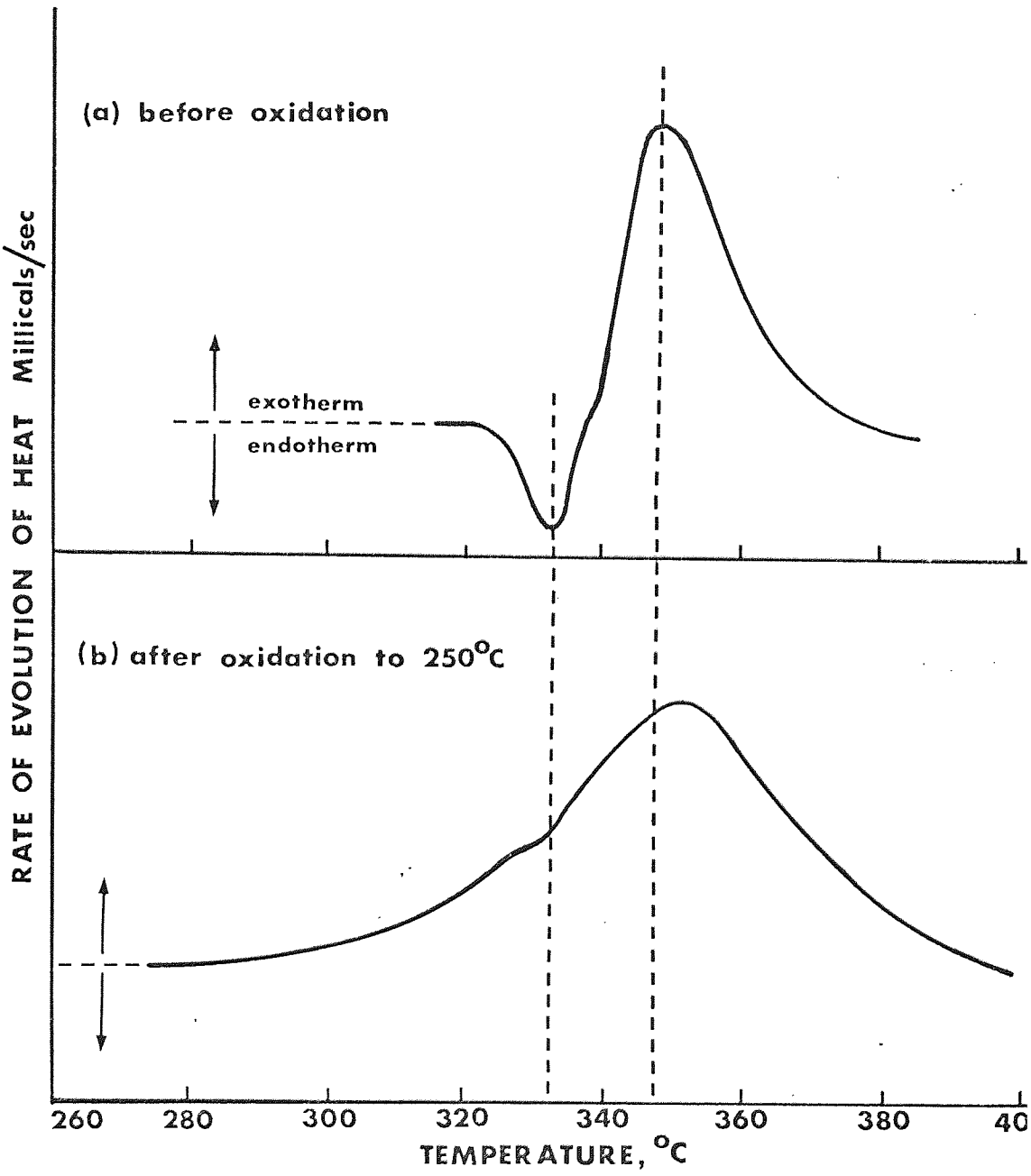

being heated under restraint at 1°C/minute to 250°C in circulating air. The reaction exotherm has very much broadened and melting appears to be suppressed by the earlier initiation of the reaction.

4.7 THE REACTION EXOTHERM FOR ACRYLIC FIBRES.

The reaction exotherms have been determined for the range of acrylics considered so far. This has been done with the D.S.C.1B differential scanning calorimeter, operating at a programme rate of 16°C/minute, with a purge of pure, dry nitrogen. The exotherms for Courtelle and the two Dralon acrylics are shown in figure 4.70. The amount of heat evolved per unit mass of the sample has been calculated in each case by integrating under the exotherm curve using a planimeter Table 4.7 below lists the values of the exotherms for all the acrylics, along with the calculated values for the heat evolved per unit mole of polyacrylonitrile in each sample.

Table 4.7

Polyacrylonitrile samples.	Amount of heat evolved Cals/Kg	Heat evolved per mole Cals (K cals)
Courtelle	115	6.7(0)
Dralon N	136	7.9(2)
Dralon T	90	4.7(7)
Orlon 81	90	4.7(7)
Pure polyacrylonitrile powder (I.C.I.)	111	5.8(8)

Hay [77] quotes the value of the heat evolved per mole of polymer as falling between 5 and 6 Cals. Gillham and Schwenker [105] are more precise and report a value of 5.85 Cal/mole.

These results agree with the author's value for the pure polymer powder. It appears paradoxical that the pure polyacrylonitrile fibres

FIGURE 4·70

THE REACTION EXOTHERMS FOR ACRYLIC FIBRES, MEASURED II

PURE N_2

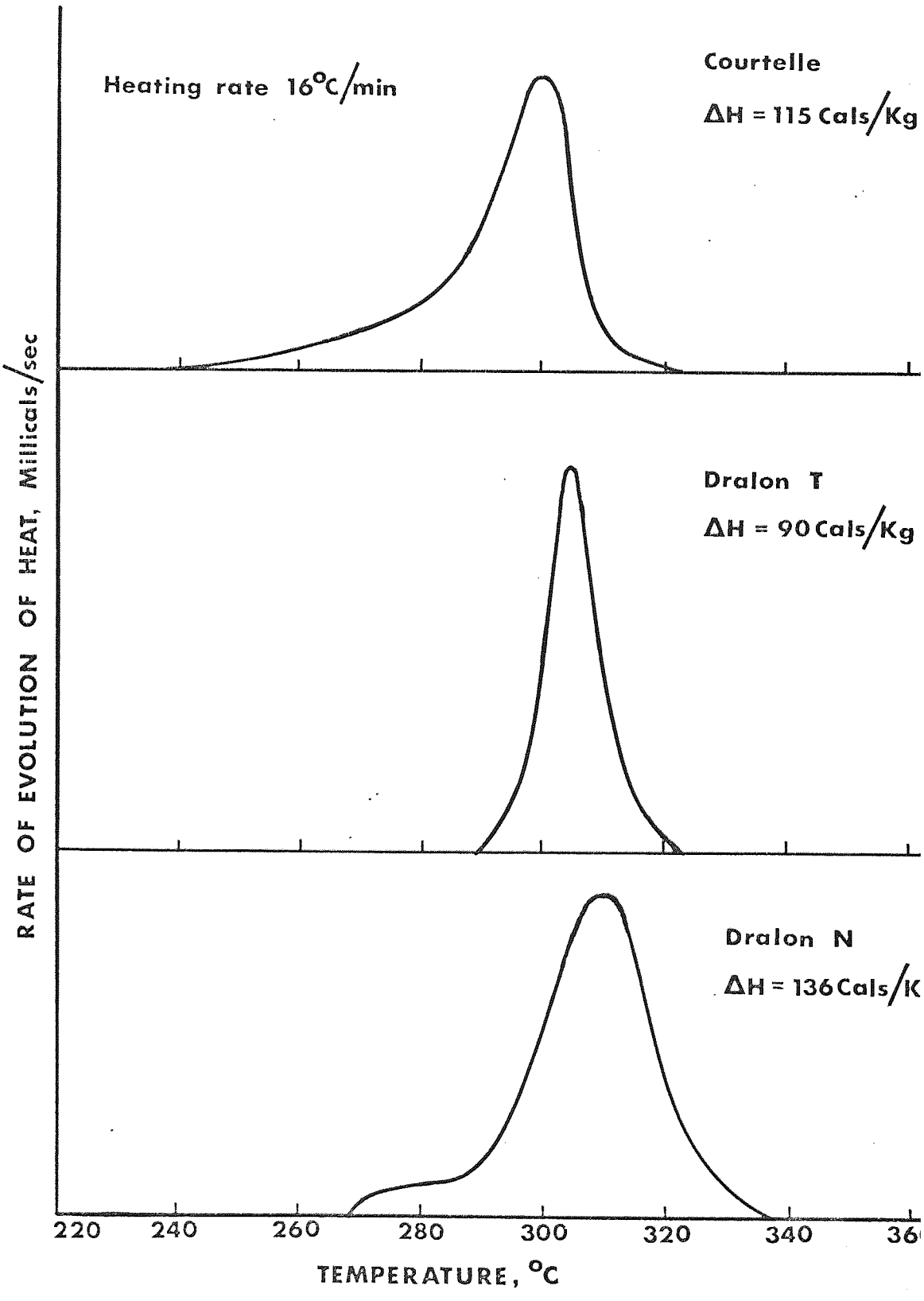

have exotherms which are smaller than the pure powder and yet the acrylic copolymers have exotherms that are larger. For the copolymers one might expect that the methylacrylate has a diluent effect. In fact, the copolymer may well have a catalysing effect. Courtelle also contains itaconic acid, which could have an additional initiating effect on the reaction.

Inspection of the exotherms in figure 4.70 lends support to the idea that the copolymer has an initiating action on the exothermic reaction. The Dralon T exotherm is very sharp and has the characteristic shape of an autocatalytic reaction. The Courtelle exotherm starts at a very much lower temperature than Dralon T and the rate of evolution of heat increases only gradually at first. The reaction must be initiated at lower temperatures by some chemical or physical mechanism, which is absent in Dralon T. The Dralon N exotherm is not catalysed to the same extent as Courtelle, but the exotherm is very much broader than for Dralon T and it is clearly not due to a simple autocatalytic reaction.

With the 16°C/minute scan used for obtaining the exotherms in figure 4.70, there is no evidence of melting prior to the exotherm peak. There is some evidence at higher temperatures, not shown on these scans, when the base line undergoes a strong endothermic drift.

4.71 The change in the residual exotherms following heat treatment.

The reaction exotherm has been measured for 1.5 denier Courtelle and Dralon T fibre, after a series of heat treatments in argon and in air, in order to follow the reducing size of the exotherm with temperature. The pyrolyses in argon were carried out in a vacuum tube furnace, from which the air was completely evacuated. Once a good vacuum was obtained, the furnace tube was filled with pure dry argon, flushed several times and the thermal programme then conducted with a constant rate of flow. The sample was tied under slight tension upon a stainless steel frame. The temperature of the fibres was

FIGURE 4·71(a)

THE DECLINE IN RESIDUAL EXOTHERM WITH TEMPERATURE

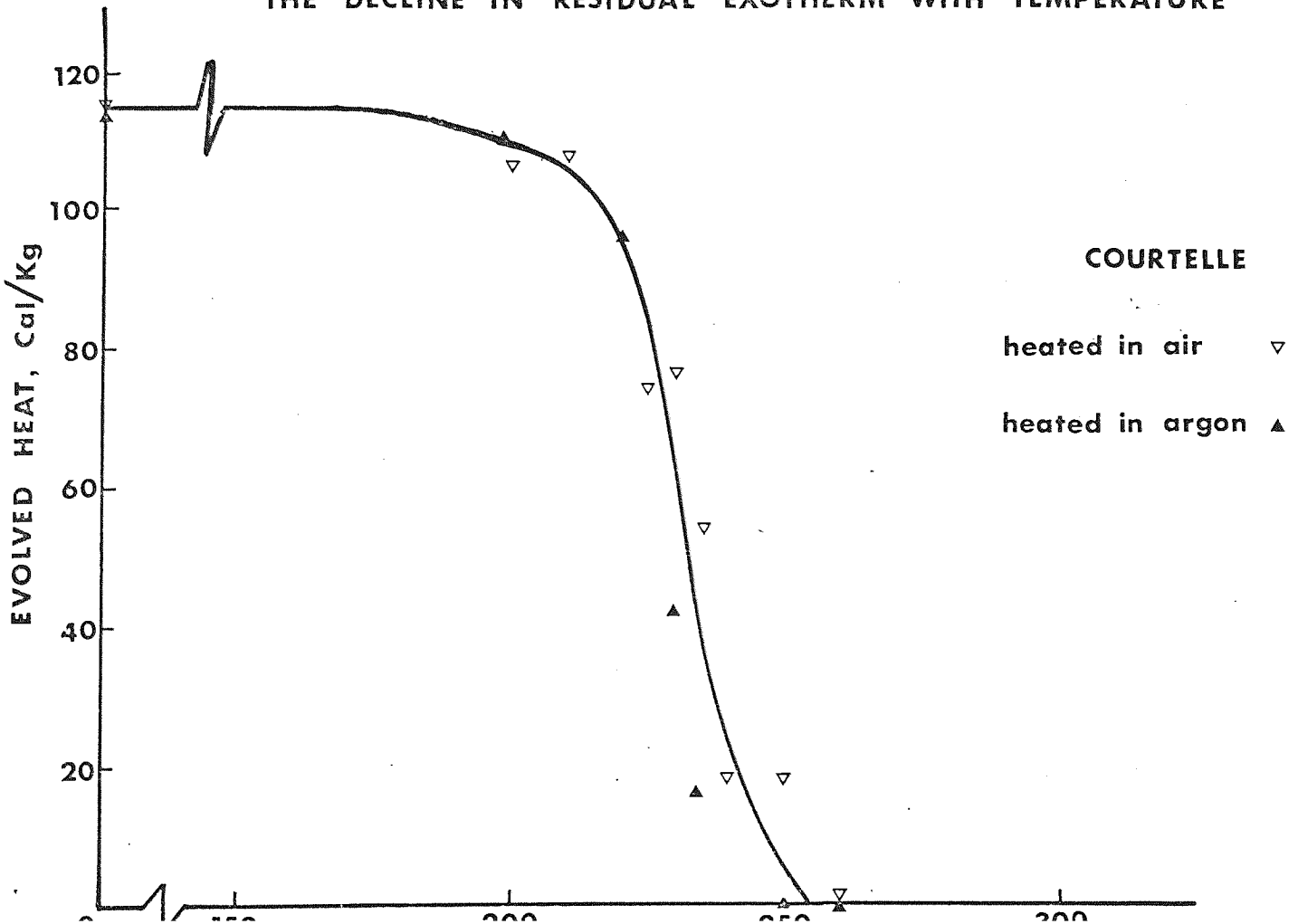

continuously recorded by a thermocouple junction, placed in intimate contact with the sample.

The temperature programme rate was $\frac{15}{12}$ °C/minute and the furnace was each time taken to the required temperature and then allowed to cool without any dwell period.

The oxidations were carried out in an air oven with the fibres tied upon the same type of frame and a thermocouple junction was again placed in intimate contact with the bundle. A constant flow of air was maintained with an air pump and a circulating fan ensured that the sample atmosphere remained consistent. The temperature programme used for all the oxidations was 1°C/minute to the final temperature, followed by a rapid quenching of the sample in the ambient atmosphere.

The residual exotherm was measured using the D.S.C. 1B, with the fibre thoroughly chopped and sealed into the standard sample pans. A programme rate of 16°C/minute was used for all the determinations and a purge of pure dry nitrogen was maintained through the cavity.

Figure 4.71(a) is a plot of the residual exotherms for the argon and air heat treated series of Courtelle samples, versus the peak programme temperature. For both heat treatments, the exotherm decays completely between 200 and 260°C. The pyrolysed fibres appear to lose their exotherm a little earlier than the oxidised samples. Figure 4.71(b) is the equivalent plot for the Dralon T fibre series. In this case the behaviour is somewhat different. From 0 to 230°C, the argon heat treatments produce no diminution of the residual exotherm. However, at 234°C the sample underwent a rapid transformation which only affected parts of the bundle. Some strands of the fibre were unchanged, while others had turned bright yellow and the remainder bright orange. The more coloured the fibre, the more it had contracted The three points plotted at 234°C in figure 4.71(b) are for the residual exotherm of each of the three differently coloured fractions. The residual exotherm is smaller the deeper the colour. By 236°C, the

FIGURE 4·71(b)

THE DECLINE IN RESIDUAL EXOTHERM WITH TEMPERATURE

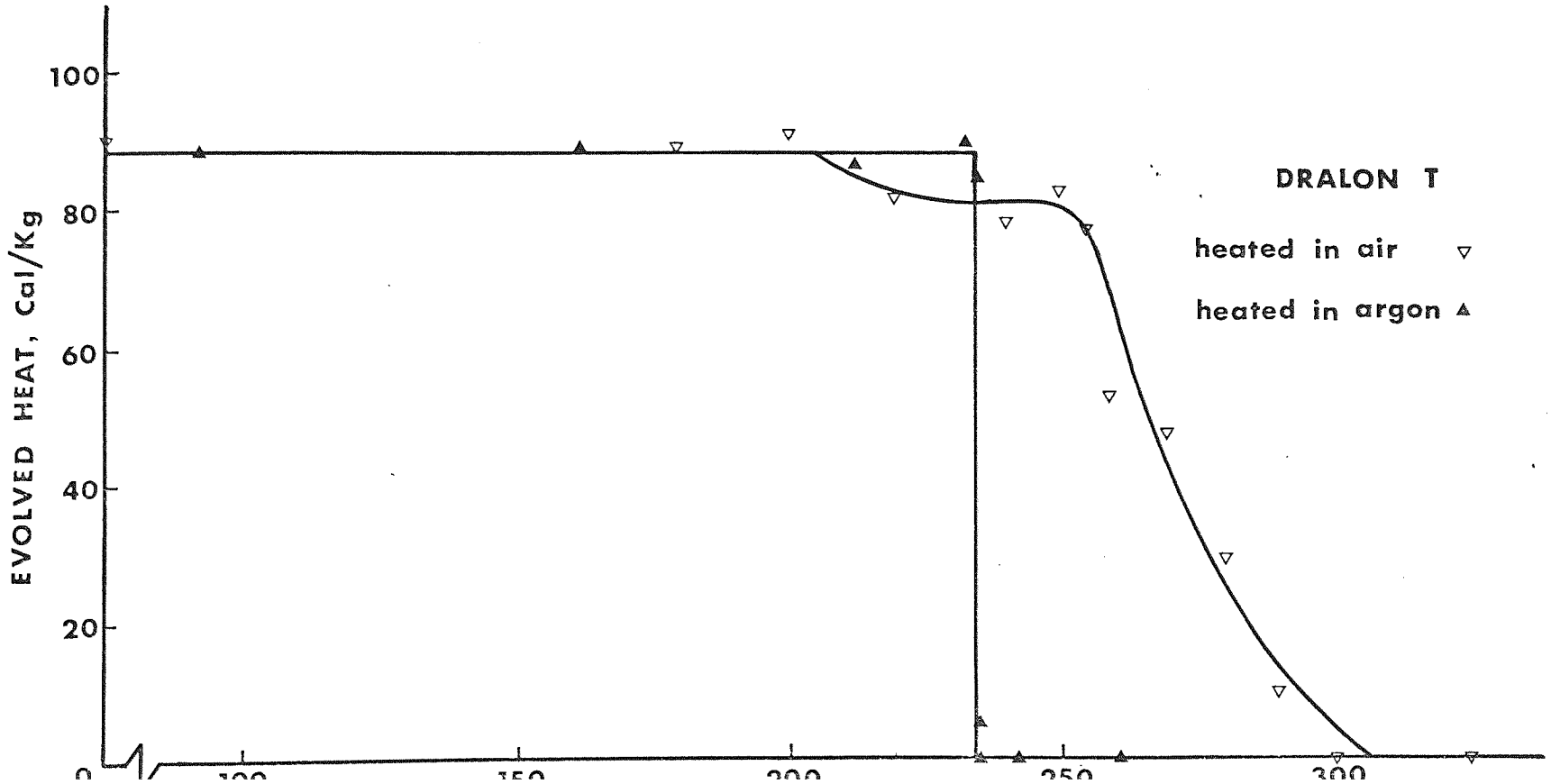

sample was uniformly orange in colour and the residual exotherm had disappeared. This behaviour is characteristic of the violent auto-catalytic reaction to which the pure polyacrylonitriles are subject when heated in inert conditions [75].

The oxidised Dralon T samples behave quite differently. The violent character of the exotherm is removed by heat treating in oxygen and the exotherm declines very much more gradually. At first there is a small decline between 200 and 240°C, but the main loss of the exotherm takes place between 250 and 300°C. This is at appreciabl higher temperatures then observed for oxidised Courtelle.

4.72 The exotherm induction period.

Pure polyacrylonitrile, heated at a constant temperature, does no exhibit a reaction exotherm until after the elapse of a given time interval, which is a function of the temperature [77, 102]. This is the isothermal exotherm induction period. The isothermal exotherm is usually of the same type as that observed for programmed heat treatmen and the amount of heat evolved is the same. No one has as yet explain the reason for this induction period.

All the acrylic samples considered in this chapter exhibited an induction period that could be measured with the D.S.C. 1B, except Courtelle. This is not to say that Courtelle doesn't have an inductio period, but simply that the initial rate of evolution of heat is so small that the instrument cannot detect it. This can be seen from the Courtelle exotherm in figure 4.70; the initial exothermic drift is very gradual, particularly under isothermal conditions and it was impossible to accurately pin point the starting times.

The induction periods were measured for the samples prepared in the same way as previously, with a flow of pure dry nitrogen through the cavity. Before placing the sample in the instrument, the cavity was heated to a temperature 10°C below that finally required. After placing the sample in the appropriate cell, the temperature was ~~cranke~~

FIGURE 4·72(a)

INDUCTION PERIOD ARRHENIUS PLOT

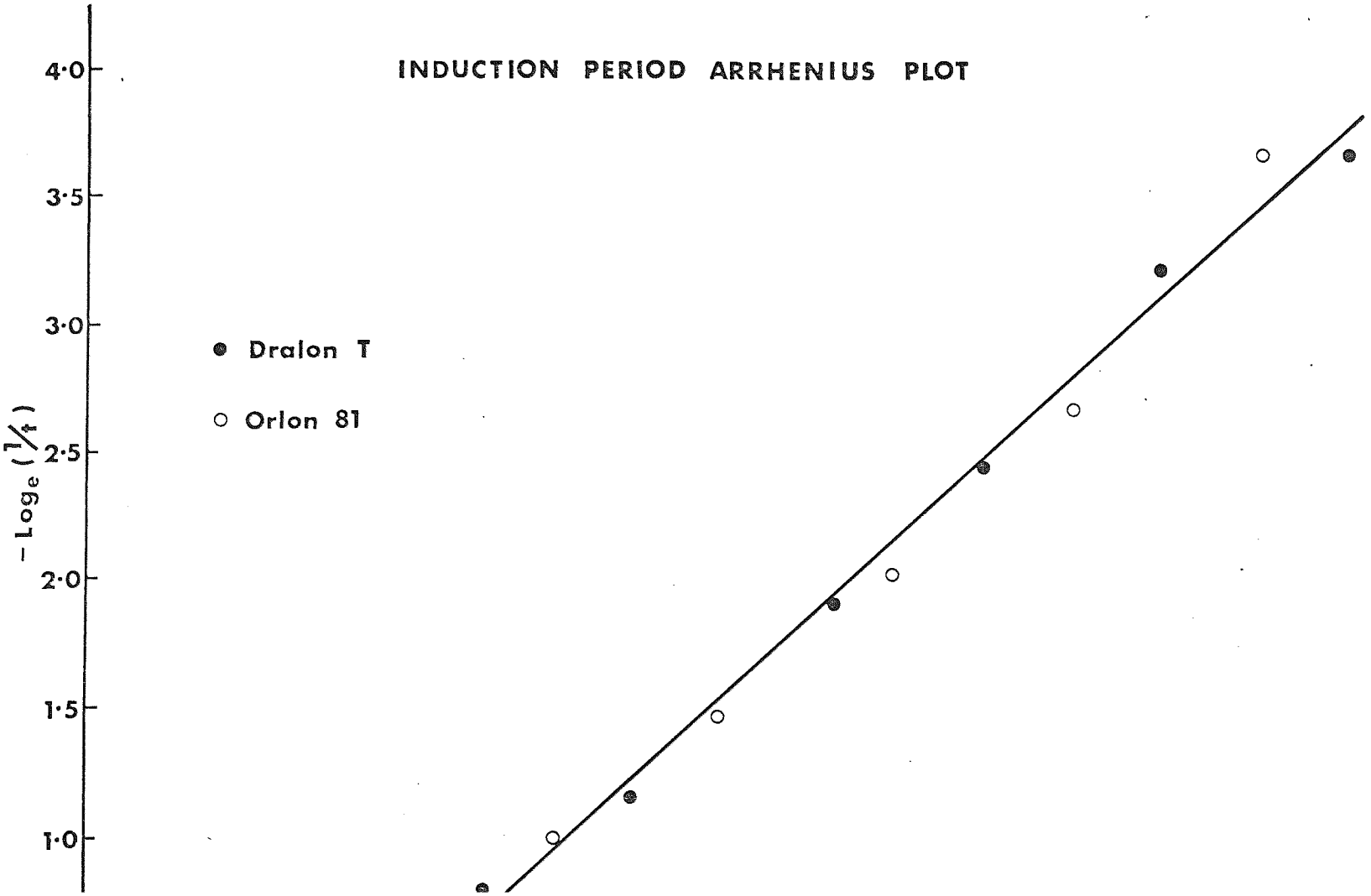

increased
A ~~up~~ to the required value at the fastest possible rate, without losing temperature control. In this way there was no temperature overshoot and the preparation time was kept to a minimum. The stop watch was started as soon as the test temperature was reached and the time taken to the start of the exotherm measured to the nearest second.

The reciprocal of the induction period is the reaction rate for each temperature and an Arrhenius plot of the reaction rate versus temperature produces a very good straight line for all the acrylics investigated. Figure 4.72(a) is the Arrhenius plot for Dralon T and Orlon 81 pure polyacrylonitrile fibres. Both sets of data are in very good agreement with the straight line fitted to them and within experimental error, both fibres have identical activation energies. This is consistent with the results obtained so far, as these two fibres also have identical glass transition temperatures and melting points and they both produce the same amount of exothermic heat.

The induction periods for Dralon N are shorter than for Dralon T. As an example of this:- at 240^{o}C the exotherm in Dralon N takes 3.78 minutes to appear, while in Dralon T it takes 40.3 minutes. The Arrhenius plot for Dralon N is shown in figure 4.72(b), and, as for Dralon T, it is quite a good straight line correlation. The activation energies for Dralon N and Dralon T are listed in table 4.72, below, together with values taken from the literature.

FIGURE 4·72 (b)

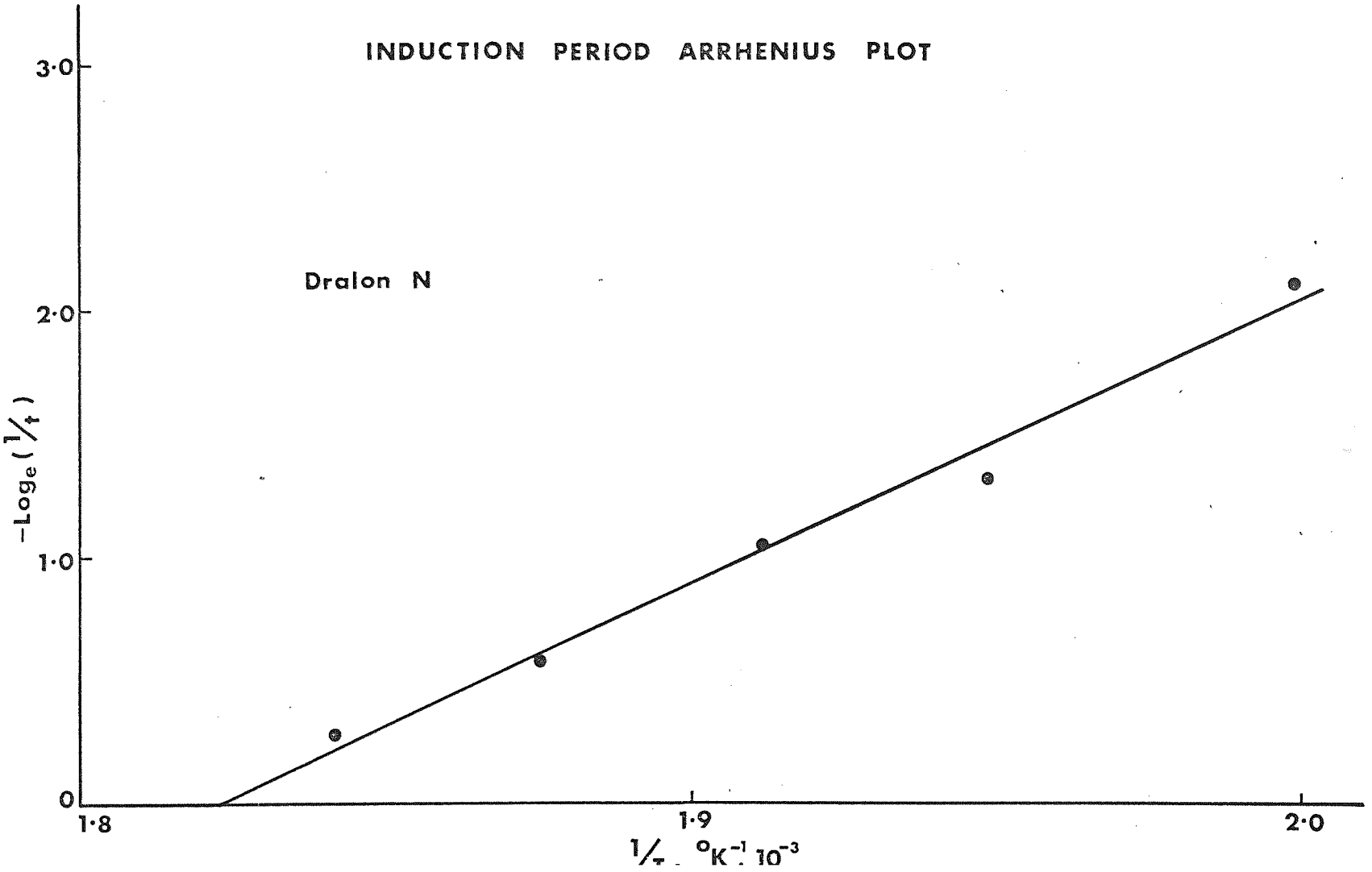
INDUCTION PERIOD ARRHENIUS PLOT
Dralon N
3·0
2·0
1·0
0
$-\log_e(1/t)$
1·8
1·9
2·0
$1/T \cdot {}^{o}K^{-1} \cdot 10^{-3}$

Table 4.72

The activation energies for exothermic/nitrile decay reactions.

Acrylic sample	Activation energy in Cals/mole (Kcals/mole)	Source & method of determination
Dralon T & Orlon 81	35.9	The author:- Exotherm induction period.
Dralon N	22.9	The author:- Exotherm induction period.
Courtelle	11.0	Reference 106:- Nitrile decay from i.r.
Pure homopolymer powder	30.0	Reference 77:- Exotherm induction period.
Misubishi polyacrylonitrile fibre.	44.0	Reference 102:- Exotherm induction period.
Pure homopolymer powder.	43.0	Reference 83:- Nitrile decay from i.r.

The activation energy for Dralon N is appreciably less than for Dralon T, possibly reflecting the initiating effect of the copolymer. The activation energy for Courtelle was obtained by a colleague of the author (working completely independently) and it was calculated from the rate of loss of the infra-red nitrile absorption [106]. The loss of the nitrile groups in the same temperature range is considered to be the source of the exotherm [56] (more evidence for this will be given in chapter 5). The Courtelle activation energy is very much

less than either of the Dralons, which is to be expected from the appearance of the exotherm at lower temperatures. This is consistent with the view that Courtelle contains a more efficient initiator than the other acrylics. Two published values for activation energies have been determined by the measurement of the induction period and these have been recorded in table 4.72. The Dralon T result falls midway between these values. Clearly, the activation energy is a function of the origin and type of sample (it is quite possibly a function of molecular weight, for example). The value due to Yu and Noh [83] is very close to that from reference [102], and it is also for a polymer of high molecular weight (M_n = 600,000). Both results could well be for polymer from the same source.

4.73 The effect of pre-oxidation on the induction period.

The oxidation of Dralon T fibre has the effect of increasing the exotherm induction period, e.g.:- fibre oxidised at 1°C/minute to 250°C in air has an induction period at 260°C of 31.53 minutes, which is compared to a value of 11.60 minutes for completely untreated material. The induction period continues to increase with the degree of pre-oxidation, until the exotherm is completely extinct. These results are at first rather surprising, because the oxidation reaction is generally believed to produce initiating groups, which should accelerate the exothermic reaction. [70], [71], [93] However, as figure 4.6 shows, the pre-oxidation of Dralon T does induce the reaction to start at lower temperatures, although the resultant exotherm is much broader than previously.

Figure 4.73 shows the Arrhenius plot for the Dralon T fibre which has been oxidised to 250°C. The activation energy calculated from the plot is 49.2 Cals/mole. This is a substantial increase on the activation energy for the unoxidised fibre of 35.9 Cals/mole. This increase in activation energy with the degree of oxidation explains the behaviour of the air heat treated series of Dralon T samples plotted

FIGURE 4·73

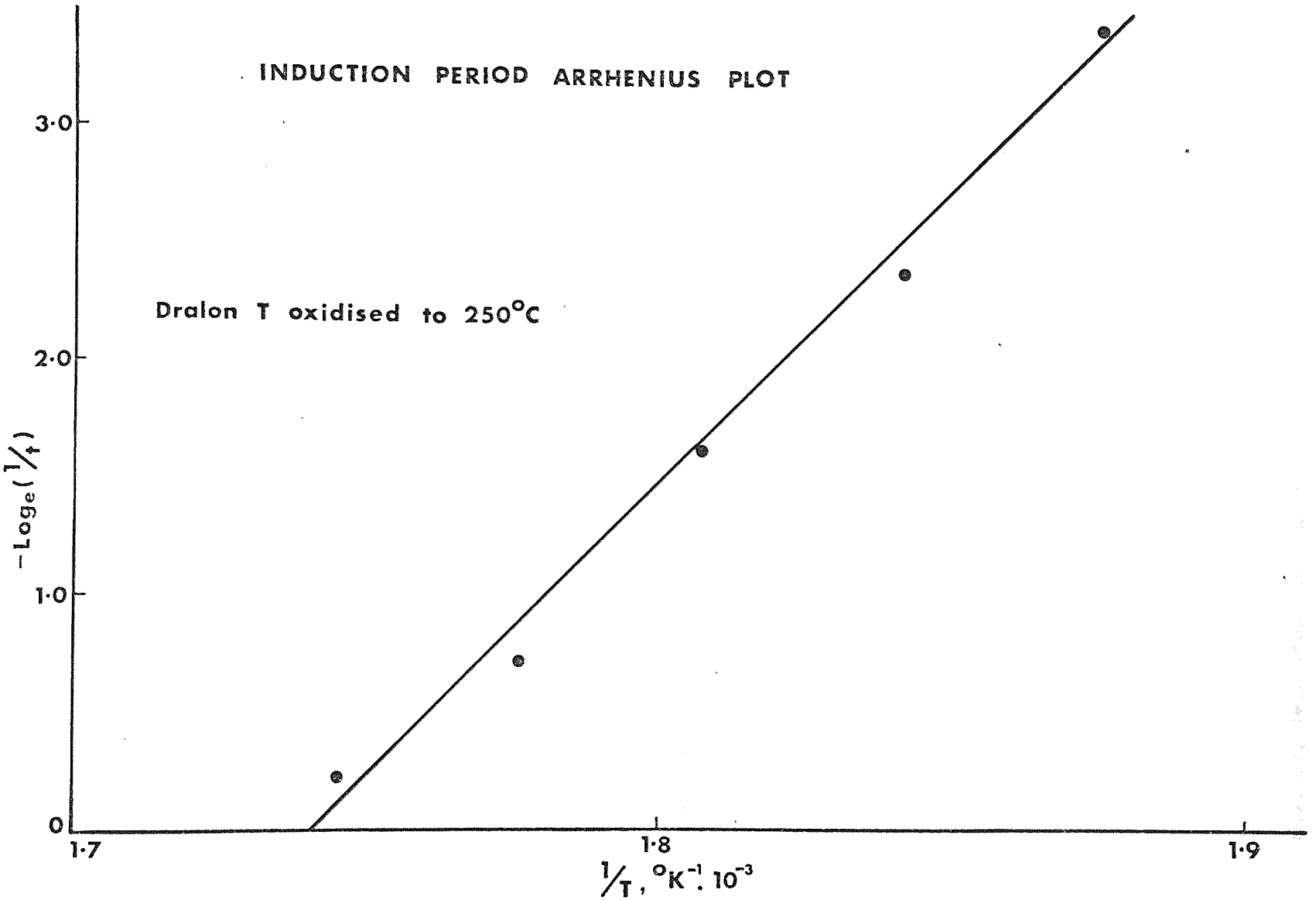
INDUCTION PERIOD ARRHENIUS PLOT
Dralon T oxidised to 250°C
3·0
2·0
1·0
0
$-\log_e(1/t)$
1·7
1·8
1·9
$1/T$, $^{\circ}K^{-1}.10^{-3}$

in figure 4.71(b). The oxidation of the fibre at increasing temperatures is progressively reducing the reaction rate, which pushes the loss of the exotherm to higher temperatures and moderates the rate at which the exotherm is lost.

SUMMARY AND CONCLUSIONS.

The origin of the isothermal induction period has yet to be explained. Hay[77] remarked upon its similarity to an Avrami process [107], but he did not elaborate upon this. The author's theory is that the similarity to a crystallisation process is more than superficial and that the induction period is in fact due to a chain relaxation/annealing process.

The colouration/exothermic reaction has been shown to be associated with the relaxation of the fibre by the results in sections 4.4 and 4.5. Any reaction taking place between the nitrile groups on the same chain molecule is dependent upon the ability of the chain to twist upon itself. This is because neighbouring nitriles are in a state of mutual repulsion, due to their permanent dipole moments [101]. Therefore, the stable conformation of the chain has the nitrile groups at lattice positions where they cannot react. Any initiating mechanism for the reaction of the nitriles requires that the chain should be capable of relaxation and this cannot take place until the polymer is above its glass transition temperature. The problem is further complicated by the presence of two glass transition temperatures, which implies that the fibre has either two phases or two types of secondary bonding.

The copolymer acrylic fibre exotherms could be situated at lower temperatures than the pure polymer, because of their lower glass transition temperatures. The methylacrylate possibly dilutes the intermolecular cohesion of the fibre, hence allowing relaxation to take place at lower temperatures. The earlier inception of the reaction is not in itself the entire explanation of why the copolymer

exotherms are larger than the pure polymer fibres'. The pure polymer powders also have larger exotherms than the pure fibres, so the explanation of the low exotherm is not just a function of the polymer content, it must also depend upon the physical state.

A feasible explanation of all these factors can be based upon the nitrile polymerisation reaction proposed by Houtz [58] and Grassie [61] and upon the formation of initiating rings in pure polyacrylonitrile. Yu and Noh [83] have shown that if it is assumed that a saturated population of initiation rings is formed before any nitrile polymerisation takes place, only 60% of the nitrile groups can participate in the polymerisation reaction. They confirm this result experimentally. The formation of initiation rings requires the controlled relaxation of the polymer and as Yu and Noh state, the process would be analogous to the crystallisation of a one-dimensional phase. Fibres, such as Dralon T and Orlon 81, are highly oriented forms of the polymer and the relaxation of the molecules to form ring structures is possibly the most energetically favourable path for the polymer to follow. The low exotherm in these samples might then result from the reduced population of nitrile groups, which would be free to participate in the polymerisation reaction.

A pure polymer powder, such as the I.C.I. material considered here, is a disordered form of the polymer. Although it has the characteristic melting point of pure polyacrylonitrile, its glass transition temperatures are low, so it will relax and react earlier than Dralon T and Orlon 81. It will not anneal to form initiation rings with as much ease as a fibre and so the initiation ring reaction will not deplete the nitrile content to the same extent. The polymerisation of the nitriles will consequently produce a greater exotherm, as they react in larger numbers.

The greater heat evolved per mole of polyacrylonitrile in the copolymers could be due to an additional initiation reaction produced

by the copolymer. Methylacrylate may initiate the polymerisation of the nitriles by the following mechanism,

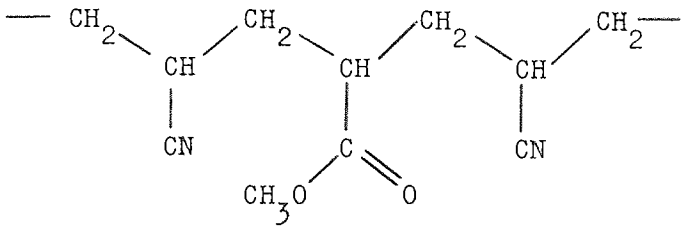

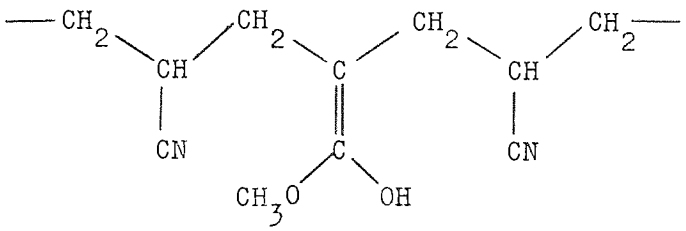

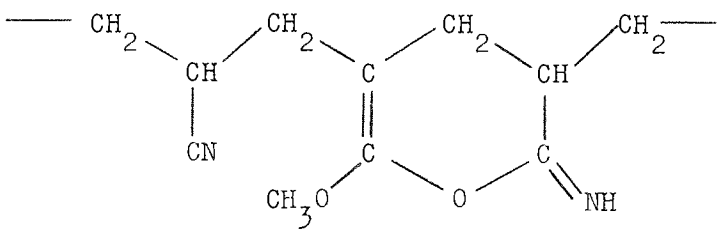

Initiation in this way might induce the nitrile polymerisation reaction to begin at lower temperatures and hence prevent a larger proportion of the nitrile groups from being consumed in the formation of initiation rings. As Courtelle contains an acid impurity, initiation could be accomplished by a second impurity reaction. This may be why Courtelle begins to colour at relatively very low temperatures.

The effect of oxidation on the induction period and rate of decay of the residual exotherm for Dralon T may also have thermophysical origins. As the induction period of Dralon T is much longer than for Dralon N and Courtelle, the oxidation reaction can proceed to a greater extent before the onset of the nitrile polymerisation reaction. If the oxidation produced polyene sequences in the chain molecule, or by some mechanism increased the degree of cohesion between neighbouring molecules, the relaxation rate of the polymer would be reduced. In fact, any mechanism which increased the effective rigidity of the chain

could have this result. Generally authors on the subject expect oxidation to introduce initiating groups (β-ketonitriles) into the polymer, which should reduce the temperature at which the exotherm takes place and possibly increase the total fraction of nitriles involved in the polymerisation reaction.[69, 92, 94] The exotherm for oxidised fibre does in fact start at a lower temperature when measured using a programmed heat treatment, under inert conditions. The initiation reaction involving the β-ketonitrile group requires the formation of a ring structure, however, so the reduction in the rate of relaxation will, nevertheless, increase the induction period.

A paper by Müller et al [86] attributes the contraction of Dralon T fibre with heat treatment to the nitrile polymerisation reaction itself. This seems to confuse cause with effect, because the reaction clearly cannot take place without relaxation and this in itself would involve a contraction of the fibre, unless restraint were applied. Without restraint contraction is inevitable, whatever the chemistry of the process. An interesting observation by Simmens [108] is significant in this respect. He found that the refractive index of fibre heat treated under restraint did not increase until appreciably higher temperatures than fibre heated without any restriction. The increase in refractive index is probably due to the chromophore and this result appears to confirm the author's hypothesis. The restraint of the fibre will have reduced the rate of chain relaxation and as a result the rate of reaction would be reduced, postponing the formation of the chromophore to higher temperatures.

CHAPTER 5.

THE MOLECULAR CHANGES ACCOMPANYING THE PYROLYSIS AND OXIDATION OF ACRYLIC FIBRES.

5.1 INFRA-RED SPECTROMETRY.

The infra-red spectrum of polyacrylonitrile has received a lot of attention from the literature and general agreement is found on the assignment and order of appearance of most of the absorption bands. (See review by Beevers [81].) Table 5.1 (below) has been drawn up to list the most important absorption bands and the frequency assignments are those found for the bands in Courtelle and Dralon T acrylics. The table is based on one published by Yamadera et al.[110]

Table 5.1

Observed frequencies and Band Assignments for Polyacrylonitrile.

Absorption wave number cm^{-1}	Intensity	Assignments
2,940	vs	$(CH_2)\ V_s$.
2,920	sh	$(CH)\ V_s$.
2,870	m	$(CH_2)\ V_a$.
2,810	vw	$(CH)\ V_a$.
2,240	vs	$(CN)\ V_s$.
1,453	vs	$(CH_2)\ \delta$.
1,375	m	$(CH)\ \delta$.
1,355	m	$(CH_2)\omega + (CC)V_a$.
1,310	w	$(CH_2)\omega - (CH)\delta$.
1,247	s	$(CH)\omega + (CH_2)\omega - (CC)V_a$.
1,115	sh	$(CC)V_s - (CH)\delta$
1,073	vs	$(CC)V_s$ $(CH_2)r - (C\text{-}C\text{-}CN)\delta$
1,015	sh	$(CH)\omega + (CC)V_a$ $(CH_2)t$
865	vw	$(CH_2)r$
778	m	$(C - CN)V + (CH_2)t$ $(C - CN)V - (CH_2)r$

FIGURE 5·1

THE INFRA-RED SPECTRA OF THE PRECURSOR FIBRES

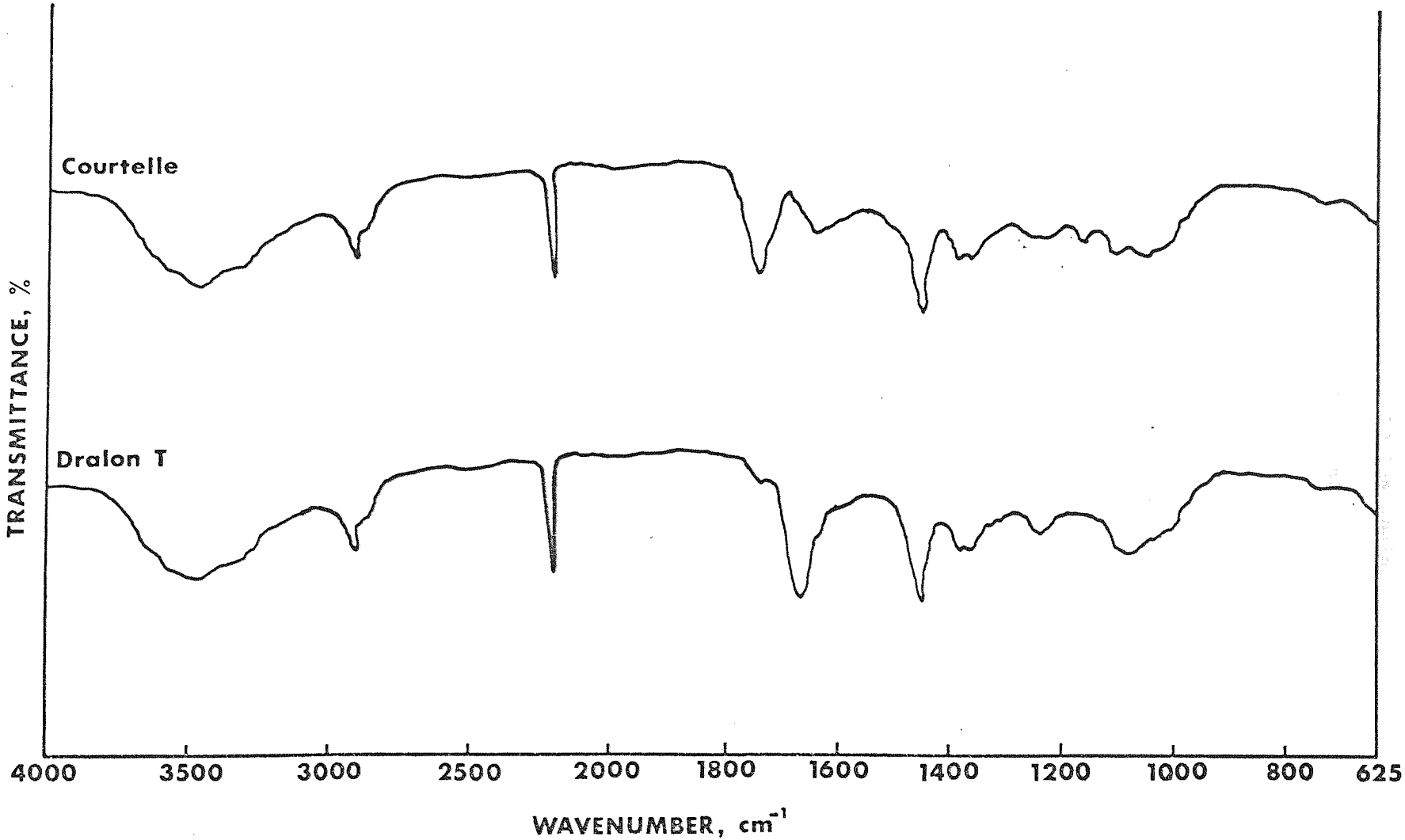

V Stretching, V_s and V_a, symmetric and antisymmetric stretching deformations.

δ Bending or deformation perpendicular to the chain.

ω Wagging or deformation parallel to the chain.

r Rocking, t twisting.

sh denotes unresolved shoulder.

vs very strong.

m medium strength.

vw very weak.

Figure 5.1 shows the infra-red spectra for Courtelle and Dralon T. The peaks in both spectra correspond quite accurately with the assignments given in table 5.1. There are additional peaks in both spectra. The peaks at 1,630 and 1,735 cm^{-1} in the Courtelle spectrum are due to absorptions by the methylacrylate copolymer. The peak at 1,670 in the Dralon T spectrum has been found to stem from a surface oil, which is applied for handling purposes by the manufacturer. This is usually removed by washing in methylene chloride.

5.11 The determination of group concentrations in the polymer.

The loss of nitrile and hydrogen from the polymer have been followed by the measurement of the peak amplitude with heat treatment of the characteristic bands in the spectra. The band intensities can be converted to a concentration value for the group concerned, as long as the extinction coefficient for their absorption frequency remains unchanged. The calculations are made using the Lambert-Beer law, which relates the fraction of the infra-red radiation transmitted to the concentration of the absorbing groups.

The Lambert-Beer Law.

$$I = I_o e^{-xc} \qquad \ldots\ldots (1)$$

I is the intensity of the infra-red radiation transmitted.

I_o is the intensity of the incident radiation.

c is the concentration of the sample, in this case it is directly proportional to the sample weight.

x is the extinction coefficient, which is assumed to be independent of the degree of heat treatment.

$$\log\left(\frac{I}{I_o}\right) = -x\,c \qquad \ldots\ldots (2)$$

For any given absorption band, the value of I_o is the transmittance of the peak base line and I is the peak transmittance. To obtain the fractional concentration of a group in a treated specimen as compared to the precursor, the ratio of expression (2) for the sample is divided by the same expression for the precursor.

$$\%\text{ of absorbing group} = \frac{\log\left(\frac{I}{I_o}\right)\text{sample}}{\log\left(\frac{I}{I_o}\right)\text{precursor}}$$

5.2 THE CHANGES IN THE INFRA-RED SPECTRA WITH HEAT TREATMENT.

Infra-red spectra were determined for the series of heat treated samples previously described in chapter 4, section 4.71. The infra-red spectral changes were very similar for the heat treated Courtelle and Dralon T sample series, except that their dependence on time and temperature were very different.

Figure 5.2(a) shows the spectra for a selection of the oxidised Courtelle samples for the temperature range 0 to 260°C. This is the temperature range in which the reaction exotherm takes place (figure 4.71(a)). The nitrile absorption band at 2,240 cm^{-1} decays a great deal in this temperature range, the 260°C sample has only approximately 20% of residual nitriles. The fibre also undergoes the colouration reaction and becomes completely blackened by 240°C. The

FIGURE 5·2(a)

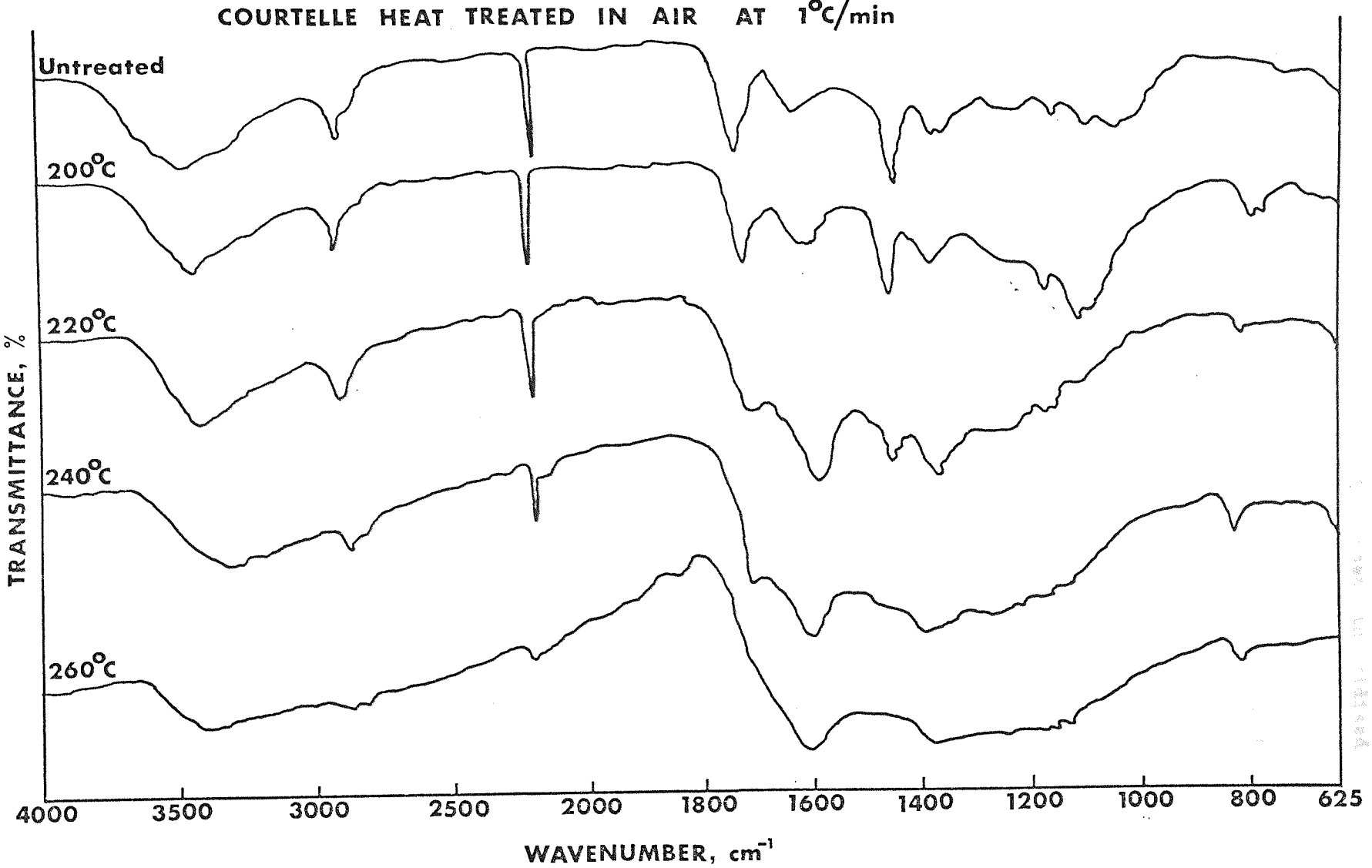
COURTELLE HEAT TREATED IN AIR AT 1°C/min
Untreated
200°C
220°C
240°C
260°C
TRANSMITTANCE, %
4000
3500
3000
2500
2000
1800
1600
1400
1200
1000
800
625
WAVENUMBER, cm⁻¹

copolymer absorption bands at 1,630 cm^{-1} and 1,735 cm^{-1} decay and disappear during this heat treatment. The shoulder at 1,700 cm^{-1} is due to an additional absorption and is also present in oxidised Dralon T fibre, which does not contain any copolymer.

Other major changes with oxidation are the development of a broad band at 1,600 cm^{-1} and the decline in the bands due to the (CH_2) stretching and bending absorptions (the 2,940 and 1,453 cm^{-1} bands, respectively). The 1,600 cm^{-1} absorption is generally attributed to the development of unsaturation in the molecule, either by the formation of polyimine groups [89], [61] or polyenes [63], [64], although either bond sequence will produce a strong absorption in this region of the spectra. The absorption which develops at about 800 cm^{-1} has been attributed to the (CH) wagging absorption in polyene sequences [62], [64]

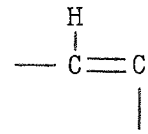

. The broad absorption between 4,000 and 3,000 cm^{-1} might be for absorbed moisture, for although the fibre is thoroughly dried before pressing the KBr disc, oxidised fibre is highly hydrophilic. Hydroperoxides and hydroxyl groups may also be contributing in this region. The nitrile absorption at 2,240 cm^{-1} becomes a double peak as the heat treatment progresses. This has been attributed to the formation of a polyene,[64] as nitrile groups pendent upon unsaturated segments of the chain would suffer a frequency shift of this order. Grassie and Mcguchan [79] attribute it to the formation of an α-iminonitrile group, by the reaction of hydrogen cyanide with the nitriles.

Figure 5.2(b) illustrates the changes which accompany the inert heat treatment of acrylic fibres. The three spectra in the figure are for the Dralon T fibre which was heated to 234°C in argon and found to have a variegated colour (section 4.71). This colouration was found to deepen after a short period of exposure to the atmosphere; the bright

FIGURE 5·2(b)

DRALON T, HEATED TO 234°C IN ARGON

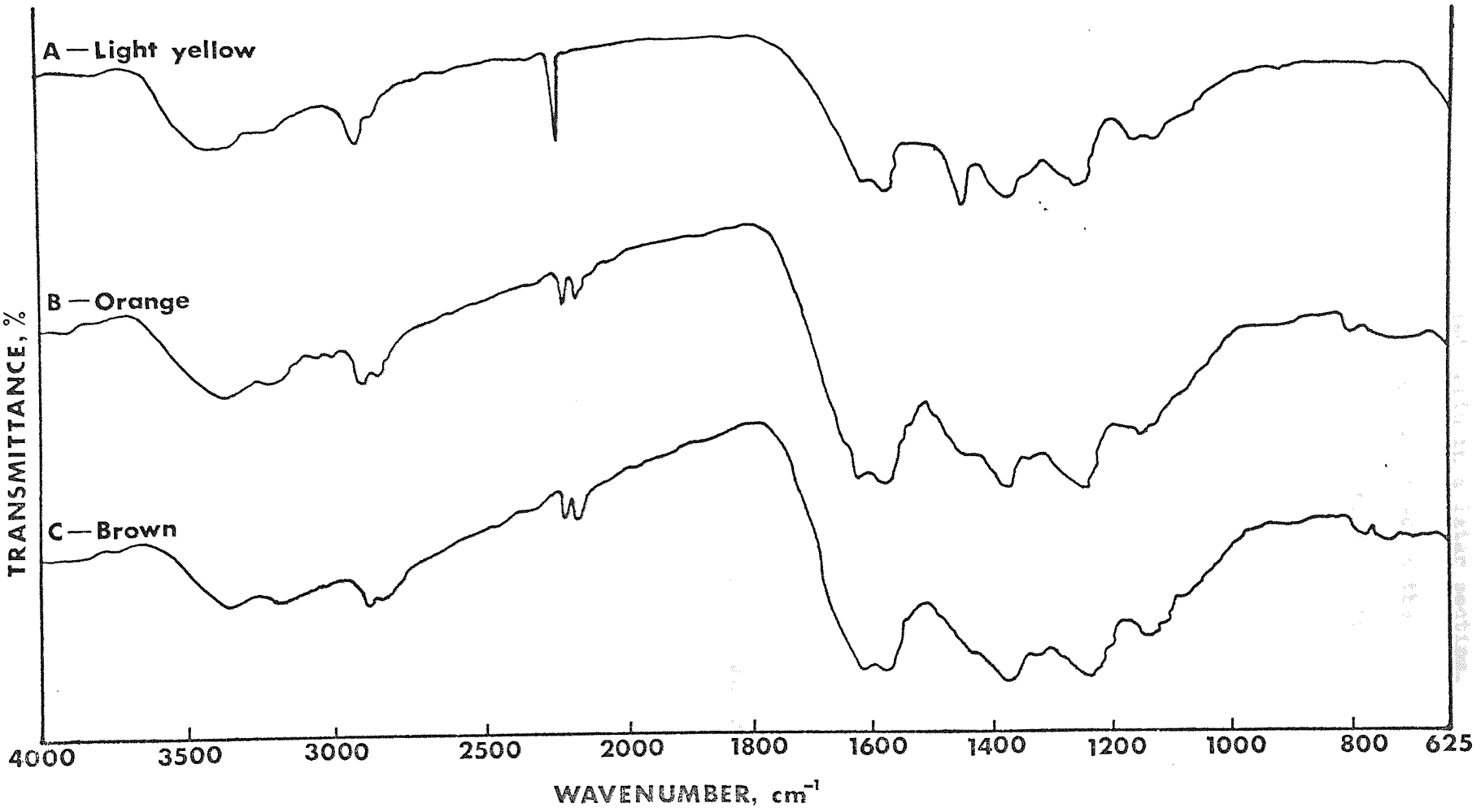

yellow fraction turned orange and the orange fraction became dark brown. This phenomena will be discussed again in a later section. However, the spectra are typical of the many published in the literature,[59, 60, 61, 78] and they are very interesting spectra, because the material has been divided purely on the basis of colour; the heat treatments are nominally the same. Courtelle undergoes identical spectral changes for inert heat treatments between 200 and 260°C.

As with the oxidised fibre, the nitrile absorption has decayed a great deal with the development of colour and the loss of the reaction exotherm (figure 4.71(b)). There is also the appearance of a second peak adjacent to the nitrile stretching absorption. The broad band at 1,600 cm^{-1} appears again, but for the pyrolysed acrylics this is partially resolved into two absorptions. The same is true for the absorption in the region of 800 cm^{-1}; the oxidised fibre had just one band here; in the pyrolysed fibre it is resolved into two. The major difference between inert heat treated and oxidised fibre is the appearance of a large band at 1,250 cm^{-1}, to be seen in figure 5.2(b). (This band appears before the chromophore.) The small band having this wave number in the precursor disappears upon oxidation, but with inert heat treatment it increases in size, prior to any diminution in the exotherm. It is particularly large in Dralon T.

These additional features of the pyrolysed polymer (including the band at 3,200 cm^{-1} and 1,150 cm^{-1}) are quite possibly the result of various types of amine group, produced by heat treatment [111] but not necessarily as a result of the exothermic/colouration reaction.

5.3 THE CHANGE IN NITRILE CONTENT WITH HEAT TREATMENT.

The nitrile contents have been calculated for the Courtelle and Dralon T series, using the Lambert-Beer law, with the 2,240 cm^{-1} nitrile stretching absorption band.

FIGURE 5·31(a)

NITRILE DECAY WITH TEMPERATURE IN COURTELLE

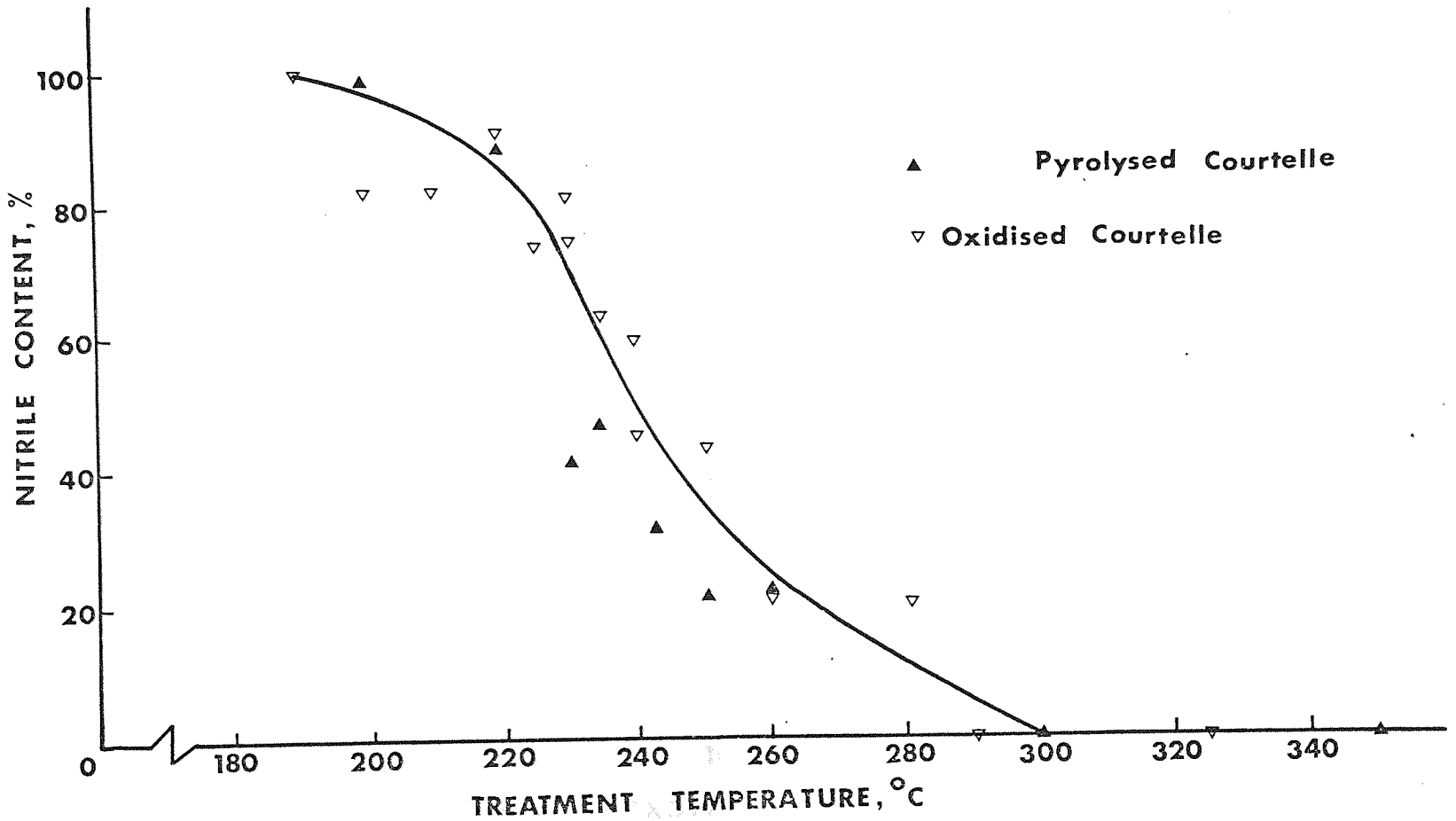

FIGURE 5·31(b)

THE EXOTHERM AS A FUNCTION OF NITRILE CONTENT

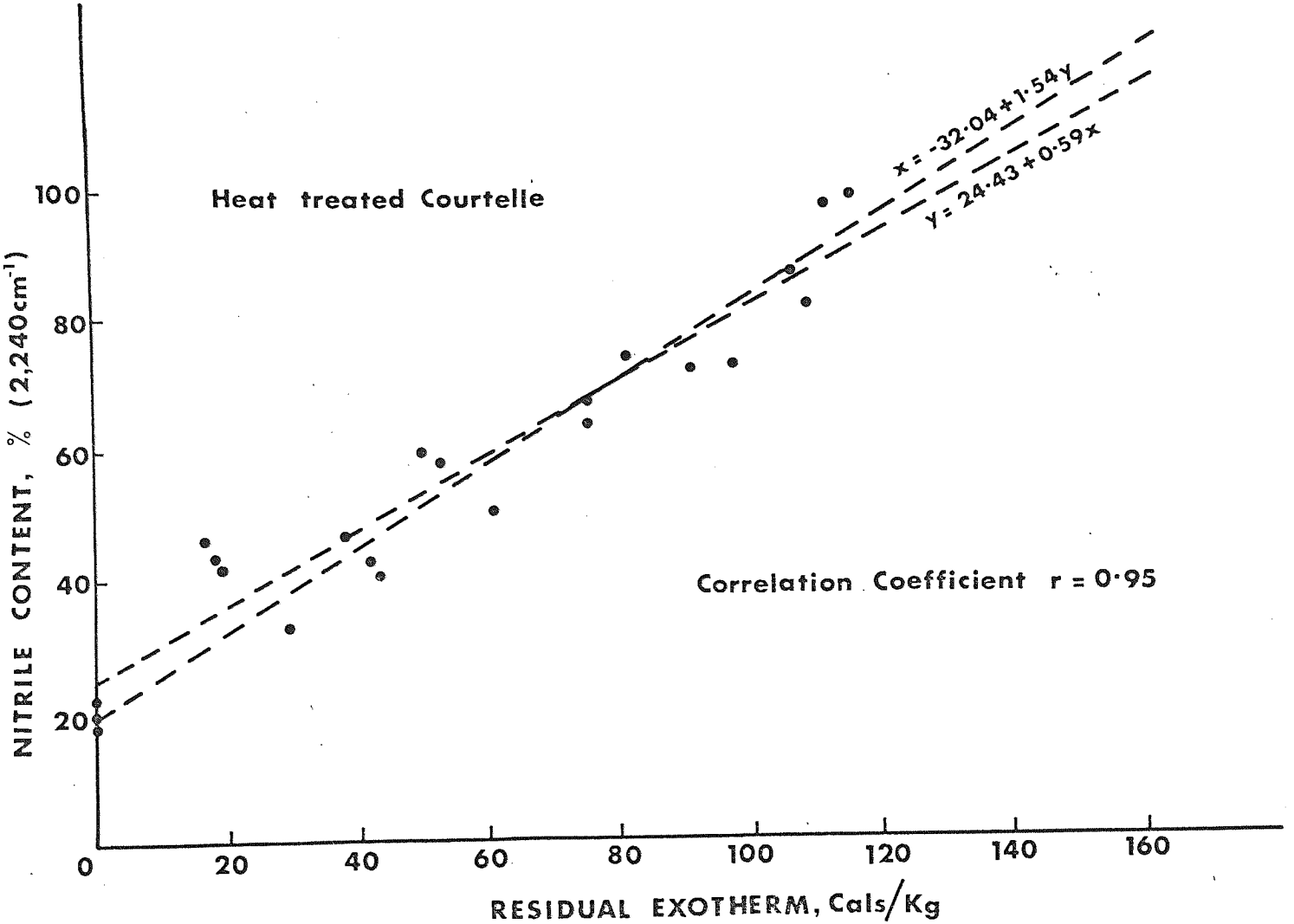

5.31 The decay in nitrile content with the degree of heat treatment, for Courtelle.

Figure 5.31(a) is a plot of the nitrile contents versus temperature, for the heat treatment series conducted in air and argon. Comparing this figure to figure 4.71(a), it can be seen that the decay in the residual exotherm corresponds to the loss of the first 80% of the nitrile groups. The final 20% fraction may be lost by a non-exothermic reaction, possibly by the elimination of HCN [56] and NH_3.

The loss of the nitrile groups appears to correlate with the loss of the residual exotherm and to examine this possibility figure 5.31(b) was plotted. This figure shows the regression lines calculated for the data, with the relevant straight line functions printed by each line. The data in the figure is from the sample series plotted in figures 4.71(a) and 5.31(a), plus a number of samples prepared by isothermal heat treatments in both air and argon. The correlation coefficient of 0.95 is very good indeed for data of this type.

The regression lines represent the extremes within which a reasonable straight line fit would lie for this data. A line drawn centrally between the regression lines intercepts the ordinate at a nitrile content of 22%. Yu and Noh [83] calculate that 19.2% would be left, if the self initiation hypothesis is accepted and they obtained an experimental value for the residue of 19 to 22%.

5.32 The decay in nitrile content with the degree of heat treatment, for Dralon T.

The decay in the nitrile concentration of Dralon T with heat treatment in air and argon is shown in figure 5.32(a). The nitrile contents have declined prior to any diminution in the reaction exotherm (figure 4.71(b)), although the fibre has coloured to some extent. In argon the fibre turns light yellow just before the sharp drop in the exotherm takes place, at 234°C. In air, it turns dark brown by 250°C, just prior to the general decline in the residual exotherm.

FIGURE 5·32(a)

NITRILE DECAY WITH TEMPERATURE IN DRALON T

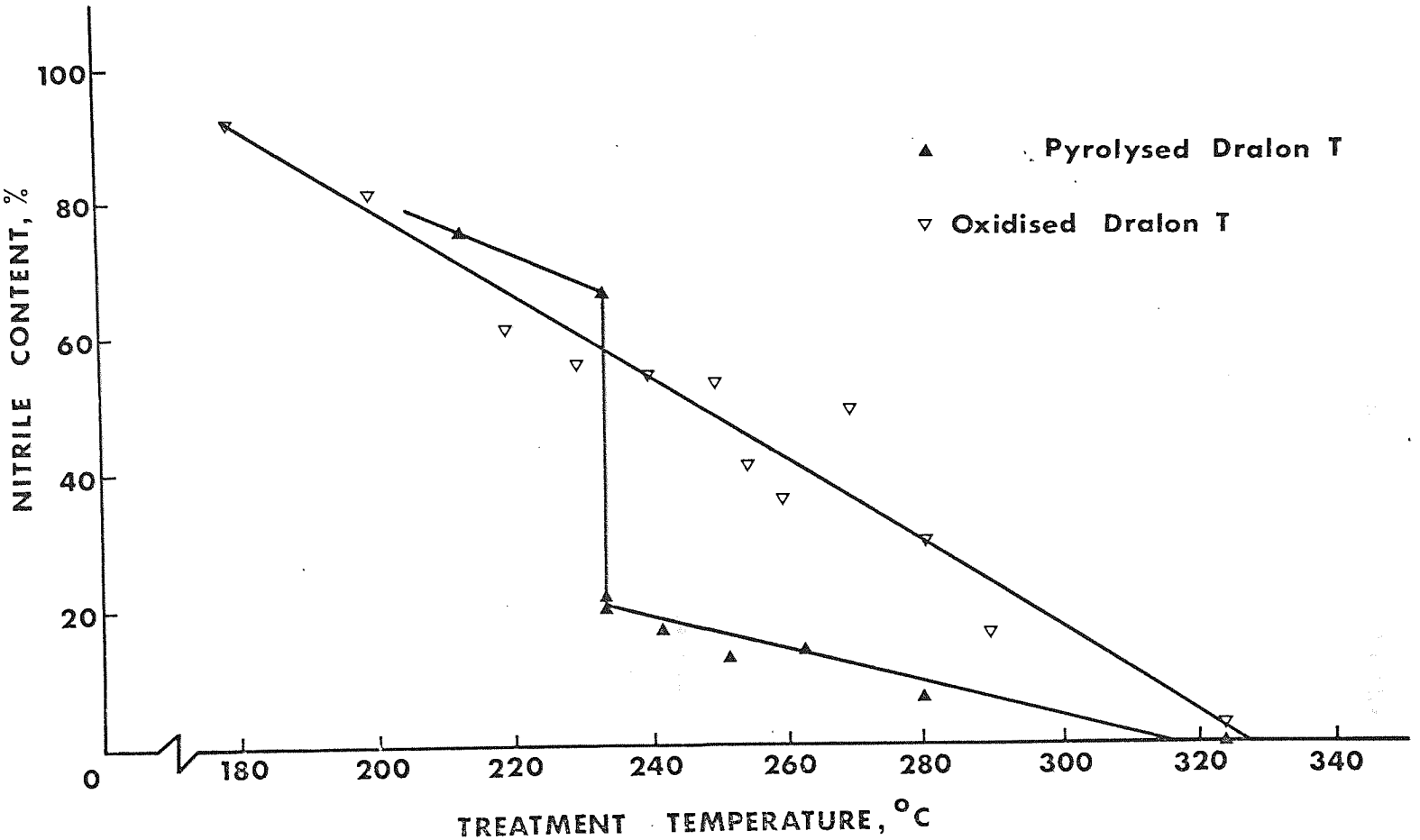

The sharp drop in the nitrile content at 234°C corresponds to the sharp drop in the residual exotherm and the sudden development of a darker chromophore. This indicates that the nitrile groups are probably involved in the exothermic/colouration reaction. While the nitrile concentration in Courtelle decays in much the same way for inert and oxidising heat treatments, the behaviour of Dralon T is quite different. The nitrile content of the oxidised Dralon T series decays very gradually, as does the residual exotherm. In a similar fashion to Courtelle, a small fraction of the nitriles remains to be lost after the complete removal of the residual exotherm.

The evidence suggests that there must be at least two reactions responsible for the loss of the nitrile infra-red absorption band in Courtelle, and at least three reactions responsible in Dralon T. A plot of the nitrile concentration versus the residual exotherm for Dralon T is shown in figure 5.32(b), and it supports this conclusion. A reasonable straight line correlation of the data is not obtained until after 45% of the nitriles have been lost. If this straight line is extrapolated back to the original exotherm value of 90 Cals/Kg, it is found that 40% of the nitrile groups are lost initially, without contributing to the reaction exotherm. The best straight line fit intercepts the ordinate at an approximately 20% nitrile residue. This figure agrees very well with the similar Courtelle result (see figure 5.31(b)) and with the value determined by Yu and Noh [83].

If the exothermic heat is due to a reaction which involves the nitrile groups (and the evidence is now very strongly for this) there must be at least three reactions involved in the loss of nitrile groups from Dralon T. The first 40% of the groups are lost without the evolution of heat and without any volatiles evolution (this latter observation is confirmed by the work of Grassie and Mcguchan [79]).

FIGURE 5·32(b)

THE EXOTHERM AS A FUNCTION OF NITRILE CONTENT

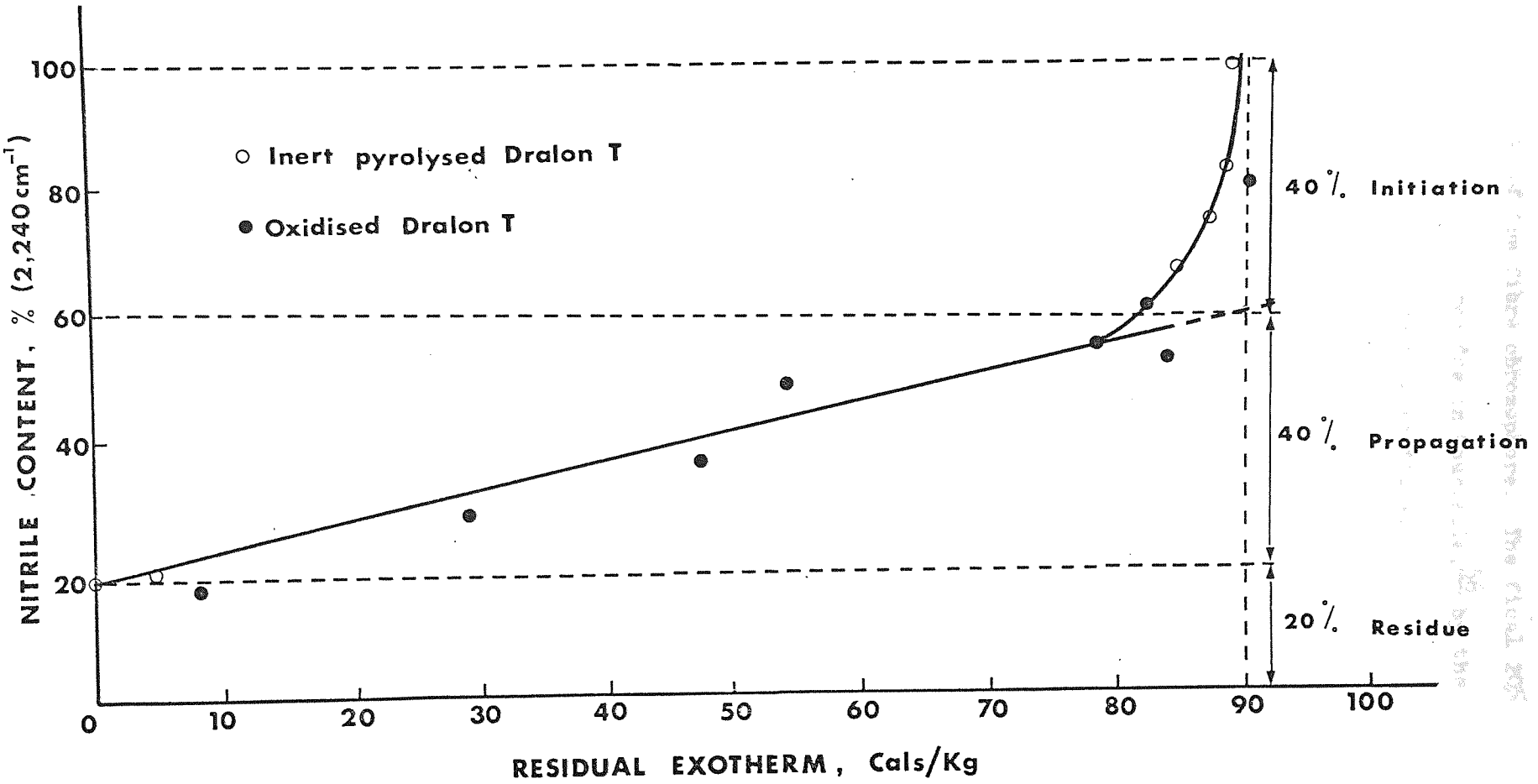

40% of the nitriles are then lost by the evolution of heat and a considerable intensification of the fibre chromophore. The final 20% residue may well be lost, as with the residue in Courtelle,[56] by the evolution of NH_3 and HCN, with no accompanying exotherm.

5.4 THE OXIDATION OF COURTELLE AND DRALON T.

The heat treatment of Courtelle and Dralon T in air produces a dehydrogenation of the polymers and the absorption and chemical combination of oxygen. Inert heat treatments also produce a dehydrogenation, particularly at high temperatures, when NH_3 and HCN are evolved. The author has further found that pyrolysed Dralon T (and Courtelle to a smaller extent) will react with oxygen at room temperature and absorb quite large quantities of oxygen in a surprisingly short time. However, it is the hydrogen losses during heat treatment which are of interest here and these are much greater with air heat treatment; this is illustrated for Courtelle in table 5.4, below.

Table 5.4

% of original hydrogen content in heat treated Courtelle fibre.

Heat treatment temperature °C	Heat treatment in argon	Heat treatment in air
180	100 %	100 %
200	98.7	93.5
220	98.7	92.0
240	97.1	70.9
260	95.0	63.2
330	75.8	47.0

FIGURE 5·4 (a)

DECLINE IN METHYLENE HYDROGEN WITH HEAT TREATMENT

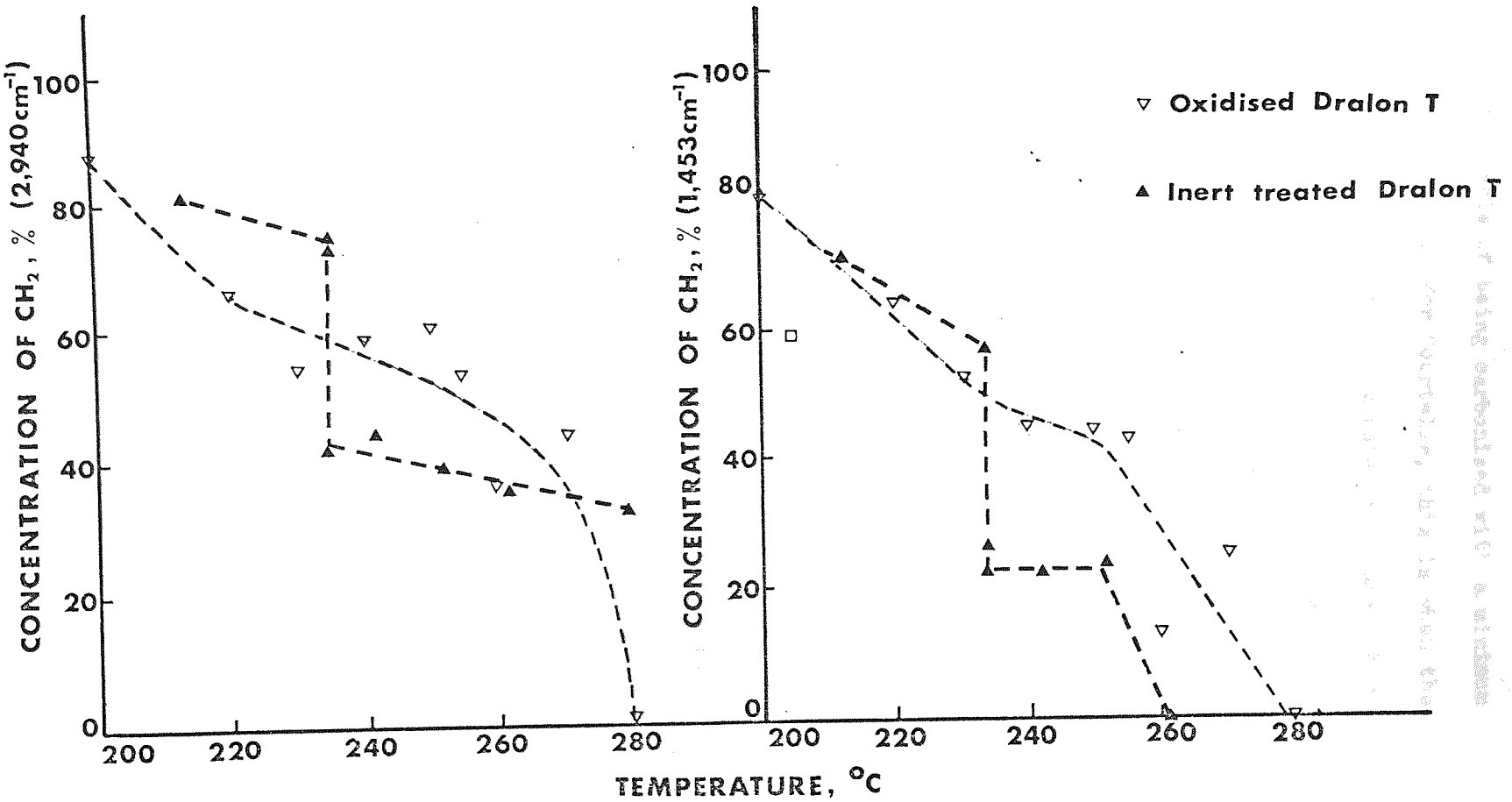

The oxygen contents are quite large once the fibre has become sufficiently stable to be capable of being carbonised with a minimum amount of weight loss and shrinkage. For Courtelle, this is when the fibre has been heated to 260°C, using the 1°C/minute programme. For a 37% loss of hydrogen, this sample has absorbed 10.1% of oxygen by weight. Dralon T requires a greater degree of oxidation than Courtelle (this fibre is less reactive than Courtelle under oxidising conditions, in almost every respect). At 260°C it has absorbed 8.2% by weight of oxygen; it is not completely stabilised until 280°C, when it has absorbed about 10%.

The most significant infra-red spectral changes during oxidation are the attenuation in the (CH_2) bands at 2,940 and 1,453 cm^{-1} and the growth in the (CH) bands at 2,920 and 1,375 cm^{-1}. Ultimately, of course, the (CH) bands decay also, but their growth between 200 and 260°C in Courtelle and 220 to 280°C in Dralon T is an indication that the oxidation is initially by attack on the methylene bridge. This is in complete agreement with the findings of Peebles et al.[69, 71]

Figure 5.4(a) shows plots of the hydrogen contents determined from the (CH_2) absorption bands for oxidised and pyrolysed Dralon T. The hydrogen loss from the pyrolysed fibre is almost all entirely due to oxidation in the atmosphere after heat treatment. This was a recent discovery by the author of an effect that has very probably affected a number of the published findings on the pyrolysis of polyacrylonitrile.[75] The stretching absorption (2,940 cm^{-1}) is lost more slowly than the bending absorption (1,453 cm^{-1}), but this latter band is a sharper absorption and probably more unambiguous as a measure of the concentration of (CH_2) groups. According to this latter absorption all the methylene hydrogens have been oxidised (to produce hydroperoxides) to leave perhaps one (CH) group at the methylene bridge and the products of the breakdown of the hydroperoxides. A plot of the weight content of hydrogen versus the fraction of (CH_2)

FIGURE 5·4(b)

CORRELATION OF HYDROGEN CONTENTS DETERMINED BY ELEMENTAL ANALYSIS AND INFRA RED ANALYSIS

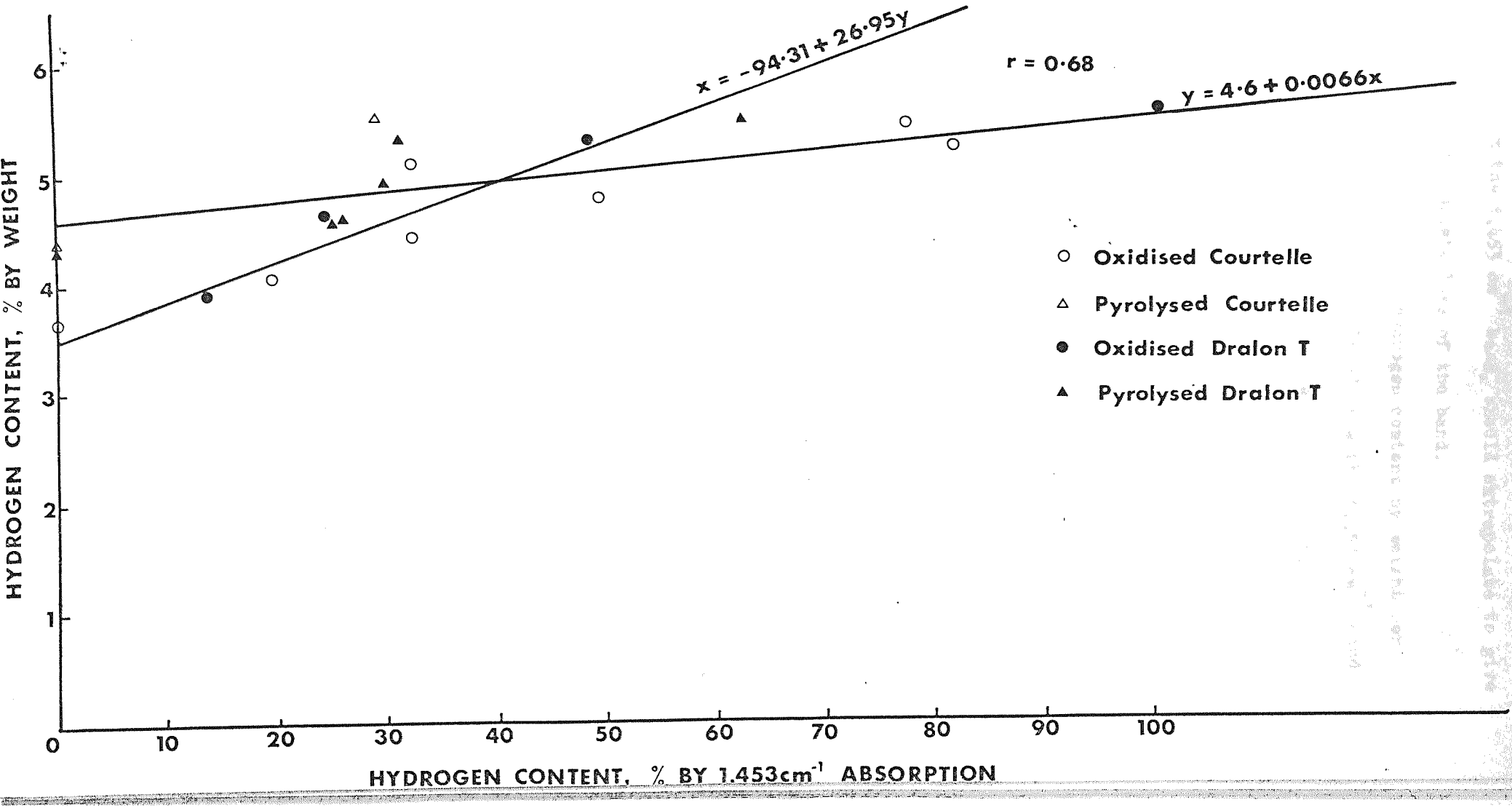

groups, calculated from the 1,453 cm^{-1} band, should extrapolate to give a fraction of $\frac{1}{3}$ for the complete loss of the band.

Figure 5.4(b) is a plot of the hydrogen content by weight per cent versus the hydrogen content calculated from the 1,453 cm^{-1} band intensity, for oxidised Dralon T and Courtelle and a number of the pyrolysed samples. The lines in the figure are for the regression analysis equations, each of which is printed along the appropriate line. The correlation coefficient (r) for the data is 0.68, which is a reasonable degree of correlation. (It is better if the oxidised and pyrolysed results are plotted separately.) The intercepts of the regression lines on the ordinate give the range in which the residual hydrogen content lies, as from 61.9 to 79.5%. Any value in this range would be a reasonable result, given the accuracy of the data. A single best fit straight line produces 30% as the amount of hydrogen lost with the total disappearance of the (CH_2) bending absorption. This is in reasonable agreement with the expected fraction of $\frac{1}{3}$.

The correlation of the (CH_2) stretching band intensity with the hydrogen contents of the heat treated samples of Courtelle and Dralon T is very good. The regression lines have been calculated for the data and these are shown in figure 5.4(c) with the equations of the lines, as before. The correlation coefficient (r) is 0.91, which indicates very good correlation. The intercept for the best fit straight line on the ordinate is at 3% hydrogen content. Clearly more than just the one third dehydrogenation expected, if one of each of the methylene hydrogens were lost. The 2,940 cm^{-1} absorption band also receives a contribution from the neighbouring 2,920 cm^{-1} band and so the loss of (CH) groups will contribute to the total attenuation in the band.

Not very much can really be deduced about the structure of the oxidised fibres from the infra-red data published in this section. The data in figures 5.4(a) to 5.4(c) shows that the hydrogen loss is mainly

FIGURE 5·4(c)

CORRELATION OF HYDROGEN CONTENTS DETERMINED BY ELEMENTAL ANALYSIS AND INFRA RED ANALYSIS

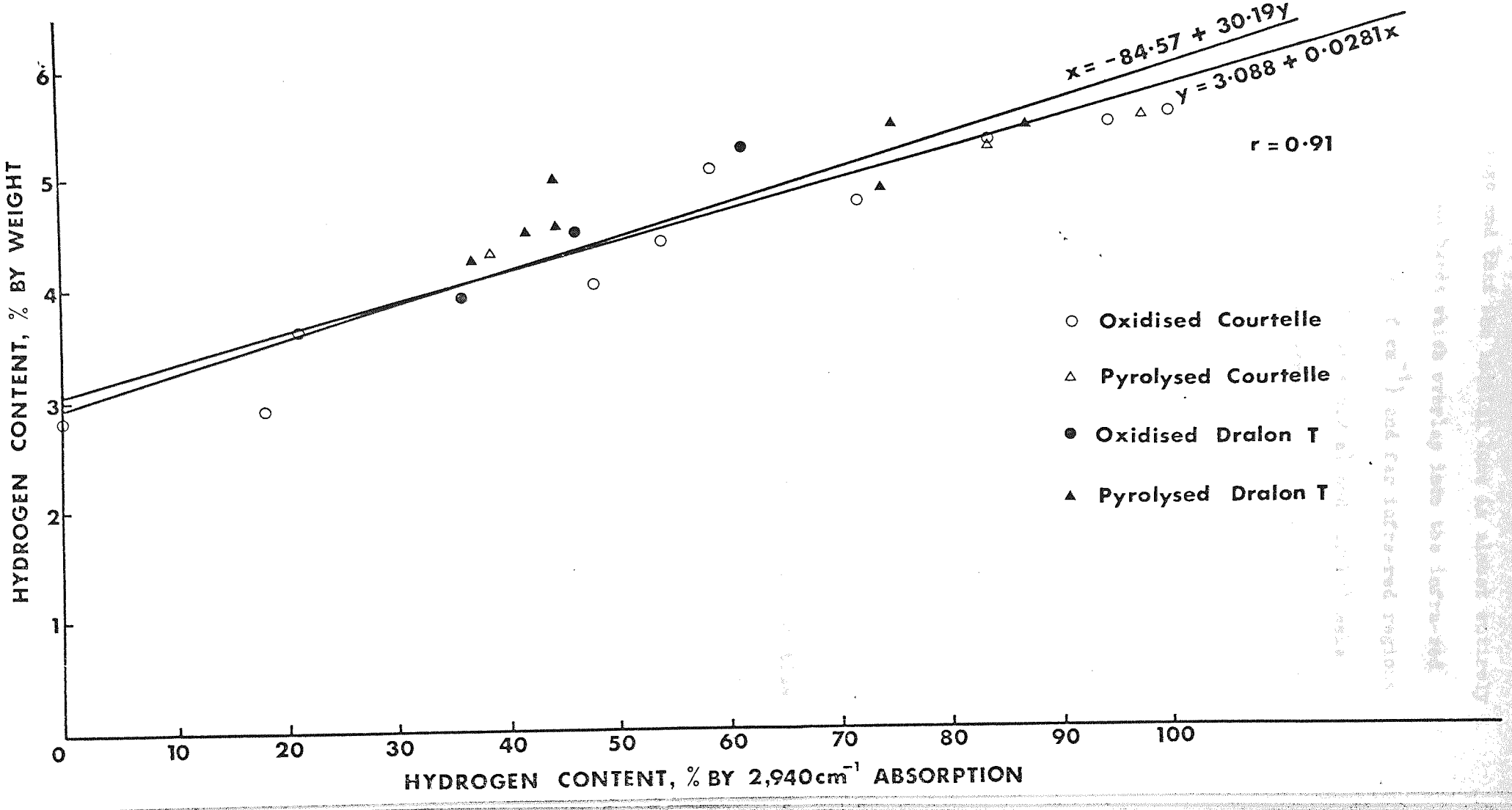

from the methylene bridge and that the initial loss is almost entirely from this source. The broad bands which overlap into the infra-red region of the visible (high values of cm^{-1}) and far infra-red regions of the spectra (see the spectra in figures 5.2(a) and 5.2(b)) make detailed assignments impossible. However, there is a broad shoulder extending from 1600 cm^{-1} to 1800 cm^{-1}, which suggests that oxygen is contained in the polymer in the form of carbonyl and carboxylic acid groups.[111] There is no evidence at all of nitrone as postulated by Peebles et al [69, 71, 90] as this should produce absorptions at 1,290 and 980 cm^{-1}. [112] Equally, there is no evidence for the epoxide type of structure suggested by Standage and Matkowsky,[94] as many of the absorptions they observe are not present in the Courtelle and Dralon T spectra.

5.5 ACRYLIC FIBRE OXIDATION AT ROOM TEMPERATURE.

A number of researchers have commented on the observation that inertly heated acrylic fibres deepen in colour over a period of time by just standing in air.[79, 113] This happens with Courtelle and Dralon N; the dark orange fibre products of the completed exothermic reaction gradually turn to a dark brown colour. With Dralon T the effect is more striking, possibly because the colour immediately after the exotherm is a much lighter orange than the other acrylics. Within a few days it turns dark brown and over a number of weeks it will turn black. The colouration is accompanied by the absorption of oxygen and a reduction in the hydrogen content. It has probably not been recognised that an oxidising reaction was involved, because most workers have been examining acrylics which contain copolymers with oxygen containing groups. Kennedy and Fontana [75] reported unexplained anomalous elemental compositions, suggesting a high degree of oxygen absorption, for a polymer which behaved very similarly to Dralon T. They did not mention sample darkening, however. The first explanation of the effect that comes to mind is the nitrone forming reaction of Peebles et al.

However, there are no signs of an increase in infra-red absorption at 1,290 cm^{-1} and 980 cm^{-1}, characteristic of the nitrone group, with increasing oxygen contents. Table 5.5(a) below gives an elemental analysis of the three inert heated Dralon T samples previously discussed in sections 4.71 and 5.2.

Table 5.5(a)

Dralon T, pyrolysed to 234°C.	Carbon %	Nitrogen %	Hydrogen %	Remainder %
A. Yellow sample	66.7(0)	25.3(0)	5.5(1)	2.4(9)
B. Orange sample	64.7(6)	23.7(0)	4.9(4)	6.5(9)
C. Brown sample	63.5(8)	23.1(5)	4.5(7)	8.7(0)

The proportions of each element are in weight percentages; the amount of oxygen absorbed is assumed to be the same as the remainder. When originally removed from the furnace, the three samples were very much lighter in colour; sample C was only light orange. All the samples have absorbed oxygen in proportion to the degree of reaction achieved during the heat treatment. The proportionate loss in hydrogen is approximately 20% compared to about 5% loss in the carbon fraction and roughly 8% in the nitrogen fraction. It appears, therefore, that the reaction has depleted the hydrogen content and possibly the nitrogen content, forming an additional chromophore in the process.

Although the greatest care was taken to eliminate possible oxygen pollution of the furnace atmosphere during pyrolysis, it was considered wise to conduct a parallel experiment in which the exclusion of oxygen was guaranteed. Dralon T fibre was taken and chopped very finely and packed into two pyrex tubes. These were then evacuated and carefully sealed using a gas torch to melt the tubes either side of the sample.

Both tubes were then tied together upon a thermocouple probe and placed along the axis of the furnace, which was also evacuated. The specimens were then heated at $\frac{15}{12}$ °C/minute to 252°C, a temperature at which the exothermic reaction was completed. After cooling, the tubes were removed from the furnace and one of them broken open to expose the sample to the atmosphere. This sample was then placed in a large sample tube and kept under observation for a week. Both samples were originally light orange, but as the week progressed the exposed sample turned dark brown. When the sample tube was originally broken open, pungent fumes emanated which were redolent of HCN and NH_3. Keeping the sample in the large sample tube produced a further accumulation of pungent fumes, which could be smelt when the cap was first removed. The second of the tubes was opened just before the sample was required for analysis, and it was only exposed to the atmosphere for as long as it took to prepare a KBr disc and a sample for elemental analysis. The elemental compositions of the samples are shown in Table 5.5(b) below, and the infra-red spectra are shown in figure 5.5.

Table 5.5(b)

Dralon T, pyrolysed to 252°C.	Carbon %	Nitrogen %	Hydrogen %	Remainder %
Unexposed sample control.	68.4(0)	23.9(9)	5.9(4)	1.5(7)
Exposed sample	65.7(9)	22.7(7)	5.0(8)	6.3(6)

The control sample contains a little oxygen, but this may be due to the absorption of water. Normally, samples are thoroughly dried before analysis, but this was not done in this case because speed was more important. The exposed sample had not absorbed as much oxygen as Sample C in table 5.5(a), probably because the exposure was not for such

FIGURE 5·5

DRALON T, HEATED TO 252°C IN VACUO

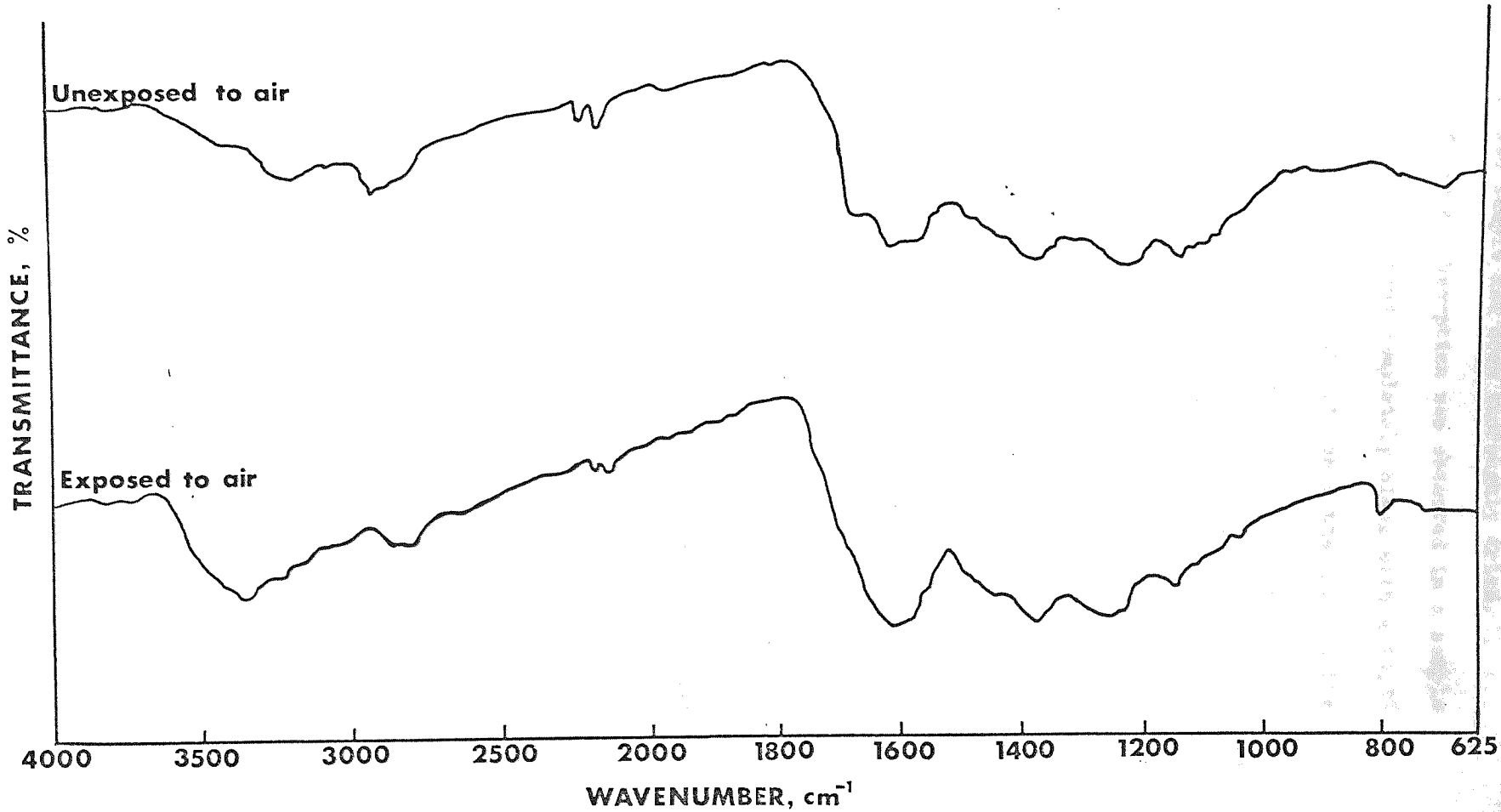

a long period. The exposed sample had been thoroughly dried.

The highest level of oxygen absorption was observed in a sample inert heated to 260°C which had turned completely black with a 10.3% oxygen content. The spectra in figure 5.5 both show the drop in the nitrile content expected, with a growth in absorption in the 1,600 cm^{-1} region. The exposed sample shows a very large increase in the 1,600 cm^{-1} region compared to the control and a much larger absorption at 800 cm^{-1}. This cannot be due to an increase in the imine content. The formation of unsaturated regions in the polymer backbone would have these consequences and it would also explain the deepening in colour of the exposed samples. The characteristic amine absorptions at 1,150, 1,250 and 3,200 cm^{-1} are present in both samples but there is a large increase in absorption at 3,400 cm^{-1} upon exposure, possibly due to an increase in OH group content.

Standage and Matkowsky have published observations of the room temperature oxidation of an almost pure polyacrylonitrile, which had been pyrolysed at 290°C.[113] This was after the author had conducted his experiments, which were carried out completely independently. Research at Rolls-Royce Ltd (Johnson, Rose and Jones, unpublished) shows that the ultra-violet irradiation of any pyrolysed acrylic, in the atmosphere, results in a deepening of the chromophore, the absorption of oxygen and a drastic reduction in the mechanical properties. A careful study of Standage and Matkowsky's oxygen absorption endotherm shows that the growth in the amount of oxygen absorbed has a diurnal pattern, as if the amount of oxidation was greatest during the hours of daylight and exposure to u.v..

5.6 THE SOLUBILITY OF HEAT TREATED COURTELLE AND DRALON T IN NITRIC ACID.

The solubility of heat treated acrylic fibres in nitric acid is a useful parameter, because taken together with the thermal, spectral and mechanical properties information, a very consistent picture of the

changes effected by pyrolysis and oxidation is presented.

The solubility of each sample was determined by immersing 0.1 grams of fibre in 100 ml. of 60% nitric acid solution, for a period of 50 hours. The dissolved fraction was determined by filtering the sample through a sintered glass crucible and washing through with 60% nitric acid. The liquid and fibrous fractions were dried at 150°C in a vacuum oven (a lower temperature, if the sample was originally heated to this temperature, or less) for 24 hours. The weight dissolved was calculated from both fractions and negligible errors were found in the results.

Solubility determinations were made for the heat treated series of Courtelle and Dralon T fibres for which the method of preparation is described in section 4.71. Figures 5.6(a) and 5.6(b) are plots of the solubility versus the peak treatment temperature for Courtelle and Dralon T heated in argon. Courtelle develops almost complete insolubility between 140 and 200°C, while Dralon T remains soluble until 490°C, where it behaves in an identical manner to Courtelle, becoming completely insoluble and remaining so throughout any further high temperature heat treatment.

The low temperature insolubility of Courtelle is very probably due to a cross-linking reaction; further evidence of this is the way in which the fibre swells to an enormous extent in the solution and can then be reprecipitated, by dilution with water, as separable fibres. There is no evidence at all of any comparable behaviour in Dralon T and there appears to be two possible explanations of this. Courtelle begins to colour and exotherm gradually at very low temperatures (the 160°C sample was light yellow) and the cross-linking reaction may be a concomitant of this; while Dralon T exotherms at high temperatures and does so rapidly, with a sudden development of colour. When Courtelle reaches the temperature range in which the major part of the exothermic reaction occurs (200 to 240°C, see figure 4.71(a)) the samples are re-solubilised in nitric acid, presumably due to the same

FIGURE 5·6(a)

PYROLYSED COURTELLE

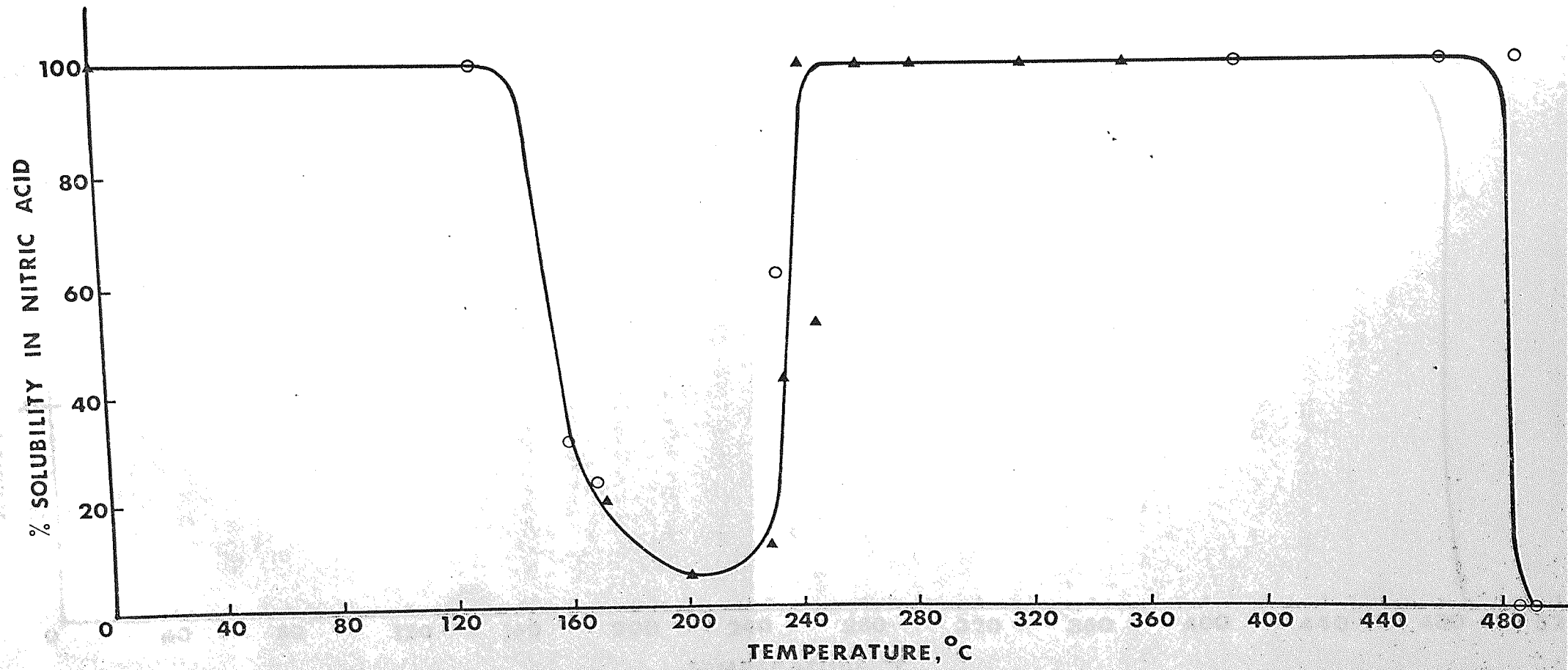

FIGURE 5·6(b)

PYROLYSED DRALON T

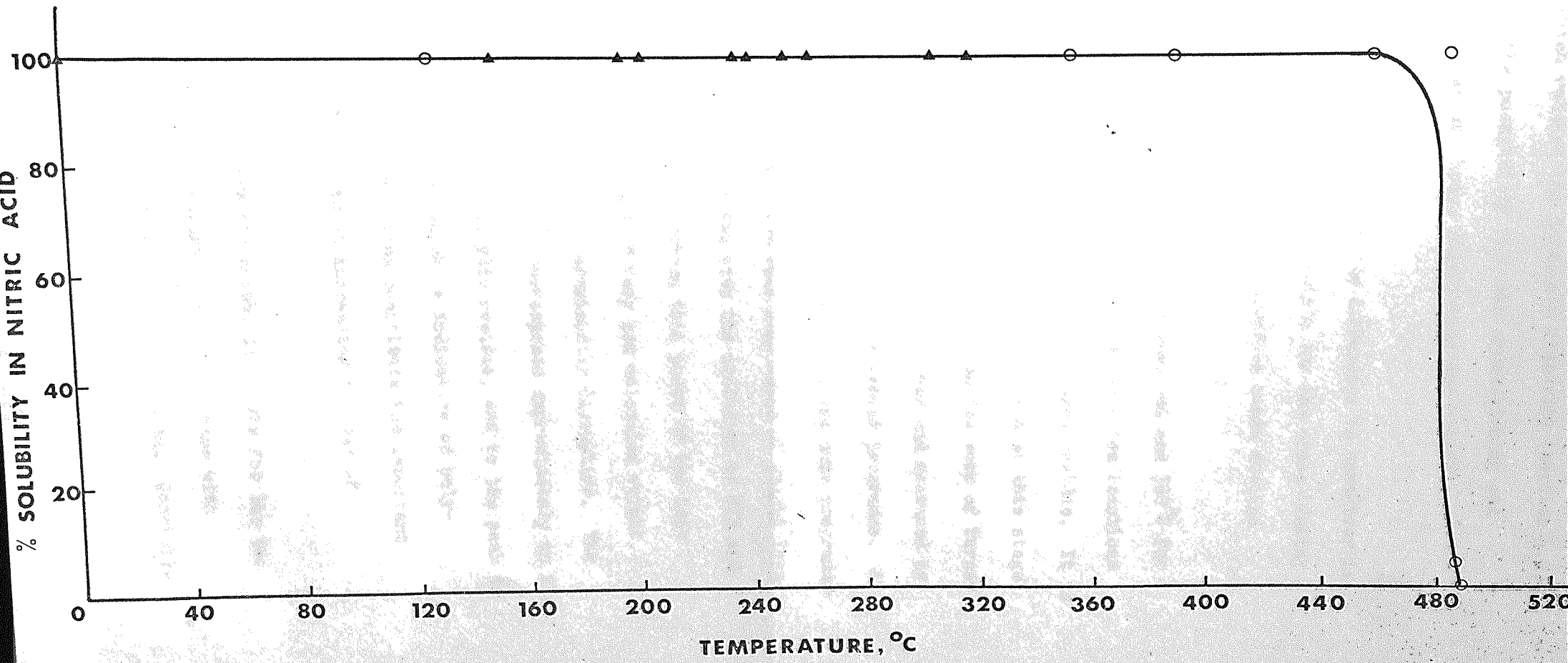

chain degradation, which reduces the intrinsic viscosity (section 4.2). In Dralon T there is the possibility that the cross-linking and degradation reactions overlap, hence eliminating any possible insolubility.

The other possible explanation of the difference in behaviour is that the copolymer in Courtelle is responsible for the cross-linking reaction. The methylacrylate infra-red absorption bands decline appreciably in the range 140 to 200°C.

The rapid development of insolubility between 480 and 500°C for Courtelle and Dralon T is evidence of the polycondensation reactions which are necessary for the formation of the carbonised residue. It is interesting to consider the nature of the gases evolved at this stage of the heat treatment. Figure 5.6(c) is taken from the work of Turner and Johnson (unpublished) and shows the gases evolved and measured by gas chromatography during a very similar heat treatment programme. A weight loss curve determined by thermogravimetry at the same programme rate is also shown in the figure. The very high rates of weight loss between 300°C and 480°C are associated with the evolution of HCN and the loss of tars from the residue. During this phase of the heat treatment the residue is soluble and of very low molecular weight. This suggests that the reactions are predominantly disruptive. The sudden drop in the solubility at 490°C corresponds approximately to the stabilisation of the weight of the acrylic residue, and to the peak in the rate of evolution of hydrogen, which is indicative of poly-condensation reactions. These reactions constitute the important carbonisation process which results in increasing degrees of crystallisation with temperature.

Figures 5.6(d) and 5.6(e) are the solubility plots for the two oxidised series of samples and contrary to the experience with pyrolysis, the two acrylics produce very similar results. Courtelle

FIGURE 5·6(c) GASES EVOLVED DURING CARBONISATION, FROM UNPRETREATED COURTELLE (Turner & Johnson)

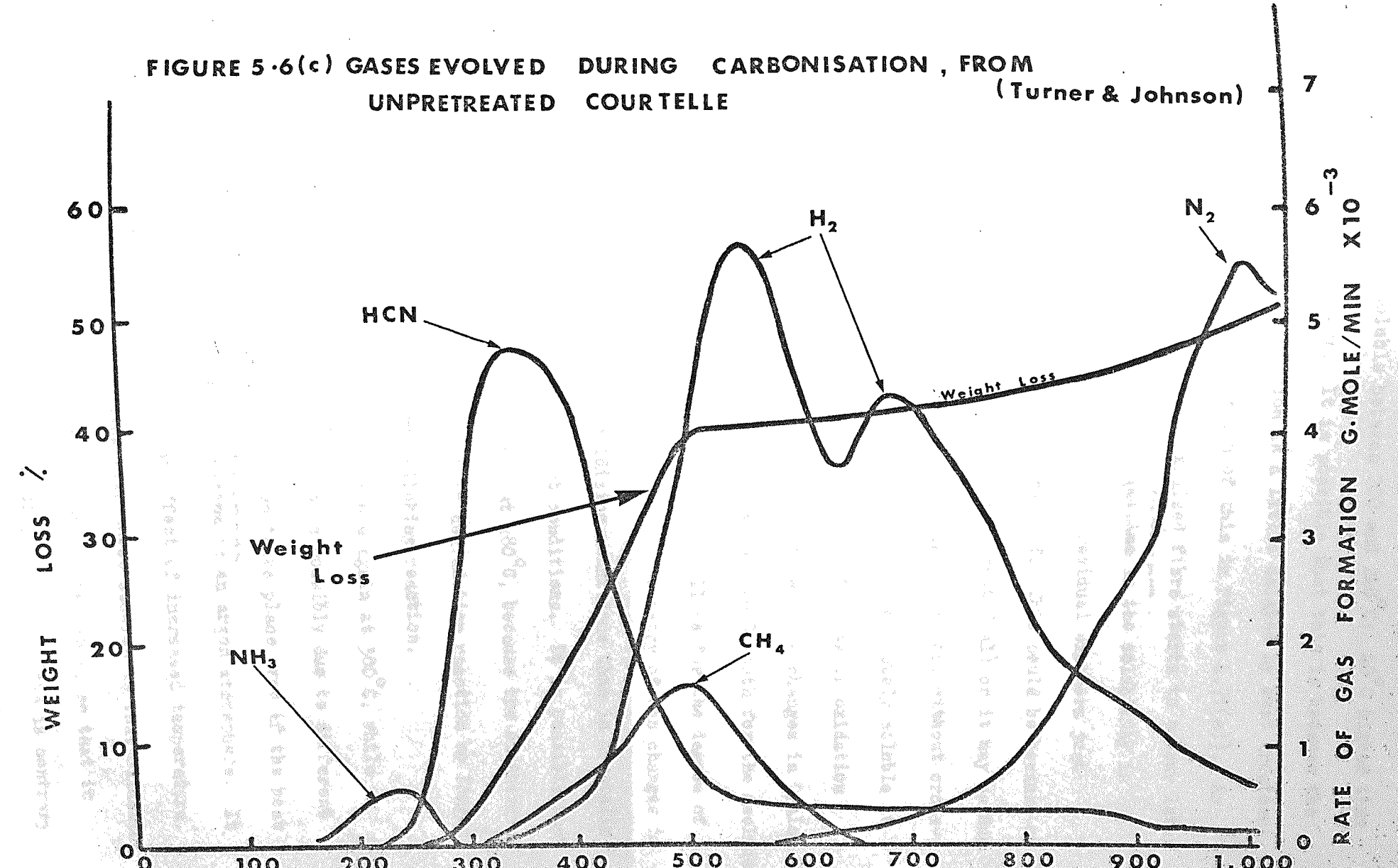

becomes partially insoluble between 200 and 240°C; 40°C higher than with inert heat treatment. It is possible that this is because the colouration/exothermic reaction is a little delayed by heat treatment in oxygen. (There is a suggestion of this in figure 4.71(a)). As figures 3.1(a) and (b) show, the oxidised fibre starts to colour later than pyrolysed Courtelle. The first minimum in the solubility is achieved at the temperature at which the residual exotherm just disappears, for both Courtelle and Dralon T. This could be because of partial cross-linking (the fibres swell a great deal) or it may be due to the formation of a structure of very high cohesion, without cross-links. The inert heat treated fibres are both completely soluble at precisely this same stage of the reaction. It is as if oxidation produces a more stable structure at this stage. The changes in Dralon T are lagging behind Courtelle by approximately 40°C, both for the decline in the exotherm and the nitrile content as well as for the degree of solubility. As observed in chapter 4, the chemistry of the changes in Dralon T are much slower under oxidising conditions than in Courtelle and very much slower than under inert conditions. It is possible that Dralon T becomes partially insoluble at 280°C, because the exothermic reaction is more gradual and the chain degradation reaction no longer overlaps a lower temperature cross-linking reaction.

Courtelle becomes completely soluble again at 300°C, while Dralon T only partially reverts; this is possibly due to different degrees of degradation. This reversion takes place even if the heat treatment is continued beyond the minimum in an argon atmosphere. It therefore appears to be entirely an effect of increased temperature.

The most significant finding with these studies is that oxidation brings about a progressive stabilisation of the fibre, so that it becomes gradually insoluble between 320 and 490°C. This is contrary behaviour to the inert heat treatments, which appear to induce increasing degrees of disruption in the fibre, until the sudden

FIGURE 5·6(d)

PREOXIDISED COURTELLE

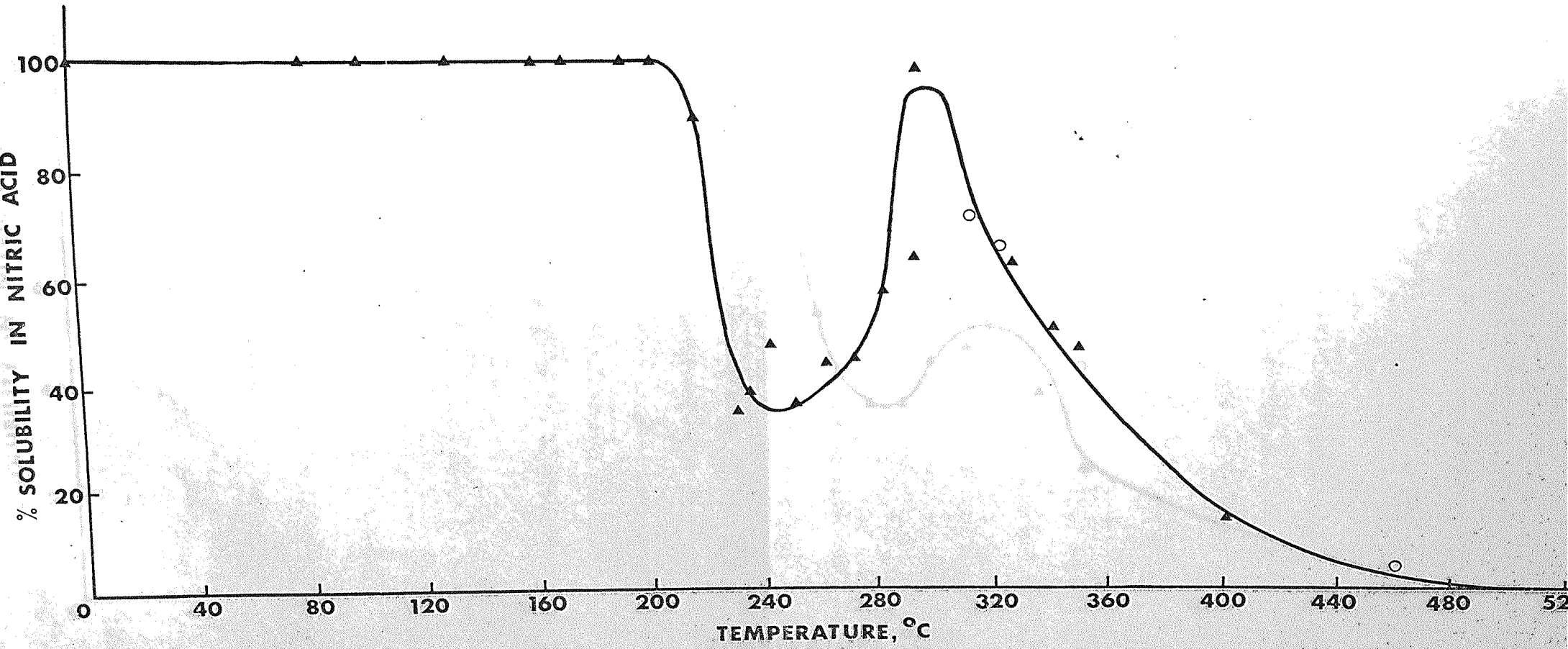

FIGURE 5·6(e)

PREOXIDISED DRALON T

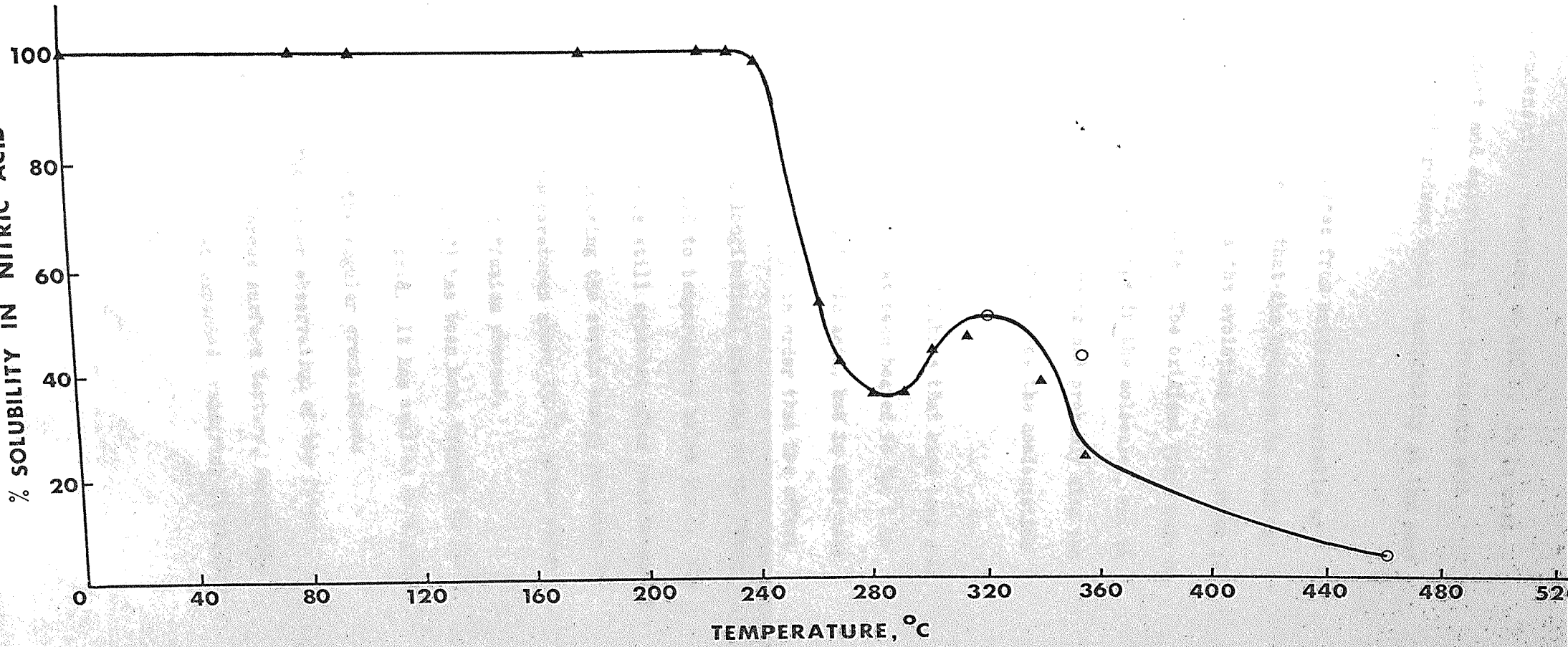

inception of the polycondensation reactions at 490°C. It is most interesting that both inert and oxidising heat treatments with Courtelle and Dralon T should produce total insolubility at the same temperature.

The analysis of the evolved gases from oxidised Courtelle at temperatures above 300°C, [114] reveals that the hydrogen is lost as HCN and water and beginning at 300°C is the evolution of CO_2, which is a major component of the gaseous products. The oxidised fibre must be condensing via the oxygen containing groups in the molecules, and it would appear that the presence of those groups and probably also the absence of a high hydrogen content is what enables the condensation processes to begin earlier.

Figure 5.6(f) shows SEM micrographs of fibres that have been acid treated. The pyrolysed Courtelle fibre has been heated to 340°C in argon. It will completely dissolve in formic acid, but in this case the reaction has been stopped prematurely, in order that the effect on the fibre may be observed. The longitudinal cracking of the fibre is typical of pyrolysed fibres heated to temperatures below 350°C. The cracks are evidence that the fibre is still oriented after heat treatment and that the solvent attack is releasing the strain energy produced by this. The effect disappears at temperatures above 350°C, after which the fibre dissolves by a continuous diffusion process.

The oxidised fibre in figure 5.6(f) has been heat treated to 230°C and has a 35% solubility in 60% nitric acid. It has swollen to a great extent and the surfaces have lost the regular crenulations characteristic of Courtelle. The closer observation of the fibre surfaces reveals that they have a fibrous surface texture, suggesting that the microfibrillar substructure has expanded, rendering it visible at these relatively low magnifications.

FIGURE 5·6(f)

INERT PYROLYSED COURTELLE AFTER ATTACK WITH FORMIC ACID

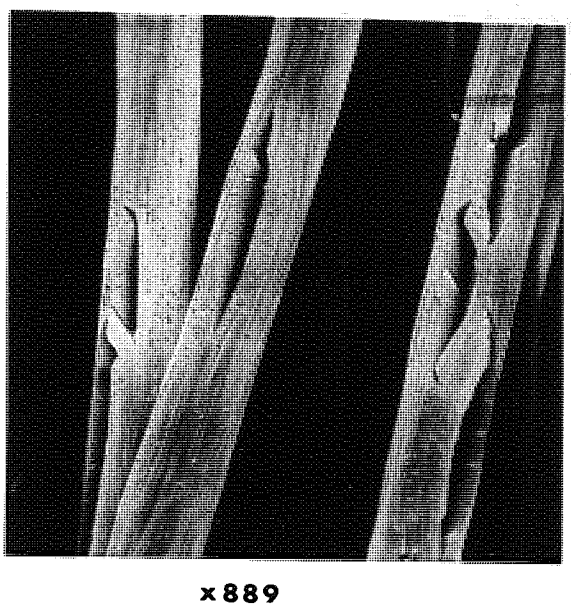

×889

×8,870

×910

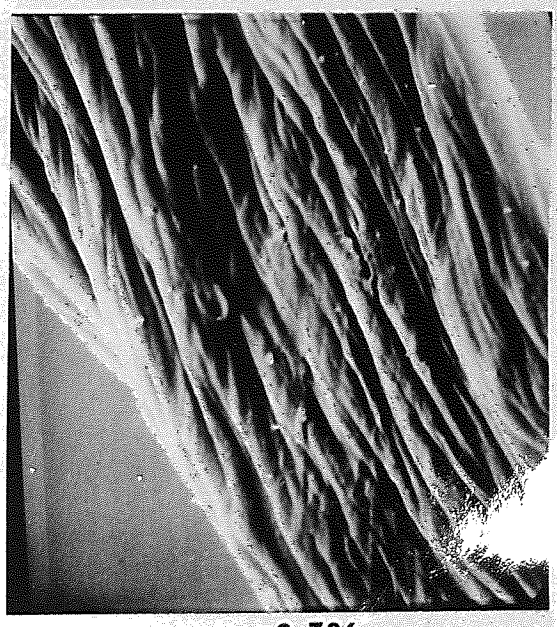

×2,786

OXIDISED COURTELLE SWOLLEN IN NITRIC ACID

TEMPERATURE, °C

SUMMARY AND CONCLUSIONS.

The spectral evidence favours the view taken in chapter 4, that the pure polyacrylonitrile fibre, Dralon T, has a self initiating reaction, which requires relatively long induction periods. The exothermic, nitrile decay reaction is preceded by a reaction(s) which consumes nitrile groups and produces amine groups. This evidence, though not direct, is undeniably in favour of the initiation ring saturation mechanism proposed by Yu and Noh.[83]

Consider the formation of an initiation ring,

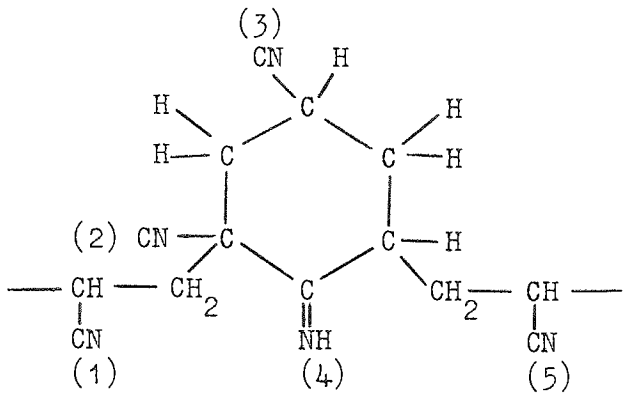

The nitrile groups have been numbered in sequence along the chain. As a result of the ring formation, which is presumably non-exothermic, nitrile (4) is destroyed by the formation of the imino group. Nitrile (3) is isolated in the ring and cannot take place in the propagation (nitrile polymerisation) reaction. Yu and Noh's statistical derivation shows that 20% of the nitriles will be destroyed, 20% will be isolated and 60% will polymerise, if the initiation ring formation reaction first goes to saturation. They further argue that the reaction should be first order and that the propagation length will be short.

The plot of nitrile content versus residual exotherm for Dralon T, in figure 5.32(b), shows very significant agreement with this interpretation of the mechanism. The first 20% of the nitrile groups are lost without any appreciable diminution in the exotherm and 20% of the nitriles are left as an unreacted residue. An apparent contradiction is that the results indicate that only 40% of the nitriles are

involved in the exothermic propagation reaction. However, further consideration of the initiation ring shows that this may in fact be reasonable. The imino group at (4) can only initiate polymerisation in one direction and the initiation itself may not be exothermic. If (4) reacts to (5), then (2) will have to form an end group and the initiation ring will have contributed just one nitrile group to the formation of a ladder segment and not the two which seemed possible. The division of the nitrile groups is now:- 20% to form the ring, 20% lost in initiating and terminating the nitrile polymerisation reaction, 40% involved in the polymerisation and 20% left as an unreacted residue. This division is indicated in figure 5.32(b), the 40% shown as the initiation reaction should be taken to include the formation of end groups and the ring.

The copolymer acrylic fibres obviously have a more efficient mechanism for initiating the polymerisation than this and it probably involves the copolymer in the reaction, as described in chapter 4. The absolute proof that the polymerisation of the nitriles is responsible for the exotherm has yet to be obtained. The indirect evidence, both in this thesis and elsewhere, is very persuasive, however. It is less certain that the product of pyrolysis is necessarily the cyclic polyimine suggested by Grassie. Work by W. D. Potter at Aston University (unpublished) shows that the sodium cyanide initiation of colouration in polyacrylonitrile produces a product of identical spectral and thermal properties to that of pyrolysed polyacrylonitrile. The mechanism that he proposes for this, however, results in a different type of cyclic product than that of Grassie et al.[60, 61] His reaction scheme is shown below:-

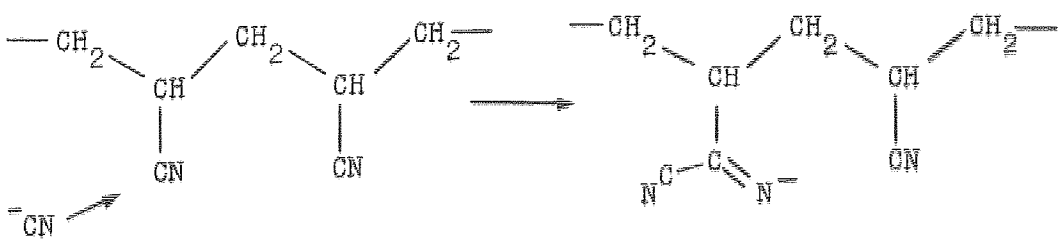

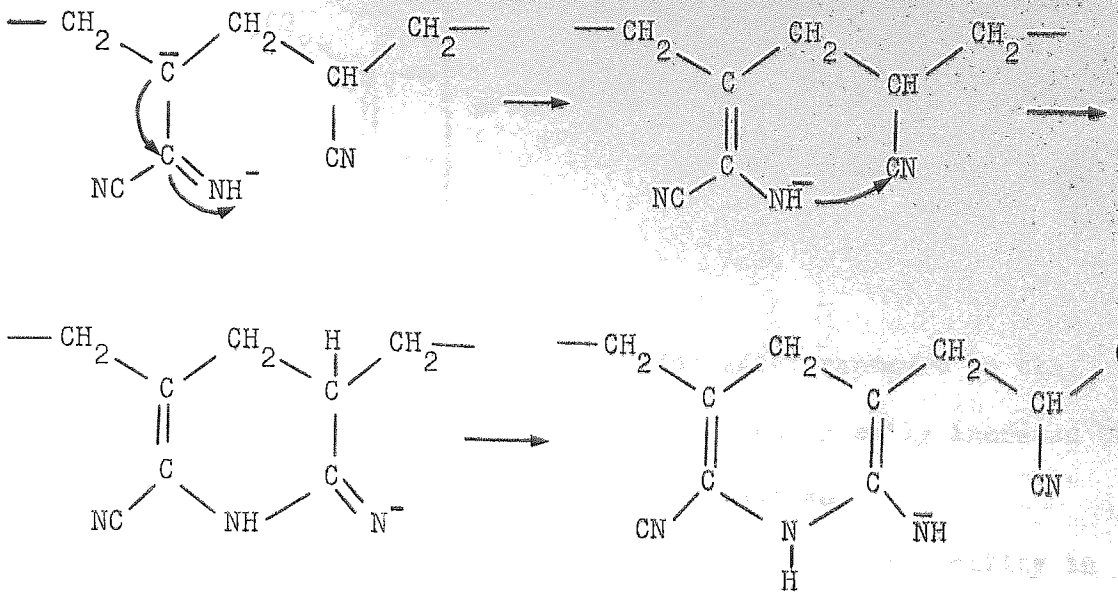

This process can continue, producing a poly 1,4, dihydropyridine type of structure.

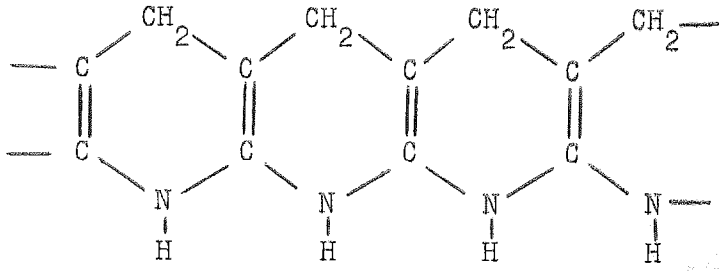

This structure is similar to one proposed by Monahan [115] and it explains the origins of all the absorption bands found in the infra-red spectra. It will be coloured, relatively thermally stable and be subject to oxidative attack. The position of the double bonds will activate the methylene hydrogens, so that they will be highly susceptible to oxidation.[84] Cook and Lyons [116] found that 1, 4 dihydropyridine was oxidised by atmospheric oxygen at room temperature. This structure, therefore, explains the very high reactivity of the pyrolysis product to oxygen in the atmosphere. The product of oxidation will probably be a mixture of dihydro and fully aromatic structures as shown below.

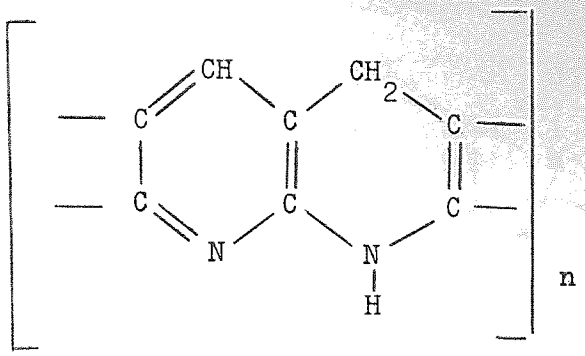

This would explain the increased colouration after exposure to the atmosphere and u.v. radiation, as the latter would greatly increase the activation of the (CH_2) and (NH) groups to oxidation.

The cross-linking reactions responsible for the insolubility in nitric acid might well be due to a propagation cross-linking type of reaction as suggested by Grassie, as this is not necessarily ruled out by the mechanism proposed by Potter. A single cross-linking bridge between opposing nitriles might take place, as follows:-

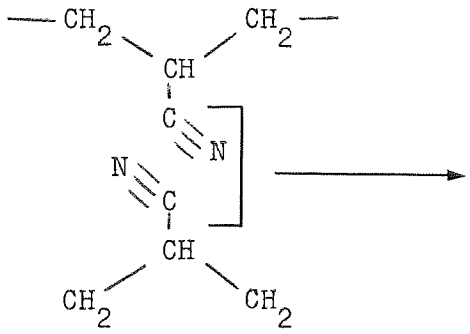

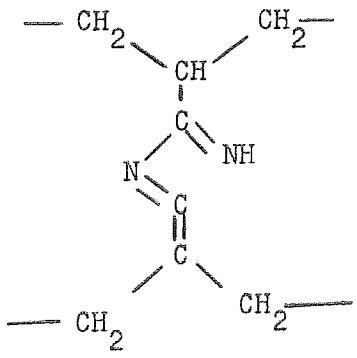

The bridge formed in this way will not be very stable, but the imino group will be capable of initiating the nitrile polymerisation reaction. The loss of the methylacrylate from Courtelle could form free radicals [117] which might allow cross-linking to take place, although the more likely consequence is the formation of unsaturation in the chain, as follows:-

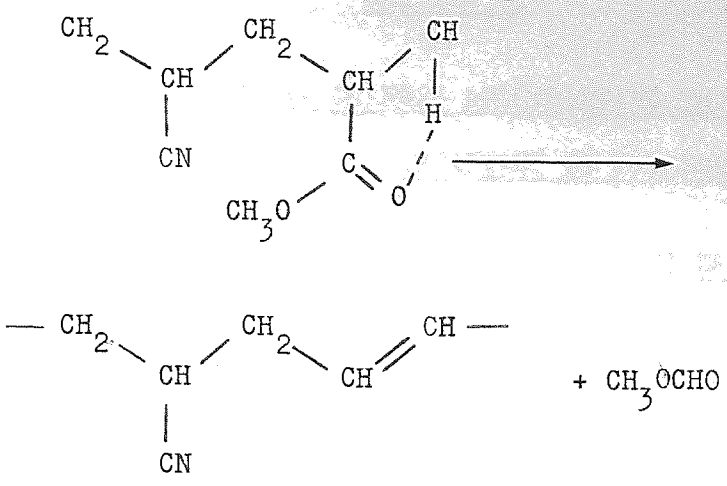

The earlier formation of cross-links in pyrolysed Courtelle has an interesting effect upon the mechanical properties of the fibre. Stretching experiments carried out at Rolls-Royce (Rose and Jones, unpublished) showed that Courtelle fibre could be stretched to greater extents and with less load if the stretching was conducted in air, rather than in argon, at 200°C. This is a temperature well above the glass transitions and below the temperatures at which a rapid exotherm would take place. It seems very possible, therefore, that the inertly heat treated fibre stretched less, because of the cross-links produced at this temperature.

CHAPTER 6.

THE PHYSICAL CHANGES ACCOMPANYING THE LOW TEMPERATURE HEAT TREATMENT OF POLYACRYLONITRILE.

6.1 THE VARIATION OF THE TENSILE PROPERTIES OF COURTELLE WITH HEAT TREATMENT.

The mechanical properties of any solid depend to a great extent upon the type of material and its morphology. A knowledge of the mechanical properties can be very useful, particularly in the case of a material such as polyacrylonitrile fibre, which becomes highly intractable during an important part of its heat treatment. Infra-red spectrometry loses its value as an analytical method at just the stage of the heat treatment when it is important to know most about the structure. This is when the fibre has completely blackened and the spectra become suppressed by large background absorptions. Clearly, optical measurements are of very limited value also. X-ray diffraction measurements are very useful, but they do present a problem of interpretation. If polyacrylonitrile could be spun to form a crystalline filament to the extent possible with polyvinylidine-chloride, for example,[35] the problem would be less difficult. These difficulties are further compounded by the fact that acrylic fibres undergo simultaneous chemical and physical changes and it is impossible to explain which effects are altering the diffraction pattern, without an independent knowledge of the mechanical properties.

A knowledge of the mechanical properties is, therefore, a useful adjunct to the interpretation of the analytical results. Some results have already been published on the mechanical property changes accompanying the heat treatment of Courtelle. The author has contributed tensile strength, modulus and extension at break data to a paper by Turner and Johnson,[56] on the pyrolysis of Courtelle. These results were considered to show that chain scission occurred during

the reaction exotherm. A paper prior to this, by Bell and Mulchandani,[118] discusses the mechanical properties for both oxidised and pyrolysed Courtelle for relatively low degrees of heat treatment. They concluded that light cross-linking takes place in both cases and that this is supported by the change in intrinsic viscosities of the fibres, dissolved in dimethylformamide. The heat treatment of polymer solutions did not, however, support this assertion.

Watt [92] has reported a few tensile results on oxidised Courtelle and concluded that little or no cross-linking is present following a normal pre-oxidation heat treatment. (This work was conducted concurrently with the authors'.)

6.11 The tensile stress-strain curve for Courtelle.

Figure 6.11 shows a set of stress-strain curves obtained for Courtelle acrylic fibre having a range of preferred orientations. The orientation angle Z^{o} is determined by the method previously described in section 2.1, from the (100) fibre diffraction arc. The lower the value of the angle the higher the degree of preferred orientation. The breaking stress increases with increasing degrees of orientation and the breaking strain decreases. The shape of the stress-strain curve is typical of fibres formed from a polymer having a helical chain conformation. Keratin and polypropylene,[119] for example, have similar stress-strain curves. The manner in which the stress-strain curves alter with the degree of preferred orientation is very typical of the behaviour of semi-crystalline polymers. Cellulose and polyethylene terephthalate behave very similarly.[119] Therefore, in spite of its anomalous X-ray fibre diagram, polyacrylonitrile behaves as a typical semi-crystalline polymer.

An important feature of the stress-strain curve, apart from the breaking stress and breaking strain, is the initial or Young's modulus. This is determined from the slope of the initial straight line portion of the stress-strain curve and it is defined in section 2.2. For the

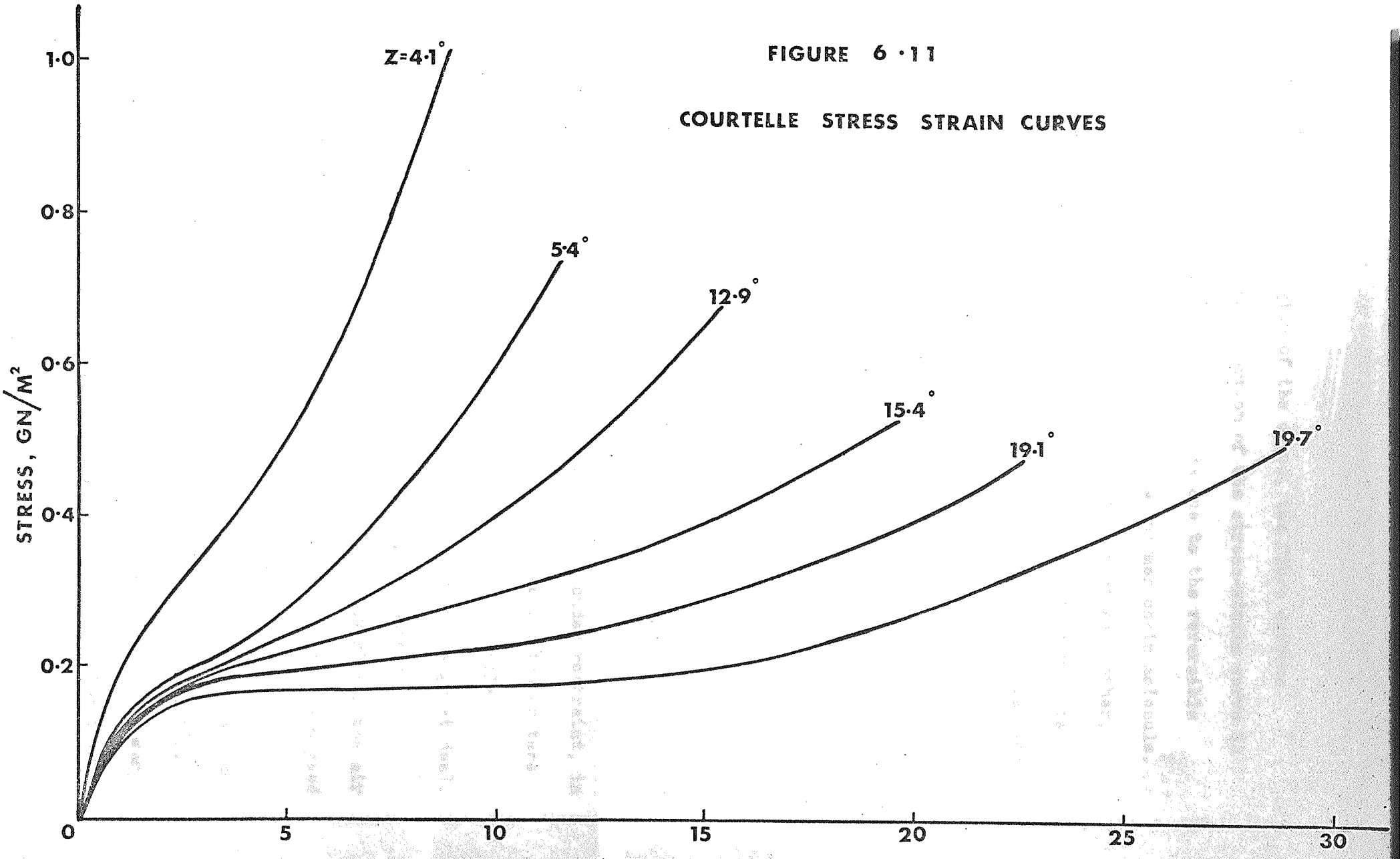

FIGURE 6·11

COURTELLE STRESS STRAIN CURVES

small strains in this region of the curve, the fibre deforms elastically, i.e. the linear portion of the stress-strain curve is completely reversible. This behaviour is due to the reversible rotation and stretching of the bonds in the polymer chain molecule. For larger strains the molecules begin to slide past each other, producing an irreversible plastic deformation. As the strain is increased further, the degree of elastic extension in the molecules increases and, as a result, the slope of the stress-strain curve can increase towards the value of the initial slope.

6.12 The change in properties with heat treatment.

Tensile tests at a standard extension rate were carried out for the oxidised and pyrolysed Courtelle series, already considered in chapters 4 and 5. The strength, elongation at break and Young's modulus were calculated in each case. Figure 6.12(a) is a plot of fibre strength versus heat treatment temperature for both series. The strength fluctuates between 0 and 170°C, which could be due to the relaxation and annealing of the fibre with heating under restraint, in the region of the glass transition temperatures. In the temperature range of greatest interest, 200 to 260°C in which the nitrile polymerisation reaction takes place, the strength decays a great deal. This decay is greatest for the pyrolysed series, the strength ultimately dropping to 0.1 GN/M^2 as compared to 0.22 GN/M^2 for the air oxidised series. The strengths remain at low values for the pyrolysed series, but above 320°C the oxidised series strengths increase.

Figure 6.12(b) is a plot of the elongation at break for the same samples. Again, there is a fluctuation in the results below 200°C. In the range in which the exotherm decay is observed, there is a very sharp drop in elongation at break. Again, the decline for the inert heated series is greatest, dropping to 1.5% as compared to 5.5% for the oxidised series. After the initial reduction in breaking elongation there is very little change, the values remaining constant

TEMPERATURE, °C

FIGURE 6·12 (a)

CHANGE IN STRENGTH WITH HEAT TREATMENT TEMPERATURE

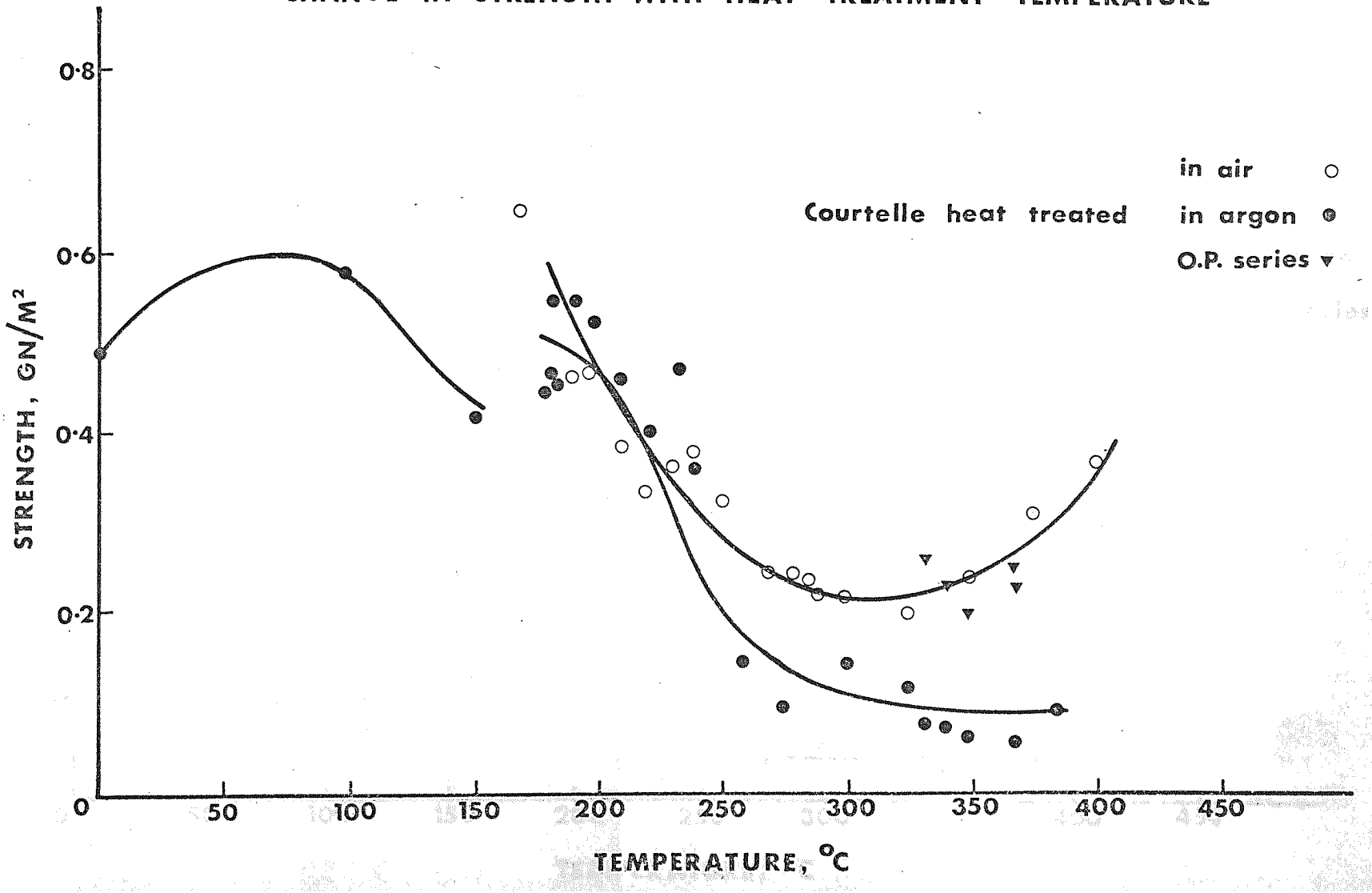

FIGURE 6·12 (b)

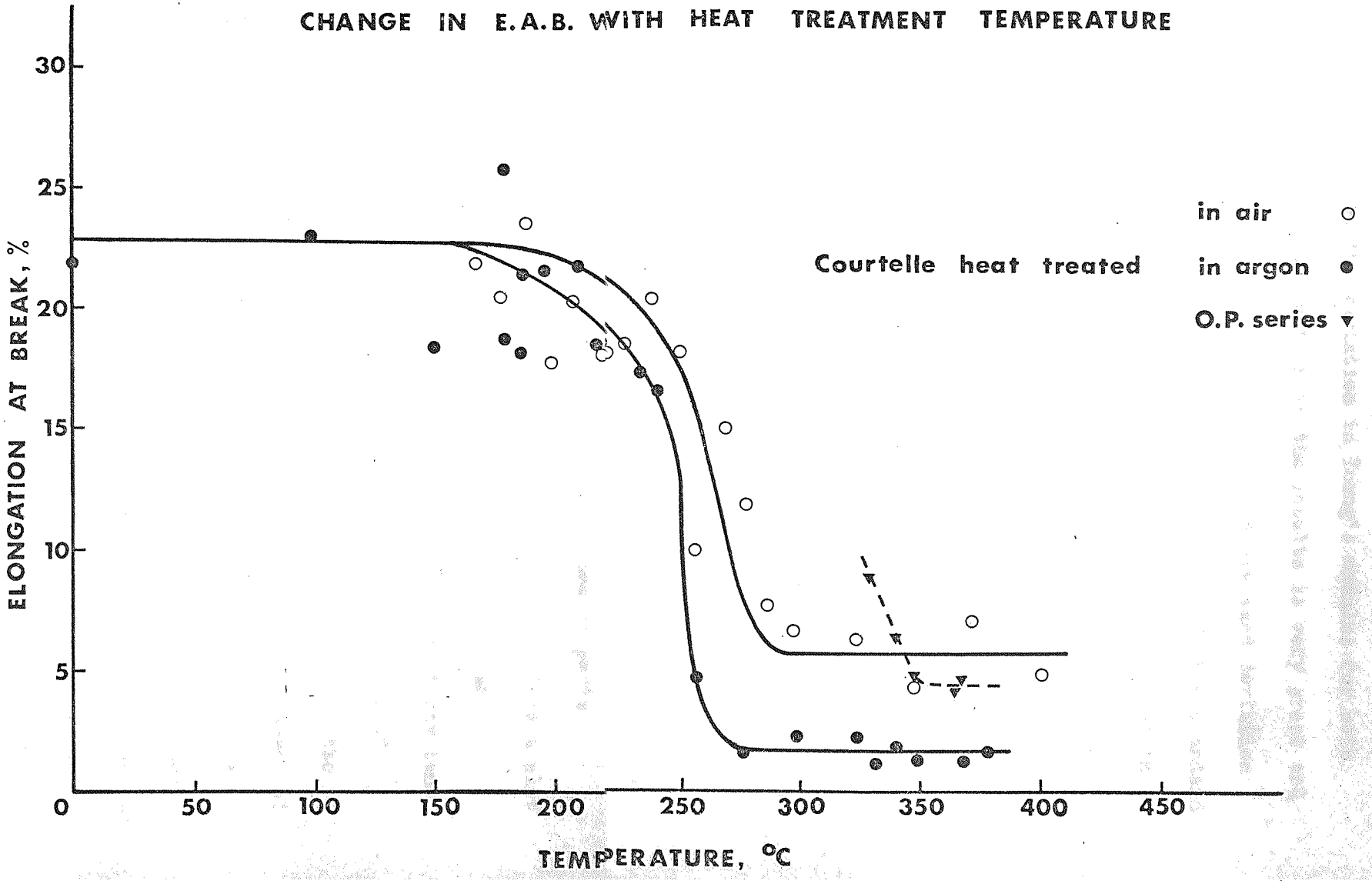
CHANGE IN E.A.B. WITH HEAT TREATMENT TEMPERATURE
ELONGATION AT BREAK, %
30
25
20
15
10
5
0
50
100
150
200
250
300
350
400
450
TEMPERATURE, °C
Courtelle heat treated
in air
in argon
O.P. series

to 400°C.

Figure 6.12(c) shows the variation in Young's modulus for both series. Up to 220°C, the fluctuation in the results is very great and little importance can be attached to them, as the standard deviation on the mean of each sample is very large. At above 250°C, the standard deviation is very small and would be barely noticeable if plotted in the figure. In the temperature range of the nitrile polymerisation reaction and within experimental error, only the pyrolysed series shows a decline in Young's modulus. The oxidised series remains reasonably constant until 300°C, above which the modulus increases. After the completion of the reaction exotherm at 260°C, the modulus of the pyrolysed series remains sensibly constant, until a sharp drop occurs at 345°C. This sharp drop is found to correspond to an apparent melting of the fibre and will be considered again in chapter 7.

The observed constancy of the Young's modulus with the nitrile polymerisation reaction in air is an important fact. This is because it implies that the intermolecular bonding has in some respects remained unchanged, in spite of the reaction. Figure 6.12(d) is a plot of Young's modulus versus time for a series of isothermal heat treatments in air between 180°C and 270°C. For forty of the forty two measurements, the Young's modulus agrees quite well with a mean of 9 GN/M^2. It is to be expected that a change in the character of the molecule should influence the elastic modulus, as this is a fundamental property of the way in which the molecules deform. The constancy of Young's modulus suggests that a sufficient population of single bonds must be present, to allow rotation and stretching in the chain molecule to the same extent as before, for the same stress. Extensive cross-linking is, therefore, unlikely and the complete polymerisation of the nitrile groups an impossibility. The decline in Young's modulus for

FIGURE 6·12(c)

THE DEPENDENCE OF YOUNG'S MODULUS ON HEAT TREATMENT

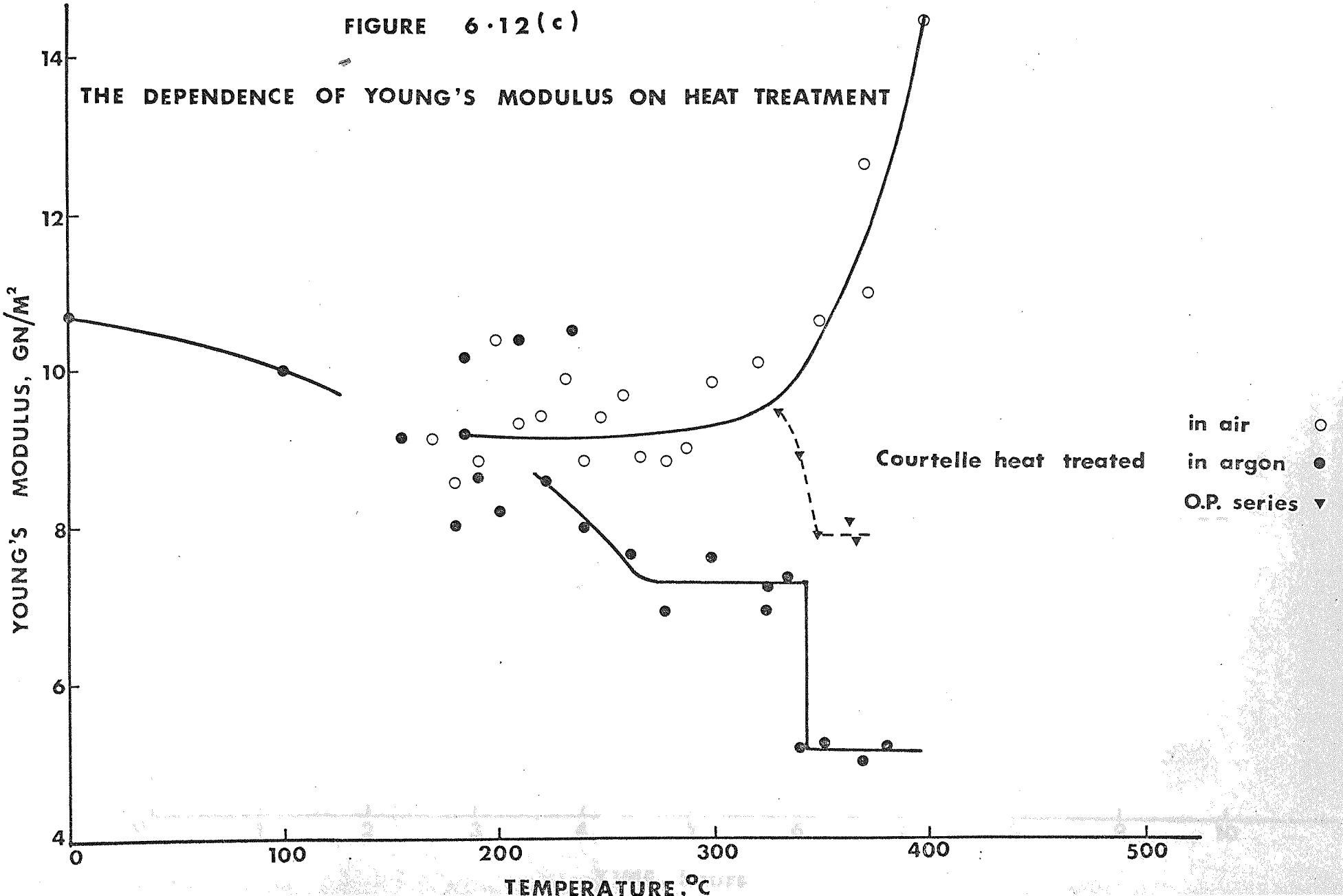

FIGURE 6·12 (d)

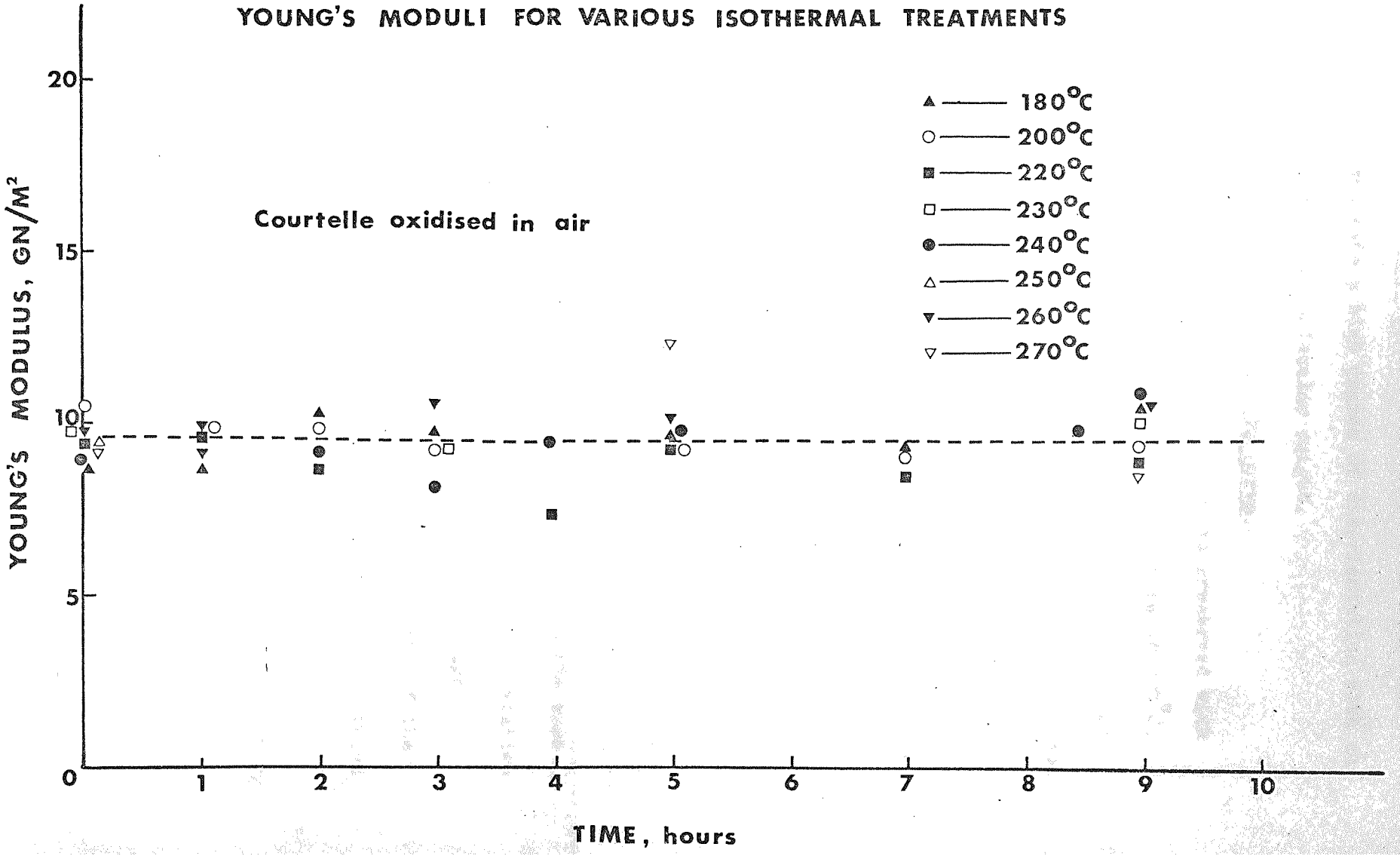
YOUNG'S MODULI FOR VARIOUS ISOTHERMAL TREATMENTS
Courtelle oxidised in air
180°C
200°C
220°C
230°C
240°C
250°C
260°C
270°C
YOUNG'S MODULUS, GN/M²
20
15
10
5
0
1
2
3
4
5
6
7
8
9
10
TIME, hours

the pyrolysed series suggests a high degree of disorientation with an accompanying degradation in the molecular weight.

6.13 The general form of the stress-strain curve.

The general shape of the stress-strain curve is preserved with increasing degrees of heat treatment, up to a temperature of 270°C. The strength and elongation at break decline simultaneously and the curve appears to be increasingly truncated with heat treatment, without any appreciable change in form. The curve shape, as shown in figure 6.11, is a function of preferred orientation. The extent of the deviation from the precursor stress-strain curve should provide us with an idea of how much the chain orientation has altered. Figure 6.13 is a plot of strength versus elongation at break for two series of heat treated samples, prepared from two different Courtelle precursors, having different preferred orientations. The precursor stress-strain curves have been drawn in the figure. The lower of the two curves, with its corresponding data, is for the Courtelle batch which has been considered in the previous sections and with which most of the experiments were performed. Between elongations at break of 2 and 17%, the correlation of the data with the stress-strain curve is excellent. At high elongations at break the results are scattered. The majority of the deviating values are for the pyrolysed samples, the same samples which deviated from the curves in earlier plots. The samples all have exceptionally high strengths and this could be due to the cross-linking reaction considered in section 5.6. Bell and Mulchandani [118] also refer to this effect. At low values of elongation at break, the pyrolysed series again deviates from the curve, as the breaking strain drops below the elastic strain observed with the precursor.

For the more highly oriented fibre the correlation is not quite so good (all these samples were pyrolysed). However, the points all plot above the curve for the fibre of low orientation, implying that the series retains a higher preferred orientation throughout inert

FIGURE 6·13

THE STRESS–STRAIN FUNCTION FOR TWO DIFFERENTLY ORIENTED FIBRES

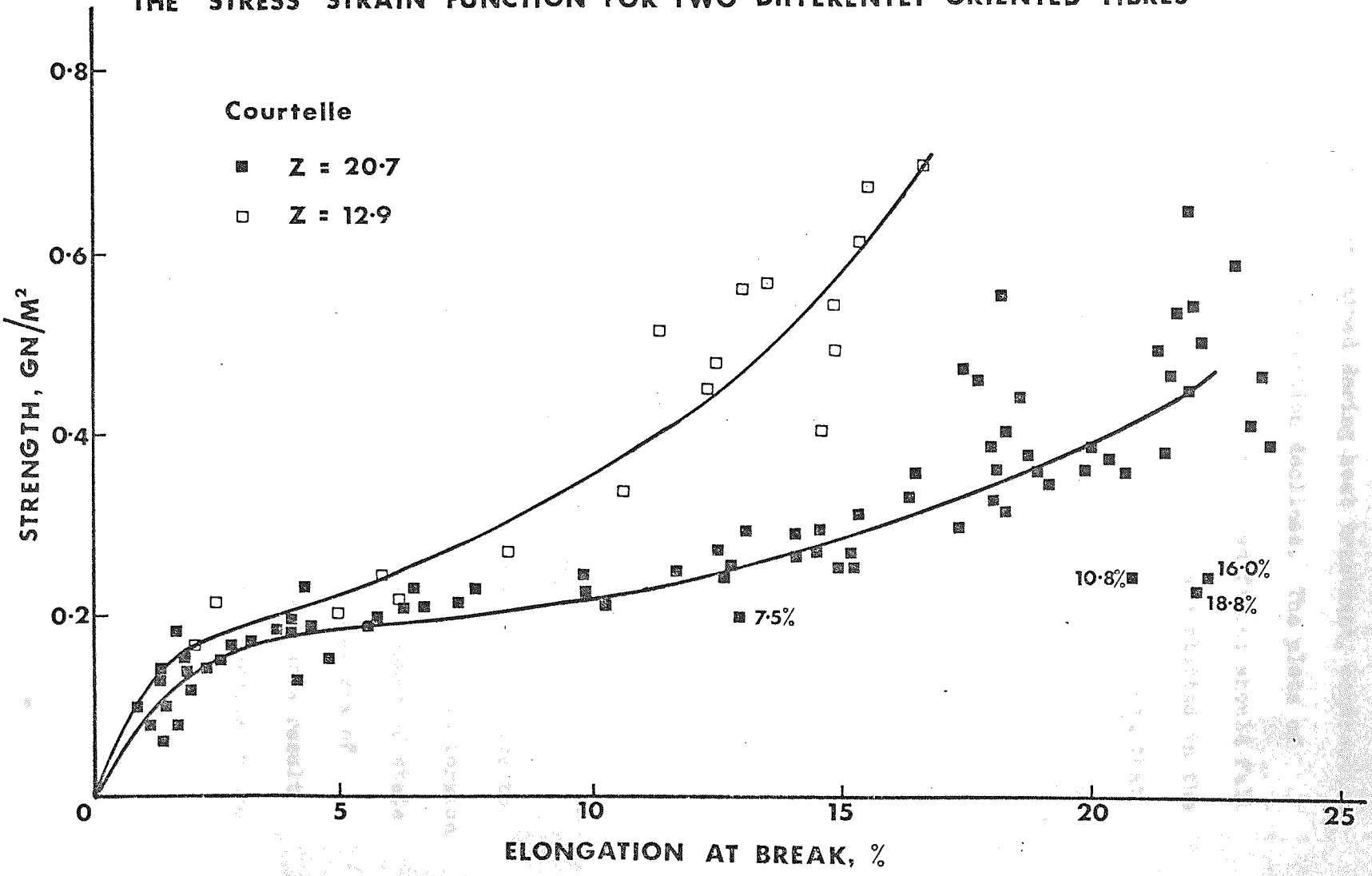

heat treatment.

If the fibre is not restrained during heat treatment, contraction takes place and the preferred orientation declines. The plots of strength against breaking elongation for contracted fibres should fall low down on figure 6.13, therefore. Several points are plotted in the figure with the degree of shrinkage indicated and it can be seen that this expectation is confirmed. Their precursor had a Z of 12.9°, but as a result of contraction the results fall below the curve for Z=20.7°.

When oxidation of the fibre is continued above 300°C, the stress-strain curve deviates completely from the precursor curve. The strength increases, while the elongation at break initially stays at 5%. This is for heat treatments following the completion of the nitrile polymerisation and the fibre is believed to be undergoing a gradual condensation reaction at this stage. For increasing carbonisation temperatures, the stress-strain curve straightens [14] and the breaking strain declines to about 1.0%.

6.2 THE CHANGE IN TORSION MODULUS WITH HEAT TREATMENT.

The torsional rigidity of textile fibres can be very sensitive to the physical state of the constituent molecules. The modulus in torsion of polymers is often used as a sensitive measure of the change of state with temperature.[120] It is also a valuable aid in the analysis of chemical changes.[121] If the chain molecules become rigid as a result of the nitrile polymerisation reaction, a corresponding increase in the torsion modulus should be observed. Any reaction increasing the restrictions in rotation about single bonds in the molecule should have the effect of increasing the rigidity of the fibre. Cross-linking is such a reaction. Chain degradation of the polymer should have the opposite effect, the fibre rigidity will decline as the chains shorten, as this increases the freedom of movement of the molecules. A loss of orientation of the fibre will usually result in a decline in rigidity, particularly if this is due to melting.

FIGURE 6·21(a)

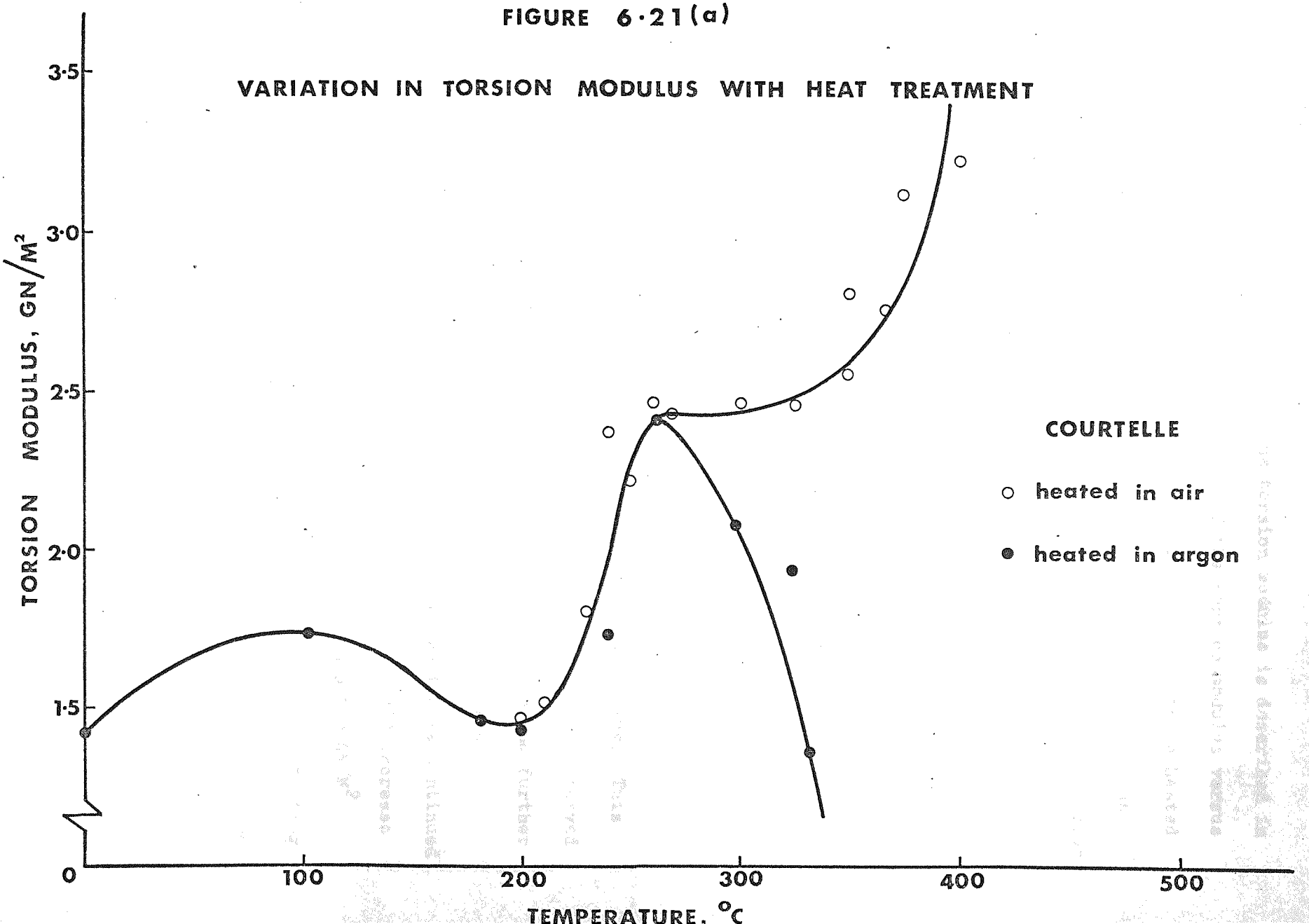
VARIATION IN TORSION MODULUS WITH HEAT TREATMENT
TORSION MODULUS, GN/M²
3·5
3·0
2·5
2·0
1·5
0
100
200
300
400
500
TEMPERATURE, °C
COURTELLE
heated in air
heated in argon

6.21 The comparison of torsion moduli for the inert and oxidised Courtelle series.

The method of measurement of the torsion modulus is described in section 2.22. Figure 6.21(a) is a plot of the torsion modulus versus heat treatment temperature, for the series of Courtelle fibres heated under restraint in argon and in air. These are the same samples as considered previously. Between room temperature and 200°C, the torsion modulus apparently goes through a peak, returning to the original value at 200°C. All the physical parameters considered so far have shown a fluctuation in this region. The temperature range in which the decline in the residual exotherm is observed, 200 to 260°C, (see figure 4.71(a)) is accompanied by a gradual increase in the torsion modulus. The exotherm, which is assumed to be due to the nitrile polymerisation reaction, is completed by 260°C. Heating above this temperature the pyrolysis results in a continuing decline in torsion modulus. After heat treatment to 350°C in argon, the fibres are adhered together and so fragile that they cannot be handled without them powdering. This very great drop in strength for these fibres has already been observed in figure 6.12(a). Heating above 260°C in air at first has no further effect on the torsion modulus, but on heating above 320°C the continuous increase in modulus is resumed. If the heating is continued in an inert atmosphere, the torsion and Young's moduli would increase progressively to very high values; e.g.:- 20 GN/M^2 and 200 GN/M^2 respectively, at 1,000°C. The initial growth in both moduli, starting in the region of 320°C, might therefore be considered as the beginning of carbonisation, through the condensation of the oxidised polymer residue.

Figure 6.21(b) is a plot of the nitrile content of the fibres determined from the infra-red spectra, versus the torsion modulus. There is clearly a reasonable correlation between the two parameters, as the nitrile content decays, the torsion modulus increases. The

FIGURE 6·21 (b)

INCREASE IN FIBRE RIGIDITY WITH NITRILE POLYMERISATION

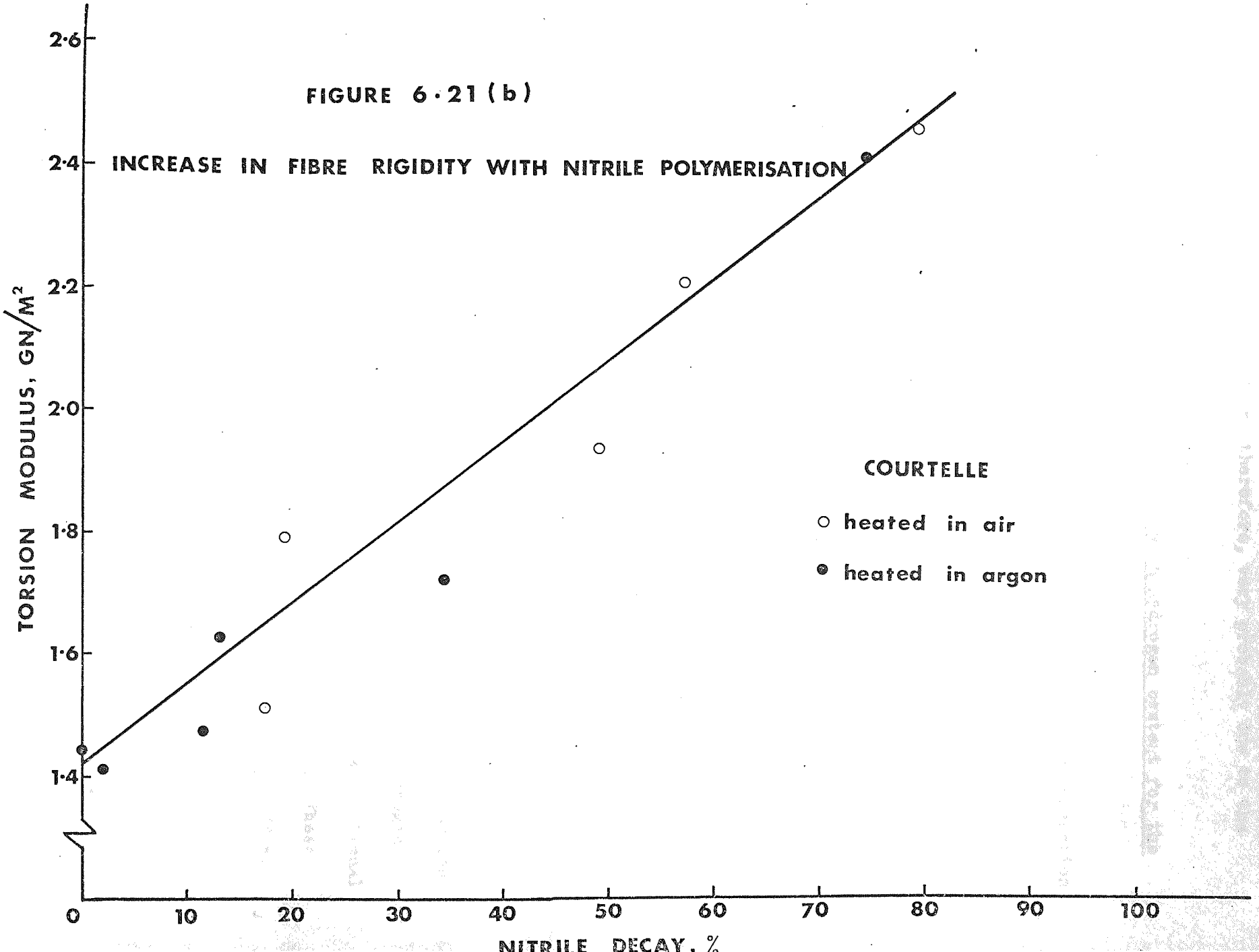

increase in fibre rigidity is, therefore, very probably due to the nitrile polymerisation reaction.

6.22 The variation of torsion modulus with hydrogen content for the oxidised Courtelle series.

The oxidation of Courtelle results in an extensive dehydrogenation of the polymer. It is interesting to observe if the torsion modulus varies with the degree of dehydrogenation, independently of the heat treatment temperature. Figure 6.22 is a plot of torsion modulus for various Courtelle fibres oxidised at a range of temperatures, for different times. The hydrogen contents have been determined by elemental analysis. The first twenty percent of hydrogen loss (from 5.66 to 4.50%) is accompanied by a large increase in torsion modulus. As observed in figure 6.21(b), this initial growth in fibre rigidity is correlated with the decay in the nitrile content, a reaction which would have occurred in the complete absence of oxygen. The dehydrogenation of the fibre down to 2.5% weight content does not further increase the torsion modulus at all. What it does is to prevent the reversion of the modulus; it either eliminates chain degradation, or substitutes a cohesive force which compensates for the effect of it. The further growth in torsion modulus for dehydrogenation below 2.5% weight content would have occurred had the additional heat treatment been conducted in the total absence of oxygen. These moduli are only achieved for heat treatments above 300°C. The effect is apparently due to the condensation of the molecular species.

The intermediate values of the hydrogen contents cannot be used to determine an empirical formula for oxidised polyacrylonitrile. This is because oxidation becomes a diffusion controlled reaction with the increasing densification of the fibre. The densification can follow from the oxidation of the precursor polymer, the formation of a polymerised nitrile product and ultimately from the oxidation of the polymerised nitrile product. The presence of the diffusion controlled

FIGURE 6·22

CHANGE IN TORSION MODULUS WITH DEHYDROGENATION

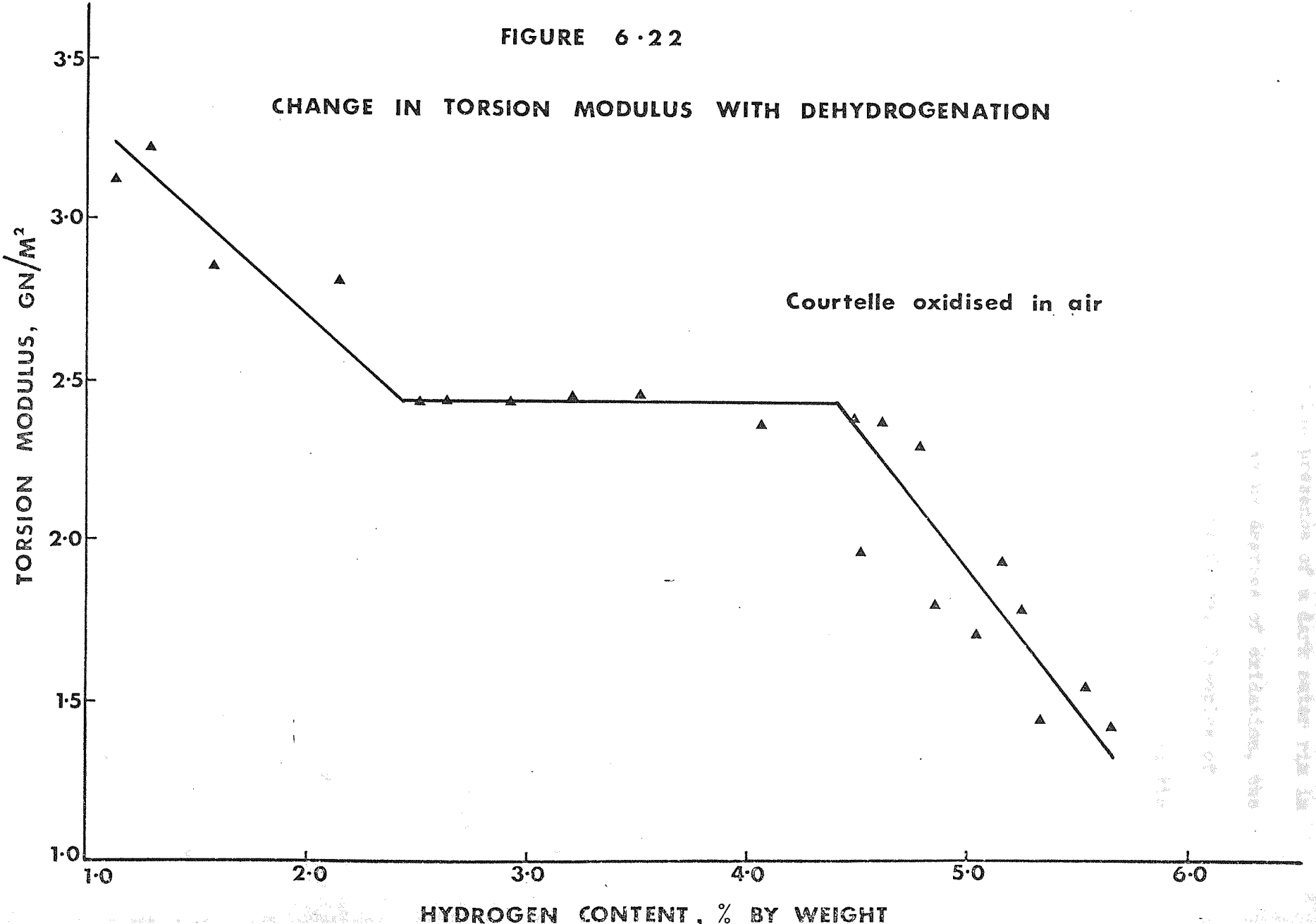

reaction is easily confirmed by the presence of a dark outer rim in the fibre cross-section. With increasing degrees of oxidation, the rim is observed to move to the centre of the fibre. Examples of reaction rims can be seen in figures 7.21 and 7.22(b). The reaction rim moves through the Courtelle fibres as dehydrogenation increases and the torsion modulus plateau in figure 6.22 is for a range of fibres having an increasingly large reaction rim. This is an additional demonstration of the independence of the torsion modulus from the degree of oxidation.

6.3 THE EFFECT OF OXIDATION ON PHYSICAL PROPERTIES, FOLLOWING INERT HEAT TREATMENT.

When considering the oxidation of polyacrylonitrile there are at least two possible reactions. There is the reaction of oxygen with the precursor polymer and the reaction with the polymer, after it has formed the polycyclic structure. Dralon T can be induced to oxidise to a very great extent without polymerisation of the nitriles, because the oxidation of this acrylic suppresses the initiation of the reaction. Dralon T can, therefore, be used as an example of polymer oxidation. This section will consider what occurs when Courtelle is pyrolysed to complete the nitrile polymerisation reaction first, before being oxidised.

Pyrolysed Courtelle fibres were prepared in the usual way by heating at $\frac{15}{12}$ °C/minute to the required temperature, in an atmosphere of pure argon, with the fibre held under restraint on a steel frame. The samples were given a post oxidation heat treatment, to approximately the same final temperature. This was done by heating the unrestrained fibre bundle at $\frac{15}{12}$ °C/minute, in a flow of atmospheric air to the desired temperature. A frame of precursor fibre was also placed in the oxidising furnace, in order that a control test could be performed. A study of the carbon fibre prepared from this series of samples is reported in chapter 7, but the discussion here will be limited to the

tensile properties of the samples themselves.

The samples have been labelled the 'OP series' and the values of strength, elongation at break and Young's modulus have been plotted in figures 6.12(a), 6.12(b) and 6.12(c), respectively. In this way, a comparison can be made between the properties obtained for the three types of heat treatment. Inspecting figure 6.12(a) the strengths of the O.P. series are virtually identical to the strengths of the fibres that have received a conventional oxidation. The strengths of the pyrolysed fibres are trebled as a result of having received the oxidising heat treatment. The elongation at break is also increased, as can be seen for the O.P. series in figure 6.12(b). The post oxidation appears to be reversing the additional degradation due to the pyrolysis. This implies that the oxidation process has a synthesising effect upon the residue, as if a cross-linking reaction is taking place. It is equally possible, however, that the effect is due to the introduction of additional cohesive forces between the molecules, perhaps hydrogen bonding is responsible for the increased properties, for example.

The effect of the post oxidation upon the Young's modulus is not so great, the modulus increases, but it is not increased to the values of the original oxidised series. The O.P. series of moduli suffer a decline in value in the same temperature region as the sharp drop in the pyrolysed series of moduli. This occurs between 340 and 350°C and it will be demonstrated in chapter 7 that this is due to a pseudo-melting behaviour, causing a loss of orientation and other effects, to be described later. The order of the effect of the post oxidation heat treatment can be appreciated from an inspection of the stress-strain curves in figure 6.3. The curve at the top of the figure is for a Courtelle fibre pyrolysed to 333°C. It is characteristic of a brittle material, being weak and having a low breaking strain. The curve below it is for the same sample, given the oxidation heat treatment

FIGURE 6·3

EFFECT OF POST OXIDATION ON THE INERT DEGRADED FIBRE

HEATED IN ARGON TO 333°C, UNDER RESTRAINT

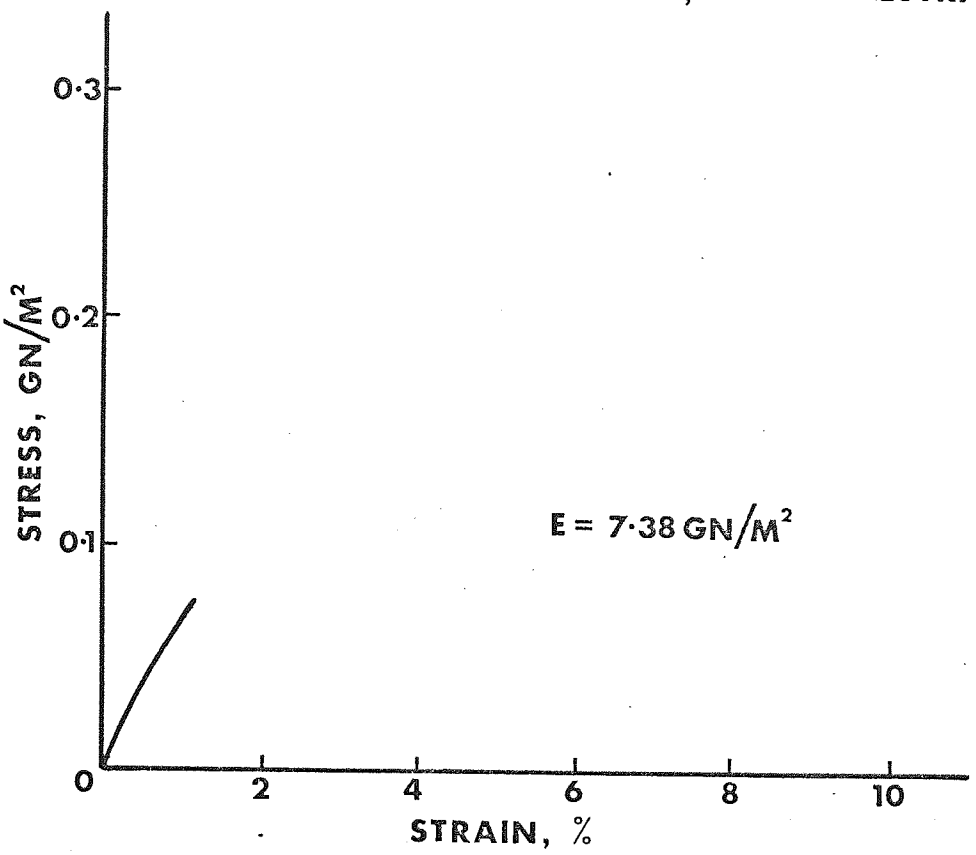

POST-OXIDISED BY HEATING IN AIR TO 333°C, UNRESTRAINED

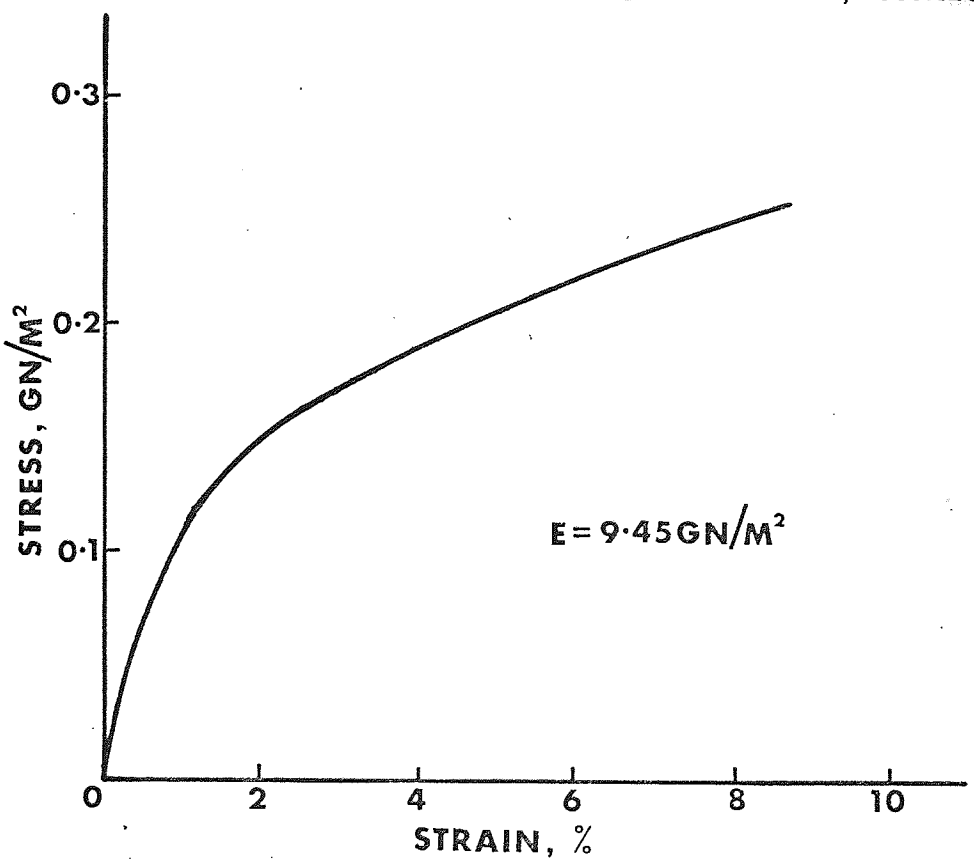

already described. The material is now very much more plastic, the modulus has been increased from approximately 7.0 GN/M^2 to 9.0 GN/M^2 and the breaking strain is increased from just over 1% to 8%. Clearly, the oxidation treatment has had quite a large effect upon the fibre's molecular state.

The O.P. series of samples were tested for solution in nitric acid, and it was found that the solubilities were identical to the fibres which had received a straightforward oxidation. It appears, therefore, that for post-oxidations at above 300°C., the same condensation reactions are taking place. This effect by itself could explain the improvement in strength and elongation at break for samples post-oxidised above 300°C. Post oxidations to temperatures below 300°C do not stimulate condensation, but nevertheless produce an improvement in mechanical properties. It is for this reason that it is suspected that the greater cohesion of the oxidised fibre might be due to the presence of additional secondary bonding forces.

Separating the nitrile polymerisation from the oxidation reaction in this way appears to make very little difference to the product, unless the pyrolysis is allowed to exceed 340°C. In fact, Thorne [106] has shown that a modest increase in carbon fibre properties can be achieved by an inert pre-treatment, if the reaction exotherm is properly controlled.

6.4 THE X-RAY DIFFRACTION OF ACRYLIC FIBRES AND THE STRUCTURE OF THE HEAT TREATED PRODUCTS.

The X-ray fibre diagrams for Courtelle and Dralon T are shown in figure 6.4(a). The fibre bundle is oriented vertically in the plane of the page, in each case. The two pairs of arcs are due to the (100) and (200) reflections and they are both produced by transverse order in the fibre. The lattice intervals are 3 and 5.2 A°. These two acrylics are typical of most polyacrylonitrile fibres in possessing a very low degree of crystalline order, and yet they do not have the

FIGURE 6.4(a) ACRYLIC FIBRE X-RAY DIFFRACTION DIAGRAMS.

Courtelle

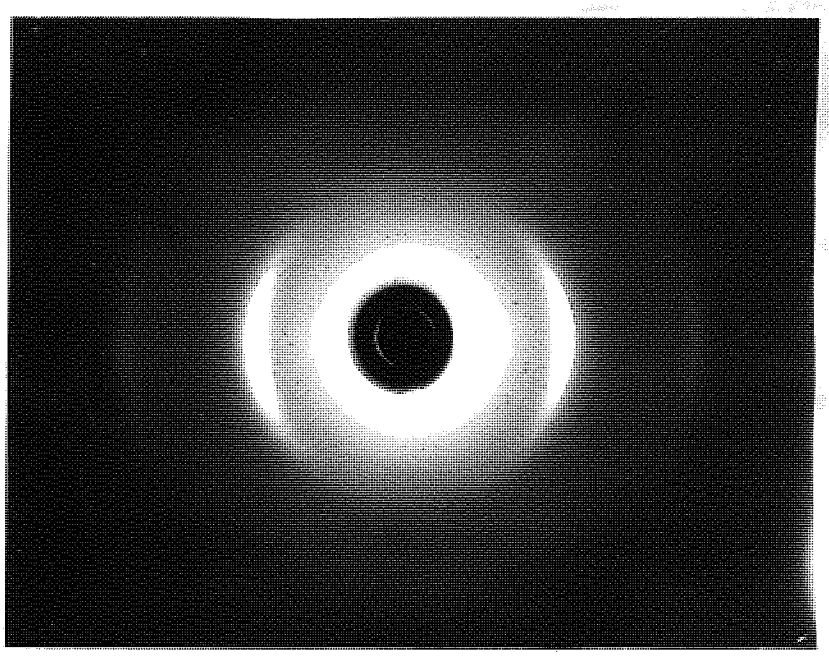

Dralon T.

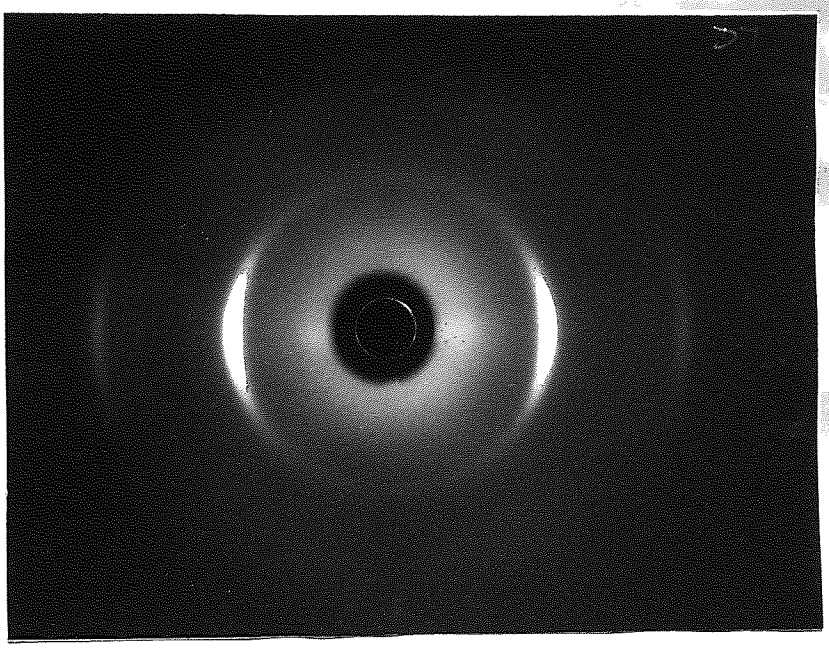

broad amorphous halo which would be typical of a completely disordered polymer. The arcs indicate that the majority of the material in both fibres has a high degree of preferred orientation, although there is a small, completely disoriented fraction. The sharper arcs for Dralon T indicate that the chain molecules have a more uniform packing than in Courtelle.

The lack of all but the equatorial arcs in most examples of polyacrylonitrile fibre indicates that it only possesses two-dimensional order. The structure has been compared to that of a nematic liquid crystal, which has a high degree of lateral order but none along the flow direction, or fibre axis.[122] Bohn et al [123] attribute the lateral order to the uniform packing of the chain molecules, with a mean separation of 5.2 A^{o} and the lack of longitudinal order to the irregular disposition of the nitrile groups, about the axis of the molecule. A paracrystalline model of the fibre has been found to produce a similar diffraction pattern.[124] This assumes that there is a three-dimensional crystal lattice which would describe the structure, but that it has become distorted, destroying all but the strongest diffraction features.

However, the highly selective use of coagulating solutions and the application of high stretch ratios has, in a few cases, produced additional weak diffraction features, including two pairs of meridional arcs.[125, 126] These suggest that the chain has a helical conformation. The problem with polyacrylonitrile is that it cannot be properly annealed without the colouration reaction intervening. This may be destroying the fibre's ability to crystallise. However, another feasible explanation is that the structure lacks longitudinal order because of the mutual repulsion of the nitrile groups, which prevents the formation of a regular helix.

A model structure suggested by Urbanczyk [122] (figure 6.4(b)) for an idealised unit cell for polyacrylonitrile explains most of the

FIGURE 6·4(b)

AN IDEALISED STRUCTURE FOR ORIENTED POLYACRYLONITRILE FIBRE (Urbanczyk)

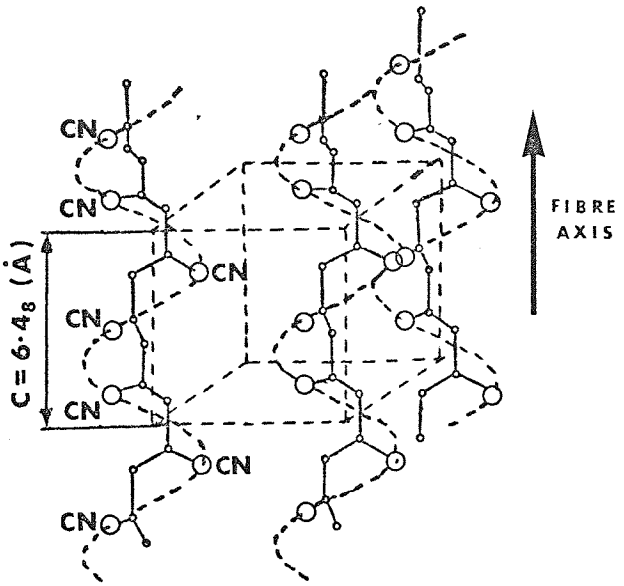

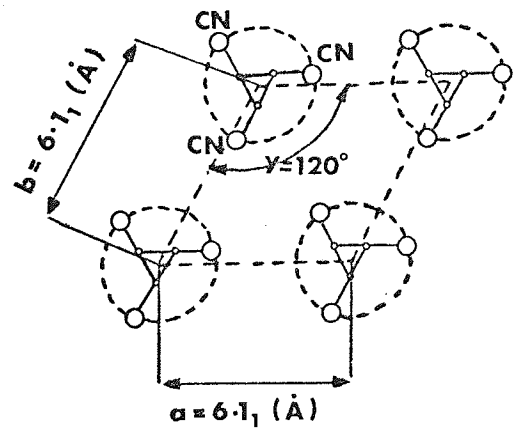

THE CRYSTAL UNIT CELL

experimental observations. It is a highly packed structure, explaining the high density of the polymer (1.2 gram/c.c.) and the molecules have a helical conformation. The crystal structures of Courtelle and Dralon T could be obtained from this model, if one imagined the helices to be stretched along the unit cell C-axis direction, so that they suffered a non-uniform distortion.

6.41 The effect of heat treatment upon the structure of the fibre.

With heat treatment in argon, the (100) and (200) diffraction arcs almost completely disappear, with the disappearance of the reaction exotherm, although a very faint, almost completely disoriented diffraction halo is sometimes observed, even after heat treatment to 400°C. Most of the resultant diffraction is for d-spacings in the range 3.5 to 4 A°, which is extremely diffuse with very little apparent preferred orientation. Post oxidation of the pyrolysed fibre produces oriented diffraction arcs, indicating that a latent type of order was present, which could not produce coherent diffraction. It is as if the molecules were oriented with their major axes roughly parallel to the fibre axis, but with their planes having random orientation, with respect to the normal to the axis. Another possibility is that the pyrolysed polymer molecule has a distorted ribbon-like structure,[74] which could produce the same effect. Oxidation appears to produce a rotation of the molecules (or an untwisting of distorted ribbon molecules) which restores the ability of the fibre to produce coherent diffraction, once the planes of the molecules are in register.

The heat treatment of acrylic fibres in air, to the point of the removal of the reaction exotherm, causes the gradual decline and loss of the 5.2 A° arc which is characteristic of the polymer, and the simultaneous appearance of a completely new, broad, diffraction arc. This second arc is often called the (002) carbon arc, even at this early stage of the heat treatment. The use of this description, however, might lead to misconceptions about the structure of oxidised

polyacrylonitrile. The (002) arc is due to the uniform d-spacing of laterally stacked molecules. The oxidised molecules are presumably in a different phase to the polymer precursor molecules, because the (002) arc can co-exist with the (100) polymer arc. The (002) arc is due to a lateral spacing of from 3.65 to 3.80 A^{o}, dependent upon the degree of heat treatment and the orientation of the precursor fibre. When the fibre is heated to 1,000^{o}C and above, this d-spacing decreases to 3.5 A^{o} and it eventually approaches the limiting value for turbostratic graphite, and in some cases the value for perfect graphite. In the graphite crystal, the C-axis will be normal to the (002) planes and in graphitised acrylic fibres the C-axis is approximately normal to the fibre axis. It is for this reason that this new arc produced by oxidation is called the (002), as it will ultimately indicate the presence of graphite layer planes.

The d-spacing of 3.8 A^{o} for oxidised fibre suggests that the molecular packing interval must be of this dimension. The molecules, therefore, can be no longer helical in conformation and they are very probably flat. This agrees with the chemical models of planar aromatic structures. The mechanical properties, however, indicate that the fibre still consists of linear chain segments to some extent, so a simple model of the oxidised fibre must take account of this.

6.42 The variation of fibre X-ray orientation with heat treatment.

The variation of fibre preferred orientation with heat treatment is an important yet difficult phenomena to evaluate. This is because the changes in the diffraction patterns are not solely due to changes in the orientation of the diffracting features. The concentration of unconverted polymer is changing continuously with heat treatment, because of the familiar chemical changes discussed in previous chapters. The orientation angle is a function of the preferred orientation and the concentration of the diffracting phase, and due allowance must be made for this.

FIGURE 6·42(a)

COURTELLE — CHANGE IN ORIENTATION WITH HEAT TREATMENT

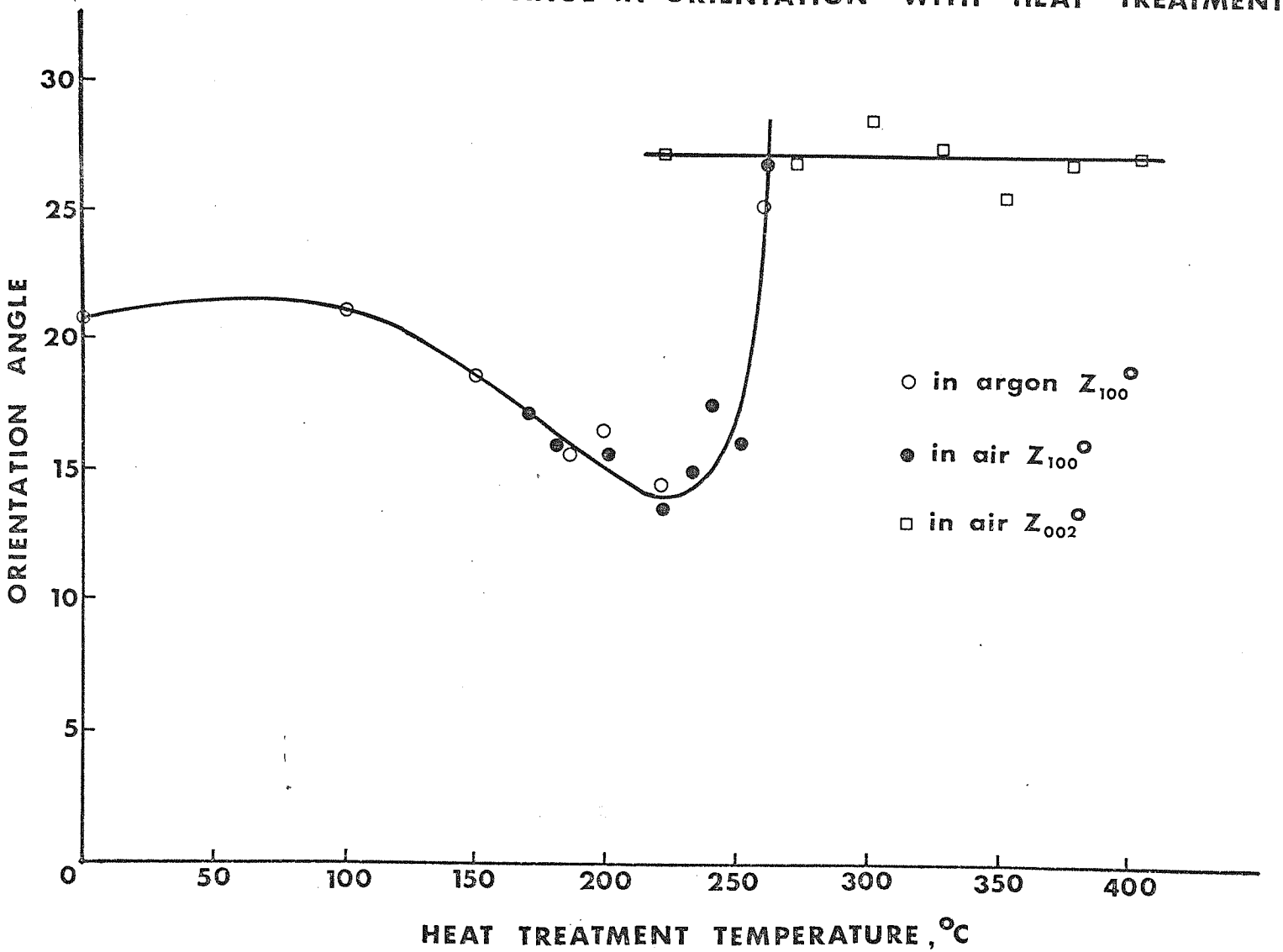

Figure 6.42(a) is a plot of the orientation angle determined from the (100) polymer arc (Z^{o}_{100}) and the (002) arc (Z^{o}_{002}), for the oxidised and pyrolysed Courtelle series of specimens. Figure 6.42(b) is the equivalent plot for the oxidised Dralon T series. Prior to reaching the temperature range in which the reaction exotherm occurs, (200^{o}C+ for Courtelle, 240^{o}C+ for Dralon T) both series of acrylics undergo an initial increase and then decline in the orientation angle. The preferred orientation of the fibre changes in the opposite sense, because the orientation angle is measured with respect to the normal to the fibre axis. This initial change is believed to be due to the competing effects of relaxation in the amorphous phase and annealing in the laterally ordered phase of the fibre. The initially poor correlation in the mechanical properties plotted in figures 6.12(a) to 6.12(c) are probably due in part to these effects.

During the nitrile polymerisation reaction and corresponding to the decline in the residual exotherms shown in figures 4.71(a) and 4.71(b), the (100)precursor polymer arc orientation angle increases very rapidly, to what are very large values for a textile fibre. This might be considered to show that the polymer fibre is relaxing and losing its preferred orientation. This is, however, not necessarily the case, because the appearance of the (002) diffraction arc takes place when the (100) orientation angle is at a minimum and it remains constant during this apparent disorientation of the unconverted polymer fraction. The (002) arc does not appear for the inert treated series, unless a post oxidation is carried out, and provided the pyrolysis temperature does not exceed 345^{o}C, the orientation angle will agree with the directly oxidised sample values.

These results,considered together with the mechanical properties, show that the major fraction of the fibre does not lose much, if any, of its preferred orientation. The minor fraction of unconverted precursor polymer remaining after the nitrile polymerisation is

FIGURE 6·42(b)

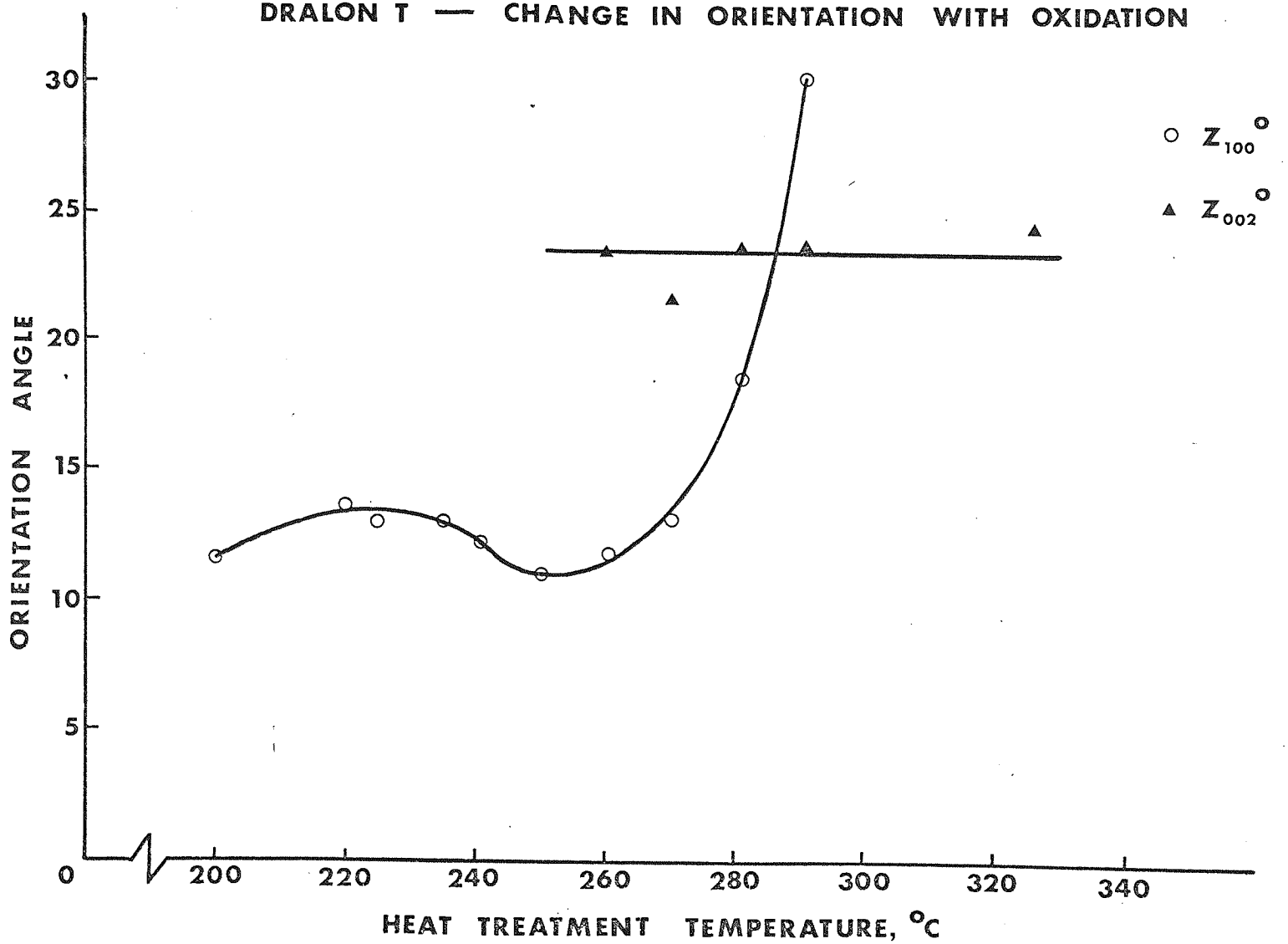
DRALON T — CHANGE IN ORIENTATION WITH OXIDATION
ORIENTATION ANGLE
30
25
20
15
10
5
0
200
220
240
260
280
300
320
340
HEAT TREATMENT TEMPERATURE, °C
Z_{100}^{o}
Z_{002}^{o}

virtually completely disoriented, however, and it is this phase which possibly acts as the loose linking material between the rigid planar segments of the molecule. Courtelle and Dralon T behave similarly with oxidation, but, as in every other respect, the changes proceed more slowly in the pure polymer fibre. As observed with the residual exotherm, the change in orientation angle with pyrolysis temperatures is very rapid in Dralon T, indicating the auto-catalytic character of the reaction in this fibre.

Bacon and Tang [127], in their study of cellulose fibre pyrolysis, attributed the orientation of the carbonised fibre to the molecular orientation of the precursor. They showed that the chain fragments produced at low temperatures could condense to produce an oriented aromatic system. Their chief argument for this was that the oriented (002) diffraction arc appeared as the (100) arc decayed. This is exactly what is observed with oxidised polyacrylonitrile.

6.5 THE CORRELATION OF THE X-RAY ORIENTATION WITH THE ELASTIC ANISOTROPY OF THE FIBRE.

From a knowledge of the modulus of the fibre in tension and in torsion one can calculate the Poisson's ratio. This is given by the expression:-

$$\frac{E}{G} = 2(1 + \mu)$$

where E is Young's modulus, G is the torsion modulus and μ is Poisson's ratio.

For an isotropic solid μ will normally have a value between 0.25 and 0.5.[128] The ratio of the Young's to the torsion modulus would, therefore, be in the range of from 2.5 to 3.0, but if the longitudinal cohesion of the fibre is greater than the lateral cohesion, the $\left(\frac{E}{G}\right)$ ratio will exceed 3. This occurs in textile fibres when they are highly crystalline with a large degree of preferred orientation. High

tenacity rayon filaments can have ratios exceeding 11, for example. The ratio is not only a function of orientation. The cross-linking of an oriented, linear polymer fibre would increase G more than E and the ratio would decrease because of a disproportionate increase in lateral cohesion.

The X-ray orientation angle for the (100) arc in Courtelle has been compared to the variation in $\left(\frac{E}{G}\right)$ with heat treatment, by plotting both quantities in the same figure. This is shown in figure 6.5. The (100) curve is for pyrolysed and oxidised Courtelle fibres and was previously plotted in figure 6.42(a). From 0 to 260°C the one curve is very much a 'mirror image' of the other. The previously discussed relaxation-annealing phenomena observed for heat treatments from 0 to 200°C is confirmed by the anisotropy ratio. The anisotropy deteriorates as the fibre relaxes and increases again as it anneals, on approaching the fibre melting range. The decline in anisotropy between 200 and 260°C, due to the nitrile polymerisation reaction, is the same for both inert and oxidative conditions. This effect is paralleled by the sharp increase in the polymer orientation angle. It was argued previously that the increase in the orientation angle is symptomatic of the loss of concentration of the precursor polymer and that the mechanical properties and (002) diffraction arc show that the preferred orientation remains substantially constant. The loss of the elastic anisotropy is not due to molecular disorientation, therefore. For the oxidised fibres between 200 and 260°C the Young's modulus remains relatively constant and it is the increase in the torsion modulus that reduces the $\left(\frac{E}{G}\right)$ ratio. The major part of the decline for the pyrolysed fibre's anisotropy is also due to this effect. The decline in $\left(\frac{E}{G}\right)$ is due to an increase in the lateral cohesion of the fibres between 200 and 260°C, which could be due to a greater lateral packing of the molecules, with increased bonding between them.

FIGURE 6·5

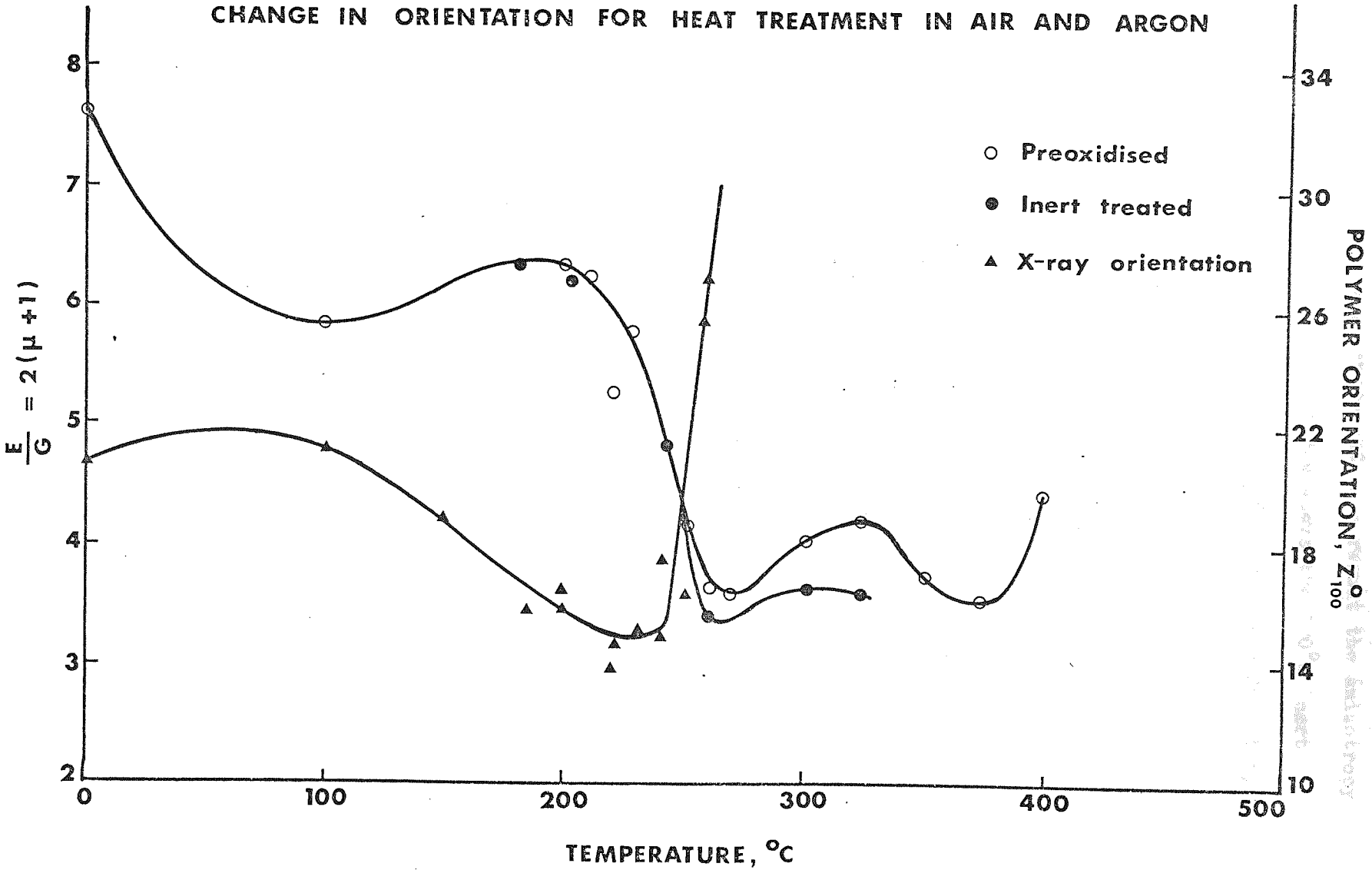
CHANGE IN ORIENTATION FOR HEAT TREATMENT IN AIR AND ARGON
Preoxidised
Inert treated
X-ray orientation
E/G = 2(μ+1)
POLYMER ORIENTATION, Z°100
TEMPERATURE, °C
0
100
200
300
400
500
2
3
4
5
6
7
8
10
14
18
22
26
30
34

Above 260°C, the pyrolysed fibre moduli both decline as the degradation becomes increasingly severe and as a result the anisotropy remains very low. The rigidity of the fibre above the 320°C inert heat treatment could not be measured because of the extreme fragility of the fibres.

The oxidised series of fibres go through a peak in anisotropy at 300°C. The moduli both start to increase above 300°C, but this peak in the ratio reflects the relative progress made by each of the parameters. E possibly improves at first with the increase in the degree of intermolecular bonding, but as the condensation process begins the effect on G is at first greater, reducing the anisotropy. By 400°C, E is increasing very rapidly as the condensation process produces larger and more oriented structures. This last phase is the final one in the change in $\left(\frac{E}{G}\right)$, the ratio continues to climb sharply with heat treatment and achieves values as high as 30 for graphitisation at 3,000°C in argon.

SUMMARY AND CONCLUSIONS.

The X-ray and mechanical property studies reveal very much greater differences between the two types of heat treatment than was implied in the spectral and thermal results. Although, as shown by the nitric acid solubilities, the inertly heat treated Courtelle samples undergo a cross-linking reaction, the reaction exotherm produces a very drastic reduction in the molecular weight, with very obvious effects on the mechanical properties. The solubility in nitric acid and the low intrinsic viscosity after heat treatment to 260°C in argon correspond to the large reduction in strength and elongation at break. The disordered X-ray diffraction pattern also confirms this.

The increase in torsion modulus, with the decline in nitrile content and the loss of the residual exotherm, is supporting evidence

for the nitrile polymerisation reaction of Grassie et al.[61] Obviously a rigid type of molecule is being formed by this reaction, albeit one of low molecular weight. The chain scission reaction might be part of the main reaction mechanism, or, as the author suspects, it may follow immediately upon it.

Oxidation has been assumed in the past to be a cross-linking reaction [50] and the partial insolubilisation in nitric acid observed during the nitrile polymerisation reaction might suggest that this is so. However, this early cross-linking of the fibre could be due to a reaction such as the propagation cross-linking reaction suggested by Grassie et al,[61] which takes place for Courtelle in argon, at lower temperatures. This reaction must be unimportant as far as the stabilising effect of oxidation is concerned. The strength and elongation at break decline during the final stages of the reaction exotherm and the fibres return to 100% solubility in nitric acid. This is characteristic of chain scission reactions, and it can be deduced from this that any cross-linking produced by oxidation has been nullified by 300°C in Courtelle.

The strength, Young's modulus, and torsion modulus all start to increase by 320°C, for heat treatment in air. This corresponds to the development of increasing insolubility in nitric acid and it is obviously due to the polycondensation reactions responsible for the initial stages of the carbonisation process. This is the most important consequence of oxidation, by comparison, pyrolysed fibre becomes increasingly degraded. The torsion modulus is unmeasurable and eventually a catastrophic fusion process occurs at 345°C and above, when the properties drop to very low values and the fibres eventually fuse into a single mass.

Although the oxidation process brings about chain scission degradation, the properties never collapse to the low values exhibited by the pyrolysed fibres. Oxidised fibres have better molecular

packing than inert heat treated material, but this alone is unlikely to be responsible for the better properties. A possible explanation for it can be found in the fact that oxidised polyacrylonitrile will only dissolve in strong mineral acids. Pyrolysed fibre will completely dissolve in formic acid, while lightly oxidised material has only a very slight solubility. The necessity of using an acid solvent suggests that both materials are hydrogen bonded, the oxidised material much more so than the pyrolysed fibre. The presence of (NH) groups in the inert heat treated fibre and the formation of carbonyl upon oxidation (whether in the ambient atmosphere or at high temperatures) means that groups capable of forming hydrogen bonds are present, and they might be present in high concentrations in the oxidised samples.

A most important feature of oxidation is the conservation of preferred orientation during the vital early degradation stage of the heat treatment. It is this initial stabilisation which prevents the ultimate disorganisation of the fibre observed at 345^{o}C. This topic will be considered further in chapter 7.

CHAPTER 7.

THE SIGNIFICANCE OF OXIDATION FOR HIGH TEMPERATURE CARBONISATION.

7.1 PRE-OXIDATION AS A STABILISATION REACTION.

A typical oxidation programme for the preparation of carbon fibre from 1.5 denier Courtelle is seven hours at 220°C. This stage of the process is carried out with the fibre restrained upon a frame for a batch process and for a continuous process, the fibre is restrained between rollers or given a constant degree of stretch, to compensate for fibre relaxation. The carbonisation of pre-oxidised fibre can be carried out without any restraint being applied. In a batch process, the bundles of fibre are simply laid in a sagger and carbonised under an atmosphere of dry nitrogen, or some other inert environment. In a continuous process the load is limited to that required for the maintenance of the tow length, but this is only necessary for preventing contraction during the oxidation process. Pre-oxidation obviously has a strong stabilising effect upon the precursor, in preventing large contractions taking place at high temperatures. A batch carbonisation is normally accomplished within 24 hours, so the high degrees of contraction obtained for the very slow heat treatment in air, shown in figure 4.4(a), will not usually be observed.

7.11 The effect of oxidation upon the contraction of acrylic fibres with processing to 1,000°C.

A standard carbonisation procedure was adopted for processing the carbon fibre in these experiments. The process used approximately 0.1 gram samples of fibre, which were contained in a graphite crucible. The crucible was purged with pure, dry argon, at a flow rate of 1 litre/minute. The temperature was programmed at 12°C/minute to 1,000°C and maintained at temperature for 30 minutes. The furnace was allowed to cool freely, which took about 12 hours to reach ambient

FIGURE 7·11(a)

FIBRE SHRINKAGE ON CARBONISATION TO 1000°C

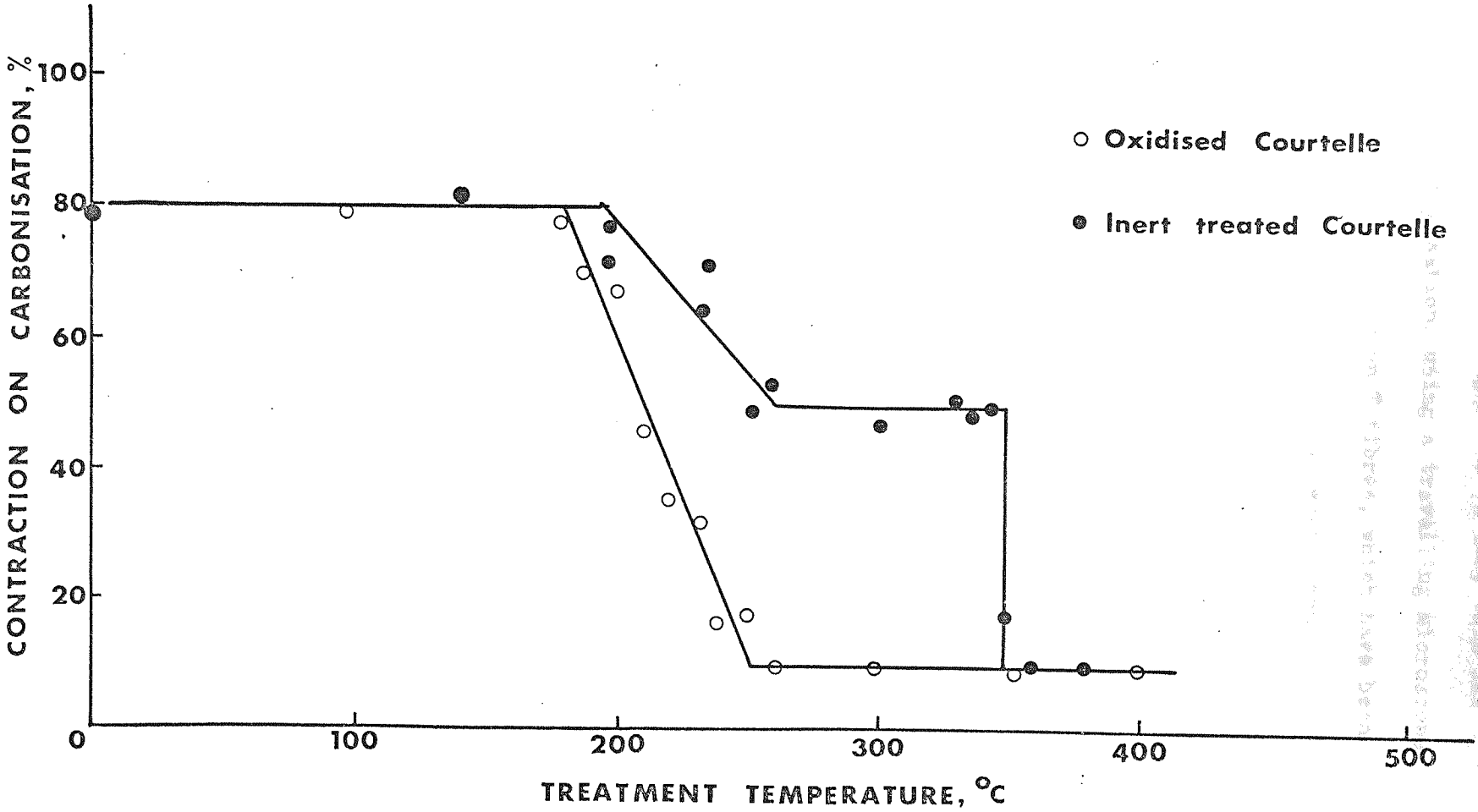

temperature. The initial sample bundle length was 10 cms, this was measured before and after carbonisation, using a travelling microscope.

The two series of Courtelle and Dralon T fibres, which have been considered in the previous sections of the thesis, were given the standard carbonisation. The samples had only been restrained during the first processing stage, the fibre bundles were perfectly free to contract during the carbonisation process itself. Weight loss and contraction were determined for each example and, whenever possible, the strength and Young's modulus were determined for the resultant carbon fibre. Figure 7.11(a) is a plot of the percentage contraction for the Courtelle samples after carbonisation, versus the peak process temperature of the initial heat treatments in air and argon. Between the 0 and 200°C heat treatment temperatures, there is no change in the degree of contraction. Complete relaxation of the samples is produced, as a result of disorientation and melting at high temperatures. Between 200 and 260°C the pre-treatments in air and argon effect increasing degrees of stabilisation. This is the range in which the nitrile polymerisation reaction takes place, with all the other resultant physical changes discussed in earlier chapters. The contractions of the pyrolysed samples are reduced to 50% at 260°C and this remains constant until heat treatment to 345°C, when it declines to 20% (the vertical drop is drawn in to emphasise the change; other changes in properties for these samples are equally sudden in the region of 345°C). The decline in the degree of contraction for oxidation between 200 and 260°C is very much greater, dropping from 80 to 8%. For increasing degrees of oxidation with pre-heat treatment above 260°C, there is no further change in percentage contraction.

A very similar picture emerges for the series of Dralon T heat treatments. There is no change in contraction between 0 and 234°C with pyrolysis, but at 234°C the nitrile polymerisation reaction takes place very rapidly and is completed by a furnace temperature of 236°C (the

FIGURE 7·11 (b)

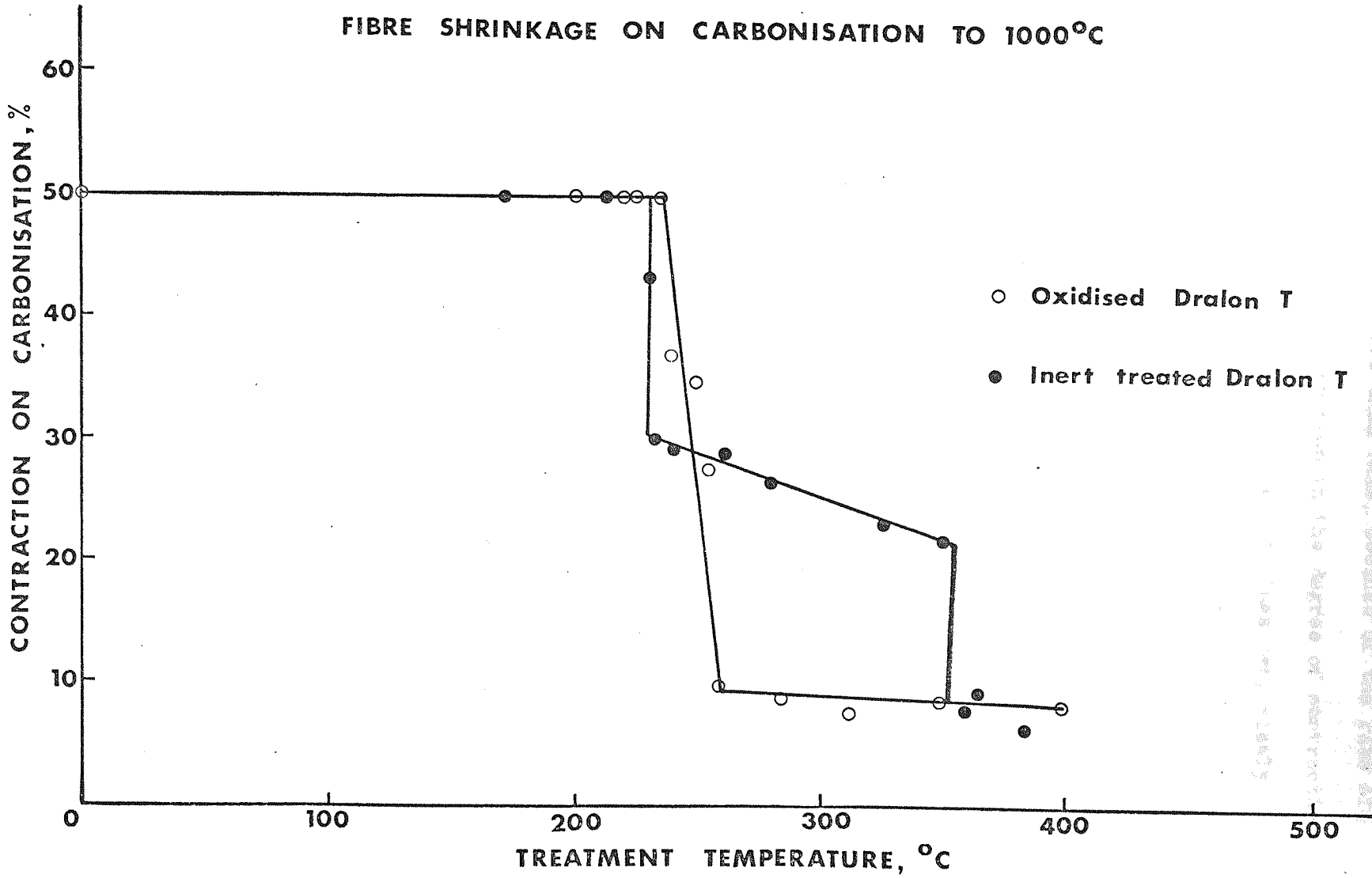
FIBRE SHRINKAGE ON CARBONISATION TO 1000°C
CONTRACTION ON CARBONISATION, %
60
50
40
30
20
10
0
100
200
300
400
500
TREATMENT TEMPERATURE, °C
Oxidised Dralon T
Inert treated Dralon T

fibre temperature is obviously more than this, because of the rate of evolution of heat). There is a sharp drop in the degree of contraction observed as a result, and the contraction then declines very slowly until 350°C, when there is another sharp reduction. The reduction in fibre relaxation for the pre-oxidised Dralon T samples starts a little later than the pyrolised samples (240°C) but it is very much greater, reducing to values of 10% contraction by 260°C. The comparison of Dralon T to Courtelle shows a similar pattern to that observed for the glass transition and melting temperatures. The relaxation of Dralon T is taking place at a consistently higher temperature but, as with the reaction exotherm, the pyrolysed Dralon T undergoes a more rapid change once the process is initiated.

The stabilisation of the pyrolysed and oxidised Courtelle fibres and the pyrolysed Dralon T fibres, corresponds to the development of the cyclised structure. The performance of the reaction in air clearly has a more effective stabilising effect in both acrylics, but the stabilisation of the Dralon T fibre is accomplished before the nitrile polymerisation has reached the half way stage. While the nitrile polymerisation reaction contributes to the stability of the fibre, the oxidation reaction clearly makes the greater contribution.

Oxidised fibre always remained unbroken on the frame throughout the heat treatment, while pyrolysed Dralon T broke at 236°C and the Courtelle fibres broke at 280°C. The continuing decline in fibre contraction above these temperatures is due to disorientation during the pyrolysis, not to a separate stabilising reaction. Nitrile polymerisation alone appears to have a stabilising effect with inert pretreatment.

7.12 The effect of oxidation on weight loss during carbonisation.

The weight loss is not such a useful measure of polymer stability as the degree of contraction, because in preparing carbon fibre it is more important to preserve the preferred orientation than to produce a

FIGURE 7·12 WEIGHT LOSS DEPENDENCE ON PRE-TREATMENT IN AIR & ARGON

FIBRE CARBONISED TO 1,000 °C

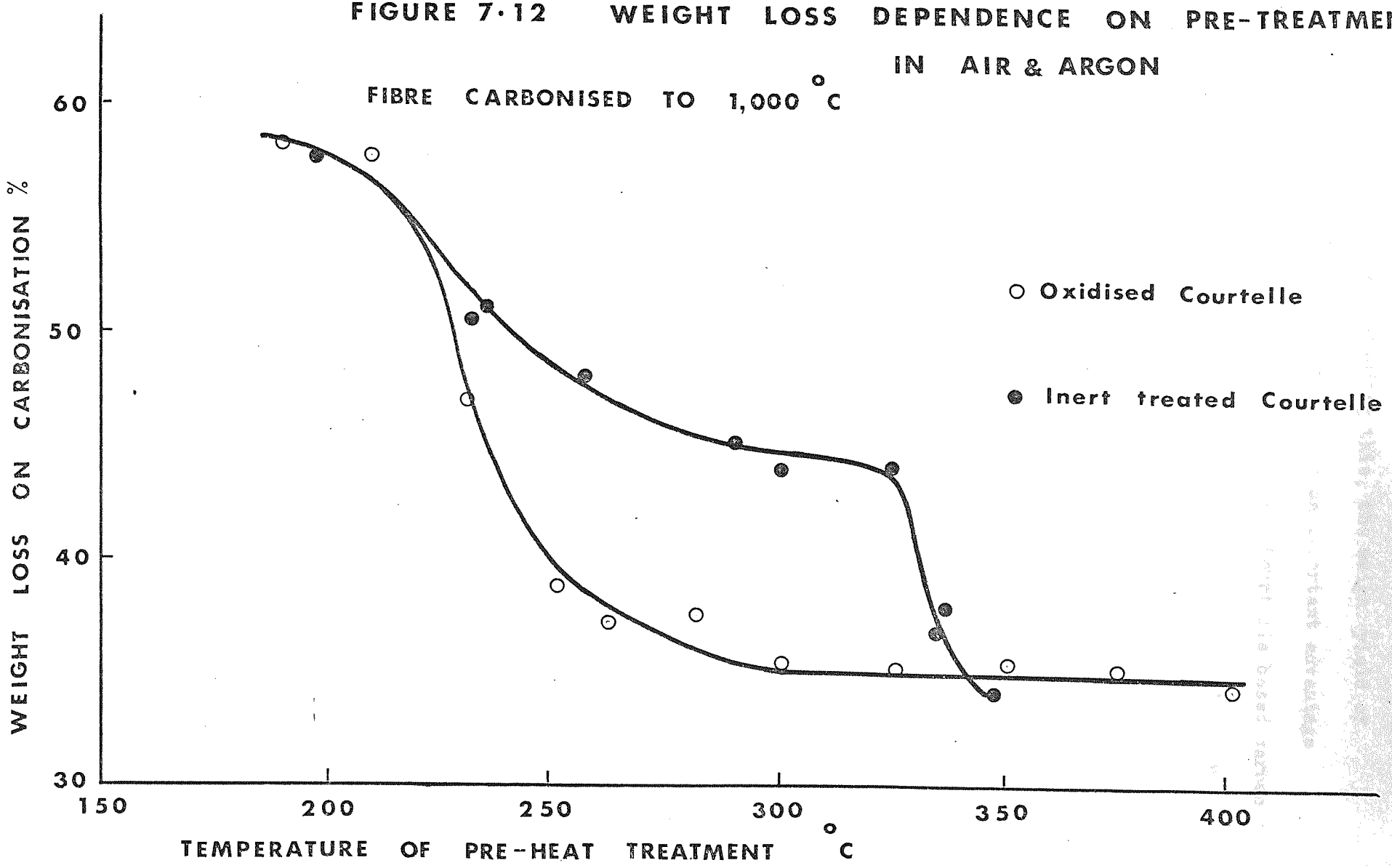

high weight yield. Notwithstanding this, the weight yield of polyacrylonitrile based carbon fibres is an important advantage compared to the use of cellulose precursors. Courtelle based carbon fibre will yield 55% by weight of the precursor as oriented carbon fibre of high strength, while cellulose rarely produces better than a 15% yield.[27]

The pyrolysis of Courtelle under restraint does not have an appreciable effect on the weight yield of carbon fibre, because carbonisation is also a pyrolysis process, and the effect of inert pre-treatment is unlikely to be significant, unless there is a rate or orientation effect upon the chemistry. The weight loss data for the pyrolysed Courtelle series is shown in figure 7.12. The weight loss is just that sustained by the samples during carbonisation. Pyrolysed Courtelle loses 10% of the precursor weight for heat treatments to 300°C, and this accounts for the apparent stabilisation accomplished between 200 and 300°C. The additional weight loss above 320°C is also due to losses during the initial pyrolysis; this corresponds to the fusion phenomena and the sharp reduction in Young's modulus. Inert pre-treatment, therefore, has little or no effect on weight stability, although it does reduce the amount of fibre relaxation.

An interesting aspect of the pyrolysis of polyacrylonitrile is the often reported observation that tars are lost during carbonisation.[78, 79, 80] An unreported observation by Turner and Johnson has shown that pyrolysis to 600°C in argon produces a 23.6% weight reduction as a result of the loss of tars. If the pyrolysis is carried out in vacuo, 26.7% by weight of the fibre is lost as tars. Kasatochkin and Kargin[80] attach a great deal of significance to these losses and consider that the tars originate from the fibre fraction that hasn't cyclised. The structure of the tars normally indicates that nitrile polymerised polymer is present, however, but that it is very low molecular weight material (Turner and Johnson unpublished). The presence of the tars

leads these authors [80] to the view that the pyrolysed fibre has a two phase structure; an oriented, relatively high molecular weight fraction and an unoriented, low molecular weight fraction, which can be extracted by vacuum.

The author has found no evidence for tar formation during the oxidation of Courtelle and there are no reported observations of tar formation with acrylic oxidation that can be found in the literature. The 1°C/min. heat treatment to 260°C in air, under restraint, produces a net weight loss of 3.25%. There has also been a total absorption of 10.13% of oxygen, however, so the true weight loss is much larger. The oxygen contents of the pre-oxidised fibres are all lost in the carbonisation to 1,000°C. Between 200 and 260°C the weight loss is considerably moderated by the pre-oxidation, as shown in figure 7.12, when it declines from 59% to 37%. By 300°C, the oxidation has completed its stabilising effect, and the major part of it is concurrent with the nitrile polymerisation reaction, as also observed with the reduction in fibre contraction. During the oxidation to 300°C, the fibre has absorbed 18.7% by weight of oxygen and suffered a net weight loss of 5.54%.

The oxidation reaction clearly involves the absorption of a great deal of oxygen and a very substantial increase in the stability of the polymer. This is in agreement with the other observations of length change and mechanical properties. The total weight loss for completely pyrolysed Courtelle is 58% compared to 41% for thoroughly oxidised fibre.

7.13 Moisture absorption by heat treated Courtelle.

In order to determine the true change in weight loss on carbonisation, it was found necessary to first extract the moisture absorbed in the fibres during storage. (Miyamichi et al [129] have reported that heat treated acrylic fabrics absorb high proportions of moisture.)

FIGURE 7·13(a)

MOISTURE CONTENTS OF HEAT TREATED COURTELLE

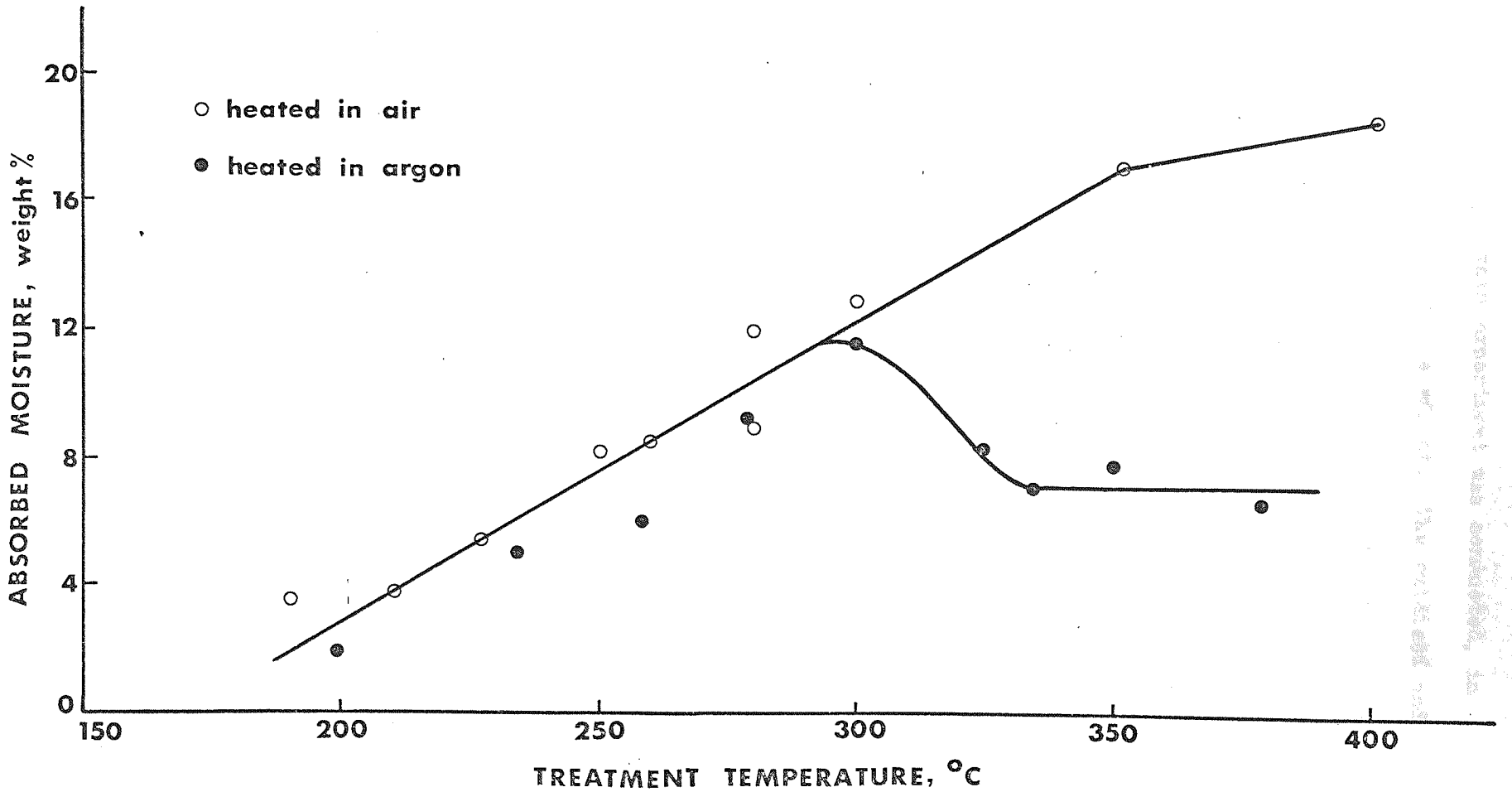

In the case of Courtelle the proportions of moisture absorbed seemed so large that a moisture regain experiment was conducted, in order to make an accurate assessment of the effect. The oxidised and pyrolysed series of Courtelle samples were given a vacuum drying heat treatment at 150°C for 24 hours. After this they were weighed and allowed to absorb moisture from the atmosphere and weighed again once equilibrium was achieved. The final weight usually agreed with the weight prior to drying.

The moisture contents are plotted against the heat treatment temperatures in figure 7.13(a). It can be seen that the moisture absorption from the ambient atmosphere can be very large indeed (the prevailing humidity was normally in the region of 60% R.H.). Oxidation to 400°C renders the fibres capable of absorbing 18% by weight of moisture. This is as large as the most extreme of the hydrophillic polymers, for absorption from the atmosphere. It is interesting to observe how the absorption for the pyrolysed samples declines for heat treatments above 300°C, while the absorption of the oxidised samples continues to increase.

The absorption of moisture in this way and to this extent must be due to the presence of a high density of hydrophillic chemical groups. Such groups have been detected in the infra-red spectra as amines and carbonyls. Continued oxidation increases the concentration of carbonyl groups which explains the increased absorption of the oxidised fibres with heat treatment. Two possible explanations can be offered for the reducing absorption of the pyrolysed samples above 300°C. One is that the hydrophillic groups might be breaking down, as the loss of volatiles increases at these temperatures.

The other possibility is that moisture absorption is only possible as long as the porous structure of the fibre is retained (porous structures have been observed in many examples of heat treated Courtelle fibres [130]). At 345°C the pyrolysed fibre disorients and

FIGURE 7·13(b)

EXAMPLES OF MELTING DURING HEAT TREATMENT

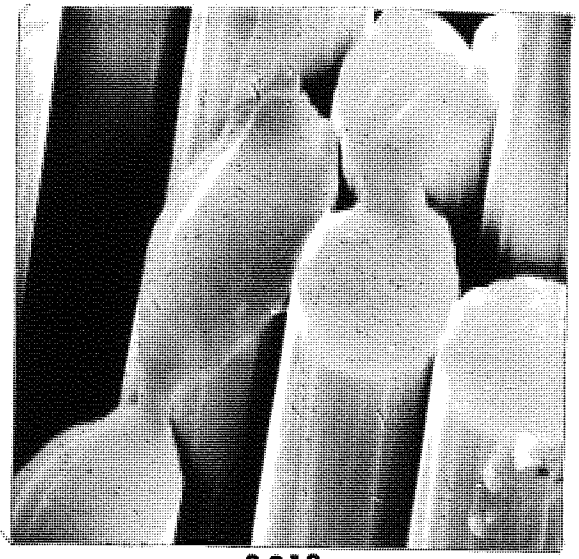

x3,318

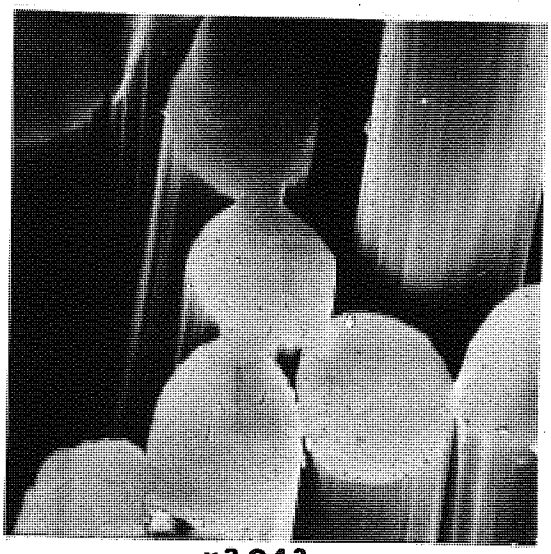

x3,043

COURTELLE HEATED IN ARGON AT $\frac{15}{12}$ °C TO 350°C

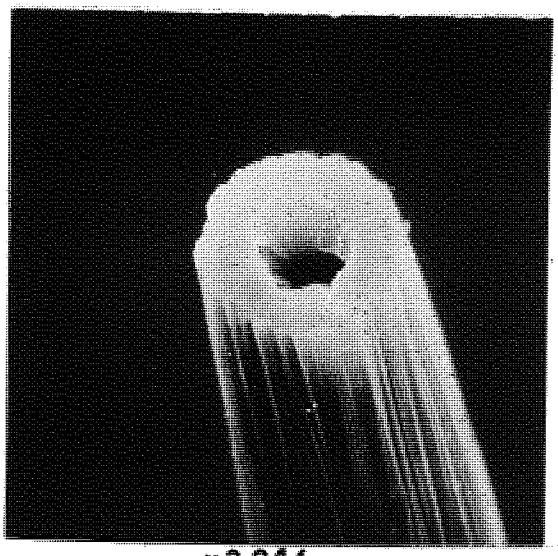

x2,946

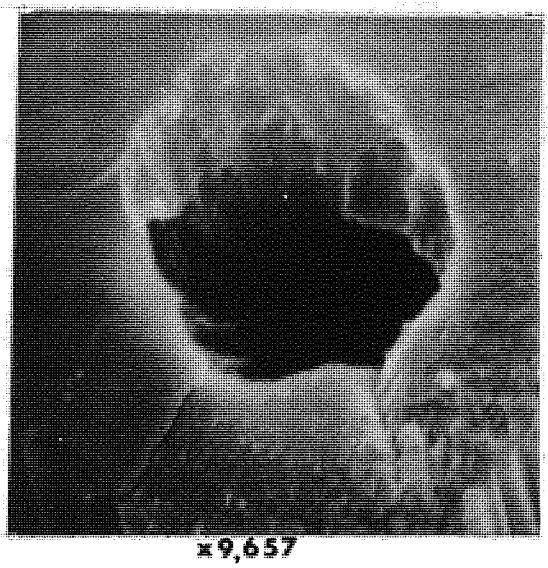

x9,657

COURTELLE OXIDISED AT 300°C FOR 18 mins CARBONISED AT 1,000°C

fuses, and it is quite probable that the pore structure of the fibre collapses, reducing the extent to which the fibre can store moisture. Figure 7.13(b) shows two SEM micrographs, which illustrate the extent of the fusion experienced at 350°C in argon. The fibres do not completely lose their identity, but where they are in direct physical contact they have adhered by melting together. For this to occur, the fibres must have been very plastic and any internal pore system would probably have collapsed as a result of this.

7.14 The dependence of carbon fibre strength and tensile modulus on fibre contraction.

The strength and modulus of carbonised polyacrylonitrile fibre have been studied by Watt et al [50] and Johnson [3]. The former has shown how contraction during oxidation reduces the strength and modulus and that the strength goes through a peak with carbonisation heat treatment temperature at 1,500°C. Johnson has also observed a peak in the tensile strength of carbon fibre and he has quoted a heat treatment temperature of 1,250°C for this. He has also shown that the Young's modulus versus treatment temperature shows a change in slope at the same temperature and that the modulus changes more gradually above 1,250°C. This author has also demonstrated how carbon fibre, behaving as a brittle material, fails from discrete flaws in the treatment range 500 to 1,250°C.[3, 131] These flaws often originate as impurity particles spun into the precursor, acting as stress-raising internal flaws after carbonisation. It has been shown that although the presence of surface flaws can seriously reduce the strength of fibre carbonised to 1,000°C, they can be modified by surface etching, to produce an increase in strength.[3, 131]

Although the strength of carbon fibre, like most materials, has a complex dependence on the type of defects present, the strength also has a very strong dependence on the Young's modulus. Thorne has shown that a wide range of acrylic fibres oxidised and carbonised to 1,000°C,

FIGURE 7·14 (a)

THE EFFECT OF FIBRE CONTRACTION ON YOUNG'S MODULUS

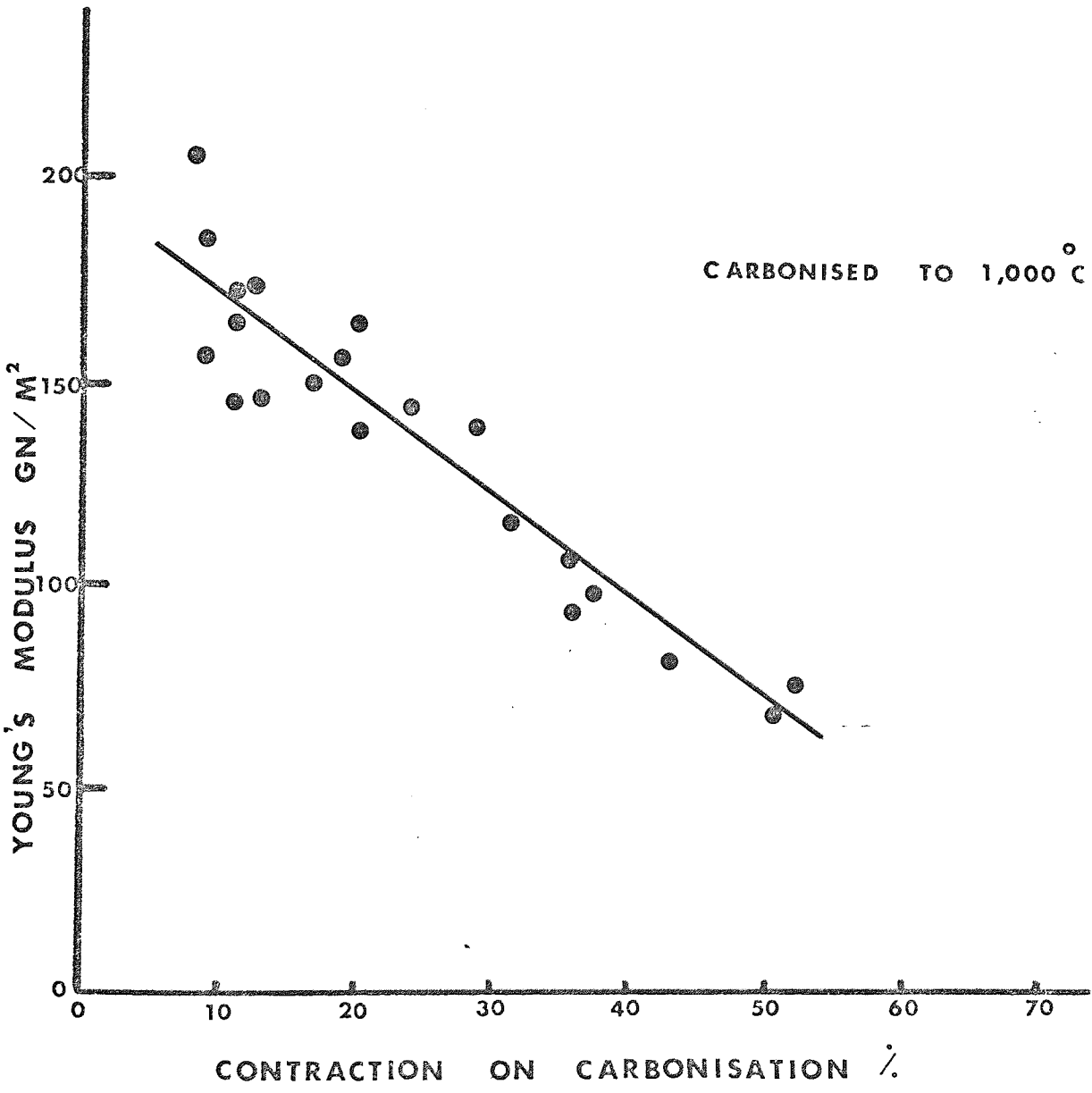

have a fixed relationship of strength to modulus.[132] The Young's modulus, which depends upon the preferred orientation of the fibre, is controlled to a great extent by the method of processing. It is also influenced by the orientation of the precursor [133] as well as by the degree of contraction experienced by the fibre during processing. For heat treatments above 1,250°C, for 1.5 denier oxidised Courtelle, the modulus increase is no longer associated with an increase in strength. The strength steadily declines as the fibre becomes increasingly graphitised.

This thesis is concerned with the influence of processing conditions upon fibre properties. It should, however, be borne in mind that the mechanical properties are influenced by other factors also. The chief advantage of pre-oxidation is that carbonisation can be accomplished rapidly without the need for the restraint demanded by the very slow distillation process.[29] High levels of pre-oxidation can induce a deterioration in the strength and modulus of the carbonised product, however. Courtelle pre-oxidised to 400°C under restraint, for example, produces a carbon fibre after heat treatment to 1,000°C, with a mean modulus of 140 GN/M^2. This is compared to a modulus of 200 GN/M^2 for the more conventional 7 hours at 220°C pre-oxidation. The author believes that this decline is due to fibre relaxation. Restraint will not completely eliminate relaxation of the fibre and relatively long times at high oxidising temperatures are certain to cause a deterioration in preferred orientation.

The result of insufficient pre-oxidation at low temperatures, for which a uniform diffusion of oxygen within the fibre is accomplished, is an undue contraction in fibre length during carbonisation. This has a very great effect upon the mechanical properties of the carbonised products, reducing their strength and modulus. Figure 7.14(a) is a plot of fibre Young's modulus versus the degree of fibre contraction, for oxidised fibre, which has been carbonised to 1,000°C. It is

FIGURE 7·14 (b)

THE EFFECT OF CONTRACTION ON FIBRE STRENGTH

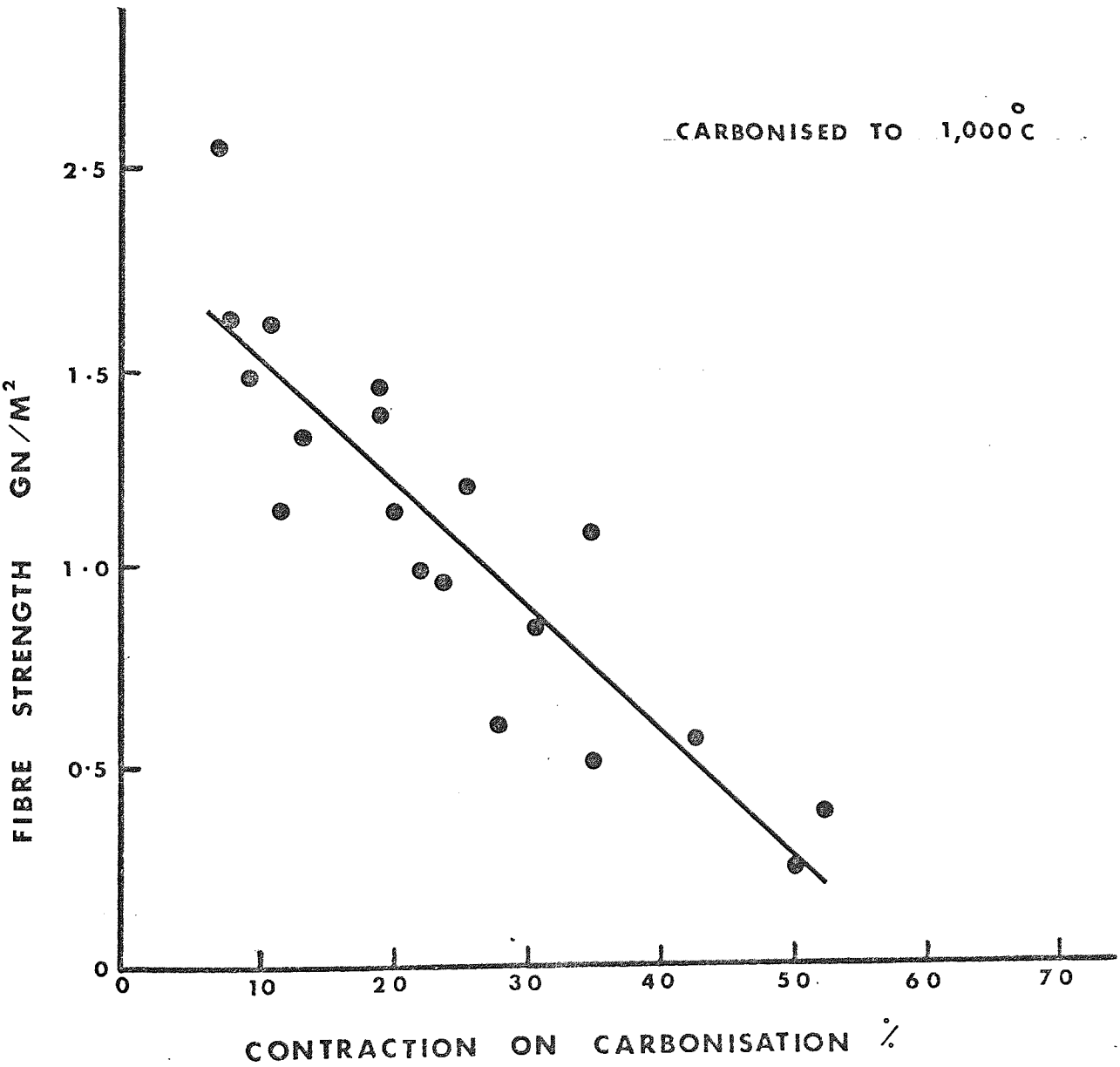

practically impossible to accurately measure the contraction and tensile properties of fibres which have contracted more than 50%, because they are very weak and cannot be pulled straight without breaking. By 60% contraction, the fibres are partially fused. Figure 7.14(b) is the equivalent plot for the fibre strengths. The correlation of the strengths with percentage contraction is very poor; this is, however, not surprising as the standard deviation on the mean strength of most batches of carbon fibre is usually high,[3] as it is for the precursor fibre itself.

The correlation of Young's modulus with contraction is quite satisfactory, as the best fit straight line in figure 7.14(a) shows. A correlation coefficient of 0.97 has been calculated for the data. Young's modulus probably declines with contraction, because of the disorientation of the fibres whilst still in a polymeric state. These contractions are probably equivalent to the low temperature relaxation of the fibre produced by unrestrained oxidation. Watt has shown [50] that this has a similar effect on the Young's modulus of carbonised and graphitised fibre. However, the shrinkage mechanism proposed by Fitzer et al [86] could not possibly produce disorientation, neither would it necessarily affect the ultimate Young's modulus.

7.2 THE MELTING OF PYROLYSED COURTELLE AND ITS SUPPRESSION BY OXIDATION.

The melting of acrylic polymer fibres has already been considered in section 4.5. Rapid heating of the precursor will produce shrinkage and fusion of the fibre at the melting point. However, it is not generally realised that the fibre pyrolysed to the completion of the reaction exotherm can subsequently melt, with very similar consequences. There is a great reluctance to believe that this is so (Watt:- unpublished comments and ref. 92) because it is generally believed that carbon fibre can be prepared from polyacrylonitrile by destructive distillation,[29, 30] and if melting occurred during this process,

separable fibres of high modulus would not be possible.

A melt endotherm can be observed for pyrolysed fibre with rapid scanning in the DSC.1B. It has been observed at 345°C (± 5°C) for a number of acrylics. Pyrolysed fibre has also been found to fuse together (see figure 7.13(b)) and a sharp reduction in properties (figure 6.12(c)) and length contraction (figures 7.11(a) and (b)) are also observed in the region of 345°C.

7.21 Oxidation as a diffusion controlled reaction.

The pre-oxidation of polyacrylonitrile fibres necessarily involves diffusion of oxygen through the fibre. When the rate of reaction of oxygen with the polymer exceeds the rate of diffusion the reaction becomes a diffusion controlled process. Diffusion control is betrayed very often by the appearance of a reaction zone, showing the extent of the progress of oxidation at the temperature of observation. Watt [30] has reported the formation of a reaction zone in 3 denier Courtelle after 2 hours exposure at 220°C. A zone doesn't appear in 1.5 denier Courtelle at 220°C, unless a complete pyrolysis of the fibre is first carried out. It, therefore, seems to be a function of the degree of nitrile polymerisation. This is supported by the formation of the zone in the oxidised Courtelle series, first discussed in section 4.71. It is first observed, very faintly, in the 240°C sample, for which the residual exotherm has declined to 20 Cals/Kg. The zone is very strong in the 260°C sample, for which the residual exotherm has just disappeared, and it is still present in Courtelle fibre heated at 1°C/minute to 325°C in air. This is shown in the SEM micrograph for a fracture surface of the fibre in figure 7.21. It has just about disappeared at 375°C as also shown in figure 7.21, but its size is a function of the fibre diameter, so this is only the approximate temperature of its disappearance.

The actual cause of a reduction in the diffusion rate could be any of a combination of effects. There is the densification due to the

FIGURE 7·21

COURTELLE FIBRES OXIDISED AT 1 °C.min^{-1}. IN AIR.

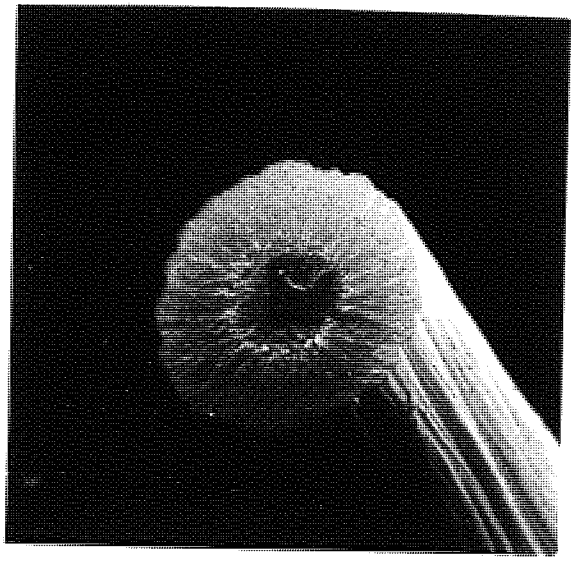

x 3,052

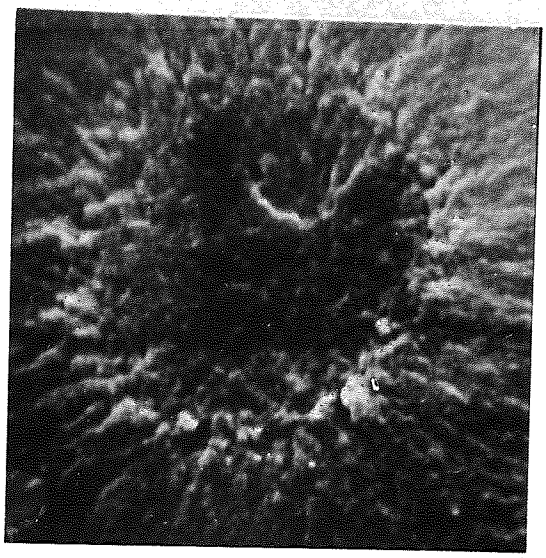

x10,080

OXIDISED TO 325 °C.

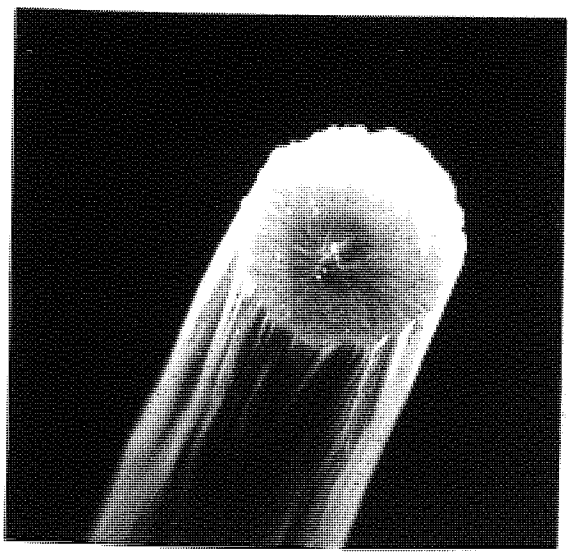

x3,060

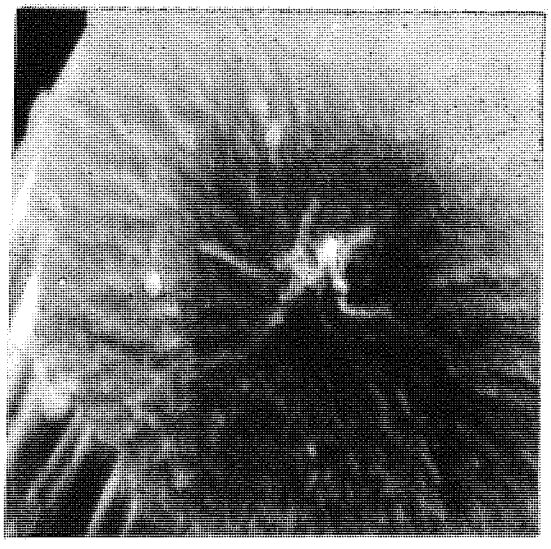

x 10,400

OXIDISED TO 375 °C.

nitrile polymerisation reaction, and the even greater densification due to the oxidation of the resultant cyclised product. Oxidation of the polymer itself, without nitrile polymerisation, might cause a reduction in the rate of diffusion, in the same way as an oxide film on a metal surface may do. This is possibly what is observed with thick fibres at low oxidation temperatures. An alternative possibility is that the diffusion rate is relatively unaffected, but that the polymerisation of the nitriles produces a more reactive polymer, again making the rate of diffusion the limiting condition. The existence of the ring can be used to produce an empirical formula for the completely oxidised, nitrile polymerised product. This might be useful, but only if it is assumed that the product is chemically homogeneous, something that is not usual with oxidised polymers.[84]

Table 7.21 below provides the elemental analysis for the 1.5 denier Courtelle sample oxidised to 375°C, in which the reaction rim has just disappeared. Also shown is the analysis for the isothermal oxidation of 1.5 denier Courtelle at 260°C for 24 hours. This last sample had also reached the point where the elemental composition had equilibriated and the reaction zone had filled the fibre cross-section.

Table 7.21

Sample Courtelle	Carbon %	Nitrogen %	Hydrogen %	Remainder (Oxygen)%
Oxidised at 1° C/Min. to 375°C.	55.83	22.49	1.18	20.50
Oxidised for 24 hrs at 260°C.	56.70	21.40	1.96	20.8

The number of atoms per carbon have been calculated as follows.

Oxidation conditions	Carbon	$\left(\frac{N}{C}\right)$	$\left(\frac{H}{C}\right)$	$\left(\frac{O}{C}\right)$
1°C/minute to 375°C	1	0.29	0.39	0.36
24 hrs at 260°C	1	0.32	0.42	0.28

These results give an empirical formula in which there are approximately three carbon atoms to each of the other three elements. This formula agrees with the stage II product of oxidation proposed by Standage and Matkowsky. (See chapter 3.) Possible structures based upon the presence of carbonyl and a cyclised molecule are shown below:-

(1)

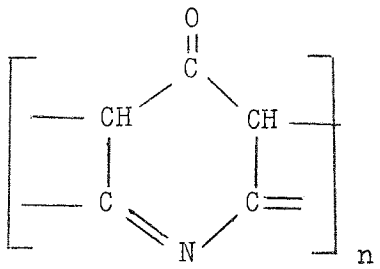

(2)

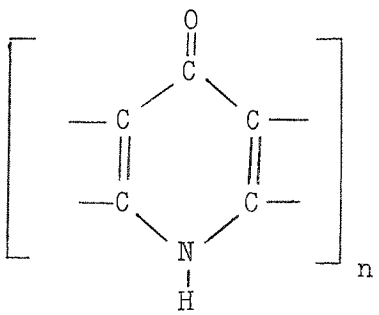

Structure (1) is based upon the Grassie model [60] and structure (2) agrees with the findings of W. D. Potter (unpublished results). Devising molecular structures in this way is a highly hypothetical exercise, however, as it is very unlikely that the hydroperoxides would all break down to produce carbonyl groups.[84] Ring opening reactions could also occur and the cyclised structures will be aromatised to some extent. Structures (1) and (2) should therefore be regarded as idealised models, which could be investigated by more positive

techniques (e.g. n.m.r. spectroscopy). Pre-oxidised acrylic fibres have been shown by photo-electron spectroscopy to contain two types of bound oxygen,[134] but this was at an earlier stage of the process than that investigated here, when hydroperoxide might still have been present in the fibre.

7.22 Molten core formation in partially oxidised fibres.

Because of the diffusion limited reaction at high temperatures, it is possible to highly oxidise the outer fraction of a fibre, with little or no oxidation of the core. A convenient method to use for the high temperature oxidation of acrylic fibres, is the fluid bed. The high thermal conductivity of fluidised particles, combined with a high rate of convection in the bed, enables the control of the reaction exotherm to be retained at high temperatures, hence preventing the fusion and burning of the fibre. A Tecam Ltd 1 KW fluid bed was used for the partial oxidation of samples of 1.5 denier Courtelle fibre. The fluid medium was fine ballatini, fluidised by a constant flow of compressed air. Samples, held under restraint, were prepared for various times at 300°C. They were found after this treatment to have diffusion rings, which could be clearly seen under the optical microscope and which appeared in the SEM to have very similar fracture faces to those previously shown in figure 7.21, for Courtelle oxidised to 325°C. Carbonisation of the samples oxidised for the shorter times resulted in the formation of cavities. The cavities were clearly due to the melting of the material in the core and its partial ejection through the wall of the fibre. An SEM micrograph of such a cavity, shown at two magnifications, can be seen in figure 7.13(b) (in the previous section). This sample had been oxidised for six minutes at 300°C. It is probable that the material in the core melted between 340 and 350°C during the carbonisation i.e. the same temperature range in which the fusion of normally pyrolysed fibres takes place.

FIGURE 7·22 (a)

CAVITIES IN 1·5den. COURTELLE FIBRES. X-RAY RADIOGRAPHS

The cavities are not continuous along the axis of the fibre, but consist of long cells which are sometimes closely spaced. C. N. Tyson (formerly of Rolls-Royce Ltd) has kindly produced X-ray microradiographs of two examples of carbonised Courtelle, containing cavities which show this. These are shown in figure 7.22(a). The microradiographs have been produced using a microfocusing X-ray camera of Tyson's own design.[135] The principle of the method is to produce a magnified radiograph by exposing the sample to a divergent beam of X-rays. The resultant magnified X-ray shadow of the fibres' internal structure is recorded on a flat plate film, placed behind the sample. The first of the two microradiographs shows how the cavities have bulged out the fibre surface, which suggests that the wall of the fibre has been subjected to pressure from the molten core, before this was relieved by the escape of the liquid material.

A better method of demonstrating the effect of an oxidised outer zone is to use a large diameter fibre. The thickest fibre available was a 60 denier monofilament Cashmilon fibre, a copolymer fibre not dissimilar to Courtelle in composition. This fibre was oxidised for 24 hours at 230^{o}C. Being a 60 denier fibre, it has a radius 6.35 times as great as 1.5 denier Courtelle fibre. Hence the differences between the oxidised and pyrolysed phases is shown to a much better effect in the scanning electron microscope. Figure 7.22(b) shows an SEM micrograph for a fractured end of an oxidised Cashmilon fibre. The oxidised outer skin is clearly visible as a separate phase of the fibre, which appears to be partially detached from the core. The large split running down the length of the skin is typical of all the fibres observed. As discussed previously, the oxidised polymer is more dense than the equivalent pyrolysed material. This implies that the oxidised outer phase has had to shrink more to achieve the greater density. As the core does not shrink to the same extent the skin has split to accommodate the resultant strain. The complete separation of the two

FIGURE 7·22(b)

PARTIALLY OXIDISED 60den. FIBRE

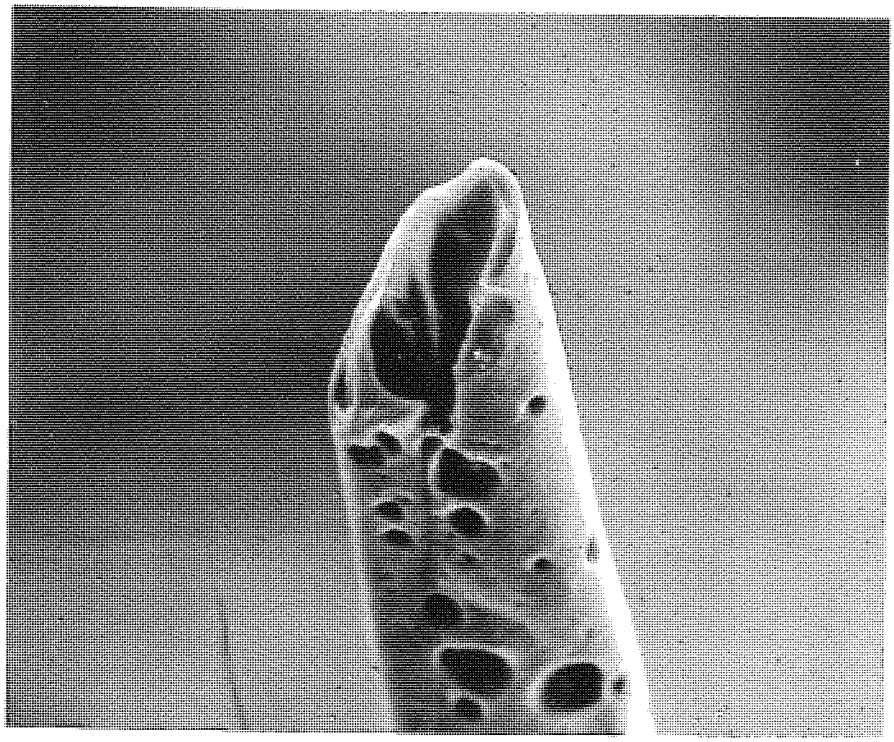

Holes and cavities in carbonised fibre

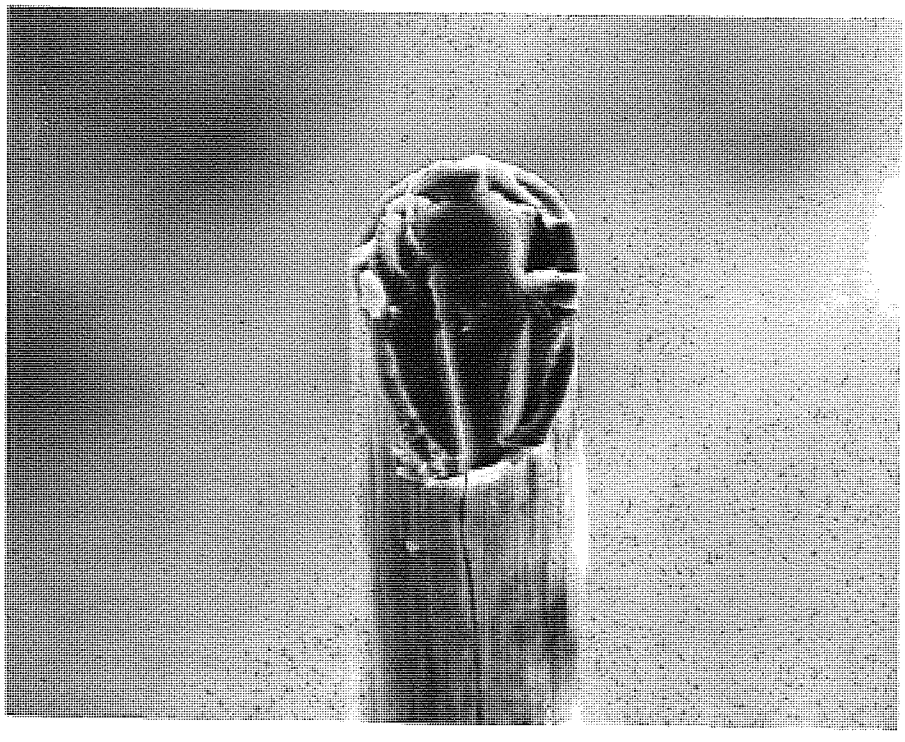

Skin and core in oxidised fibre

phases would be produced by this mechanism.

Apart from the obvious disadvantage of core melting, the existence of a diffusion zone will also be a source of surface flaws. Even if the core does not melt, the differential shrinkage of the two phases might produce surface cracking, which could cause a catastrophic reduction in carbon fibre strength.

The carbonisation of the partially oxidised 60 denier fibre to 1,000^{o}C, has a most dramatic effect. This can be seen in the micrograph above that of the partially oxidised fibre, in figure 7.22(b). The core has melted and a large amount of material erupted through a great variety of holes and fissures in the surface. As this is a large diameter fibre, the manner of the molten material's exit is more easily appreciated than with 1.5 denier Courtelle. Many of the fibres show total collapse with large cracks running along the surface. The molten material must be from the unoxidised fraction of the fibre and the disgorged material would normally be observed as tars, as will be seen from the fibre weight loss pattern.

An X-ray microradiograph of carbonised 60 denier fibres can be seen in figure 7.22(c). The central cavity runs the whole length of the fibre and the variation in optical density of the fibre shows the holes which run out to the surface from the centre.

Cavities are never found in inert heat treated fibre and if the melting of the core is the same melting which causes surface fusion with pyrolysis, the formation of cavities must be due to the oxidised fibre wall. The containment effect of the wall probably causes the core material to volatilise under pressure, producing the forces necessary for the violent escape of the tars. If both phenomena are the same melting process, the weight loss patterns for purely inert processed and partially oxidised 60 denier fibres should be very similar. This has been shown to be the case, using thermogravimetric analysis. A Stanton Thermobalance was used for this purpose, with a

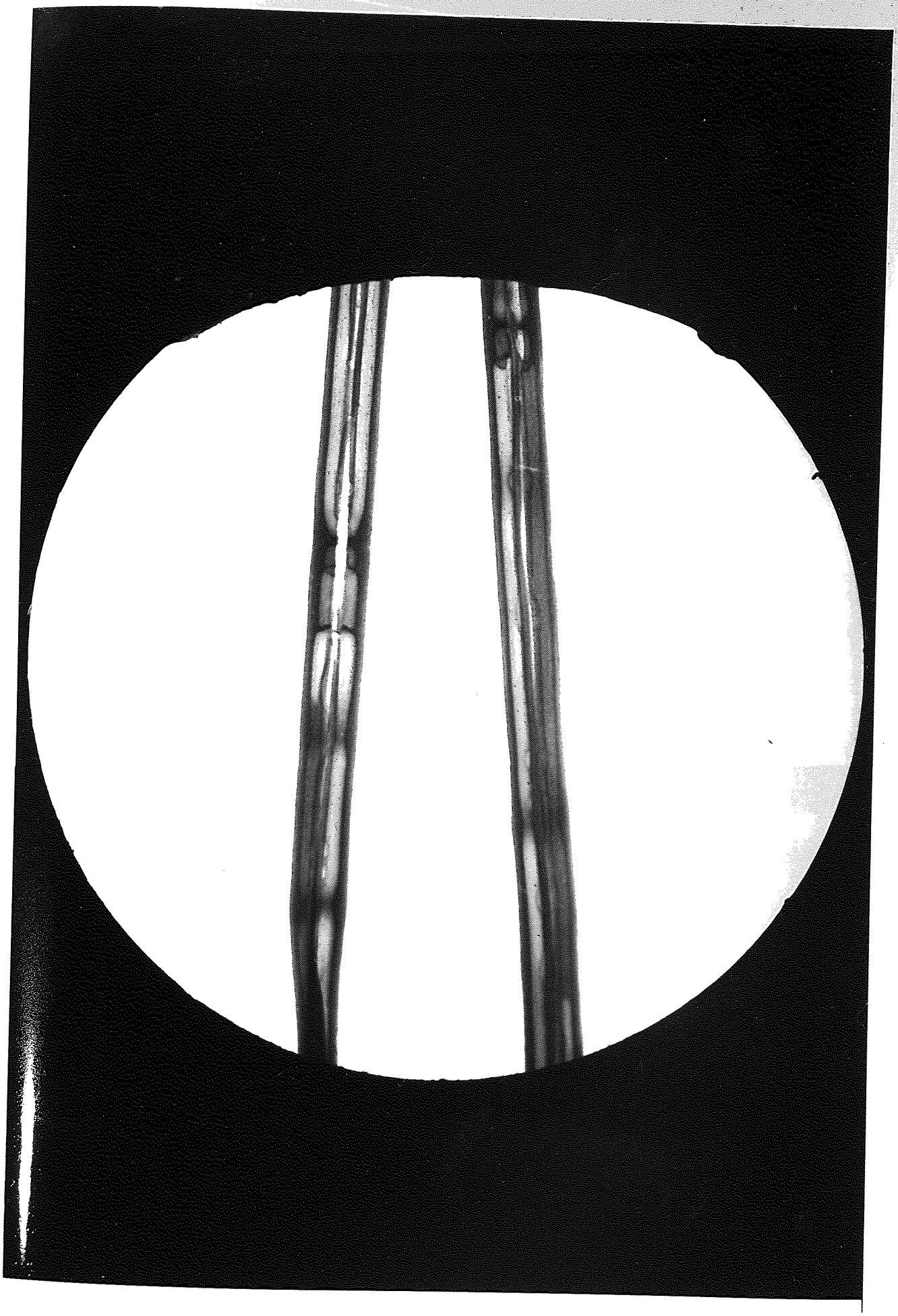

FIGURE 7·22(c)

CAVITIES AND HOLES IN 60den. FIBRE. X-RAY RADIOGRAPHS

of 3°C/minute.

Three samples of 60 denier acrylic were studied and the resultant weight loss curves for them are shown in figure 7.22(d). Sample A is simply untreated precursor fibre and the weight loss curve for this is characteristic of the behaviour of completely pyrolysed polyacrylonitrile. Sample B is the partially oxidised fibre already considered above, while sample C is 60 denier fibre which has received a very high level of oxidation (> 100 hours at 300°C in air). It is of interest to note that this last fibre still retains a diffusion ring, but on carbonisation to 1,000°C the core shows only slight cavity formation. The weight loss curve for sample C is quite typical of a well oxidised polyacrylonitrile fibre. It is usually linear, although the small step in weight loss at 450°C is exceptional.

The total weight losses shown in figure 7.22(d) cannot be compared directly, because samples B and C have lost weight during oxidation; B has lost 4.6% and C 14.3%. The weight loss shown by each sample between 0 and 130°C should also be taken into account. This is due to the removal of absorbed moisture. If both factors are considered, the true weight loss per gram of precursor fibre can be calculated. These are, for A 52%, for B 40% and for C 41% after heat treatment to 1,000°C. Although larger cavities have formed in B, the weight loss of C is as great, due to the much larger weight loss sustained during oxidation. The sharp decrease in weight at 300°C for sample A corresponds to the reaction exotherm. This is commonly observed for polyacrylonitriles which have sharp exotherms under inert conditions. Grassie and Macguchan have shown this with several samples.[79] There are similarities between the TGA curves for A and B. They exhibit the same weight loss pattern, beginning at ~ 340°C and finishing at ~ 520°C. This similarity of behaviour corresponds to the formation of central cores in sample B and to the sticking of fibres in sample A. This is reasonable evidence for the view that both phenomena are due to the

FIGURE 7·22 (d)

T.G.A. CURVES FOR 60den. ACRYLIC

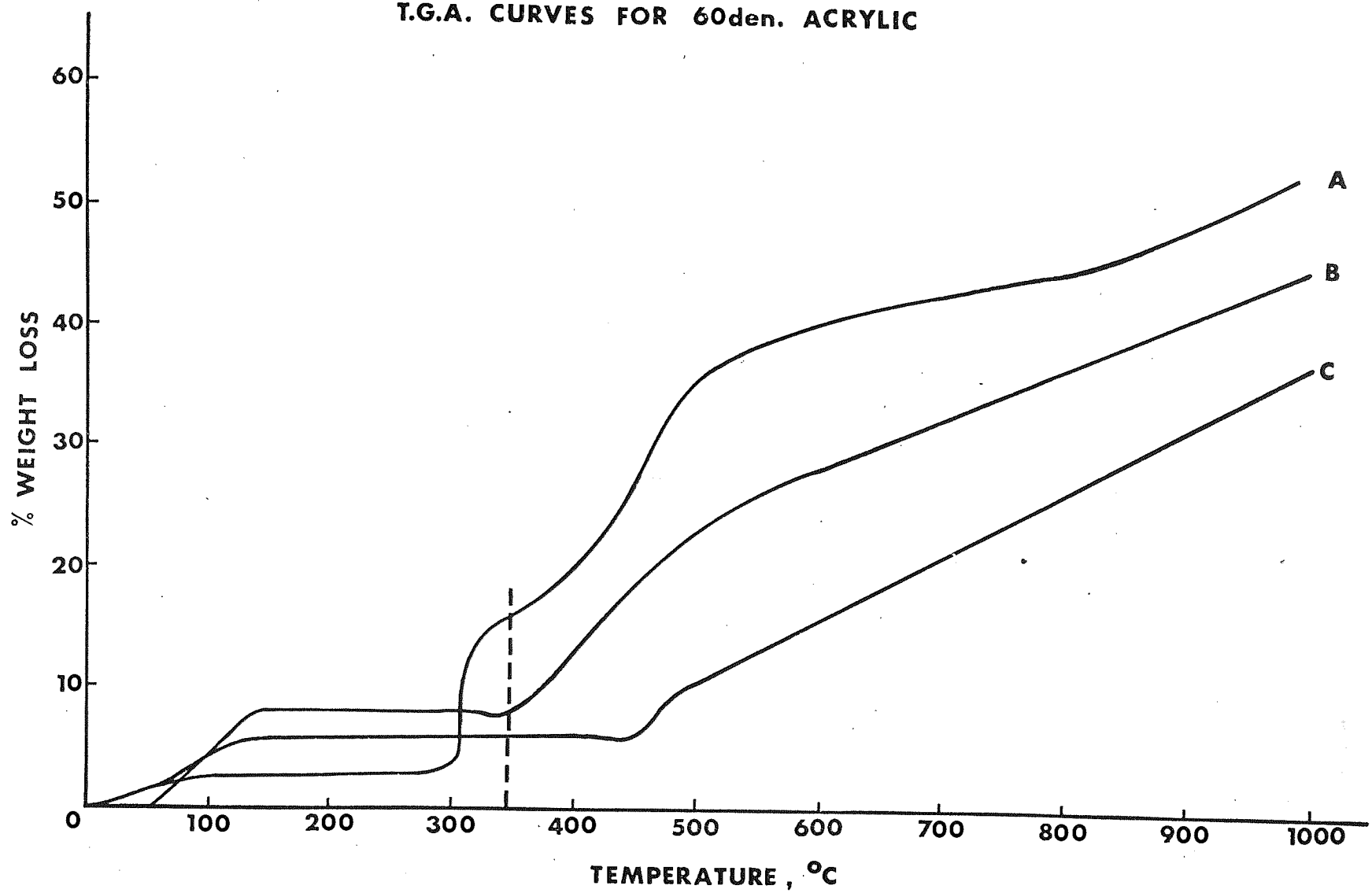

same melting process. A large proportion of the weight losses between 340°C and 520°C is found to be associated with the formation of low molecular weight tars. Above 500°C the weight loss from sample B is linear, as it is for sample C. If a 60 denier fibre could be prepared without any internal cavities, the weight loss curve should be entirely straight and the inflection at 450°C for curve C would be absent.

7.23 The dependence of carbon fibre strength and modulus on the degree of pyrolysis.

The effects of separating the pyrolysis from the oxidation reactions has already been discussed in terms of the mechanical properties and solubility of the fibre. In this section, the effect upon carbon fibre properties will be discussed. A series of Courtelle samples (the OP series) have been inert pre-treated under restraint to temperatures in the range 280 to 400°C and then given an oxidation to the same temperature at the same programme rate, but without restraint, in a flow of air. Each oxidation was conducted with a control sample of untreated precursor held under restraint, which was subsequently carbonised and tested with the experimental sample. After pyrolysis above 280°C, there is very little X-ray diffraction, the mechanical properties are poor and become increasingly so with heat treatment, and the samples produced cannot be carbonised without prior oxidation, because they would otherwise fuse. After oxidation, however, the mechanical properties are improved, the fibres can be separated and carbonised without fusing. Oxidation also invariably introduces lateral order into the fibre, which produces an X-ray diffraction arc. This can be used to determine the preferred orientation of the fibre.

The samples were carbonised at 12°C/minute to 1,000°C and held at temperature for 30 minutes before cooling. The furnace was thoroughly evacuated before commencing the process and a purge of high purity argon was used at a rate of 1 litre/minute throughout the programme. The strength and modulus were determined for each batch

FIGURE 7·23(a)

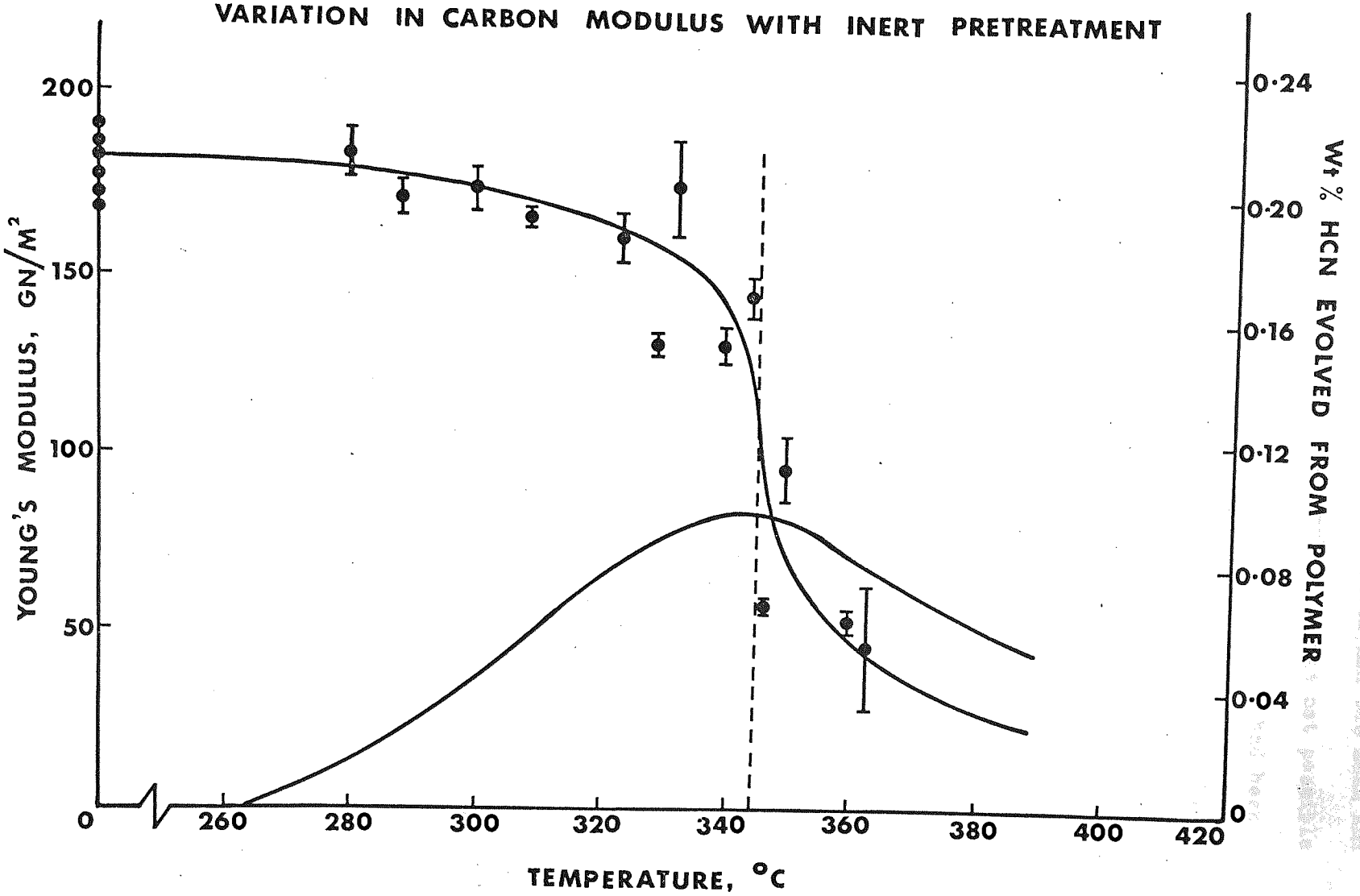
VARIATION IN CARBON MODULUS WITH INERT PRETREATMENT
YOUNG'S MODULUS, GN/M²
200
150
100
50
0
260
280
300
320
340
360
380
400
420
TEMPERATURE, °C
0·24
0·20
0·16
0·12
0·08
0·04
0
Wt % HCN EVOLVED FROM POLYMER

where this was possible. This was done in the way described in Chapter 2; twelve fibres were tested from each batch and the mean and 95% confidence limits calculated for each sample. It was not possible to test the carbon fibres prepared from the precursors that had been pyrolysed above 370°C, because they were too firmly fused together, and oxidation did not sufficiently assist their separation. The Young's moduli for the samples are plotted in figure 7.23(a). Some of the oxidised control values have been plotted in the figure in order to show the range of results, and, as they have received no inert preheat treatment, they are plotted at 0°C. All the other moduli are plotted against the maximum temperature of inert pre-heat treatment. 95% confidence limits on the mean of each result are shown as horizontal bars for each data point.

Figure 7.23(a) shows that between 340°C and 360°C the inert pretreatment is bringing about a sharp reduction in Young's modulus. This does not happen for straightforward oxidation, as the moduli remain between 170 and 190 GN/M^2 for the control samples. Inert heat treatments above 340°C have already come to have some significance from a consideration of fibre length changes during carbonisation; the amount of contraction drops very sharply at 345°C (figure 7.11(a)). The same occurs for the Young's modulus of the pyrolysed fibre (figure 6.12(c)). A vertical hatched line has been drawn in figure 7.23(a) to correspond to 345°C. This has been quoted as the melting point for polyacrylonitrile.[81] It would seem more sensible to talk about the melting of the pyrolysis product, as the nitrile polymerisation reaction has been completed by 260°C. The drop in Young's modulus is associated with the same process that causes fibre fusion and, in the presence of an oxidised zone, fibre cavity formation.

The only chemical event that appears to be associated with the transition at 345°C and the drop in Young's modulus, is the evolution of HCN. The formation of ammonia occurs too early to have any

FIGURE 7·23(b)

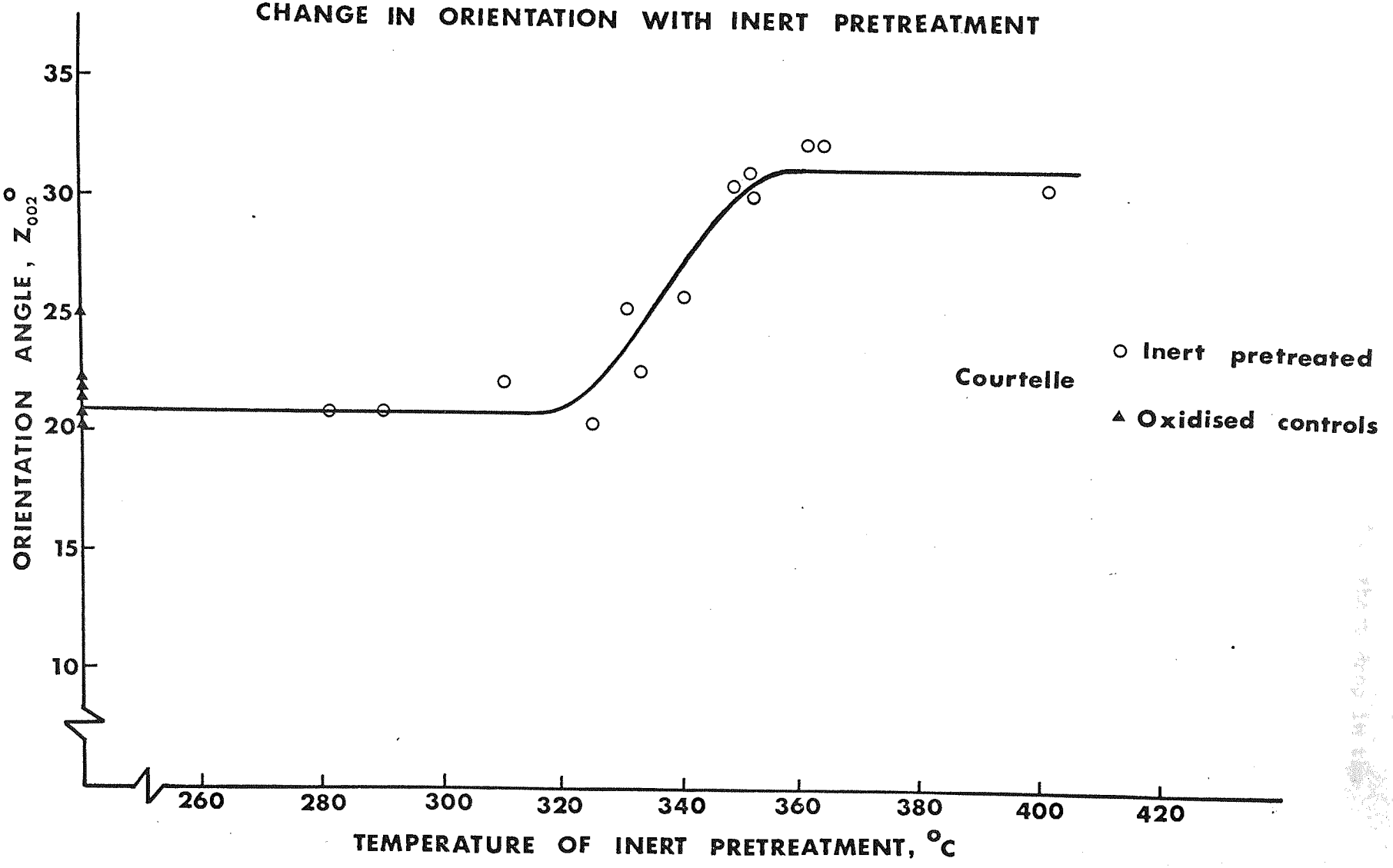
CHANGE IN ORIENTATION WITH INERT PRETREATMENT
ORIENTATION ANGLE, Z_{002}°
35
30
25
20
15
10
260
280
300
320
340
360
380
400
420
TEMPERATURE OF INERT PRETREATMENT, °C
Courtelle
○ Inert pretreated
▲ Oxidised controls

correlation and the formation of hydrogen takes place too late. The HCN evolution curve is also shown in figure 7.23(a) and the peak in the curve corresponds exactly to 345°C and to the sharp drop in the Young's modulus.

HCN is lost in two regions of the pyrolysis process;[114] between 260 and 500°C, as shown in figure 7.23(a) (and peaking at ~350°C) and between 500 and 1,000°C (peaking at ~ 600°C). Not all the nitrogen is lost by this means, as Watt has shown,[49] purely inert heat treatment accounts for 23.2% loss of the original molar content of nitriles in Courtelle. This value is in quite good agreement with the 22% remanent content of nitrile groups, found to be present after the completion of the pyrolysis reaction exotherm (see figure 5.31(b)). Most of the nitrogen loss with carbonisation is in the form of molecular nitrogen which is evolved at above 600°C; the structure which binds the nitrogen must therefore be very stable.

The decline in carbon fibre modulus for inert pre-treatments beyond 360°C is very great and possibly continues on to values of 28 GN/M^2, which is the expected value of Young's modulus for isotropic graphite. Such a large decline in modulus could only be due to the disorientation of the structure. The orientation of the carbonised OP series has been determined by the calculation of the orientation angle, Z°. As described before, this is the half angular width, measured at half the peak intensity, for the intensity distribution measured around the (002) X-ray diffraction arc. Figure 7.23(b) is a graph of orientation angle versus inert pre-heat treatment temperature, for the carbon fibre series for which the modulus has been plotted in figure 7.23(a). As in that figure, the control values are plotted at 0°C.

From an orientation angle of 21° at 325°C, agreeing with the mean control value, the angle increases with temperature to 32.5° at 360°C. It is interesting to observe that though this is a large increase in orientation angle, the fibre has not completely disoriented on heating

Figure 7.23(c)

X-ray fibre diagrams for carbonised fibre.

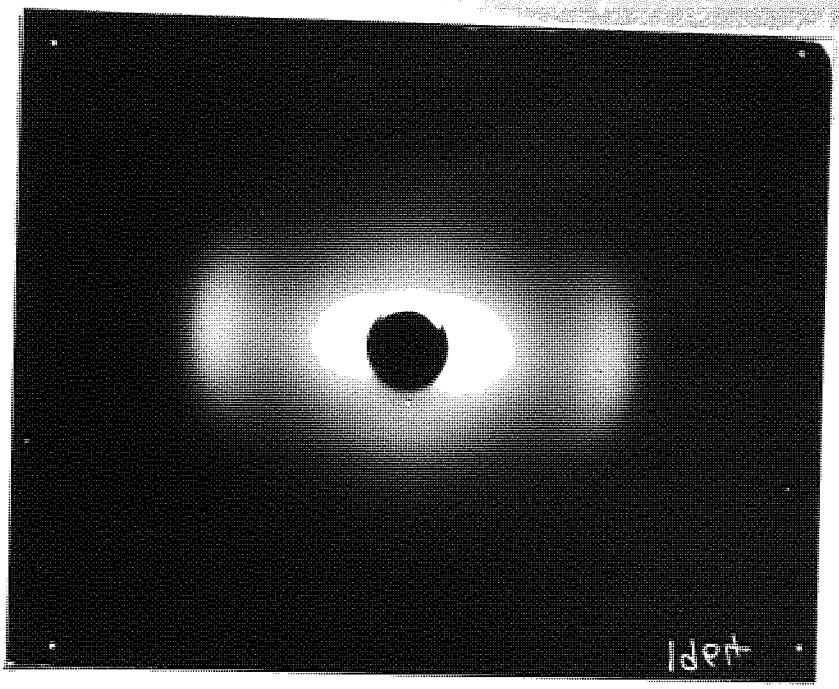

Courtelle, inert pretreated to 325°C,

oxidised and carbonised.

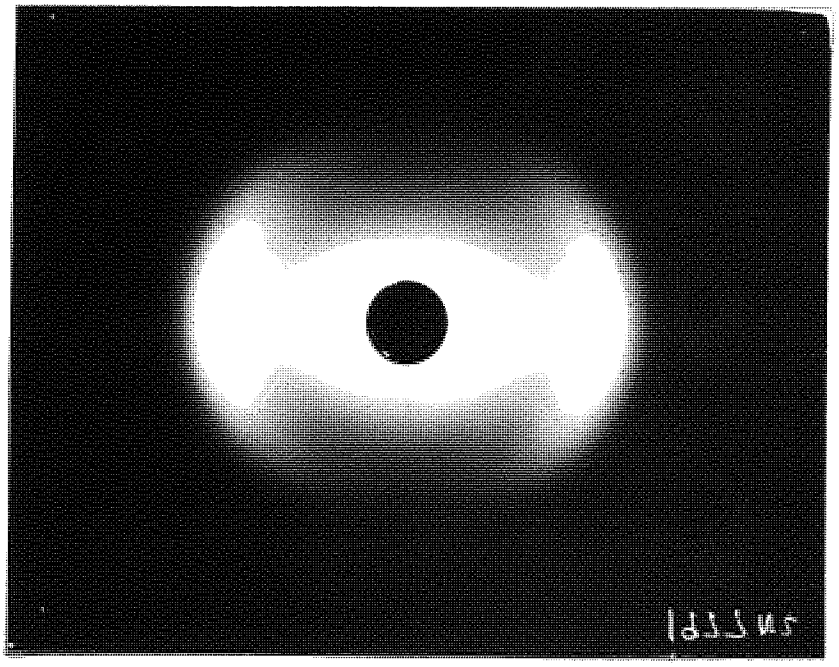

Courtelle, inert pretreated to 363°C,

oxidised and carbonised.

above 345°C. Fusion of the fibres is, therefore, not due to a complete melting of the structure, which should produce a complet disordering of the X-ray diffraction pattern. A comparison of the X-ray fibre diagrams is interesting. Figure 7.23(c) compares the X-ray fibre diagram of a fibre inert heat treated to 325°C and then oxidised and carbonised, with a fibre which was inert heat treated to 363°C, prior to subsequent processing. The two fibre diagrams represent the samples at each extreme of the change shown in figure 7.23(b).

The 325°C sample can be seen to be much more highly oriented than the 363°C sample (the difference may appear to be much greater than the difference in orientation angles suggests to most readers). The (002) diffraction arc and the low angle pattern each side of the central aperture, both show the relative degree of preferred orientation. A particularly significant difference between the patterns is the presence of an amorphous halo, extending down to low angles in the 363°C sample, which is almost completely absent in the 325°C sample. This suggests that melting is the result of a two phase structure, in which one phase completely disorders while the other remains oriented to some extent.

SUMMARY AND CONCLUSIONS.

The stabilising effect of oxidation is shown quite graphically by the effect it has on fibre contraction with carbonisation. Courtelle is completely stabilised by the completion of the reaction exotherm and the product of this reaction, almost certainly a cyclised molecule, must have an important part to play in the stability of the material. In the case of Dralon T, the length is stabilised before the reaction exotherm is completed, but the carbon fibre properties are only satisfactory if the exotherm is removed while the fibre is held under restraint. This is because the fibres soften and adhere during carbonisation, which has a deleterious effect on strength. Dralon T

oxidised to 300°C to remove the exotherm and then carbonised, shows no adhesion and the properties are at least as good as Courtelle based fibre.

After the completion of the inert reaction exotherm, pyrolysed and oxidised fibres have many similarities; the major differences appear for heat treatments to higher temperatures. The pyrolysed fibres continue to degrade and the evolution of HCN appears to be symptomatic of this. However, the fibre is still polymeric at 345°C, which is why the fibre is capable of large shrinkages at this temperature. Pyrolysis effectively increases the melting point of the fibre from 281°C (for Courtelle) to 345°C, but oxidation completely removes the possibility of melting. Oxidised fibre is undergoing extensive condensation reactions from 300°C upwards and by 345°C the fibre has been rendered incapable of melting or disorienting, unless extremely long relaxation times are permitted.

The successful oxidation of polyacrylonitrile to form a carbonisable product no doubt depends upon the formation of the cyclised structure. However, without an oxidation process, it seems improbable that carbon fibre of good properties could be prepared. This conflicts with the generally held belief that carbon fibre of good properties can be prepared by a completely inert distillation process.[29, 30] A clue to the reasons for the success of the distillation method can be found in a recent observation by one of the original inventors.[113] Fibre maintained in an atmosphere of nitrogen at 335°C was found to absorb 10.2% by weight of oxygen, after two hours in the furnace and yet the nitrogen contained only 50 p.p.m. of oxygen. This amount of oxygen absorbed at below 345°C would be quite sufficient to stabilise the fibre against melting. One of the essential features of the distillation process is that very slow heating rates are used (the Rolls-Royce process required 5 days for the temperature to reach 1,000°C). With these very slow rates and a sufficient level of

oxygen impurity in the purge gas, the distillation process might in practice have involved the use of an oxidation stage.

The major advantage of the 1,4 dihydropyridine structure proposed by Potter is that it will have a very high oxidation potential. It will oxidise at room temperature in the atmosphere and it should be quite capable of absorbing oxygen to the extent observed by Standage and Matkowsky.[113] The hydrogenated naphthiridine structure proposed by Grassie will not have this property. The empirical formula derived for fully oxidised fibre shows that there is one oxygen atom per former monomer unit and infra-red spectroscopy shows that some of this will be in the form of carbonyl groups. Hydrogen bonding between these groups and the (NH) group in the dihydropyridine structure could explain the superior properties obtained with oxidised fibre and the presence of both groups explains the solubility of the materials in acids and their remarkable hydroscopicity.

The HCN loss might be due to the disintegration of the uncyclised segments of the chain. As the chain length shortens the melting point of the pyrolysed polymer is reduced and it is quite reasonable to find the melting temperature at the peak in the rate of evolution of HCN. The fibre clearly disorients as a result of thermal degradation and melting in argon and the reduction in Young's modulus of the carbonised fibre will be due to this.

Watt [30] had attributed the formation of cavities in 3 denier Courtelle fibre to the shrinkage of the material in the core. The experiments with 60 denier fibre demonstrate that this is unlikely to be the case and that core melting is the most probable explanation of the effect.

CHAPTER 8.

THE PREPARATION OF CARBON FIBRES AT VERY HIGH TEMPERATURES.

8.1 THE GRAPHITISATION OF OXIDISED POLYACRYLONITRILE FIBRES.

It is generally recognised that the carbonisation of organic materials to produce graphite can be considered to consist of three overlapping stages. The initial, low temperature, stage usually involves the breakdown and aromatisation of the precursor material. This is the pyrolysis stage, which is usually completed by 500°C. From 500 to 1,000°C, the formation of the carbon residue takes place, following the elimination of the other atomic species, although some hydrogen can be present until 2,000°C. Polyacrylonitrile based carbon will also contain a small weight percentage of nitrogen, at this stage. 1,000°C carbon has a primitive crystal structure, consisting of very small crystallites, completely lacking in three-dimensional order. Further heat treatment of carbons above 1,000°C, and particularly in the temperature range above 1800°C, produces a growth in mean crystallite size and generally an improvement in the degree of crystalline order. This process is generally called the graphitisation of the carbon, though this is not always meant to imply that the carbon will necessarily form a perfect graphite by heat treatment alone.

Two parameters are used when defining the size of a graphite crystallite, L_c and L_a. L_c is determined from the width of the (002) X-ray diffraction arc profile and provides a measure of the mean thickness of the crystallites, in the direction parallel to the graphite C-axis. L_a is determined from the (100) or (110) diffraction arc profile and is a measure of the mean graphite layer diameter i.e. it is the mean dimension of the crystallites perpendicular to the C-axis. Johnson and Tyson [20] have reported layer diameters in Rolls-Royce carbon fibre, which have been calculated from the low angle diffraction pattern. The parameter they use is designated by the symbol $\bar{l}_c$. This

parameter is the mean of the chord lengths which constitute the major axes of the graphite layers, e.g. if the crystals are rectangular prisms, $\bar{\ell}_c$ will have a mean value intermediate between L_a and the length of the diagonal ($1.414\ L_a$), if L_a has been determined from the (100) arc. The crystallites are usually found to be approximately rectangular with $\bar{\ell}_c$ having values between 1.2x and 1.4x L_a. The advantage of $\bar{\ell}_c$ is that it is independent of crystallite shape.

An important parameter is the inter-layer d-spacing, which measures the average separation of the graphite layer planes. The d-spacing can be used as a measure of the degree to which the carbon has graphitised. Turbostratic graphite (discussed in Chapter 1) is not expected to have an interlayer spacing of less than 3.44A°.[10, 47, 48] The d-spacing measured for any fibre will be the mean of the range of d-spacings present. If this mean is less than 3.44A°, the possibility exists that three-dimensional (i.e. perfect) graphite might be present.

J. R. Marjoram of Rolls-Royce has carried out a very wide range of X-ray diffraction measurements with graphitised polyacrylonitrile fibres of various origins, prepared by different methods. His results are as yet unpublished, but are available in a Rolls-Royce report.[16] D. J. Johnson and C. N. Tyson have collaborated with the research group at Rolls-Royce and their publications [17, 20] concern the structure of carbon fibres, which were prepared as part of the Rolls-Royce research programme. This initial review of the structural changes accompanying the heat treatment of oxidised polyacrylonitrile will draw on these workers' results. The later parts of this chapter concerning stress graphitised and two-phase graphite fibres have arisen as a result of the author's own researches.

From the first appearance of the (002) diffraction arc with the oxidation of the fibre, there is a linear increase in preferred orientation with heat treatment temperature. Typical orientation angles (measured from the (002) arc) are 25° at 260°C (immediately

after oxidation), 20° at 1,000°C and 5° at 2,800°C. At first the orientation grows with the condensation of the aromatic products of pyrolysis, this is before true crystallisation can be said to be taking place. Oxidised fibres show a strong (002) arc and a very weak (100), which are their only diffraction features. (The (100) arc is that characteristic of the graphite structure and should not be confused with the polymer (100) arc, which disappears with oxidation.) This indicates that the oxidised polymer consists of relatively flat, uniformly stacked sheets. However, even the most poorly developed graphite should exhibit a (110) diffraction arc and as this is absent, the presence of the (100) indicates that the sheets are possibly only extensive in one direction; i.e. they are ribbon like. The (110) first appears for heat treatments between 400 and 600°C, which could be due to the previously considered, molecular condensation processes.

Tyson and Johnson [17] have calculated the proportion of carbon within the fibre, which is in a wholly amorphous form; i.e. separate from the layer structure. For fibre heat treated to 1,000°C, they estimate that 30% of the carbon is in an amorphous phase and that this reduces to 5% by 2,000°C. Crystallisation of the structure, therefore, is taking place throughout this temperature range, which at first produces an aggregate of very small crystallites. Growth in mean crystallite sizes only becomes significant late in this temperature range, as normal graphitising temperatures are approached.

A typical 1,000°C carbon fibre has an L_c value of approximately 10 A°, with a similar value for L_a or $\bar{l}_c$. The inter-layer d-spacing is approximately 3.6 A°. This implies that each crystallite consists of three layer planes on average, which is only marginally larger than the unit cell dimensions. This only just qualifies the solid as a crystalline material and then only as a turbostratic graphite, limited to two-dimensional order within the layer planes. However, these fibres can have Young's moduli of 240 GN/M^2 and strengths of 2.8 GN/M^2.

Figure 8.1 shows a micrograph of a carbonised, oxidised Rhodiaceta acrylic fibre. This is a picture of the fibre fracture surface. It is similar to the fracture surfaces obtained for strong, brittle solids, such as glass,[136] and shows very little evidence of a crystalline microstructure. The fibre has failed from a surface flaw, which is a common feature of the fracture of carbon fibres and indicates that their strengths can be limited by surface imperfections.[3]

It is commonly observed that graphitised normally oxidised polyacrylonitrile fibres lack three-dimensional order. The X-ray diffraction pattern usually only exhibits diffraction arcs of the type (00ℓ) and $(\ell k0)$, for which ℓ and k cannot be simultaneously zero. The (002) (100) and (110) diffraction arcs are present and are due to diffraction from the layer planes. Marjoram has found that the intra-layer atomic intervals are approximately similar to the graphite crystal values (private communication). Perret and Ruland,[137] working with graphitised polyacrylonitrile and also using sophisticated techniques, found that the interatomic distances in the layers were appreciably different from the crystal values. The C-C bond length in graphite is 1.421 A^{o}, while they determined a value of 1.416 A^{o} for 2,000^{o}C fibre and 1.418 A^{o} for 3,000^{o}C fibre. This could be due to a bending of the layer planes causing an apparent bond shortening. This distortion would anneal out with increasing heat treatment. C-C bond lengths are also short for low orders of layer size, such as those found in organic molecules formed from small numbers of aromatic rings. Therefore, an alternative explanation of the low C-C distances might be that the layer planes are very small. The growth in size of the layers with temperature should then increase the bond length. Like most authors,[2, 17, 21] Perret and Ruland consider that polyacrylonitrile carbon is non-graphitic and non-graphitising.

To be considered as a graphitising carbon the d-spacing should be capable of reduction below 3.44 A^{o} with heat treatment and X-ray

FIGURE 8·1

RHODIACETA ACRYLIC FIBRES OXIDISED & CARBONISED.

Carbonised at 1,000°C ----- 2,500°C.

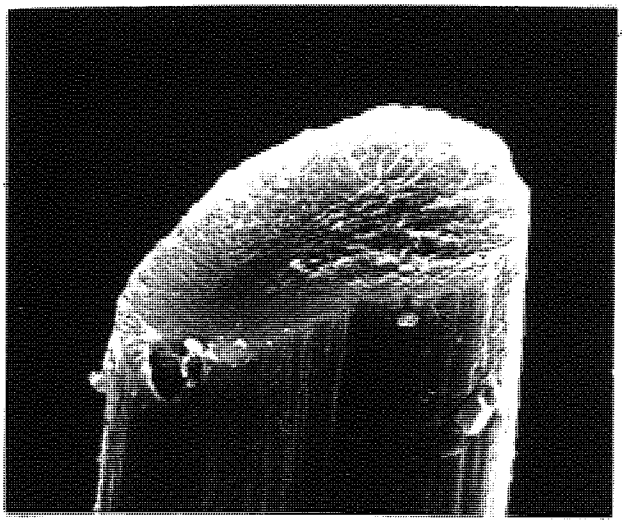

x3,220

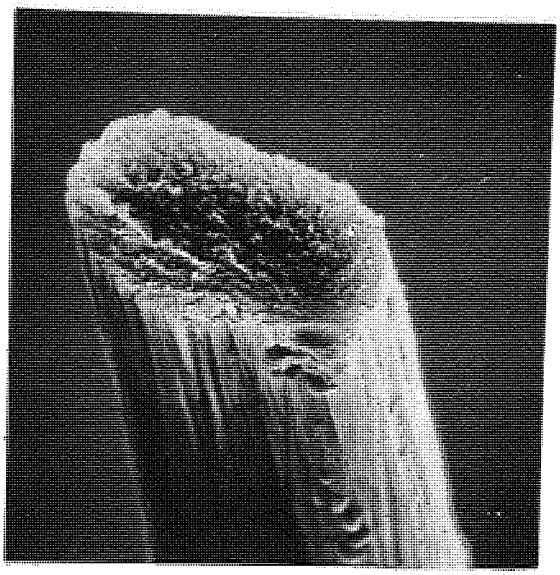

x2,793

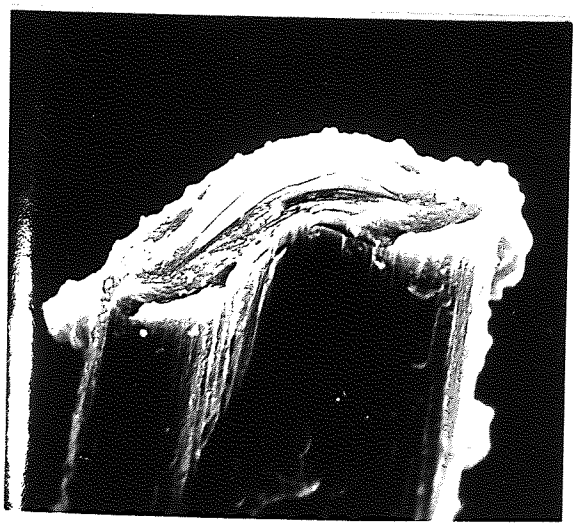

x2,880

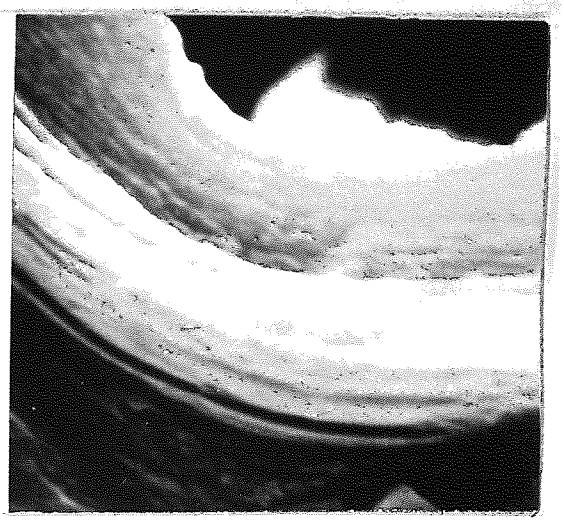

x 11,130

PARTIALLY OXIDISED AT 300°C.

GRAPHITISED AT 2,560°C.

diffraction arcs such as the (101) and (112) should ultimately appear. When completely graphitised all the possible X-ray diffraction arcs should be present and the d-spacing should be 3.354 A^{o}. Johnson and Tyson [17] have shown that Rolls-Royce prepared carbon fibres are turbostratic and, for material heat treated to 2,800°C, they quote a d-spacing of 3.42 A^{o}, with a mean L_a of 65 A^{o} and a mean L_c of 75 A^{o}. For $\bar{l}_c$ they quote values of 26 A^{o} at 1,000°C increasing to 100 A^{o} at 2,800°C.

A diagram of Johnson and Tyson's proposed structure is shown in Chapter 1. Johnson and Tyson also observed three-dimensional graphite in disintegrated Rolls-Royce fibre.[17] It was observed as crystalline flakes in the electron microscope. They consider that this represents a very small fraction of the total fibre structure, but that it can have important strength reducing effects.

8.11 Three-dimensional graphite in graphitised 9 denier Courtelle.

The appearance of three-dimensional graphite in graphitised acrylic fibres is not as uncommon as a reading of the literature would indicate. The reason for this is possibly that most of the published research work has been conducted with a limited range of acrylics and heat treatment procedures. In fact, most of the published work to date is for 1.5 denier Courtelle based material. Johnson and Tyson's observation of trace quantities of three-dimensional graphite fragments in Rolls-Royce fibre probably originates in the manner of this fibre's preparation. Before the appearance of 1.5 denier Courtelle, Rolls-Royce graphitised fibre was prepared by the heat treatment of stretched 9 denier Courtelle. The fibre was stretched in boiling water to between 300 and 400% of its original length, before distillation or oxidation and ultimate graphitisation. It was in occasional examples of these fibres that Johnson and Tyson originally observed completely crystalline graphite.

The author has discovered that three-dimensional graphite will form in oxidised 9 denier Courtelle. Fibres were prepared by taking

9 denier Courtelle fibre and stretching on a micrometer screw stretching frame, in an air circulating oven at 150°C. The fibres were oxidised at temperatures and times which ensured that thorough penetration of oxygen to the fibre interior took place. For this purpose each sample was investigated to ensure that the oxidation diffusion rim had reached the centre of the fibre. The oxidation was carried out with the fibre still under the stressed condition upon the stretching frame. The samples were all carbonised at a rate of 12°C/min. to 1,000°C and then graphitised for 30 minutes at 2,650°C. Both operations were carried out with the fibre maintained in a stream of pure, dry argon. Four stretch ratios were studied, 0, 100, 200 and 300%. Each batch of fibres was measured for strength and modulus in the usual way. Twelve fibres were selected from each batch and, after fracture, the fibre ends were mounted for examination in the "Stereoscan" scanning electron microscope. X-ray diffraction measurements were also made; from fibre diagrams and Debye Scherrer powder photographs. All the data collected is shown in table 8.11, below.

Table 8.11

Graphitised 9 denier Courtelle Stretched	Young's Modulus GN/M^2	Tensile Strength GN/M^2	d_{002} A^o	L_c A^o	L_a A^o	Z_{002} ^{o}
0%	289	0.47	3.380	97.5	365	6.8
100%	428	0.89	3.377	105	413	5.9
200%	391	1.26	3.393	98.5	243	6.8
300%	398	1.10	3.385	109	306	6.8

Studying the parameters in the table, it can be seen that stretching from 0 to 100% improves the modulus and strength quite substantially. The strengths shown here, however, are quite a lot lower than Watt et al [32] and Standage and Prescott [29] obtained; (the

latter with a slow distillation process). The striking feature of the results are the low values for the inter-layer d-spacing d_{002}. These values are appreciably lower than the 3.44 A^{o} spacing expected for turbostratic graphite. However, the X-ray diffraction data does not indicate that there is any significant structural difference between the four batches, although the 0% stretch sample has very low properties. It is surprising that the preferred orientations are so much the same, because at 1,000^{o}C the 0% stretch fibre had a very low relative degree of preferred orientation.

All the fibres showed (h k ℓ) and (h o ℓ) X-ray diffraction arcs, characteristic of the presence of completely crystalline graphite. Of equal interest was the presence of a discretely layered fine structure within the fracture surfaces of fibres from the 0 and 100% stretched samples, which were absent in the remaining two batches. An example of this is shown in the SEM micrographs in figure 8.11. These are pictures, at three magnifications, of the lamellar fine structure in a fibre from the 0% stretched sample. The fracture surfaces were not exactly similar in showing such a regular structure as that seen in the figure. Some fractures showed a high degree of 'pull out' of the lamellae, due very probably to shearing of the layers upon one another. Many fractures showed less lamellae and a few none at all. Fractures with the highest degree of this structure were normally exceptionally weak; the fracture in figure 8.11 was produced by a breaking stress of 0.23 GN/M^{2}. This bears out Johnson and Tyson's assumption that three-dimensional graphite can have a weakening effect upon the fibre.[17]

The dimensions of the lamellae are not of the same order as the X-ray crystallographic parameters. The lamellae thicknesses are in the region of 1,000 A^{o} (though here we are limited by the resolution of the SEM to a maximum resolution of 150 A^{o}) and an L_a for the phase would appear to be very large. In concentrating our attention upon the fracture faces of the fibres, it would be easy to exaggerate the extent

LAMELLAE PRESENT IN GRAPHITISED COURTELLE

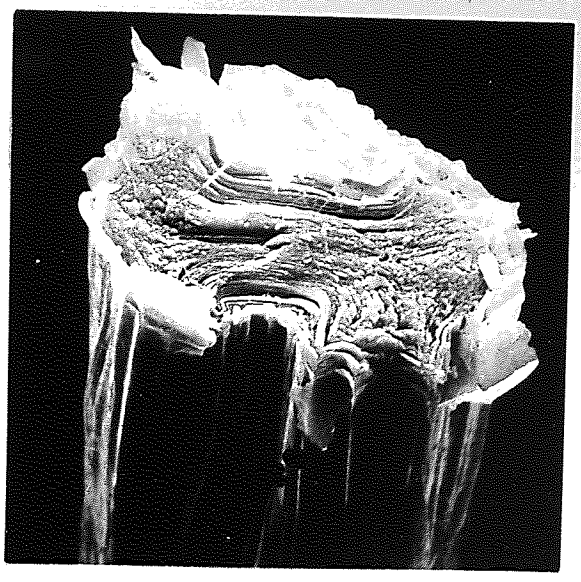

x3,185

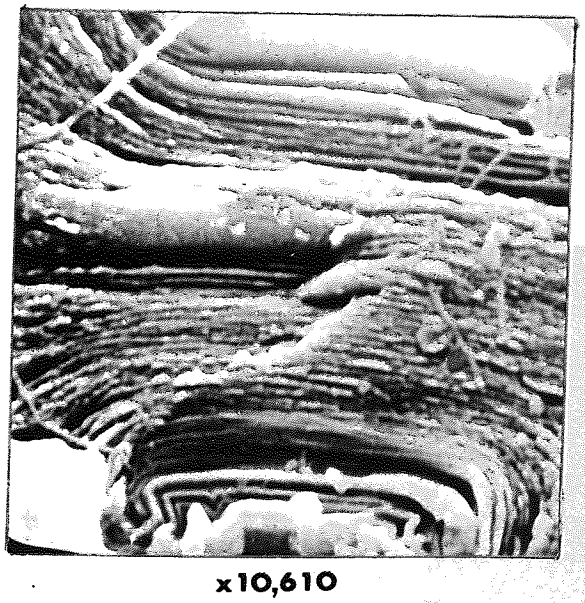

x10,610

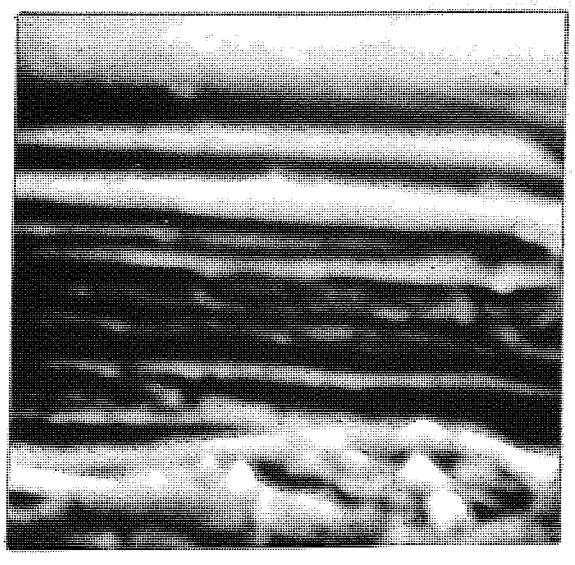

x32,410

to which the fibres consist of a lamellar structure. If they are a strength reducing feature of the structure, they will appear in the fracture faces with a high relative frequency. An approximate estimate of the concentration of three-dimensional graphite has been made by comparing the peak intensity of the (110) arc with the (112). These are neighbouring diffraction peaks, which should be identical in intensity for a perfectly crystalline graphite and, being close in the value of their Bragg angles, they should be subject to similar intensity corrections. The (110) arc is due to diffraction from all the crystallites in the fibre, while the (112) arc is merely from the three-dimensional phase. Taking the ratio of the arc peak intensities, it is found that the graphitised 0% stretched 9 denier fibre has 36% of perfectly crystalline graphite and the more highly stretched fibres, approximately 25%. A feature of the 0 and 100% stretched fibres is that the (002) diffraction arc profile is the sum of two Gaussian intensity distributions, which is a clear indication that the fibre has a two phase crystal structure. Graphite and normally graphitised acrylics exhibit just one intensity distribution, which is usually quite accurately Gaussian in form. The 200% and 300% stretched sample (002) arcs are of this type.

As the lamellar structure only appears in the fibres which exhibit a two phase (002) intensity distribution, it is reasonable to assume that one phase is due to the lamellae. The d-spacing for this second phase shows that the lamellae must have an almost perfectly crystalline graphite structure and it is possible that the crystalline fragments observed by Johnson and Tyson were from structures of this type. Three-dimensional diffraction from the 200 and 300% stretched fibres may stem from a second phase which cannot be resolved by X-ray techniques. Alternatively, the fibres may have a structure intermediate to a turbostratic and graphitic crystal lattice, as if the fibres were in the process of graphitising at the temperature of preparation.

The structure of the precursor fibre should have an important influence upon the crystalline development of the carbon. It is generally observed that acrylic fibres can have a fibrillar fine structure [2, 17, 21] and the formation and orientation of the fibrils will depend upon the method of coagulation and the amount of stretch applied to the fibre during preparation. Unstretched 9 denier Courtelle may contain regions where the polymer is relatively poorly oriented and in which the fibrils are large or even non-existent. In these regions of the fibre, uninhibited crystal growth might be possible, resulting in the formation of large crystallites. Prescott demonstrated [138] that as 9 denier fibre is stretched, the fibre volume is increased. This is an unexpected result, if one considers the behaviour of typical semi-crystalline polymer fibres. Stretching usually produces an increase in crystalline order, which reduces the volume of the fibre and increases the density. Unstretched 9 denier Courtelle has a density of 1.20 g/c.c., while highly stretched fibre can have densities below 1.0 g/c.c.. This is consistent with the view that internal voids are formed with stretching. This could be due to the formation of microfibrils, which are separated from their neighbours by elongated voids.

It is not understood why any limitation to the degree of graphite crystal growth should limit the degree of crystalline perfection possible. It has been generally observed, however, that three-dimensional graphite is never found in carbons in which the L_a dimension is less than a particular threshold value. Pinnick [139] reports that this value is 150 A^o, while Warren suggested that 100 A^o was a more acceptable value. The fibrillar fine structure of graphitised Courtelle might limit the value of L_a, so that the degree of crystal perfection is restricted in the way observed. Takahashi et al [141] have derived an empirical formula which expresses the measured value of the d-spacing, $\bar{d}$, in terms of the layer diameter, L_a.

The expression is,

$$\bar{d} = 3.354 + \frac{9.5}{L_a}$$

Other authors consider that the constant should be 7.4 [142] or 20.5,[13] rather than 9.5. 3.354 is the d-spacing for perfectly crystalline graphite, in A^{o}. For an L_a of 110 A^{o}, $\bar{d}$ = 3.44 A^{o}, the minimum layer spacing for turbostratic graphite. As L_a increases in value, the d-spacing approaches the value for perfect graphite.

This formula has been shown to be valid for a very wide range of carbons, with varying degrees of graphitisability. Following the work of Franklin [47, 48] and Warren,[46, 140] a graphitising but non-graphitised carbon is considered to be a mixture of the two crystal types. $\bar{d}$ is, therefore, in this view, dependent upon the relative proportions of crystallites with d = 3.354 A^{o} and d = 3.44 A^{o}. If this were the case for the graphite fibres prepared from 9 denier Courtelle, the proportion of three-dimensional graphite in all the samples would have to be very much greater than that actually observed. Ruland et al [143, 171] have shown that a distorted ribbon model of the graphite layers in carbon fibres might have greater validity than the turbostratic structure. This will be considered later in the chapter, but for the present the Takahashi formula will be treated as valid, because of the favourable empirical evidence for it, rather than any agreement with the two-phase concept.

Courtauld's scientists (unpublished communications) quote a mean value for the fibril diameter in 9 denier Courtelle as 300 A^{o} ± 15%. They have found that the stretching of the fibre does not reduce the diameter of the fibrils but obviously some sort of structural re-ordering must occur. Prescott [138] has shown that carbonisation and graphitisation reduces the fibril diameter to a mean of 175 A^{o}.

If the growth of L_a is limited to this diameter (assuming that the crystals grow no further than this along the length of the fibril) then $\bar{d}$, calculated from Takahashi et al's formula, will be 3.408 A°. All the $\bar{d}$ values in table 8.11 (shown as d_{002}) are appreciably below this value. In the case of the fibres containing the lamellar graphite, this is understandable, as the d-spacing for the fibre would be reduced by the contribution from the non-fibrillar phase.

Using exactly the same precursor and preparing the fibre by a distillation process or with low degrees of pre-oxidation, Prescott found that $\bar{d}$ never fell below 3.41 A°, the value predicted by the Takahashi formula. As the only difference between the author's methods and Prescott's is that a very long and thorough oxidation method was used by the former, then the initial chemistry of the preparation process is clearly having a very significant effect upon the structure of the graphitised fibre.

8.12 The microfibrillar fine structure of graphitised fibres.

Several authors have described the fibrillar fine structure to be observed in graphitised 1.5 denier Courtelle [2, 17, 21] and other polyacrylonitrile based graphite fibres.[109] Their descriptions of the structure are generally in good agreement. The fibrils are considered to be very long and to be separated by elongated pores. Two varieties of fibril have been found to be present, a narrow one, about 100 A° in diameter and a larger one apparently formed as a bundle of microfibrils, which are 800 to 1,000 A° in diameter. This latter, macrofibril, can be observed in microtomed 1,000°C acrylic carbon fibre.[2] The author has also observed them in longitudinally splintered graphitised Courtelle, using the Stereoscan scanning electron microscope. This is shown in figure 8.12(a). The series of micrographs at increasing magnifications show that the structure is quite uniform, with a fibril diameter of approximately 1,000 A°. The 38,500x magnification shows that the fibrils are long compared to their diameter but not of

FIGURE 8·12(a)

THE FIBRILLAR FINE STRUCTURE OF GRAPHITISED COURTELLE

x 3,640

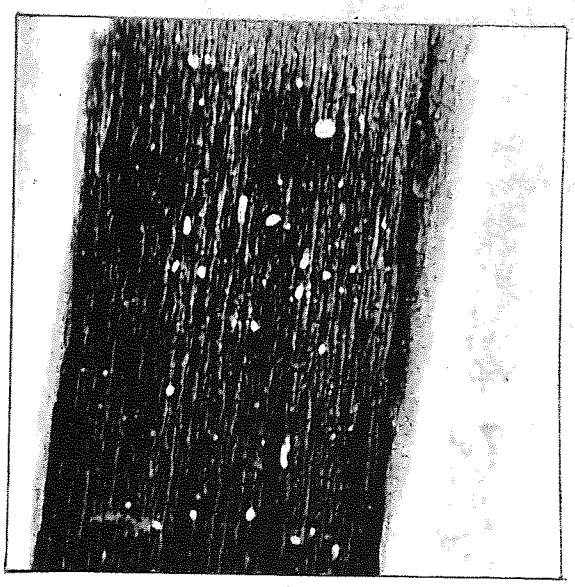

x10,500

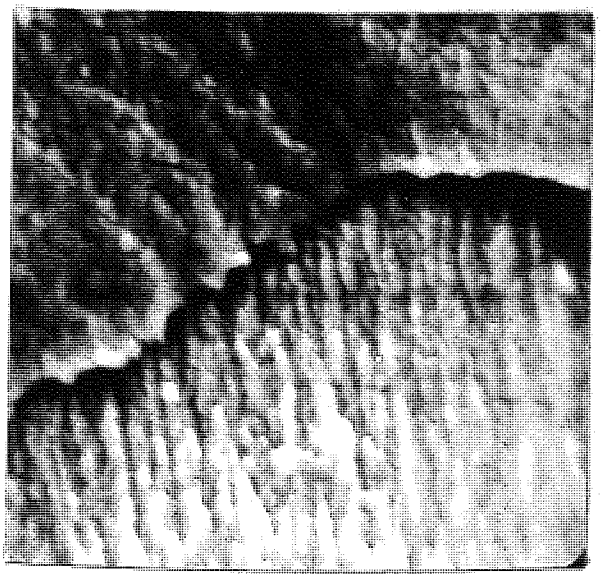

x 32,200

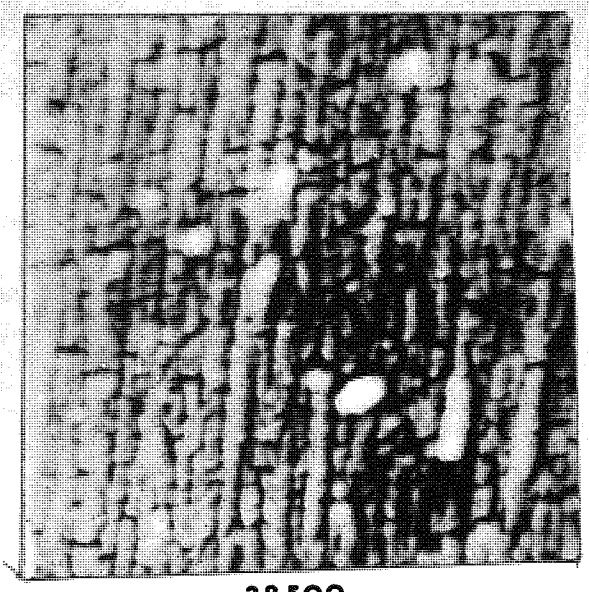

x38,500

unlimited length, as distinct transverse voids can be quite clearly observed at intervals along their lengths. This view of the fibre is very reminiscent of the longitudinal fine structures which Scott has shown in acrylic polymer fibres that have been 'peeled' to reveal their interiors.[144]

Bacon and Tang [127] have observed a fibrillar structure in graphitised Cellulose, which is another polymer fibre, known to possess a fibrillar fine structure. Fracture surfaces of Thornel 50 graphitised Cellulose fibre reveal a coarse fibrillar structure, which is very similar to that shown in figure 8.12(a) for the graphitised acrylic fibre. Thornel 50 is a high modulus carbon fibre, produced by Union Carbide Ltd, and prepared by the high temperature stretching of a high tenacity rayon. A typical fracture surface of a Thornel 50 fibre is shown in figure 8.12(b). The macrofibrillar features are of approximately the same diameter as those shown in the Courtelle based fibre and, in fact, Bacon and Silvaggi [145, 146] quote 500 A^{o} as the mean diameter. The fine structure within the fibrils is described as a honeycomb micropore structure, consisting of turbostratic graphite crystallites.

The fibril diameters quoted in the literature, being of the order of 100 A^{o} for the smallest species, indicates that three-dimensional graphite is unlikely to form. This is assuming that the fibril boundary represents a barrier to crystal growth and that Takahashi et al's formula applies. Tyson and Johnson [17] find that their L_a values are in the range 20 to 110 A^{o}. The upper value is the same as Takahashi et al's threshold value and three-dimensional graphite formation is therefore unlikely. They also quote a mean fibril diameter of 75 A^{o}, a value very similar to the mean value of L_a.

In comparing the fibril diameter with the L_a value, one is assuming that the crystal L_a dimension is the same parallel to the fibril axis, as it is normal to it. Without exploring the reasons

THORNEL 50 – GRAPHITISED CELLULOSE

x3,073

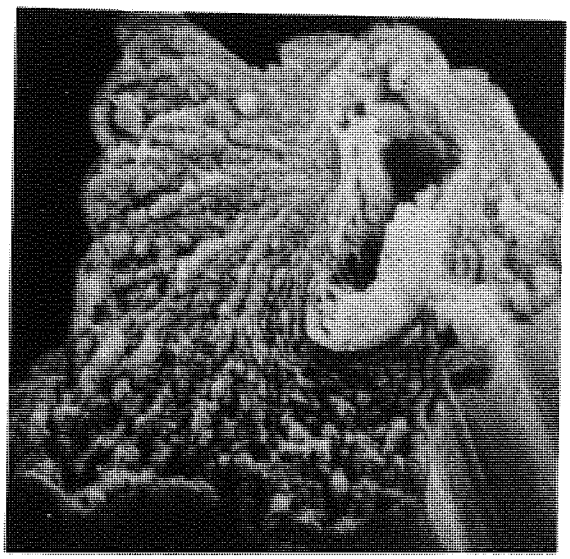

x 10,250

x 30,660

for this, it is nevertheless found to be the case.[17] The (100) arc for the X-ray fibre diagram is normally of uniform intensity along its length, indicating that the L_a value is constant for all orientations. The L_c value, i.e. thickness of the crystallites, will also be limited by the diameter of the fibrils. It follows from these assumptions and observations that when crystal growth is complete, the L_c and L_a values should be equal and have the same value as the mean fibril diameter. Figure 8.12(c) is a plot of the L_c values for a series of graphitised 1.5 denier Courtelle samples, versus the corresponding L_a values, which have been calculated from Takahashi et al's formula, using the measured d-spacings. These samples are from a stress-graphitisation experiment. The one series of fibres have been stretched while being graphitised, while the other series are control batches which were present during the hot stretching. The main difference between these samples and those investigated by Johnson and Tyson is that they have been graphitised for much longer times; 5 hours or more at temperature, as compared to the more usual half an hour.

The ~~straight~~ hatched line in figure 8.12(c) is for $L_a = L_c$ and the curve fitted to the data points crosses this line at $L_a = L_c = 180$ A°, approximately. If a 'fibril limit' to the growth in crystallite size is to be accepted, then the mean fibril diameter must be 180 A° or more. It is interesting that this value is close to that calculated by Prescott, from the data supplied by Courtaulds, i.e. a fibril diameter of 175 A°. It should be noted that the sample having an L_c in excess of 175 A° is a hot stretched batch and hot stretching provides the possibility of sealing the inter fibrillar boundaries by straightening.

While it is satisfying to have this result agree with that of Prescott, it is unfortunate that it disagrees with Johnson and Tyson. They obtained the fibril diameter using transmission electron microscopy of the precursor fibre, after complete degradation of the

FIGURE 8·12(c) GRAPHITE CRYSTAL THICKNESS v DIAMETER

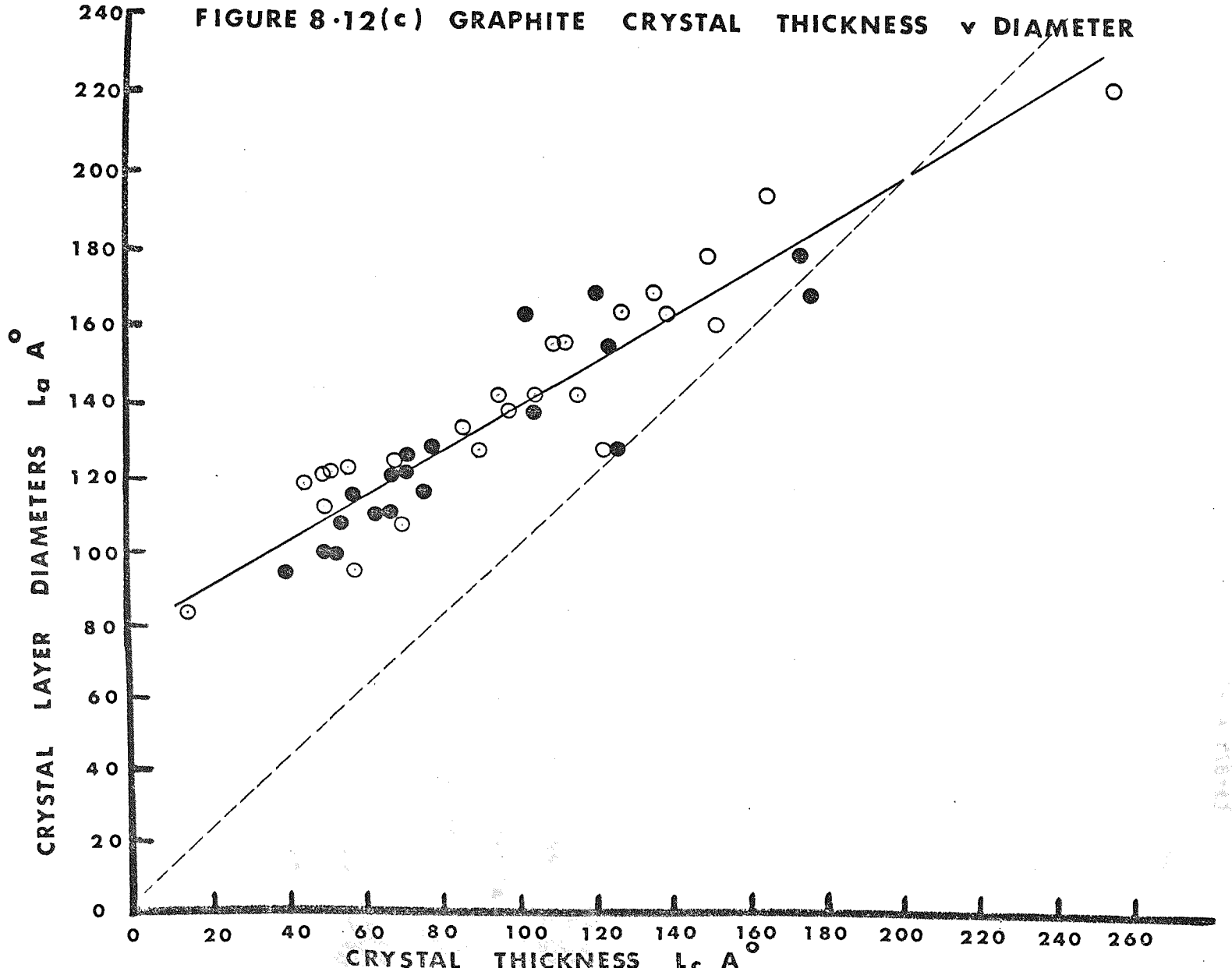

structure with ultrasonic radiation. The figure they quote of 75 A° is low compared to results for carbonised fibres published by other workers and yet a collapse of 50% of the precursor fibre diameter has to be allowed for. This suggests that they anticipate a fibril diameter of about 40 A° in the graphitised fibre. This figure is so low that it is difficult not to believe that the ultrasonic disintegration has split the fibrils into smaller units.

8.13 The formation of continuous lamellae in graphitised polyacrylonitrile fibres.

One of the more remarkable effects observed with the graphitisation of polyacrylonitrile fibres is the formation of graphite lamellae. The discovery of this very different, continuous crystal phase in graphite fibres has already been published by the author;[147] (a copy of this paper accompanies the thesis). The appearance of graphite lamellae is associated with the partial oxidation of oriented acrylic fibres. Oxidised acrylic fibres can be prepared by a short high temperature oxidation, such that only an outer diffusion zone of the fibre cross-section receives adequate oxidation. (This is discussed in Chapter 7.) In some cases the unoxidised interior of the fibre melts on heating to 1,000°C. When such fibres are heated to above 2,000°C, concentric lamellae are formed around the central cavity in the fibre. Figure 8.13(a) shows two examples of graphitised 1.5 denier Courtelle fibres, which originally received an oxidation for 6 minutes at 300°C, in a fluid bed. The fibres have been fractured to reveal the central cavity, around which the lamellae have grown. The micrographs labelled a, and b, in figure 8.13(a), are for the same fibre fracture surface at two magnifications. These micrographs show that one or more of the lamellae has sheared out from the fibre core like a telescope tube. It is white, because the primary beam of the SEM has passed through the tube, with little attenuation. This indicates that the material in the tube must be very thin. Micrographs, c, and d, are the same fracture

FIGURE 8·13(a)

GRAPHITE LAMELLAE IN PARTIALLY OXIDISED COURTELLE, GRAPHITISED AT 2,650°C

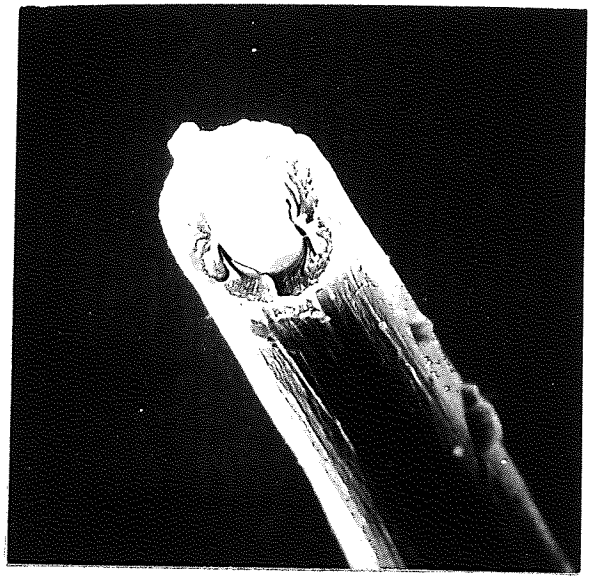

x 2,870

a

x 9,590

b

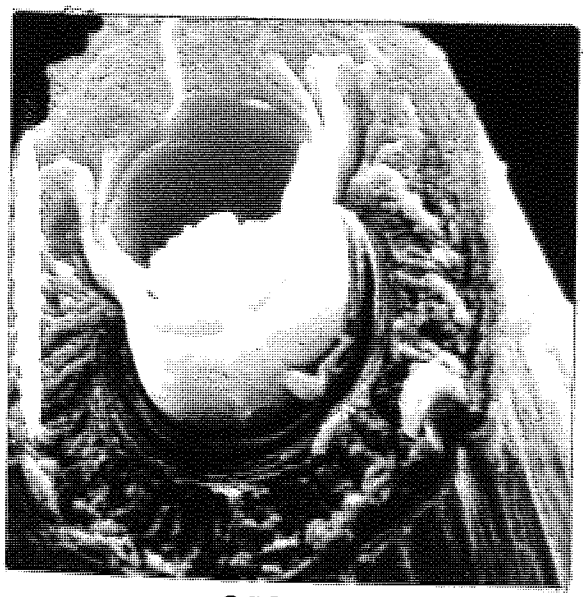

x 9,590

c

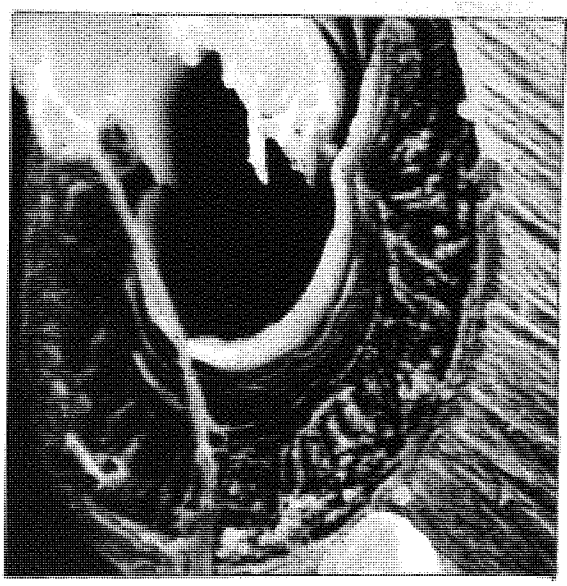

x 9,690

d

face but viewed from opposite directions for a fibre from the same batch. These micrographs show the individual, discrete lamellae, very clearly, and that they are continuous around the central cavity. Again, there are sheared out lamellae, which are transparent to the primary beam. The material at the surface of the fibre appears to be partially organised into layers, and this poses the question as to whether it is simply the free surface area that allows the carbon to organise itself into sheets. In fact, lamellae have not been observed in these fibres, independently of a free surface. However, this does not appear to be a sufficient criterion for the formation process. Holes, of themselves, are not necessarily associated with lamellar graphite, the prior melting of the fibre core also appears to be a necessary precondition to the effect. It cannot be due to excessive oxidation, as thought to be the case in 9 denier fibre.

Figure 8.1 (section 8.1) compares the fracture surface of a conventionally graphitised, oxidised Rhodiaceta fibre, with two fracture surfaces of graphitised, partially oxidised fibres. The conventional graphite fibre can be seen to have a much rougher surface than the equivalent carbonised fibre, this is possibly symptomatic of the coarser crystal structure possessed by the more highly heat treated fibre. The partially oxidised fibres have a very different fine structure after graphitisation than the fully oxidised fibre. In this case the partial oxidation was carried out in an air oven, at 300^{o}C for ten minutes. The fibres have holes or cavities in the centre, but, because of the shape of the fibre and the number of prominent lamellae, it is not obvious looking at the fractures. The cavities are very narrow indeed, but, nevertheless, internal melting of the fibres has taken place and after graphitisation a lamellar fine structure has developed. The lamellae around the central cavity have sheared some way out of the surface and, as with the Courtelle example, their thinness has rendered them transparent to the SEM primary beam. Apart from the whitened lamellae themselves, the remainder of the fibre

cross-section appears to exhibit a concentric layer structure.

X-ray crystallographic studies of these two examples of graphitised, partially oxidised acrylic fibres, reveals that they have a two-phase structure. The evidence for this is the double Gaussian distribution obtained for the (002) diffraction arc. In this respect they are similar to the graphitised 9 denier Courtelle fibres considered previously. A table of the X-ray parameters and the mechanical properties of the fibres is shown below.

Table 8.13

Graphitised, partially oxidised acrylic fibres.	Young's Modulus GN/M^2	Tensile Strength GN/M^2	d_{002} A^o	L_c A^o	L_a A^o
Courtelle heated to 2,650°C.	402	1.32	3.379	130 380	380
Rhodiaceta heated to 2,560°C.	365	1.10	3.393	142 290	243

The strengths of both samples are very low and should be compared to values of about 2.00 GN/M^2, which are quite reasonable values for completely oxidised fibre, graphitised to these temperatures. The moduli, however, are relatively good compared to values of approximately 340 GN/M^2, usually achieved for fibre heat treated in the normal way. These high values for Young's modulus are quite surprising, when one considers that the fibres are filled with cavities, the presence of the highly oriented lamellar phase is very probably responsible for this. Further heat treatment of the partially oxidised Rhodiaceta fibre to 3,100°C resulted in a fibre batch with a mean modulus of 930 GN/M^2, which is very close to the theoretical modulus for single crystal graphite (1,026 GN/M^2) and the sort of value one would hope to obtain with graphite whiskers. Unfortunately,

the strengths of these fibres were extremely low for such high moduli, being only 1.4 GN/M^2 approximately.

The interlayer d-spacings were low for both the fibres shown in table 8.13 and as with most of the other graphitised fibres considered in this work, this indicated the presence of perfectly ordered graphite. X-ray diffraction arcs of the type (h k ℓ) (h, k and $\ell \neq 0$) and (h o ℓ) were present in the powder diffraction pattern. The proportion of three-dimensional crystal was quite large and it may have been present in both the lamellar and alternative phases of the fibre. The two (002) Gaussian intensity distributions were separated graphically and the L_c values for each phase calculated individually. Both L_c values for each sample are included in table 8.13. The larger of the L_c values is probably from the lamellar phase and the thinness of the individually sheared lamellae in the micrographs indicates that L_c is a measure of the mean lamella thickness. (At an accelerating voltage of 20 kV, the penetration of the SEM primary beam will only be a few hundred angstroms.) The L_a values shown in the table were calculated from the formula of Takahashi et al. These will be mean values for the two phases.

It is interesting to speculate what value of L_a a completely cylindrical sheet of graphite would have, if determined by X-ray diffraction of the sheet, oriented as a cylinder perpendicularly to the incident beam. Measured perpendicularly to the axis of such a cylinder, L_a is equal to the circumference, in theory. However, measured with X-rays the L_a value will be small, due to the curvature of the layers and the measured value will bear some relationship to the wavelength of the X-ray beam. As the lamellae in graphitised, partially oxidised acrylics appear to be cylindrical about the fibre axis, the value of L_a cannot be related to the size of the crystal.

A very impressive example of lamella formation in graphitised acrylic fibres is provided by 60 denier Cashmilon fibre. This fibre

FIGURE 8·13(b)

SURFACE LAMELLAE IN GRAPHITISED 60den. FIBRE

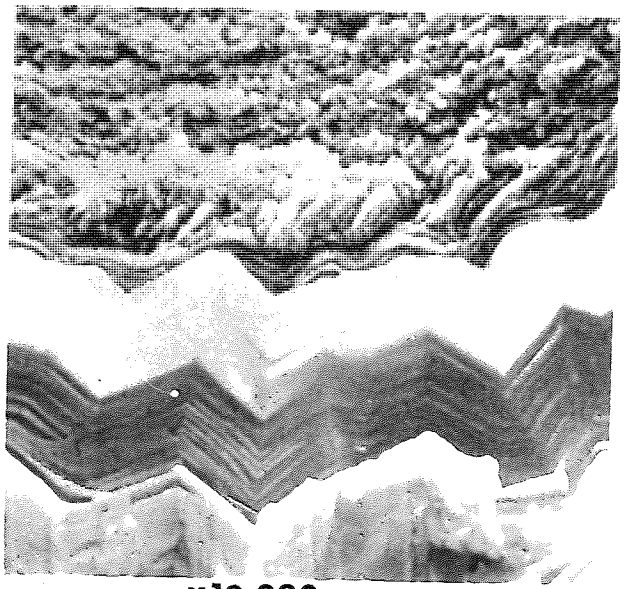

×10,290

×30,730

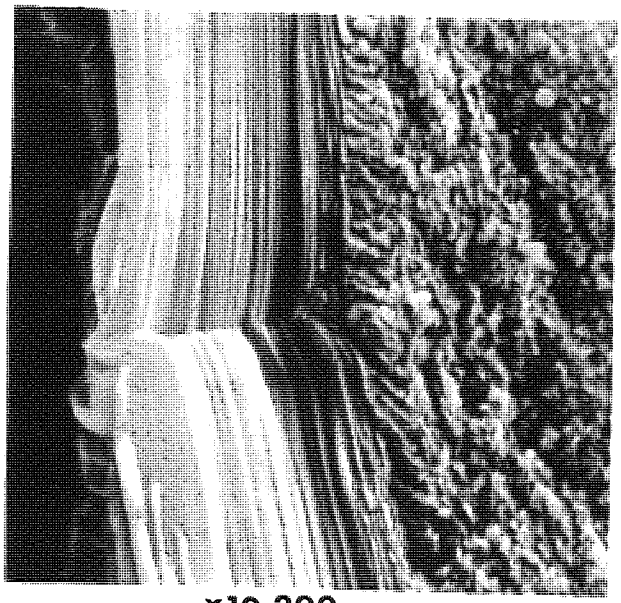

×10,290

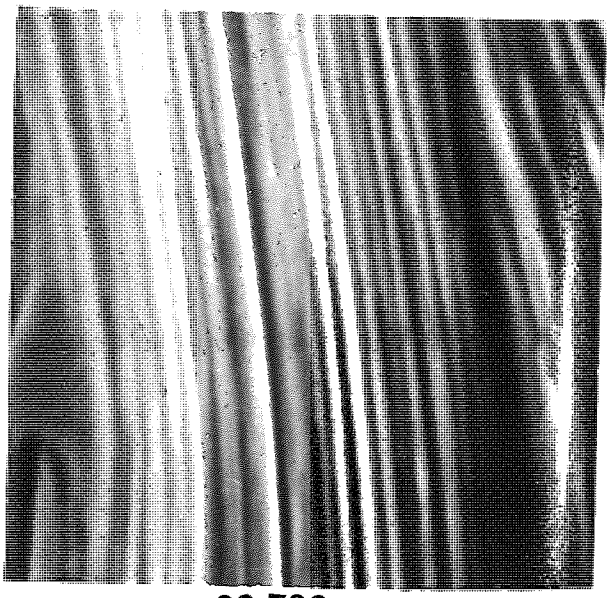

×30,730

was discussed in chapter 7 as an example of how core melting can occur, as a result of partial oxidation. In this case the lamellae are formed upon the external surface of the fibre, ostensibly completely contradicting the findings with Courtelle and Rhodiaceta, in which the lamellae appeared to be formed in the remainder of the molten phase, left inside the fibre. There is no sign whatever of any lamella formation around the inside surface of the cavity wall in the 60 denier fibre. Figure 8.13(b) shows SEM micrographs of the surface lamellar structure. The two right hand high magnification micrographs are of parts of the structure shown in the corresponding low magnification micrographs. The outside wall of the fibre has become wrinkled as a result of shrinkage, but the lamellae are quite continuous, bending through the sharp corners without any apparent discontinuity. They are also remarkably parallel for very great distances (which cannot really be shown here). An X-ray fibre diagram of graphitised 60 denier fibre answers the problem of the absence of parallel lamellae upon the interior cavity wall. This is shown below, as figure 8.13(c).

Figure 8.13(c)

X-ray fibre diagram for graphitised 60 denier fibre.

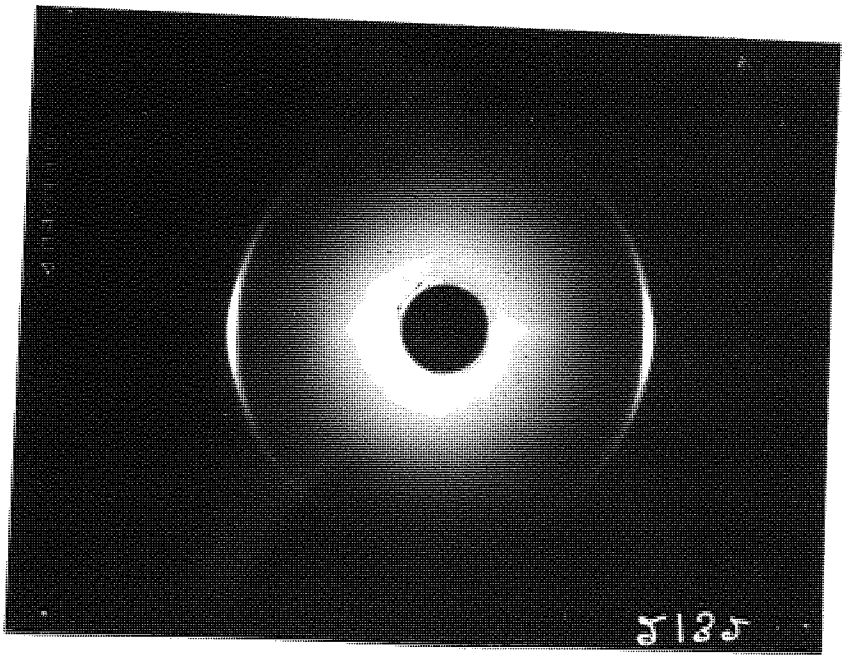

The (002) arc consists of two overlapping intensity distributions. The very bright equatorial arcs are for a very highly oriented species, while the major proportion of the material contributing to the wide arc is very highly disoriented. Of particular significance is the long equatorial low angle pattern, i.e. the pair of equatorial streaks emanating from the centre of the fibre diagram. The low angle pattern is for a range of d-spacings extending from the unit cell C-dimension (6.708 A^{o}) to several hundreds of angstroms, and the diffracting features are highly oriented and parallel to the fibre axis.

These results imply that only the surface of the fibre remained oriented during heat treatment and was hence capable of forming the well aligned lamellae observed in figure 8.13(b). The melting at above 350^{o}C must have destroyed the orientation of the material in the interior of the fibre, removing its capacity to form oriented graphite. This did not happen in the Courtelle and Rhodiaceta cored fibres, both these were completely and highly oriented after graphitisation. The formation of the lamellae in the 60 denier fibre depended on the melting process, because highly oxidised fibres which showed very little loss of material from the core, also showed no graphitic layers or any evidence of their potential formation. The explanation of their origin must be that it is due to the molten material which, having been ejected from the fibre core at 350^{o}C+, graphitised upon the oriented, oxidised fibre surface.

It has long been recognised that melting can be an important step in the crystal development of graphitising carbons. Kipling and Shooter have contributed several studies,[148, 149] demonstrating that many graphitising carbons pass through a molten phase. The existence of a viscous state during the carbonisation enables the aromatic products of pyrolysis i.e. the crystal nuclei, to orient themselves into a semi-ordered state. This is the mesomorphic state often observed with heat treated pitches and tars, which appears to possess a smectic or nematic

order. Franklin was the first to observe [12] that the hydrogen content of the precursor had an influence upon the degre of graphitisability. As an example of a non-graphitising precursor, she considered polyvinylidinechloride. This is because it condenses at very low temperatures, to produce a very highly cross linked char [34, 35, 150] which does not pass through a molten phase and hence cannot reorient to produce a completely graphitic carbon. It is the archetypal turbostratic, non-graphitising carbon. Polyvinylchloride retains its hydrogen to more advanced stages of its thermal degradation, because it is not all lost as hydrogen chloride. This polymer can, therefore, go through a mesomorphic phase and condense in an oriented, well ordered form, producing a graphitising carbon. These examples of extremes in the behaviour of organic precursors have parallels in the behaviour of polyacrylonitrile.

Completely pyrolysed polyacrylonitrile behaves in many respects like polyvinylchloride. It does not become as liquid or graphitise as easily, but its behaviour in two-phase fibres demonstrates the way in which it forms very extensive, highly crystalline graphite. Pyrolysed polyacrylonitrile remains very hydrogen rich to quite high temperatures. It contains 4.2% by weight of hydrogen at 350°C, which represents approximately 1.9 hydrogen atoms per carbon, and does not show evidence of condensation (i.e. cross-linking) until very high temperatures (480+°C). Oxidised polyacrylonitrile is similar to polyvinylidine-chloride, in that it forms a carbon of very poor order, which one would not expect to be graphitisable. Possibly because its hydrogen content is depleted by oxidation early on in the heat treatment, it does not pass through a mesomorphic phase. Condensation begins at relatively low temperatures (300+°C), which in an unoriented char would probably result in a highly disordered graphite.

The one major difference between the materials considered by the early workers on this topic and the present day carbon fibre

precursors is that these latter materials are highly oriented and tend to retain a large part of this orientation throughout carbonisation. In the case of polyacrylonitrile and possibly other materials, this seems to remove the necessity for a mesomorphic stage in the preparation. It does not seem impossible to the author that an apparently non-graphitising precursor as considered by Franklin, might be rendered graphitising, if it were originally obtained in a highly oriented form, or if it were hot stretched at graphitising temperatures.

8.14 Crystalline orientation in the plane perpendicular to the fibre axis.

The concentric lamellar structure indicates that the C-axes of the crystallites are oriented radially in the transverse plane of the fibre. Inspection of figure 8.13(a) shows that the phase of the fibre between the lamellae and the surface of the fibre might be radially ordered, with the crystal C-axes oriented circumferentially to the fibre axis. This is not obvious, however. Radially oriented crystallites can be very clearly observed in the fracture surfaces of fibres which have been partially oxidised and graphitised, but which have not melted in the core to the extent of forming a cavity. Figure 8.14(a) shows an example of such a fibre. This fibre was oxidised for a longer time at 300°C than the previously considered 1.5 denier Courtelle; 18 minutes instead of 6 minutes. The first SEM micrograph in figure 8.14(a) shows the fracture surface for the fibre immediately following oxidation in which the two regions of the fibre are quite easily discerned. Following graphitisation to 2,650°C, the oxidised region of the fibre has formed radially oriented crystallite, while the core has remained relatively featureless. It is quite possible that the core material has melted and that the higher degree of surface oxidation in this case has produced a stronger retaining skin, capable of withstanding the pressure of the molten core. The centre picture in figure 8.14(a) is a 20 kV SEM micrograph, which is the maximum accelerating voltage

COURTELLE PARTIALLY OXIDISED & GRAPHITISED

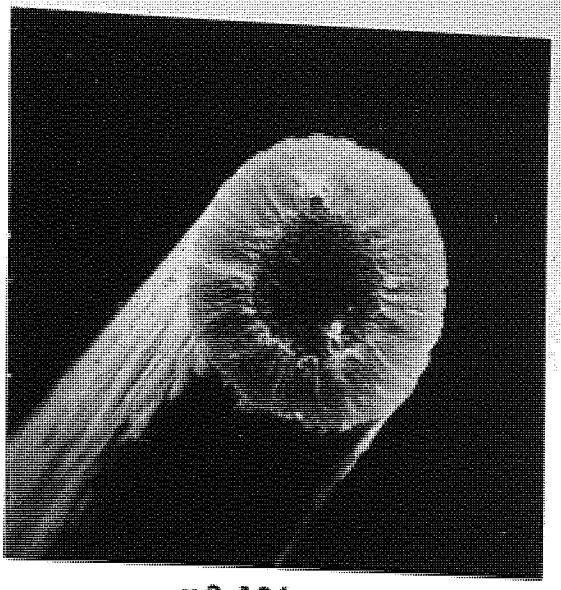

OXIDISED AT 300°C

x 3,136

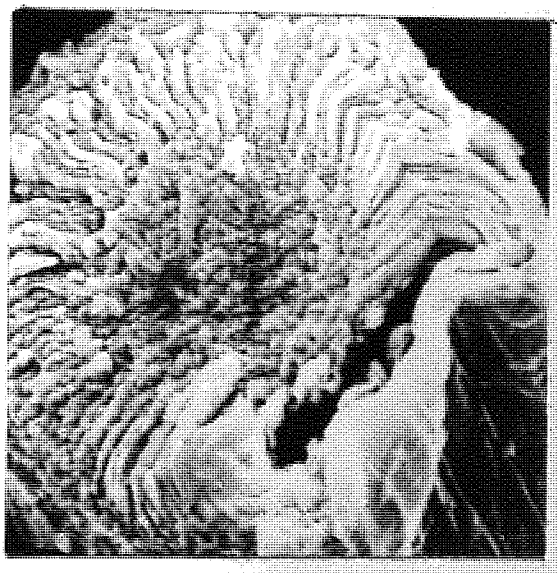

GRAPHITISED AT 2,650°C
(20KV)

x 10,430

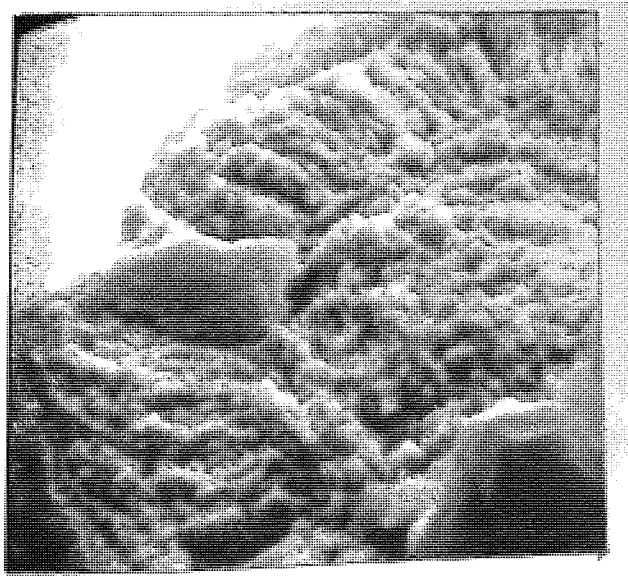

(30KV)

x 11,700

available with the Rolls-Royce instrument. The picture clearly shows the radially oriented crystallites but it is not clear from it that the angles formed by the crystallites are in the vertical plane to the fracture face. The third of the micrographs was taken using a Mk 2 Stereoscan instrument with a 30 kV accelerating voltage. This last picture was taken to show what could be a large crystallite jutting well out of the fibre fracture surface, on the middle left hand side. With the higher accelerating voltage, a deeper penetration of the fibre is achieved, which shows the radial structure much better. The crystallite just mentioned appears to have obtuse angles of the order of 120°, which is characteristic of graphite crystallites. The same applies to a similar structure which can be seen in the bottom right hand corner of the micrograph.

This fibre is by no means as crystalline as the fibre discussed in section 8.13, its mean d-spacing is 3.43 A° and it has an L_c of 69 A°. There is also no significant indication that it has a two-phase structure. Clearly, it is not as crystalline as the fibre containing the lamellar phase. The mechanical properties are also low, it has a mean Young's modulus of 280 GN/M^2 and a strength of 1.06 GN/M^2. This fibre has inferior properties to the lamellar phase material, which might be because the lamellae have a stiffening and strengthening effect upon the fibres which contain them. The core material in the weaker fibre might have very poor properties, because it possibly melted at first and without a free surface available as a substrate, it would not be able to graphitise into an oriented state.

Microscopy studies of polished graphite fibre cross-sections in polarised light, offer very useful complementary evidence to the study of fibre fracture surfaces. Graphitised, fully oxidised cellulose and polyacrylonitrile fibres [151], [152] show a strong radial orientation of the crystallite C-axes particularly at the fibre surface, when studied between crossed polarisers. This result was at first surprising,

because the fracture surfaces of such fibres studied in the SEM show fibrous fractures, which are considered to show that the structure consists of an aggregate of micro-fibrils.[147] Lamellar formation is often observed near the outside surface of graphitised fibres, but this is usually limited to just a few layers. Electron microscopy has shown that highly graphitic crystals are present on the surface of the higher temperature fibres [14] and these have been shown to correspond to the oriented surface layers. Raman spectroscopy has been used to study similar fibre surfaces [153] and the findings confirm that a high surface orientation exists, with the C-axes oriented radially.

The optical findings are not just limited to the surface structure; although this may be more strongly oriented, the mass of the crystallites are usually ordered with the C-axes radially oriented within the transverse plane. This suggests that the microfibril fine structure has merely a subordinate role in determining the crystal growth processes. Though it may limit the ultimate size of the crystallites, it does not govern their lateral orientation. If the fibrils behaved as part of the continuum during graphitisation, the individual crystallites would be able to respond to the forces bringing about their lateral orientation. If the fibrils acted as independent entities, the material within them is unlikely to orient itself so as to form layers parallel to the surface of the fibre, but is more likely to orient itself parallel to the surface of the fibril. This would result in an apparent random orientation of the crystallites in the transverse plane, even if the fibrils themselves were organised in concentric layers. The fibrils must therefore be part of the matrix continuum, and a subsidiary feature as far as crystallisation is concerned.

Knibbs [154] has carried out a detailed study of the effect of oxidation of the precursor upon the orientation in the fibre cross-section, using polarised light microscopy. His results are well worth

while summarising, because they are supporting evidence for the author's own findings. For very small amounts of oxidation, he finds that there is very little orientation at all in the graphitised fibre and the centre is completely isotropic (he suspects that holes may be present in some cores). With increasing degrees of oxidation he finds at first that the outer zone of the fibre forms an oriented layer with the C-axes radially oriented. This must correspond to the lamellar phase. At this stage the centre remains isotropic. With further oxidation again, the outer zone of the fibre remains with the C-axes radially oriented and the inner zone becomes ordered, with the C-axes having a circumferential orientation. After complete oxidation of the fibre, the graphitised material is completely ordered, with the crystallites adopting the same orientation, with the C-axes all radially disposed.

A possible explanation of the transverse fine structure can be based upon the melting behaviour of the fibre. The degree of softening and melting is controlled by the amount of oxidation received by the fibre. With little or no oxidation, the fibre almost completely disorients and graphitisation results in an isotropic transverse organisation of the crystallites. Order starts to appear with increasing degrees of oxidation, because the orientation of the precursor polymer is preserved at the fibre surface and hence provides a substrate on which epitaxial crystal growth can take place. If the core of the fibre loses material to form a cavity and the fibre is sufficiently oxidised, the cavity wall will also provide a substrate for oriented crystal growth. The oriented lamellae shown in figure 8.14(b), diagram (a) show this structure. Lamellae will form early in the graphitisation process, as the molten residue is a graphitising material crystallising upon an oriented substrate. Once the lamellae are formed, the carbon between the lamellar zones is subjected to a radial tensile force. This is because the fibre has to shrink, as the

THE TRANSVERSE FINE STRUCTURE IN GRAPHITISED PARTIALLY OXIDISED ACRYLIC FIBRES

(a)

Lightly oxidised Courtelle (6mins. at 300 °C) Graphitised at 2,650 °C

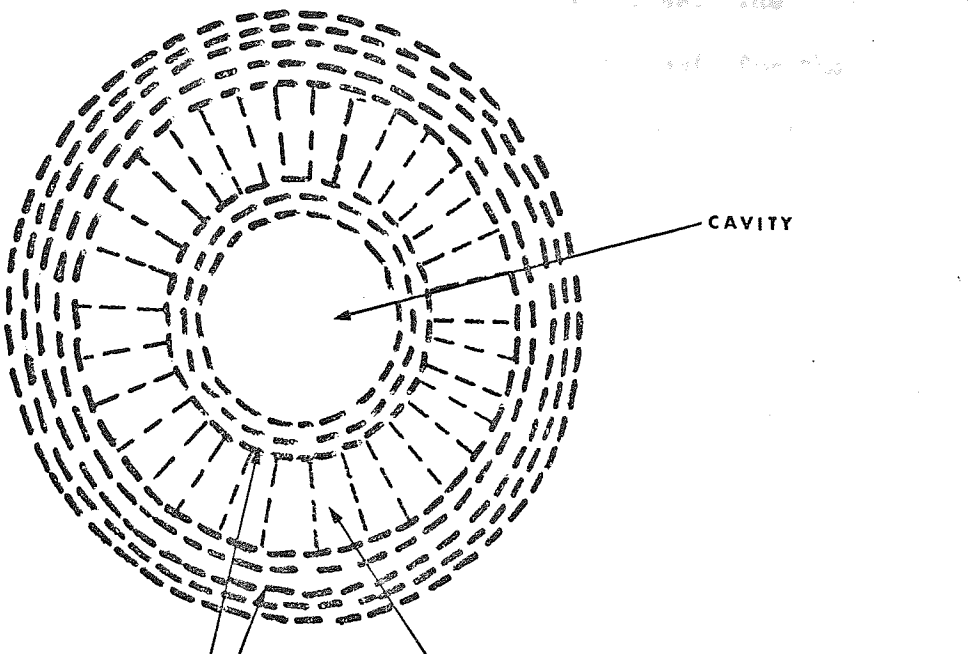

(b)

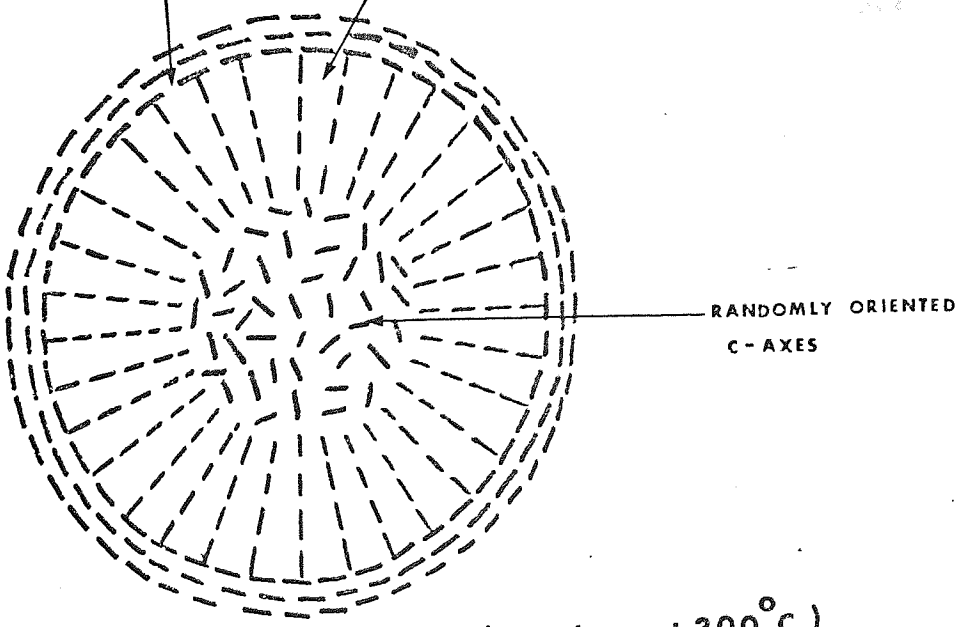

More highly oxidised than above (18mins. at 300 °C)

Graphitised at 2,650 °C

carbon crystallises to produce a denser structure; the lamellae may well pack closer together, but they cannot shrink to accommodate the core material. They may wrinkle, however, as in the 60 denier fibre, but this might not completely compensate for the forces. The crystallites inside the fibre must, therefore, compensate for the radial forces by orienting into a radial configuration, with their C-axes lying circumferentially to the fibre axis. This is the explanation of the texture of the fibre seen between the fibre surface and cavity lamellae shown in figure 8.13(a) and it is also represented in diagram (a) figure 8.14(b). In the case where the core material is left completely disoriented by the melting, but without cavity formation, the radial forces still develop with temperature. The surface still has a well oriented crystal structure, which withstands the shrinkage forces of internal crystallisation and the completely disoriented carbon core cannot be reoriented, without the presence of a substrate. The intermediately oxidised material is oriented, but because it is only lightly oxidised it passes through a plastic phase in which the crystallites orient radially, to compensate for the radial tensile forces, generated by condensation in the core. This produces the structures shown in figure 8.14(a) and shown diagrammatically in figure 8.14(b), diagram (b).

If the precursor fibre is completely stabilised, by uniform oxidation throughout the fibre, then the crystallisation of the fibre will take place homogeneously. The fibre contracts uniformly and the resultant compression forces must tend to orient the crystallites with their C-axes radial to the fibre axis. The layer planes might not be as concentrically ordered as with the lamellae, but they would produce the optical activity observed by Knibbs.[154]

8.2 THE STRESS-GRAPHITISATION OF POLYACRYLONITRILE BASED CARBON FIBRE.

The application of stress to polycrystalline graphites at high annealing temperatures often results in an increase in the preferred

orientation. With an increase in preferred orientation, there should be an increase in the tensile modulus, parallel to the principle axis of orientation. This is because the anisotropy of the graphite crystal favours the parallel orientation of the basal planes. Experience has shown that this applies to the Acheson type of synthetic graphite, pyrolytically deposited graphite [155] and even to the so-called vitreous carbons.[156]

8.21 The temperature dependence of hot stretching.

The use of hot stretching to improve the tensile properties of carbon fibres has now become a standard part of the technology, although it was only pioneered relatively recently. Bacon and co-workers [157] have shown that hot stretching increases the preferred orientation of cellulose based carbon fibres, with a consequent improvement in tensile modulus and strength. While the author and his collaborators were the first to show this effect with polyacrylonitrile based fibres.[158] (This work has been published and a copy of the paper is available with the thesis.)

The method of hot stretching is described in chapter 2 (section 4). With normally oxidised Courtelle fibres, carbonised to 1,000°C, no yielding of the fibre can be induced until the fibre achieves 1,700°C. This is shown in figure 8.21. The amount of stretch is dependent to some extent upon the load, but the fibre had to have a large load upon it before it would yield at all. The load was always close to the breaking point and the curves in figure 8.21 are really failure envelopes for the fibre loops, as the maximum stretch was usually terminated by fracture. The suddenness of the initiation of stretching was suggestive of a thermal transition, not unlike the glass transitions seen in the original precursor fibre.

This sharp change from a brittle to a plastic phase has led the author and his collaborators to look for parallel changes in the physical parameters of the fibre in the region of 1,700°C. Of

FIGURE 8·21

MAXIMUM DEGREE OF STRETCH OBTAINED AT TEMPERATURE

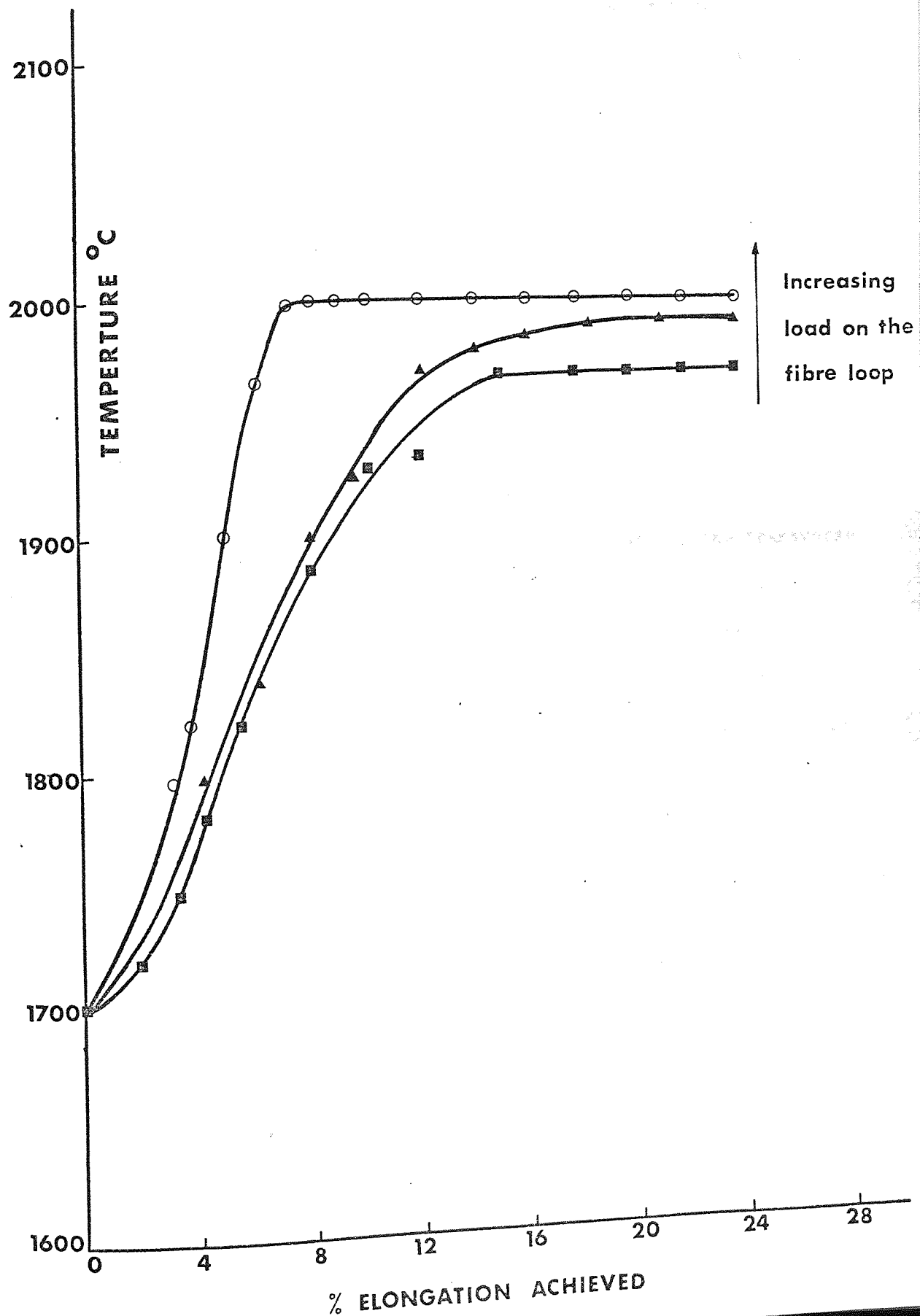

particular significance is the transition in the rate of change of the ratio of the tensile and torsion moduli, $(\frac{E}{G})$ at 1,800°C, as observed by Jones and Johnson.[159] This parameter measures the degree of elastic anisotropy and hence increases with the growth in preferred orientation. The growth in the values of L_c and L_a, the dimensions of the crystallites, also increases in rate above this temperature.[16] This is, in fact, often the case with graphitisable carbons. The amorphous content measured by Tyson and Johnson [17] declines by this temperature and the degree of structural homogeneity measured by low angle diffraction also shows a sharp rise in value.[20] The amorphous content in carbons is often attributed to a cross-linking phase, which might be considered in this case to be tying the fibrillar regions together.[2, 14] If the amorphous phase were indeed a cross-linking system, then it might well consist of covalent bonds which would thermally rupture by 1700°C, a temperature at which diamond is observed to graphitise.[7] The rapid growth in $(\frac{E}{G})$ could then be easily explained by a relative decline in the value of G with the loss of the transverse bonding formerly rendered by the cross-links. Young's modulus, E, increases linearly with temperature in this range, as does the preferred orientation of the fibre. Therefore, although one might expect the torsion modulus, G, to decrease in value with the growth in mean crystallite size and orientation, the observed decline may well include the loss due to the breakdown of inter crystalline bonding.[160]

The electronic properties of the fibre also show a discontinuity, at 1,750°C. Collaborative work between the author and Ingram, Robson and Assabghy [161, 162] has shown that the g-anisotropy of the fibre first appears at this temperature. This is a parameter measured using electron spin resonance spectrometry. Work with single crystal graphite indicated that it should be observable with graphitised fibre if it consisted of oriented crystallites of sufficient size. The first appearance of g-anisotropy corresponds to the development of oriented

crystalline, electronic behaviour. It could be due to the development of trace quantities of three-dimensional graphite at this stage, but more likely it is simply the result of the development of long range mobility for the π-electrons; i.e. when the characteristic metallic conduction of graphite begins at a micro-crystalline level.

The first appearance of developing lamellae is found at temperatures just above 1,800°C,[147] this is no doubt a consequence of the increased level of crystal growth. The discovery that the carbon fibre becomes plastic in this temperature region must be linked with the crystallisation mechanism. Whether this mechanism is initially controlled by a cross-linking phase must for the present remain a matter of speculation. It is interesting, however, that Cellulose based carbon fibre can be hot stretched by 100% of its length at 1,000°C and by a further 100% at 2,500°C. (Bacon, unpublished communication.) Pre-oxidised polyacrylonitrile fibre (Courtelle) can only be stretched above 1,700°C and even then the maximum stretch achieved so far has been 30%.

8.22 The change in mechanical properties as a result of stress-graphitisation.

As anticipated, the hot stretching of carbonised Courtelle fibres above 1,700°C had the effect of increasing the Young's modulus and the degree of orientation of the graphite basal planes. Each stretching experiment was conducted in the presence of a control sample which was placed sufficiently close to the experimental sample, so as to experience the same heat treatment conditions. Figure 8.22(a) is a plot of Young's modulus versus the orientation angle for the graphite basal planes. The orientation angle is approximately the mean angle of inclination of the crystallite graphite basal planes to the fibre axis. As the orientation angle approaches 0°, the basal planes become oriented parallel to the fibre axis with the C-axes oriented perpendicularly. However, an orientation angle of zero would be

FIGURE 8·22(a)

VARIATION OF MODULUS WITH PREFERRED ORIENTATION

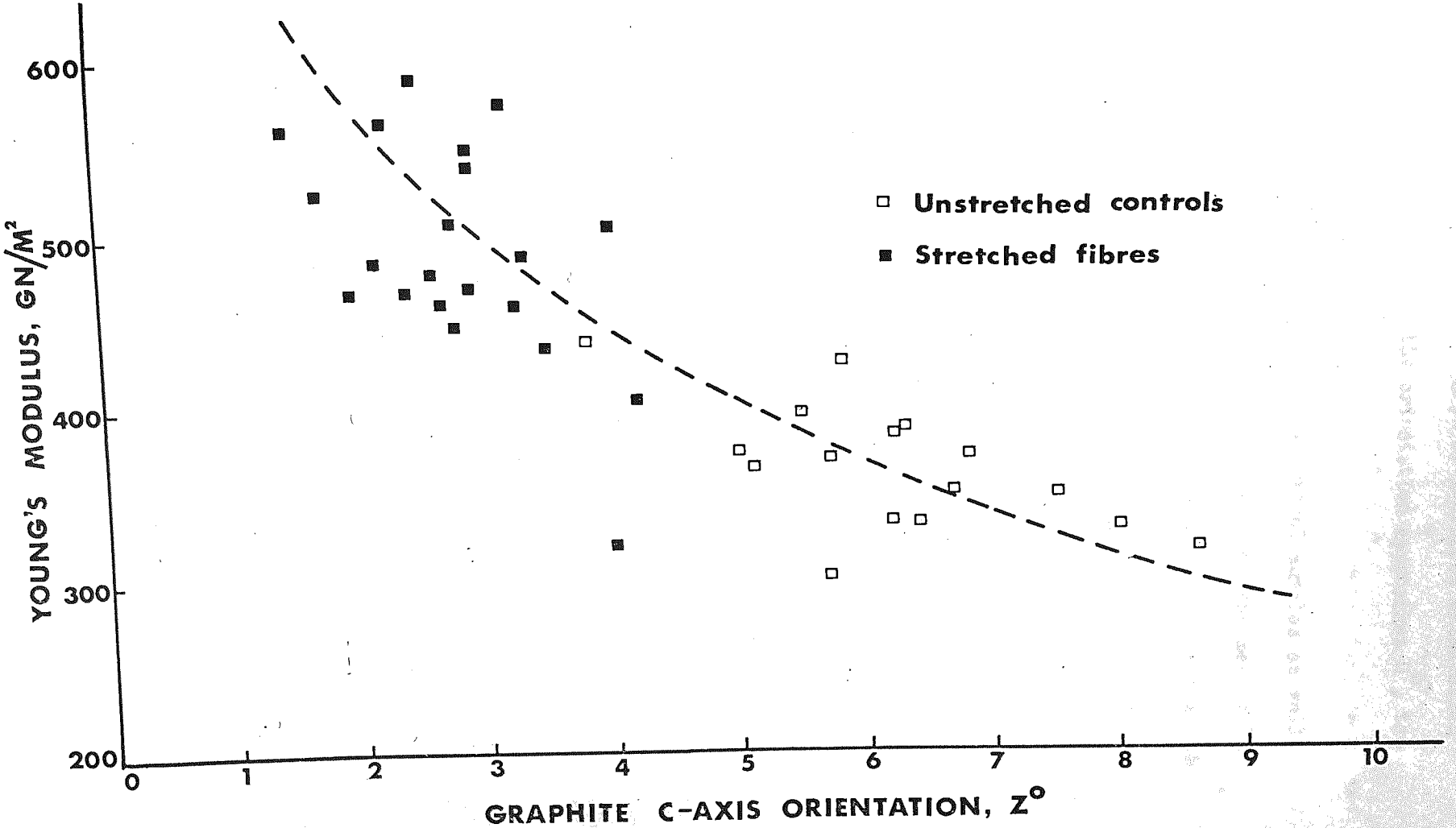

unmeasurable, because of the instrumental limitations involved. It would, however, represent the maximum degree of preferred orientation feasible with a carbon fibre and as the orientation approaches 0^{o}, the Young's modulus will go to a maximum.

Figure 8.22(a) shows the results for the control samples as well as for the hot stretched fibres. The Young's moduli are the mean value for a dozen single fibre measurements and the orientation angle has been measured for a small bundle of fibres, selected from the test loop. The hot stretching experiments were conducted at a range of temperatures and the controls hence cover a range of degrees of crystallisation. The effect of stretching is to increase the preferred orientation in each case, which reduces the value of Z_{002} and improves the Young's modulus. Hot stretching also increases the crystallinity of the fibre, which is exhibited as a reduction in the inter-layer d-spacing and an increase in L_c and L_a. Table 8.22, below, compares a selection of stretched fibres with their controls, as an illustration of this.

Table 8.22

Graphitisation Temperature, ^{o}C	% Stretch at temperature	$d_{002}.A^{o}$	$L_c.A^{o}$
1,990	0	3.444	50
"	20.0	3.432	70
2,270	0	3.436	76
"	30.0	3.428	122
2,600	0	3.410	119
"	24.0	3.407	148
2,970	0	3.407	170
"	23.0	3.397	250

FIGURE 8·22(b)

RECIPROCAL OF YOUNG'S MODULUS VERSUS ORIENTATION

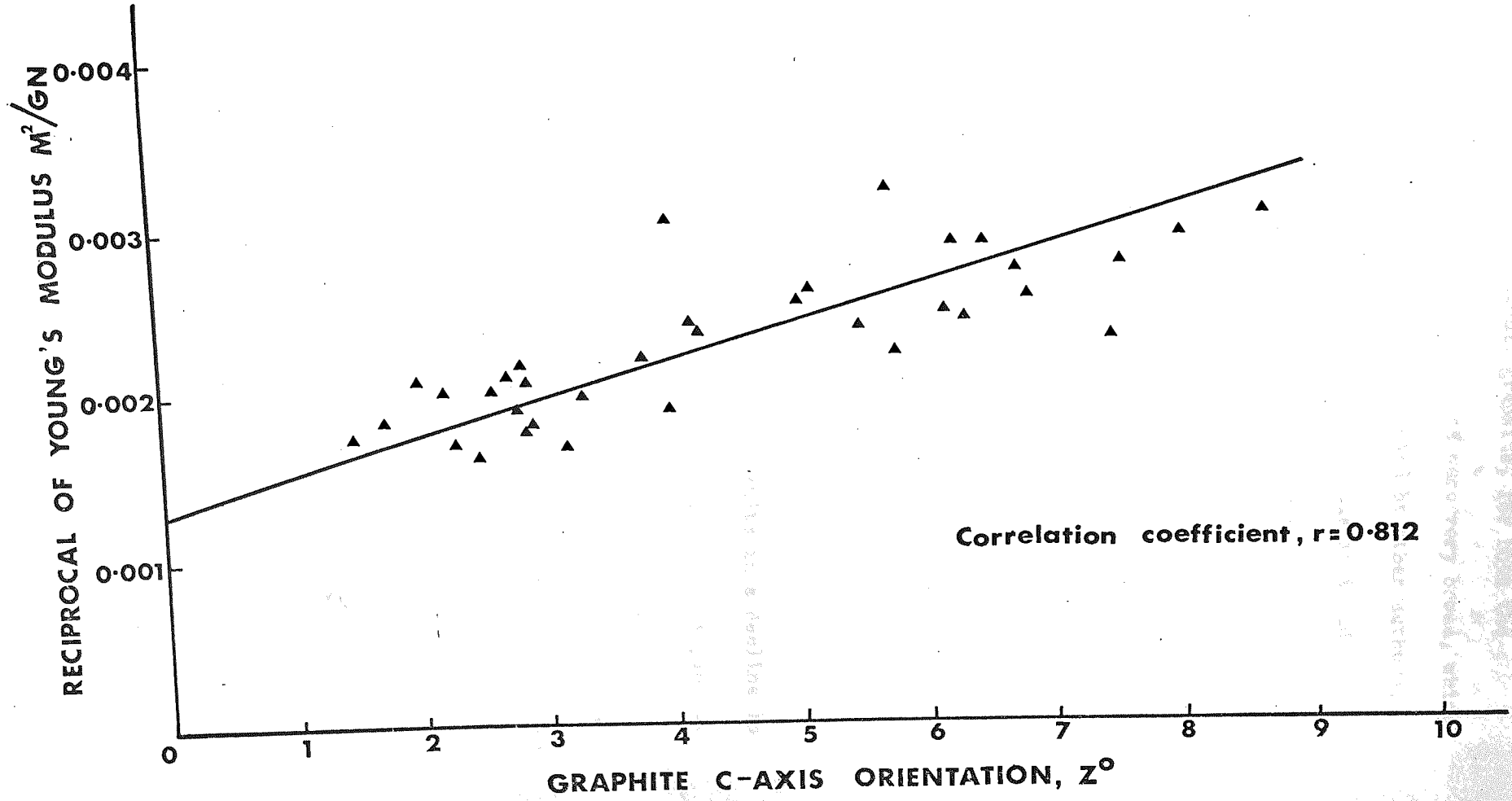

The samples with L_a values significantly above 110 A^o (as calculated by Takahashi's formula) were found to have X-ray diffraction arcs characteristic of three-dimensional graphite, for both the stretched and control fibres. Some of the arcs were very broad, which may explain why they have been so often overlooked by other authors, but in the more crystalline fibres they were quite distinct and suggested perfect crystalline contents of 30% and more.

The hatched curve drawn in figure 8.22(a) is for a suggested function relating the reciprocal of the Young's modulus to the orientation angle. Figure 8.22(b) is a plot of the reciprocal of the Young's modulus versus the orientation angle and the line drawn through the data is a best straight line fit. The correlation coefficient, r, has been calculated for the data and this is 0.812, a very good value considering the statistical scatter normally found in this work.

The strength of graphitised Courtelle fibre is improved by hot stretching. This is in some respects surprising, because increasing heat treatment temperatures without stretching results in a decline in strength for temperatures above 1,200°C.[3] Figure 8.22(c) is a plot of strength versus orientation angle for the stretched fibres and unstretched controls. The lines in the figure are best straight line fits and the correlation coefficient for each group of results has been calculated separately. The control strengths clearly decline with increasing preferred orientation and the correlation coefficient, r, is 0.671; a reasonable value for positive correlation. Stretched fibre strengths have all increased above their corresponding control values, but the correlation coefficient is only 0.234; a low value, indicating that the strength at least does not decline with increasing preferred orientation.

These observations are evidence that the strength limiting factor in graphite fibre is the low shear resistance of the graphite crystal in planes other than those parallel to the C-axis. Although the

FIGURE 8·22(c)

VARIATION OF STRENGTH WITH PREFERRED ORIENTATION

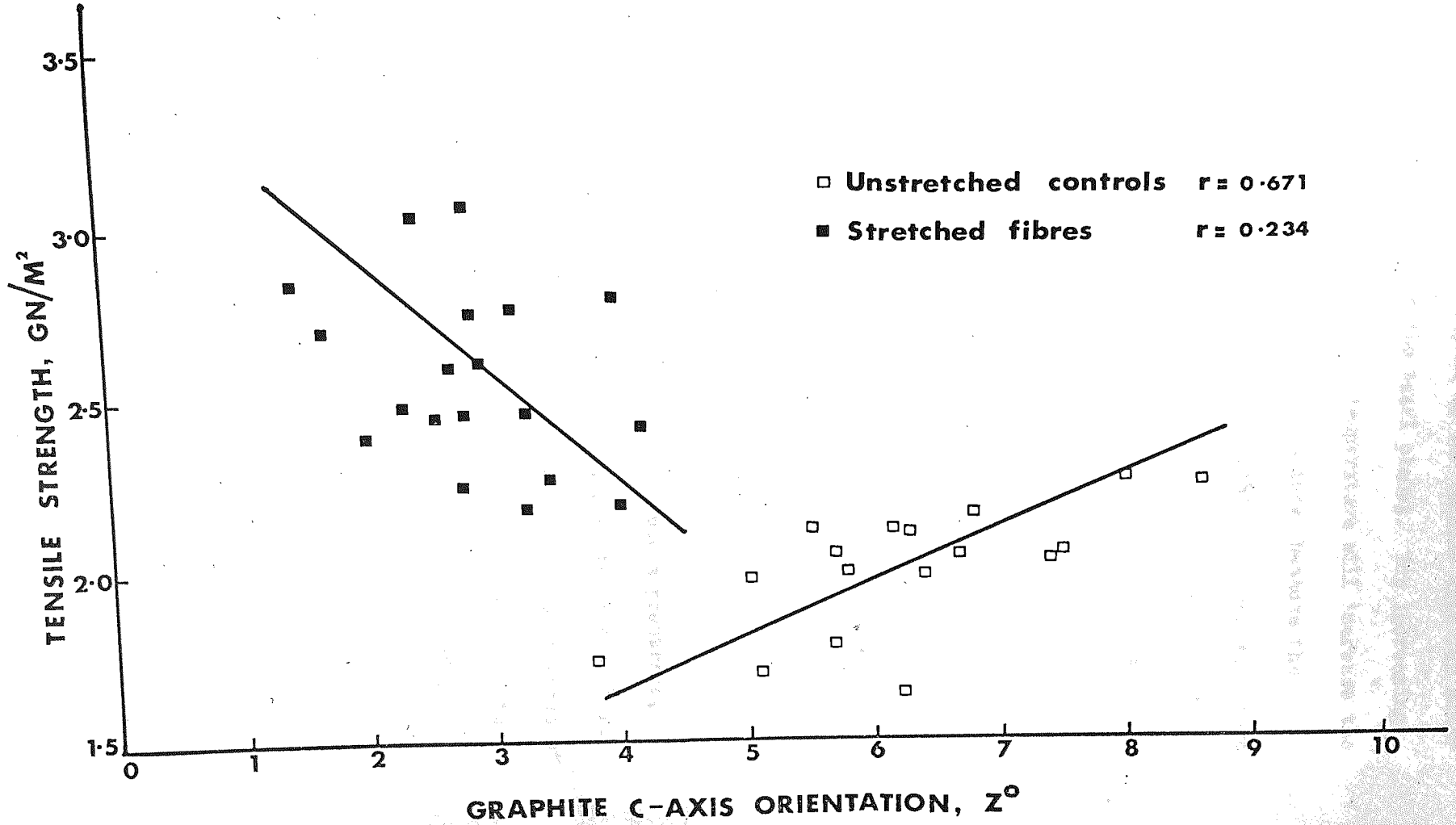

orientation angle in an unstretched fibre might be small, the crystals are sufficiently disoriented with respect to the tensile axis for shear failure to be initiated parallel to the basal planes. The increasing growth in the mean crystallite sizes with temperature will increase the susceptibility of the fibre to this type of fracture, because the amount of grain boundary material capable of inhibiting shear will have been depleted by the growing crystals. Increases in preferred orientation might at first fail to compensate for this mechanism, as the weakness of the inter-layer van der Waal's bonding will be dominant up to quite high levels of preferred orientation. Hot stretching provides a very large improvement in preferred orientation, as a result of which the proportion of very well oriented crystallites able to block the path of a shear crack increases to a point where a strength improvement is obtained.

This description of the fracture of graphite fibre is not generally accepted by other workers in the field. Bacon and his co-workers,[163] using carbon fibre prepared from a cellulose precursor, attribute the low strength relative to the modulus to the microfibril structure. They assert that the strength is limited by the weakness of the inter fibrillar bonding phase, which they believe breaks down to produce anelasticity in bending. The author does not understand, however, why the rupture of inter fibrillar bonds, when the fibre is in tension, should lead to total fracture of the fibre.

The mechanical properties of polyacrylonitrile based carbon fibres can differ quite a lot from cellulose based material. The breaking strain of Bacon's cellulose based fibre (which has to be hot stretched to produce useful properties) never exceeds 0.5%.[157] Polyacrylonitrile based fibre achieves a breaking strain of 1.3% after heat treatment to 1,200°C.[3] This then declines to values of approximately 0.5% at 3,000°C,[158] when it has similar properties to the cellulose based fibre with the same modulus. Hot stretched Courtelle carbon fibre however,

has very similar properties to cellulose based material. This is observed for the mechanical properties and the crystal structure. Figure 8.22(d) is a plot of tensile strength versus Young's modulus for the stretched fibres and their controls and the lines are best straight line fits. The correlation coefficient for the controls is 0.061, therefore there is no correlation. The correlation coefficient for the stretched samples is 0.753, giving quite reasonable correlation. The stress-strain curves for these fibres were treated as straight lines and so the ratio of the strength to the modulus provides the breaking strain. For the controls, the breaking strain is declining with increasing Young's modulus to 0.5%. The stretched fibres all have approximately the same breaking strain of 0.5%, given by the slope of the line fitted to the results. This same line fits the results of Bacon et al. for cellulose based fibre.[157] The higher breaking strains for the controls does not disagree with the shear mechanism proposed for the fracture of graphitised fibre. Fibre which fractures as a result of a degree of microplasticity should have a greater fracture strain than completely brittle fibres. Although, by most comparisons, both types of fibre would be considered to be brittle materials.

Carbon fibres from any precursor generally have extremely low strengths for the moduli obtained. Bacon et al. calculate that a perfect single crystal of graphite, tested in parallel to the basal planes, should have a tensile strength which is 18% of the Young's modulus.[163] This should provide strengths some thirty six times greater than those found for carbon fibres. With such a disparity between theory and practice, it is probably premature to attach too much importance to any one theory of strength in carbon fibres. It is possible that a number of mechanisms are responsible for their weakness. Thermally induced cracks and dislocations are just two sources of weakness that can be postulated. Johnson et al.[164] and

FIGURE 8·22(d)

STRENGTH AS A FUNCTION OF MODULUS

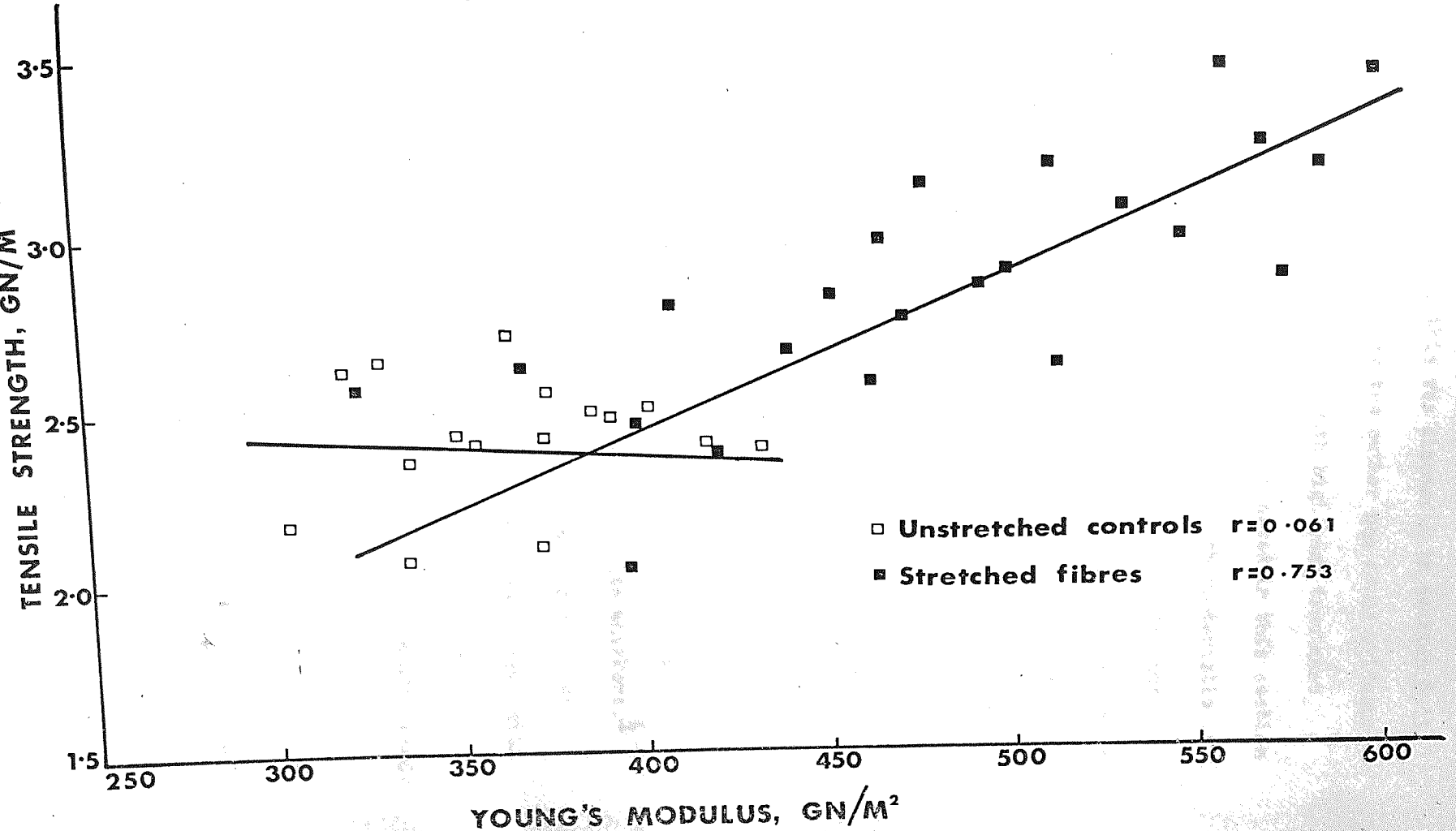

Johnson and Tyson [17, 20] believe that the presence of three-dimensional graphite is a source of weakness, this was discussed in section 8.11. This is an interesting theory, because the author has found evidence for three-dimensional graphite appearing with high heat treatment temperatures. Half of the control specimens discussed in this section produced X-ray diffraction arcs with Miller indices characteristic of the single crystal. However, this was also the case with the hot stretched specimens, a larger proportion of these contained completely crystalline material and yet their strengths had been improved by stretching. It is probably too early in the progress of carbon fibre research to be precise about the effect of structure. If a graphite fibre could be prepared, say by stretching, with an orientation angle of 0^{o}, then it would be possible to test the theory that microshear is responsible for graphite fibre weakness. Such a fibre should have a strength more commensurate with the high Young's modulus. The etching away of surface flaws and the annealing out of dislocation might then produce a material with strengths comparable to graphite whiskers.[6]

It is interesting to compare the effect of fibre contraction during carbonisation upon the modulus of the graphitised fibre, with the effect of stretching at a fixed graphitisation temperature. Figure 8.22(e) is a composite graph, where the percentage length change is plotted on the left hand side of the scale for the hot stretching process and on the right hand side for contraction during carbonisation. The contracted fibres are from the experiments conducted with various degrees of pre-oxidation of the polymer fibre which are described in chapter 7. Each modulus value is the result of single fibre tests on twelve fibres, and the bars drawn through the data points are for the 95% limits of confidence, on the mean of the modulus; i.e. there is a 95% probability that the mean of a second test on the same sample will fall on the bar. The best fit line for the stress graphitised fibres has a very similar slope to the line for the contracted fibres which

FIGURE 8·22(e)

DEPENDENCE OF MODULUS ON FIBRE LENGTH CHANGES FOR GRAPHITISED FIBRES

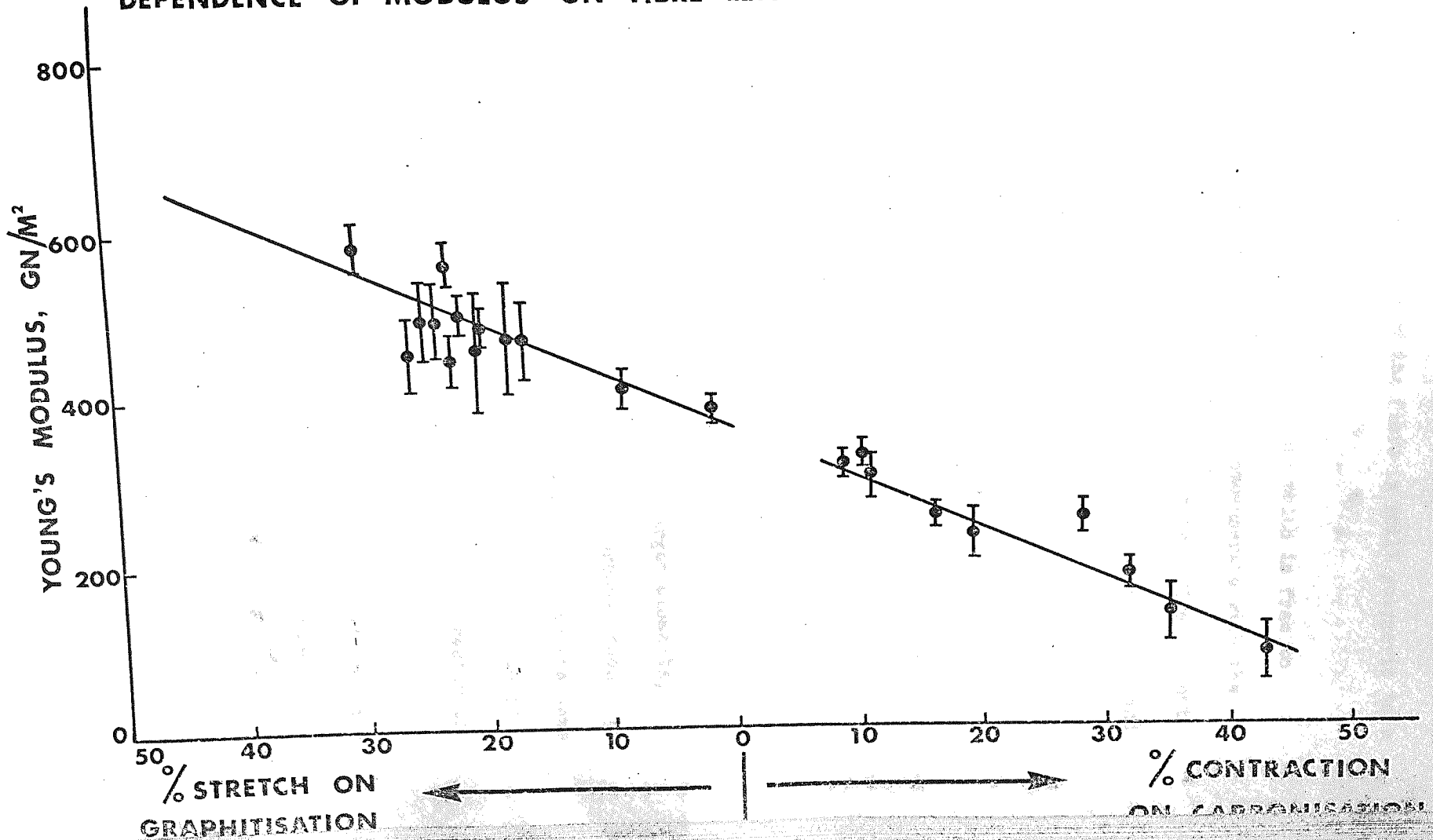

had been graphitised at 2,650°C. The effect of stretching at 2,600°C (in this case) is equal and opposite to the effect of fibre contraction mainly taking place below 350°C, when the fibre is still polymeric to a large extent.

The relaxation of an oriented polymer fibre which is free to contract will result in a reduction in length commensurate with the loss in orientation. If the agreement shown in figure 8.22(e) is not fortuitous, the structural element responsible for the orientation and contraction of the polymer fibres, is primarily responsible for the orientation of the graphite fibre. Stretching the fibre at 2,600°C produces the same amount of orientation that stretching at 150°C would produce, if this latter process could be conducted without any plastic flow of the polymer (the contraction process is without plastic flow). This is striking evidence for the view that the precursor polymer molecules are responsible for the conservation of orientation and not a macro-molecular feature, such as the microfibril. They must remain oriented to a large extent, albeit in the form of larger elements, during the entire heat treatment process; i.e. the carbon-carbon backbone chains must be incorporated into the layer planes in the same oriented state. The initial ladder polymer formation reaction would facilitate this process if the ladder molecules condensed directly to form the graphite layer planes.

Experience with cellulose indicates that a similar relationship exists between precursor and graphite fibre orientation. Indeed, Bacon in his original paper discussing this topic,[127] considered that the molecules condensed in an oriented state to form the partially oriented layer planes of the final structure. A major difference between cellulose and polyacrylonitrile fibre is that it is not possible to completely restrain the former during the initial pyrolysis. It becomes very weak as a result of the degradation reactions and is unable to withstand the relaxation forces. As a result of this, it is

allowed to contract a great deal, under load. After carbonisation to 1,000°C, the modulus of the fibre is very low and by no means comparable to the properties obtained for polyacrylonitrile fibre, which can be oxidised under total restraint. It appears very likely, therefore, that the inferior properties are partly due to the disorientation following fibre shrinkage. This seems to be further confirmed by the fact that stress-graphitisation produces graphite fibres with identical properties for both precursors.

8.3 THE STRUCTURE OF CARBON/GRAPHITE FIBRES.

The structure of carbon fibre can be considered in two alternative ways. It can be regarded as an assemblage of microcrystallites, growing in size and increasing in orientation with heat treatment temperature. Or, alternatively, as a paracrystalline lattice, in which the long range order is perturbed by various distortions in the lattice, producing an apparent microcrystalline fine structure. The structure of semi-crystalline polymer fibres have been variously described with these models. The microcrystalline model has a counterpart in the fringed micelle model used for many fibres [119] and the paracrystalline lattice has been used to describe the structure of polyacrylonitrile fibres.[124]

Models produced as a result of the analysis of X-ray diffraction data will usually be based upon discrete crystalline building blocks, because the theories of line broadening which are used to calculate L_a and L_c assume that this will be the type of structure possessed by a polycrystalline solid. Very high resolution transmission electron microscopy has shown that high modulus graphite fibre has a continuous ribbon-like structure, however. The inter-layer d-spacing of ~3.40 A° of graphite can be easily resolved with the high quality electron microscopes now available. Hugo et al.[165] have shown continuous layer planes running along the surface of Thornel 50 fibres, by direct transmission through surface crenulations. Better order is expected at

the surface of graphite fibres, as shown by SEM micrographs and electron diffraction. However, very long ribbon-like lamellae have been detected by Harling [166] in longitudinal sections of Thornel 50, confirming that though the perfection of the structure may be somewhat less internally, it consists of the same basic ribbon-like features. Exceptionally good electron micrographs of fibre transverse cross-sections produced by Harling [166] for both cellulose and polyacrylonitrile based graphite fibres exhibit the same ribbon structure as seen in longitudinal sections. Individual ribbons appear to represent the microfibrils previously observed in lower resolution microscopy. Johnson,[167] Allen et al.[164] and Fordeaux et al.[143] have also published similar evidence, these latter workers have shown that the X-ray diffraction evidence is quite compatible with the observed structures. Figure 8.3 is a schematic representation of the ribbon structure.[168] Inspection of the drawing shows how an assembly of continuous sheets could be interpreted as a microcrystalline body. In the parts of the fibre having a lamellar structure, the ribbons would be lying parallel to a prior substrate, such as the surface of the fibre or an internal void, where the ribbons could easily coalesce to form a continuous sheet. This type of structure belongs more to the paracrystal concept of crystalline order than to the more conventional idea of crystals separated by various types of grain boundary.

Growth in crystal size, perfection and preferred orientation with heat treatment temperature is more easily understood with a structure of this type than with the turbostratic microcrystal model. Kinks and wrinkles in a graphite ribbon would tend to straighten between undistorted regions and to take up the same orientation, because of simple energy considerations. The graphite layer structure is essentially planar and high temperature annealing will allow distorted bonds to straighten. Dislocated regions of the layers could produce sufficient mobility in the ribbon, so that a straightening process

FIGURE 8·3

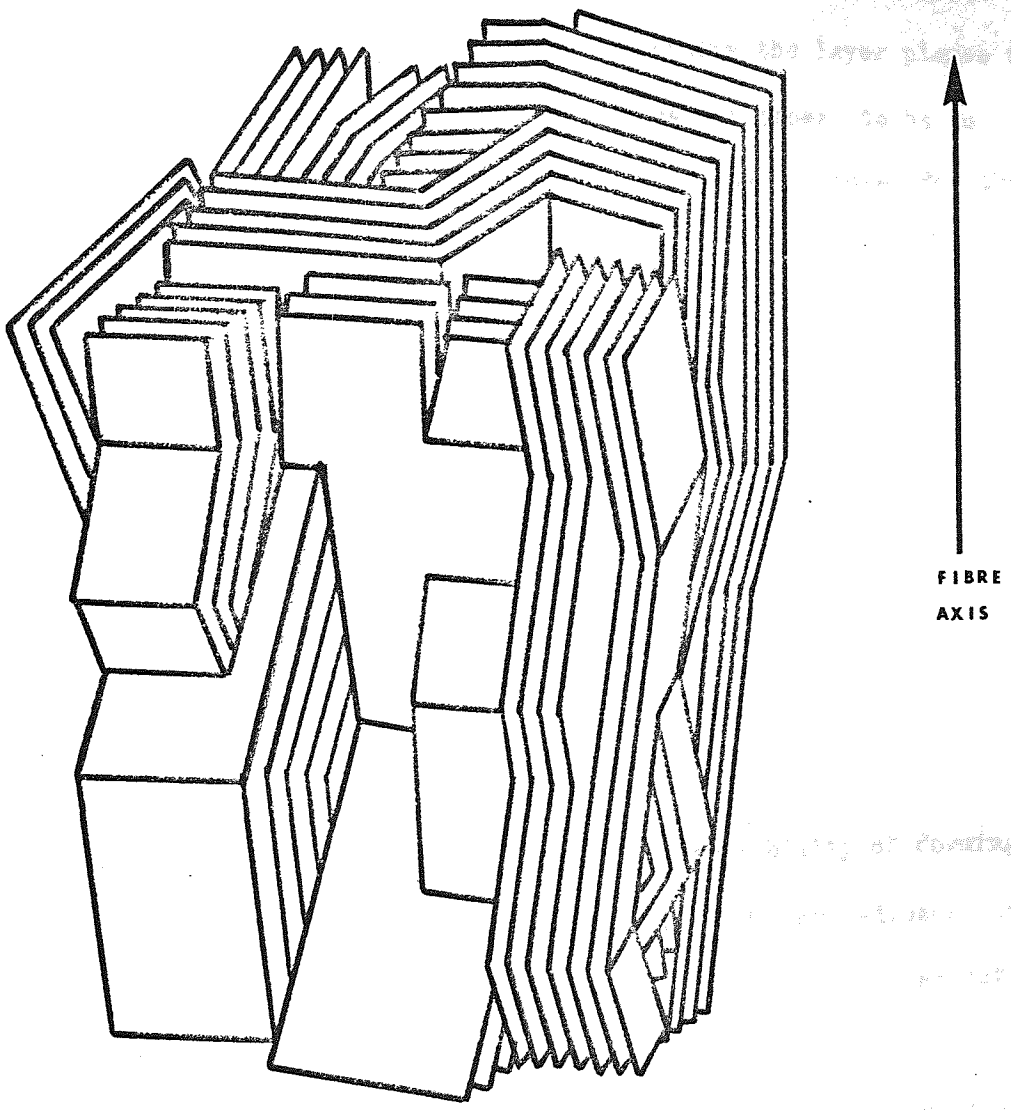

A SCHEMATIC REPRESENTATION OF THE RIBBON—STRUCTURE IN GRAPHITISED CARBON FIBRE (Allen et. al.)

could take place. Movement of the layers in the ribbons would permit the d-spacing to decrease as the layer packing improved. This type of mechanism would explain why so much three-dimensional graphite can be formed from an apparently turbostratic carbon. For a turbostratic carbon to form a perfectly crystalline graphite the layer planes would have to rotate about the C-axis. This does not appear to be as energetically favourable as the annealing process proposed for the ribbon model. The increase in preferred orientation with heat treatment is also more difficult to understand with the turbostratic crystal model. This requires that the crystals rotate in the fibre to form the oriented fibrils observed and there is no obvious mechanism for doing this, except the contraction of the fibre diameter. However, it is much more simple to consider that a long range oriented structure is already present which develops from a primitive form of ribbon structure, during the early stages of the carbonisation process.

The assumption of a continuous, well oriented ribbon structure for graphite fibres suggests a theoretical possibility of forming an almost completely crystalline fibre, having 100% three-dimensional order. This is suggested by the appearance of increasing amounts of three-dimensional graphite with heat treatment and stress-graphitisation. It is surprising that not many authors have made these same observations, when perfect crystallinity is observed it is usually attributed to special conditions, such as the presence of boron in the fibre.[164]

8.31 The possibility of perfectly crystalline graphite fibre.

Ergun[18] and Ezekiel [19] have observed as much as 45% of graphite crystal in a single batch of fibre, which has led the former worker to expect that it might be a general phenomenon. Ezekiel has observed very many different graphite fibre batches which have very low d-spacings suggesting three-dimensional order, but he has not investigated the possibility further.

FIGURE 8·31(a)

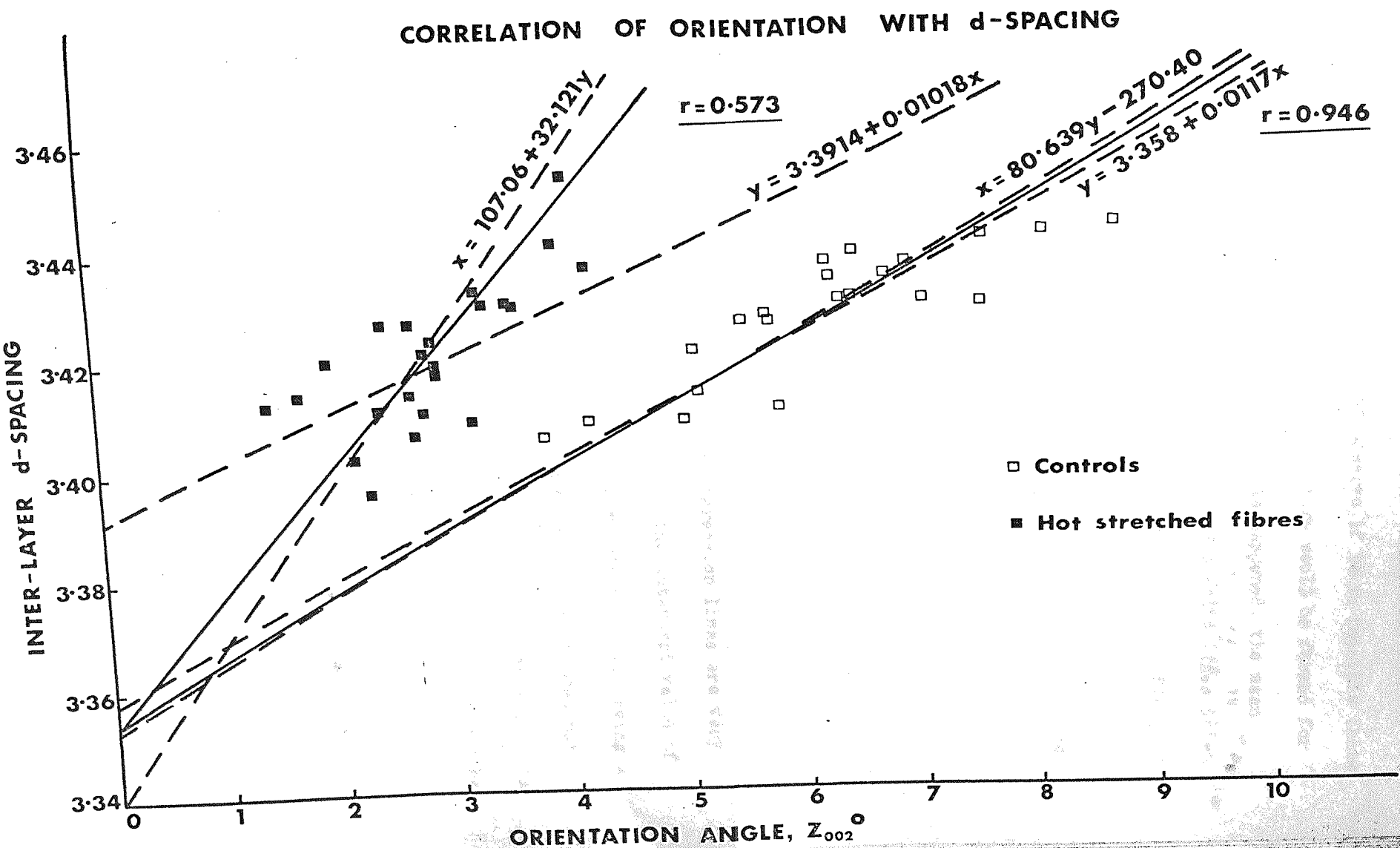
CORRELATION OF ORIENTATION WITH d-SPACING
x = 107·06 + 32·121y
r = 0·573
Y = 3·3914 + 0·01018x
x = 80·639y − 270·40
r = 0·946
y = 3·358 + 0·0117x
INTER-LAYER d-SPACING
3·46
3·44
3·42
3·40
3·38
3·36
3·34
0
1
2
3
4
5
6
7
8
9
10
ORIENTATION ANGLE, Z002 °
Controls
Hot stretched fibres

Figure 8.31(a) is a plot of orientation angle versus inter-layer d-spacing for the stress-graphitised series of samples and for their control samples. The purpose of the plot is to extrapolate back to an orientation angle of 0^{o}, in order to observe if it is feasible that a completely three-dimensional graphite structure would be formed for the complete orientation of the fibre. If this happened, the mean d-spacing for the structure should be 3.354 A^{o}. The solid lines drawn through the data points are not drawn from best straight line fits, but are drawn deliberately through an inter-layer d-spacing of 3.354 A^{o}. Regression lines have been calculated for each set of data, these are drawn in as hatched lines, with the appropriate straight line function printed along them. Regression lines are calculated assuming that only one of the two parameters is in error, in each case. The hatched lines, therefore, represent the extremes in which a reasonable best fit straight line must fall. A correlation coefficient has been calculated for each set of data and for the control values it is 0.946, a very high value, showing good correlation. The regression lines are very close and they cross the ordinate very near to the intercept value of 3.354 A^{o}. The hot stretched data does not correlate so well, having a correlation coefficient of 0.573. This could be because it does not cover such a wide range of Z_{002} values as the controls. However, it is quite a reasonable, positive correlation and the line drawn through the intercept at 3.354 A^{o} falls within the intercept values of the regression lines.

It appears to be a reasonable hypothesis that the total orientation of a graphite fibre should produce complete graphitisation. As the orientation angle approaches 0^{o}, it is to be expected that L_c and L_a should rise exponentially to very high values indeed. Figure 8.31(b) suggests that this might be the case. It is a plot of the crystallite L_c dimension for the hot stretched and control series of samples versus the orientation angle. The curves are exponential in form and indicate

FIGURE 8·31(b)

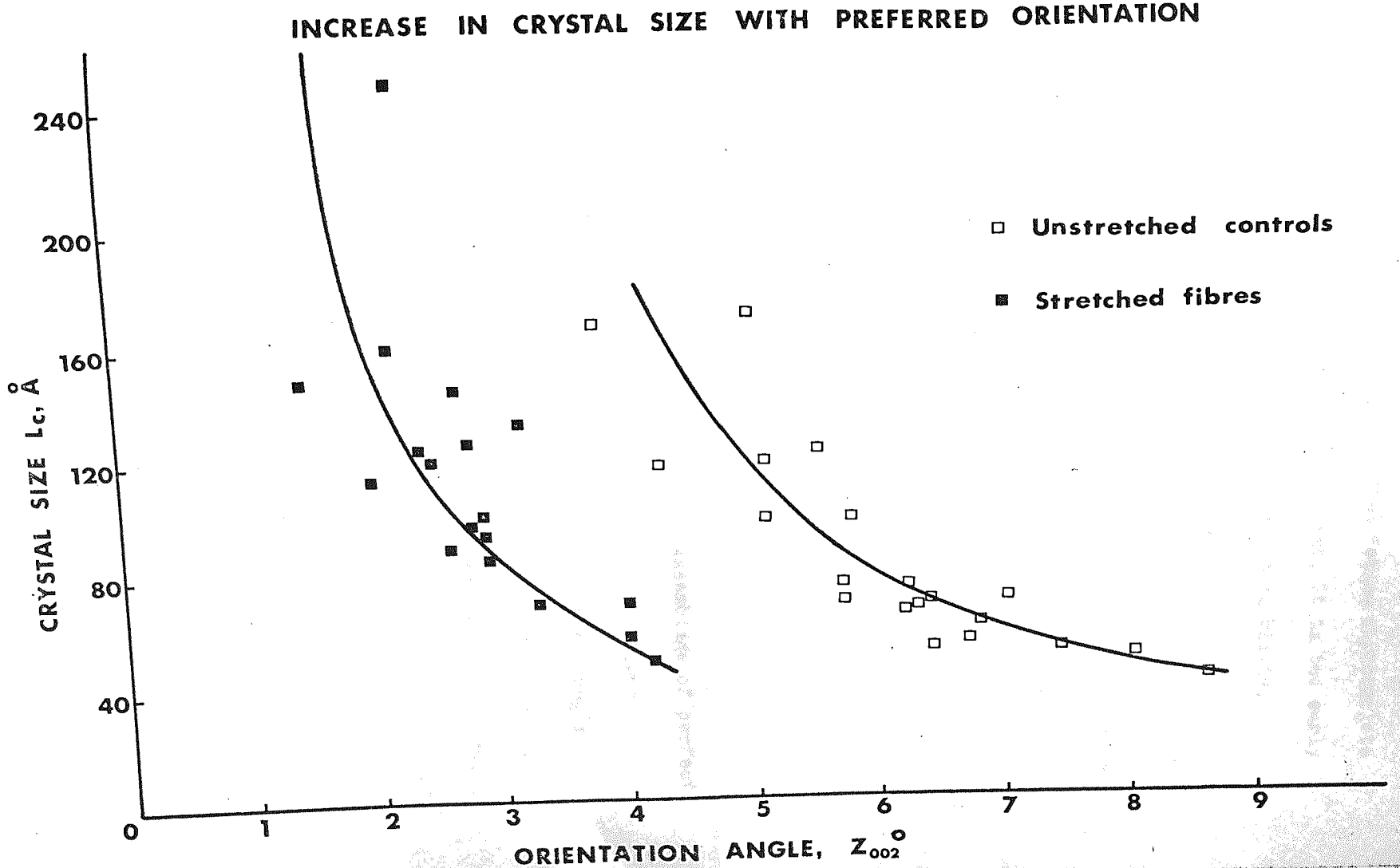
INCREASE IN CRYSTAL SIZE WITH PREFERRED ORIENTATION
Unstretched controls
Stretched fibres
CRYSTAL SIZE Lc, Å
240
200
160
120
80
40
0
1
2
3
4
5
6
7
8
9
ORIENTATION ANGLE, Z002°

that very low values of orientation angle might result in very high crystallite sizes indeed. It is for the very low values of Z_{002} that the strength should rise to values which are a reasonable proportion of the Young's modulus. There may be a fundamental reason why complete orientation of the fibre is not achievable, however, it is too early in the development of carbon fibres to dismiss the possibility.

8.32 The orientation angle and the ribbon model.

Figures 8.31(a) and 8.31(b) show that stress-graphitisation has its greatest effect on the preferred orientation of the fibre. Although it increases the crystallite sizes, the effect on Z_{002} is very much greater. This seems to be in agreement with the ribbon model; the ribbons can be pulled straight to some extent, but the crystallisation processes within the ribbons are limited by the thermal rate processes. The improvement of crystallinity with hot stretching might be entirely due to the healing of boundary voids within the ribbons.[158]

A relationship between the Young's modulus and the orientation angle can be derived by treating the fibre as an assemblage of perfect crystallites, each contributing to the elasticity of the fibre according to its orientation. It has been shown that the Young's modulus of polycrystalline materials will fall within boundaries given by two alternative models of the structure.[169] These models are due to Voigt and Reuss. The Voigt model assumes that the crystals are linked together in such a way that an applied stress will produce a constant deformation in all the crystals. This produces uniform strain in the body. It is as if the crystals are embedded in an isotropic matrix of very high stiffness, which forces the crystals to deform in the tensile direction to the same extent, whatever the modulus of the crystal in that direction. The Voigt curve for graphite is shown in figure 8.32. It shows that the modulus of the body should be high for quite low values of preferred orientation. The Reuss model assumes that the crystals are subject to constant stress in the tensile direction.

FIGURE 8·32

DEPENDENCE OF CARBON FIBRE MODULUS ON ORIENTATION ANGLE

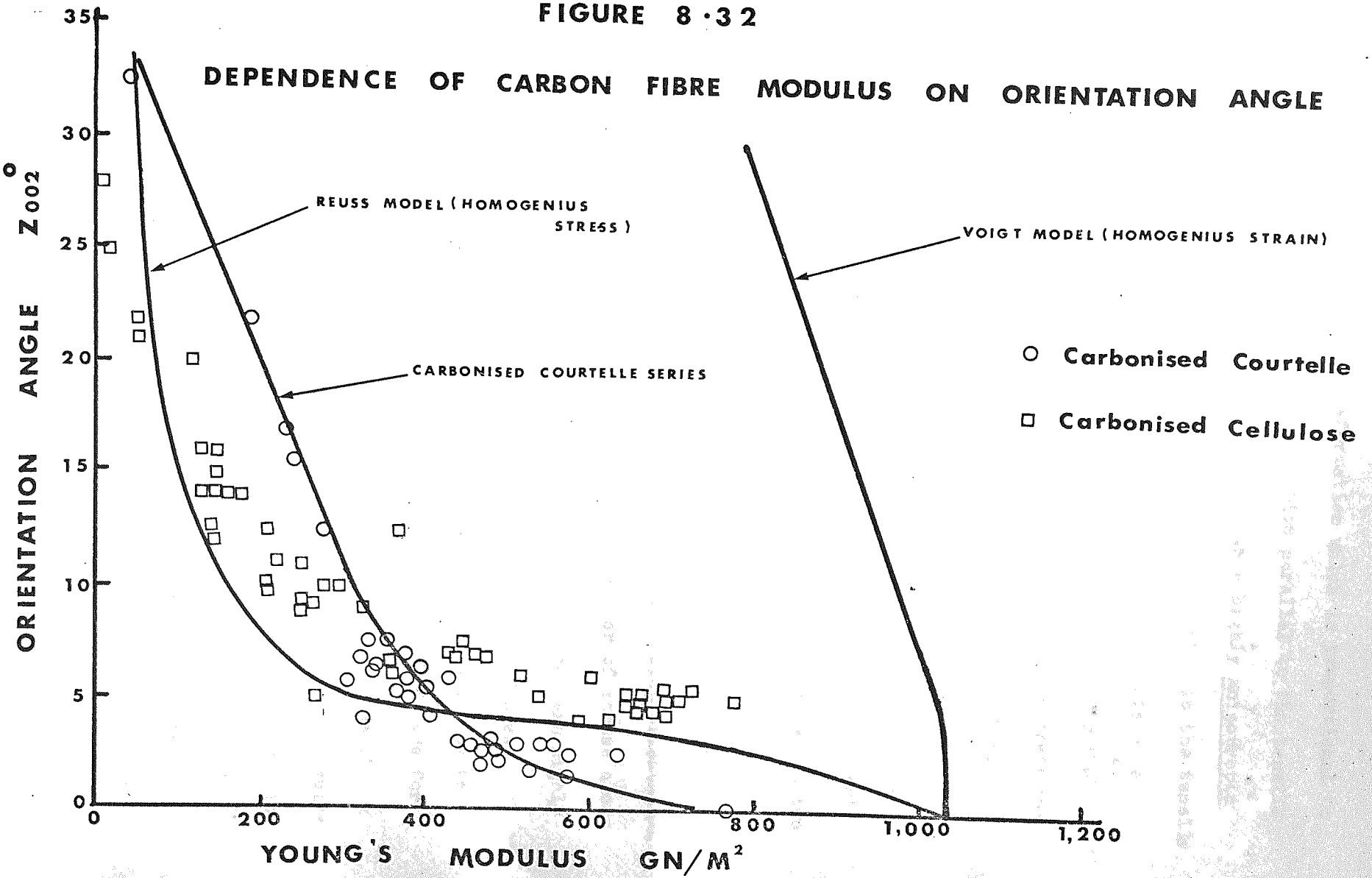

Whatever the orientation of a crystal, the application of a given stress to it will only produce a deformation which is proportional to the modulus of that crystal, in the direction parallel to the tensile axis. It is as if the crystals are embedded in a highly anisotropic matrix, which only applies the full stress to the crystal in the tensile direction and lacks completely any transverse cohesion. This model should apply to highly oriented polymer fibres. The curve for the Reuss model is also drawn in figure 8.32. For low values of preferred orientation, the Young's modulus is very low. When the orientation angle is 0° (when the preferred orientation is perfect) both models give the theoretical Young's modulus (i.e. the modulus parallel to the graphite basal planes) of 1,035 GN/M^2. Bulk graphites produce Young's moduli which generally fall mid-way between the values given by the two models [170] as do many crystalline solids.

The ribbon model strongly suggests that the Reuss model should describe the dependence of carbon fibre Young's modulus upon orientation. Because the ribbons should allow the efficient transfer of stress along the fibre without much transverse deformation, even if they are highly disoriented. The results for a very wide range of carbon fibres prepared from Courtelle have been plotted in figure 8.32 and a curve fitted to them. A lot of the results plotted above 300 GN/M^2 are for the hot stretched series of fibres and their controls. The result plotted for $Z_{002} = 0^{\circ}$ has been obtained by extrapolation of the results in figure 8.22(b). Also plotted in figure 8.32 are a series of results published by Bacon and Schalamon [157] for cellulose based carbon fibres.

All the results shown in the figure are very far from being in agreement with the Voigt model, on the other hand for high values of modulus, the agreement of both series of samples with the Reuss model is excellent. The Courtelle series falls below the Reuss curve to terminate at a modulus of 753 GN/M^2 (B in the figure) somewhat below the theoretical modulus. It would be very surprising if it did not,

as the structure is unlikely to be perfect. Below 250 GN/M^2 the cellulose based carbon fibre agrees much better with the Reuss curve than the Courtelle based material, the curves have diverged quite a lot by 200 GN/M^2 (this is the modulus characteristic of 1,000°C fibre). It is for moduli in the region of 200 GN/M^2 that Courtelle carbon fibre has much higher strengths than cellulose based fibre. This could be due to the cross-linking phase suggested by various authors.[2, 14, 17, 160] Such a phase would give the fibre higher transverse stiffness and bias the orientation-modulus plot towards the Voigt curve. None of the data in the plot is for fibres heat treated below 1,000°C, the Courtelle result at $Z_{002} = 32.5^\circ$ (A in the figure) is a fibre which has been allowed to disorient with inert heat treatment prior to oxidation and carbonisation. For moduli below 50 GN/M^2 the cellulose and polyacrylonitrile based carbon fibres both agree with the Reuss curve.

This agreement between the data for the two precursors and the Reuss curve is strong support for the ribbon model of carbon fibre fine structure. It is even more remarkable that other precursors have similar agreement, such as petroleum pitch [42] and hot stretched 'glassy' carbon fibres.[156] A ribbon model of graphite structure has far more general application than this. Carbon blacks have been shown to have a coiled ribbon structure [172] and recent work with vitreous carbon shows it to consist of tangled ribbons of turbostratic graphite.

SUMMARY AND CONCLUSIONS.

The low temperature chemistry of heat treatment obviously has a very important influence on structure development in acrylic based carbon fibre. Without oxidation, it is clearly impossible to make graphite fibres that are separable and have good mechanical properties. However, the experience with 9 denier Courtelle shows that the mechanical properties will suffer if excessive oxidation is employed. This was the experience with 1.5 denier Courtelle and was discussed in

Chapter 7. The author believes that this deterioration in properties might be due to the early disorientation of the precursor and that this might allow the formation of a lamellar structure to occur at graphitising temperatures.

On the other hand, oxidation acts as a stabilising reaction, due to the earlier inception of polycondensation reactions at 300°C. It is expected, therefore, that it would conserve the microstructure of the precursor fibre, as melting and disorientation are prevented. The existence of a microfibrillar fine structure in graphite fibre very probably stems from the precursor, although it is not impossible that it is created during heat treatment; microfibrils in pitch based fibres must originate after pyrolysis for example. Prescott's experience with 9 denier Courtelle demonstrates that the microfibrils might limit the extent of possible crystal growth, while the author's work shows that in some cases they may not be present and in other cases they can be destroyed by melting.

The development of a graphite lamellar phase can be a source of fibre weakness, the 9 denier based material is almost certainly of low strength and modulus because of it. However, the concentric lamellar structure produces much better properties than one would expect from a hollow fibre and the very high modulus of the Rhodiaceta based material is most encouraging. If one is searching for a continuous fibre to rival graphite whiskers, it would be interesting to learn more about the development of this type of structure. The formation of curved graphite structures having a tubular or scroll-like conformation is becoming more commonly observed; it was recently reported from the pyrolysis of phenol.[174] This type of structure is inherently of high modulus and it may be possible to make filaments of very high strength possessing it, without recourse to the sophisticated methods used for making whiskers.

The frequency with which three-dimensional graphite was observed

in high modulus fibres leads to the conclusion that polyacrylonitrile is a graphitising polymer. It does not graphitise with the facility of polyvinylchloride but it is one of the few fibrous polymers which graphitises to form an oriented crystal structure. No doubt other polymers will be introduced which have this characteristic, which is the single most important advantage of polyacrylonitrile and one that is lacking in most competing precursors at present.

The ribbon model is almost certainly an accurate picture of the structure of high modulus carbon fibre. It has the additional advantage of explaining how increasing heat treatment temperatures produce an improvement in preferred orientation. The microfibrillar structure is unlikely to be the source of preferred orientation, because, as the two-phase graphite fibres showed, they have no controlling effect on the transverse distribution of the crystallites in the fibre.

The improvement in strength and Young's modulus by hot stretching appears to be equivalent to the original stretching of the precursor, to produce high preferred orientation. If a polymer precursor could be stabilised chemically after being given an extremely high preferred orientation, it might be possible to produce a graphite fibre with very high mechanical properties, without the necessity of a hot stretching phase.

CHAPTER 9.

CONCLUSIONS AND SUGGESTIONS FOR FUTURE RESEARCH.

(1) Polyacrylonitrile is a suitable precursor for the preparation of carbon fibres, because it reacts with heat treatment to produce a more thermally stable product. Oxidation of this product is, however, essential, if carbon fibre of high strength and modulus is to be prepared from it.

(2) The stable product of pyrolysis is produced by the polymerisation of the nitrile groups. Evidence produced in this thesis supports the hypothesis of W. D. Potter (University of Aston) that a poly 1,4, dihydropyridine structure is formed. Oxidation of this structure by heat treatment in air or under ambient atmospheric conditions, results in the formation of an aromatic product, which also contains cyclic molecules with carbonyl and other oxygen containing groups.

(3) It has been confirmed that pure polyacrylonitrile fibres probably form a saturated population of initiating rings, before the polymerisation of the nitriles can be initiated. Copolymer fibres, containing methylacrylate can initiate the polymerisation of the nitriles at lower temperatures and as a consequence of this, a larger proportion of them contribute to the cyclised product.

(4) Courtelle has so far proved to be a more satisfactory precursor for carbon fibre production than most other acrylics. This appears to be because stabilisation is accomplished at lower temperatures, through the polymerisation of the nitriles, without the violent exotherm and fibre sticking associated with other acrylics. Courtelle also oxidises at lower temperatures, which further suppresses fibre melting. However, these are purely practical advantages, because Dralon T processed with due regard to its chemistry, will produce carbon fibre with properties at least as good as Courtelle based material. This is

further confirmed by recent results published by Ezekiel.[175]

(5) Oxidation improves the stability of heat treated polyacrylonitrile, by inducing the polycondensation reactions responsible for forming a stable carbon, to commence at lower temperatures. Oxidation in air at 1 ^{o}C/minute begins to produce condensation at 300 ^{o}C, as compared to 480 ^{o}C for a similar programme conducted in argon. These results agree with the general observation that the presence of oxygen in heat treated chars assists carbonisation, while the presence of hydrogen inhibits it.

(6) Stretching at graphitising temperatures increases the modulus and strength of acrylic based carbon fibre. Maximum stretches of 30% have been achieved with carbonised Courtelle, which is much less than the 200% stretches reported for cellulose based material. As acrylic based carbon fibre has a much higher orientation than the equivalent carbonised cellulose material, the disparity in stretch ratios is understandable.

The increase in orientation produced by hot stretching, is found to be equal and opposite to the disorientation produced by contraction during carbonisation. This indicates that the orientation of the precursor is preserved throughout carbonisation, as a result of the condensation of the molecules, while they still retain their original extended conformation.

(7) The partial oxidation of acrylic fibres at high temperatures can have a decisive influence on the degree of crystalline development produced by graphitisation. If the fibre core melts, continuous lamellae can be formed by crystal growth upon the oxidised substrate. This type of structure can result in very high Young's moduli, for which values comparable to those determined for graphite whiskers have been observed.

(8) Polyacrylonitrile has been found to be a graphitisable polymer. It is not as graphitisable as some vinyl polymers and oxidation does reduce the amount of crystallinity produced under given conditions. Nevertheless, varying fractions of three-dimensional graphite crystal have been found in high temperature fibres. This sometimes constitutes as much as 40% of the total carbon content.

(9) The variation of carbon fibre Young's modulus with the (002) orientation angle, suggests that the Reuss model of crystalline orientation is the most valid. This favours the view that the fibre is compounded of continuous ribbons of crystallites, which are about as thick as they are broad, but which extend for many thousands of angstroms along the length of the fibre. This model of the structure explains the X-ray and electron diffraction results and the micro-fibrillar fine structure normally observed in pre-oxidised, graphitised fibre. The gradual appearance of three-dimensional graphite with heat treatment, could be due to the annealing out of distortions in these ribbons.

(10) If a graphite fibre with an orientation angle (Z_{002}) of 0^{o} could be prepared, it would have a modulus in excess of 1,000 GN/M^2. The strength would probably be a substantial fraction of this and the fibre would probably be perfect single crystal graphite.

Suggestions for future research.

With the subject at the very beginnings of its development, there are many promising future possible lines of research, which could be directed towards producing carbon fibres more cheaply and with improved properties. Just a few of the more relevant possibilities will be considered here.

An important approach to the problem of obtaining improved properties that has not received much attention at present, is to obtain high values of precursor preferred orientation. The choice of

spinning method, molecular weight, and stretching techniques are just some of the variables which should be investigated. If very high values of preferred orientation could be achieved at this stage, it might be possible to obtain Young's moduli in excess of 700 GN/M^2, without the use of an expensive hot stretching stage. Obtaining high values of Young's modulus is probably an easier task than that of improving the strength. Improvements in strength depend upon obtaining cleaner precursors, which are more homogeneous, and processing methods which can totally eliminate damage to the fibre surface, due to melting and localised oxidative attack.

It might be advantageous to oxidise acrylic fibres using an organic peroxide, which could be dispersed throughout the fibre during the spinning stage. By a suitable choice of initiating agent for the nitrile polymerisation reaction, it might be possible to produce the equivalent of the present pre-oxidised fibre, at much lower temperatures. In this way, the amount of chain degradation might be reduced, to the benefit of the properties of the carbonised fibre. The appearance of two-phase structures will also be avoided, which would be advantageous to the preparation of 1,000^{o}C carbon fibre, as the two-phase structure is normally deleterious in fibre of this type.

A more long term approach should be to try to synthesise polymers which have the advantageous properties of the oxidised product of polyacrylonitrile. They must be thermally stable and be readily carbonisable i.e. be able to form highly oriented carbon, without any large losses due to the formation of reaction byproducts. In particular, it would be an advantage to keep the loss of gaseous products to a minimum, as these form pores which weaken the structure. Therefore, a precursor which has a very high initial carbon content is required, as long as it can be spun into a fibre. This specification suggests the use of a ladder type of polymer, such as polybenzimidiazole.

If a high molecular weight poly 1,4-dihydropyridine could be synthesised and oxidised, it would provide a necessary further insight into the mechanism of carbonisation and it might itself produce excellent carbon fibre if it could be spun with very high preferred orientations.

ACKNOWLEDGEMENTS

The author wishes to thank his supervisors for their help and encouragement in this work,

Professor G. Scott,
Department of Chemistry,
University of Aston,
in Birmingham.

Dr J. W. Johnson,
Rolls-Royce (1971) Ltd,
D.E.D. Laboratories,
Derby.

Thanks are also due to Mr J. R. Marjoram and Mr W. N. Turner (both of Rolls-Royce) for providing routine X-ray diffraction and elemental analysis services, and to Mrs J. W. Watkins for her valuable experimental assistance and to Mrs N. Heseltine for typing the manuscript.

REFERENCES.

1. Report from the select committee on science and technology. Session 1968 - 69. "Carbon Fibres". H.M.S.O. 1969.
2. Moreton, R., Watt, W., and Johnson, W., Nature, 213, 690, 1967.
3. Johnson, J. W., Applied Polymer Symposia 9, 229,1969.
4. Jackson, P. W., and Marjoram, J. R., Nature 218, 83, 1968.
5. Jackson, P. W., and Marjoram, J. R., J. Mat. Sci. 5, 9, 1970.
6. Bacon, R., J. Appl. Physics, 31, 2, 1960.
7. Ubbelohde, A. R., and Lewis, F. A., "Graphite and its crystal compounds", Oxford, 1960.
8. Bernal, J. D., Proc. Roy. Soc., A., 106, 749, 1924.
9. Reynolds, W. N., "The physical properties of graphite", Elsevier, 1968.
10. Bacon, G. E., Acta Cryst., 3, 320, 1950.
11. Gray, R., and Gasparoux, H., "Les Carbones", Masson, Paris, 1961.
12. Franklin, R. E., Proc. Roy. Soc., A, 209, 196, 1951.
13. Mitchell, S. J., and Thomas, C. R., Carbon 9, 253, 1971.
14. Shindo, A., Government Industrial Research Institute, Osaka, Report No. 317, 1961.
15. Shindo, A., J. Ceram. Ass. Japan, 69, C195, 1961.
16. Marjoram, J. R., Rolls-Royce Report, RR(OH)320, 1968.
17. Johnson, D. J., and Tyson, C. N., B. J. Appl. Physics (J. Phys. D) (2), 2, 787, 1969.
18. Ergun, S., 9th Biennial conf. on carbon, (Boston), paper SS-21, June 16-20, 1969.
19. Ezekiel, H. M., 10th Symp. A.S.M.E., (New Mexico), January 29th, 1970.
20. Johnson, D. J., and Tyson, C. N., B. J. Appl. Physics (J. Phys. D.), 3, 526, 1970.

21. Badami, D. V., Joiner, J. C., and Jones, G. A., Nature, 215, 386, 1967.

22. United States Patent, No. 223,898, 27th January, 1880.

23. Scientific American, 16th November, 1959.

24. Swann, J. W., British Patent No. 5,978, 31st December, 1883.

25. United States Patent, No. 3,107,152, 15th October, 1963.

26. United States Patent, No. 1,093,084, 16th March 1965.

27. Ross, S. E., Text. Res. J., 38, 906, 1968.

28. British Patent No. 911,542, 28th November, 1962.

29. Standage, A. E., and Prescott, R., Nature, 211, 169, 1966.

30. Watt, W., and Johnson, W., 3rd Conf. "Industrial Carbons and Graphite", 417, 1970 (S.C.I., London)

31. Canadian Patent, No. 790,509, April 1965.

32. Watt, W., Phillips, L. N., and Johnson, W., The Engineer, May 27, 1966.

33. British Patent No. 1,110, 791, April 1965.

34. Everett, D. H., Adams, L. B., Boucher, E. A., and Cooper, R. N., 3rd Conf. "Industrial Carbons and Graphite", 1970 (S.C.I., London)

35. Everett, D. H., Boucher, E. A., and Cooper, R. N., Carbon, 8, 597, 1970.

36. Stuetz, E. D., United States Patent, No. 3,449,077, June 10th, 1969.

37. Accontius, O. E., British Patent, No. 1,188,146, April 15th, 1970.

38. Amano, Y., Japanese Patent, No. 20,609, October 5th, 1963.

39. Amano, Y., Japanese Patent, No. 16,681, August 13th, 1964.

40. Watanabe, U., Japanese Patent, No. 12,615, 1963.

41. Otani, S., Carbon, 3, 31, 1965.

42. Hawthorne, H. M., Baker, C., Bentall, R. H., and Linger, K. R., Nature, 227, 946, 1970.

43. Ezekiel, H. M., Applied Polymer Symposia, 9, 315, 1969.

44. Shindo, A., Nakanishi, Y., and Soma, I., Applied Polymer Symposia, 9, 305, 1969.

45. Bragg, L., "The crystalline state", Bell, 1, 33, 1962.

46. Warren, B. E., Phys. Rev., 59, 633, 1941.

47. Franklin, R. E., Acta. Cryst., 3, 107, 1950.

48. Franklin, R. E., Acta. Cryst., 3, 158, 1950.

49. Watt, W., Nature, 222, 265, 1969.

50. Watt, W., and Johnson, W., Applied Polymer Symposia, 9, 215, 1969.

51. Meredith, R., J. Text. Inst., 45, 489, 1954.

52. Johnson, W., 3rd Conf. "Industrial Carbon and Graphite", 447, 1970, (S.C.I., London).

53. O'Neil, M. J., Anal. Chem., 36, 1238, 1964.

54. Thornton, P. R., "Scanning electron microscopy", Chapman and Hall, 1968.

55. Grassie, N., "The chemistry of high polymer degradation processes". Butterworth, 1957.

56. Turner, W. N., and Johnson, F. C., J. Appl. Polymer Sci., 13, 2,073, 1963.

57. Geddes, W. C., Tech. Rev. 31, Rubber and Plastics Research Association, Shawbury, 1966.

58. Houtz, R. C., Text. Res. J., 20, 786, 1950.

59. Grassie, N., and McNeil, I.C., J. Polymer Sci., 27, 207, 1958.

60. Grassie, N., and Hay, J. N., S.C.I. Monograph, 13, 1961.

61. Grassie, N., and Hay, J. N., J. Polymer Sci. 56, 189, 1962.

62. Conley, R. T., and Bieron, J. F., J. Appl. Polymer Sci. 7, 1757, 1963.

63. Berlin, A. A., Dubinskaya, A. M., and Moshkovski, Y. S., Vyskomol, Soyed. 6: 11, 1938, 1964.

64. Fester, W., Textil-Rundschau, 20, 1, 1965.

65. Fester, W., J. Polymer Sci., C-16, 755, 1967.

66. Schurz, J., J. Polymer Sci., 28, 438, 1958.

67. Schurz, J., Skoda, W., and Bayzer, Z., Z. physik. Chem (Leipzig), 210, 35, 1959.

68. Takata, T., Hiroi, I., and Taniyama, M., J. Polymer. Sci., A2, 1,567, 1964.

69. Brandup, J., and Peebles, L. H., Macromolecules, 1, 64, 1968.

70. Kirby, J. R., Brandup, J., and Peebles, L. H., Makromolecules, 1, 53, 1968.

71. Kirby, J. R., Brandup, J., and Peebles, L. H., Makromolecules, 1, 59, 1968.

72. Meredith, R., and Bay-Sung Hsu, J. Polymer Sci. 61, 271, 1962.

73. Andrews, R. D., and Kimmel, R. M., Polymer Letters, 3, 167, 1965.

74. Miyamichi, K., Okamoto, M., Ishizuka, O., and Katayama, M., J. of Soc. of Fibre Sci. and Tech. Japan, 22, 12, 538, 1966.

75. Kennedy, J. P., and Fontana, C. M., J. Polymer Sci., 39, 506, 1959.

76. Thompson, E. V., J. Polymer Sci., B4, 361, 1966.

77. Hay, J. N., J. Polymer Sci., A1, 6, 2,127, 1968.

78. Madorsky, S. L., and Strauss, S., J. Res. Nat. Bur. Standards, 61, 77, 1958.

79. Grassie, N., and McGuchan, R., European Polymer J. 6, 1,277, 1970.

80. Kasatochkin, V. I. and Kargin, V. A, Doklady Akad. Nauk SSSR 191, 5, 1,084, 1970.

81. Beevers, R. B., Macromol. Revs., 3, 240, 1968.

82. Baily, J. E., and Clarke, A. J., Chemistry in Britain, 6, 484, 1970.

83. Noh, I., and Yu, J. J. Polymer Sci. B4, 721, 1966.

84. Scott, G., "Atmospheric oxidation and antioxidants". Elsevier, 1965.

85. Vosborough, W. G., Text. Res. J., 30, 882, 1960.

86. Müller, D. J., Fitzer, E., and Fiedler, A. K., Conf. on carbon fibres, 2, 1971 (Plastics Institute, London).

87. Danner, B., and Maybeck, J., Conf. on carbon fibres, 6, 1971, (Plastics Institute, London).

88. Makschin, W., and Ulbricht, J., Faserforschung und Textiltechnik 7, 321, 1969.

89. Peebles, L. H., and Brandup, J., Makromol. Chem., 98, 189, 1966.

90. Peebles, L. H., J. Polymer Sci., A-1, 5, 2,637, 1967.

91. Brandup, J., Makromolecules, 1, 72, 1968.

92. Watt, W., 3rd Conf. "Industrial Carbons and Graphite", 447, 1970 (S.C.I., London)

93. Watt, W., and Green, J., Conf. on carbon fibres, 4, 1971, (Plastics Institute, London)

94. Standage, A. E., and Matkowsky, R. D., Nature, 224, 688, 1969.

95. Sanders, R. E., Chem. Process. Eng., 49, 100, 1968.

96. Onyon, P. F., "Viscometry", Chapter 6 in 'Techniques of polymer characterisation' ed. Allen, P. W., Academic Press, 1959.

97. Fujisaki, Y., and Kobayashi, H., Kobunshi Kagaku, 19, 81, 1962.

98. Cotten, G. R., and Schneider, W. C., Kolloid-Z, 192, 16, 1963.

99. Wiesener, E. and Henkel, H., Faserforschung und Textiltechnik, 19, 369, 1968.

100. Tobolski, A. V., J. Chem. Phys. 37, 1,139, 1962.

101. Krigbaum, W. R., and Tokita, N., J. Polymer Sci. 43, 467, 1960.

102. Dunn, P. and Ennis, B. C., J. Appl. Polymer Sci., 14, 1,795, 1970.

103. Layden, G. K., J. Appl. Polymer Sci., 15, 1,283, 1971.

104. Boyer, R. F., J. Appl. Physics, 25, 825, 1954.

105. Gillham, J. K., and Schwenker, R. F., Applied Polymer Symposia, 2, 59, 1969.

106. Thorne, D. N., Rolls-Royce Report, RR(OH)M.234. 1970.

107. Sharples, A., "Introduction to polymer crystallisation", Arnold, 1966.

108. Simmens, S. C., Conf. "Microstructure of Materials" September, 1968, (Royal Microscopical Society, Oxford).

109. Fialkov, A. S., Dokladi Akedemii Nauk S.S.R. 173, 147, 1967.

110. Yamadera, R., Tadokoro, H., and Murahashi, S., J. Chem. Phys., 4, 1,233, 1964.

111. Bellamy, L. J., "The infra-red spectra of complex molecules", Methuen, 1958.

112. Liepens, R., Campbell, D., and Walker, C., J. Polymer Sci. A-1, 6, 3,059, 1968.

113. Standage, A. E., and Matkowsky, R. D., Nature, Physical Sci. 232, 42, 1971.

114. Turner, W. N., and Johnson, F. C., Rolls-Royce Report, RR(OH)379, 1969.

115. Monahan, A. R., J. Polymer Sci. A-1, 4, 2,391, 1966.

116. Cook, N. C., and Lyons, J. E., J. Amer. Chem. Soc., 87, 3,283, 1965.

117. Encyclopedia of Pol. Sci. and Tech. Ed. Mark. H. F. et al. 686, 4, 1966, Wiley.

118. Bell, J. W. and Mulchandani, R. K., J. Soc. Dyers and Colourists, 81, 55, 1965.

119. Hearle, J. W. S., and Peters, R. H. "Fibre structure", 621, Butterworths 1963.

120. Ferry, J. D., "Viscoelastic properties of polymers" Wiley, 1970.

121. Gillham, J. K., Applied Polymer Symposia 2, 45, 1966.

122. Urbanczyk, G. W., Przeglad Wlokiennizy 15, 216, 1961.

123. Bohn, C. R., Schaefgen, J. R., and Statton, W. O., J. Polymer Sci., 55, 531, 1961.

124. Lindenmeyer, P. H., and Hoseman, R., J. Appl. Phys. 34, 42, 1963.

125. Mikhailov, N. V., and Klesman, V. O., Soobsch. o Nauchno. Issled Rabot. Primorsk. Otd. Vses. Khim. Obshchestua, 43, 1955.

126. Katayama, M., and Kambara, S., Sen-i Gakkaishi, 10, 3, 1954.

127. Bacon, R., and Tang, N. M., Carbon, 2, 221, 1964.

128. Honwink, R., "Elasticity, plasticity and structure of matter". Dover, 1958.

129. Miyamichi, K., and Katayama, M., J. of Soc. of Textiles and Cellulose Industries, Japan. 21, 640, 1965.

130. Spencer, D. H., Hooker, M. A., Thomas, A. C., and Napier, B. A., 3rd Conf. "Industrial Carbons and Graphite", 1970. (S.C.I., London)

131. Johnson, J. W., and Thorne, D. J., Carbon, 7, 659, 1969.

131. Also Thorne, D. J., 3rd Conf. "Industrial Carbons and Graphite", 175, 1970 (S.C.I., London).

132. Thorne, D. J., Nature, 225, 1,039, 1970.

133. Moreton, R., 3rd Conf. "Industrial Carbons and Graphite", 243, 1970 (S.C.I., London).

134. Barber, M., Swift, P., Evans, E. L., and Thomas, J. M., Nature, 227, 1,132, 1970.

135. Tyson, C. N., "An X-ray microscope for studying carbon fibres" Rolls-Royce Report, No. RR(OH)490, 1970.

136. Proctor, B. A., Composites, 85, June, 1971.

137. Perret, R. and Ruland, W., J. Appl. Cryst. 1, 257, 1968.

138. Prescott, R., "The Rolls-Royce carbon fibre development programme to December 1966". Rolls-Royce Report No. RR(OH)276, 1967.

139. Pinnick, H. T., J. Chem. Phys., 20, 756, 1952.

140. Warren, B. E., Proceedings of the 1st and 2nd Carbon conferences, 49, 1956 (Buffalo).

141. Takahashi, H., Kuroda, H., and Akamatu, H., Carbon 2, 432, 1965.

142. Maahs, H., Carbon, 7, 509, 1969.

143. Fourdeux, A., Hérinckx, C., Perret, R., and Ruland, W., C. R. Acad. Sc. Paris, 269, 1,597, 1969.

144. Scott, R. G., Conf. "Microstructure of Materials" September, 1968, (Royal Microscopical Society, Oxford)

145. Bacon, R., and Silvaggi, A. F., Carbon, 6, 231, 1968.

146. Bacon, R., and Silvaggi, A. F., Carbon, 9, 321, 1971.

147. Scott, G., Johnson, J. W., and Rose, P. G., 3rd Conf. "Industrial Carbons and Graphite", 444, 1970 (S.C.I., London).

148. Kipling, J. J., and Shooter, P. V., 2nd Conf. "Industrial Carbons and Graphite" 15, 1965 (S.C.I., London).

149. Kipling, J. J., and Shooter, P. V., Carbon, 4, 1, 1966.

150. Everett, D. H., and Redman, E., Fuel, 42, 219, 1963.

151. Butler, B. L., and Dieffendorf, J., 9th Conf. on Carbon, Paper SS-25, 161, June 16th, 1969 (Boston).

152. Butler, B. L., and Dieffendorf, J., 10th Symposium, "Carbon Composite Technology" 107, 1971 (ASME, New Mexico).

153. Tunistra, F., and Koenig, J. L., J. Composite Materials, 4, 492, 1970.

154. Knibbs, R. H., (to be published) J. of Royal Microscopy Soc. 1971.

155. Fishbach, D. B., Carbon, 7, 196, 1969.

156. Hawthorne, H. M., Conf. on carbon fibres, 1971 (Plastics Institute, London)

157. Bacon, R., and Schalamon, W. A., Applied Polymer Symposia 9, 285, 1969.

158. Johnson, J. W., Marjoram, J. R., and Rose, P. G., Nature, 221, 5,178, 1969.

159. Jones, W. R., and Johnson, J. W., (to be published) Carbon, 1971.

160. Johnson, J. W., Conf., "Fibres for Composites:- Strength, Structure and Stability". 3, 1969. (Institute of Physics, Brighton).

161. Robson, D., Assabghy, F. Y. I., Ingram, D. J. E., and Rose, P. G., Nature, 221, 5,175, 1969.

162. Robson, D., Assabghy, F. Y. I., Ingram, D. J. E., and Rose, P. G., 3rd Conf. "Industrial Carbons and Graphite". 1970 (S.C.I. London).

163. Bacon, R., Williams, W., and Steffens, D. A., J. Appl. Physics, 41, 4,893, 1970.

164. Johnson, D. J., Allen, S., Cooper, G. A., and Mayer, R. M., 3rd Conf. "Industrial Carbons and Graphite" 1970 (S.C.I., London)

165. Hugo, J. A., Phillips, V. A., and Roberts, B. W., Nature, 226, 144, 1970.

166. Harling, D. F., JEOL News, Ge (2), 22, 1971.

167. Johnson, D. J., Nature, 226, 750, 1970.

168. Allen, S., Cooper, G. A., and Mayer, R. M., I.M.S. Report 7, November 1969 (N.P.L.).

169. Hill, R., Proc. Phys. Soc. A65, 349, 1952.

170. Goggin, P. R., and Reynolds, W. M., Phil. Mag., 16, 317, 1967.

171. Ruland, W., Applied Polymer Symposia, 9, 296, 1969.

172. Ban, L. L., and Hess, W. M., 9th Conf. on Carbon, Paper SS-27, June 16th, 1969 (Boston).

173. Jenkins, G. M., and Kawamura, K., Nature, 231, 175, 1971.

174. Weisbeck, R., Carbon, 9, 525, 1971.

175. Ezekiel, H. M., Fibre Sci. and Tech. 3, 243, 1971.